THE UNIVERSITY
of EDINBURGH

REGULATION OF COHESIN CLEAVAGE DURING MEIOSIS IN *SACCHAROMYCES CEREVISIAE*

Stefan Galander

Thesis presented for the degree of Doctor of Philosophy

University of Edinburgh

2017

DECLARATION

I declare that this thesis was composed by myself and the research presented within is my own work, unless stated otherwise. This work has not been submitted for any other degree or professional qualification except as specified.

Stefan Galander
2016

ACKNOWLEDGEMENTS

I consider myself extremely lucky that, over the past 3.5 years, I met some truly exceptional people. While my PhD has been a lot of hard work, my colleagues, my family and my friends have provided me with an incredible amount of support and I know that without them, it would have been infinitely harder. I am exceptionally grateful to everyone who has walked part of this journey with me. In particular, I would like to thank the following people:

Adèle, thank you so much for all of your support and encouragement throughout the years! I have learnt so much from you and I am really glad that you allowed me to join the lab. I am especially grateful for all of the freedom you have given me and for allowing me to follow my own ideas! I have had a great time, both scientifically and personally. I don't think I could have done my PhD in a better environment and I am so glad to have been part of an amazing team!

Nadine, it has not even been three months since you left and I already miss you! You have been such a great friend over the past years and I am so grateful for all the time you have invested discussing my project with me – your input has really helped me a lot. I hope that wherever I go in the future there will be someone as dedicated, honest and caring as you!

Kitty, I always look back at the time you've been in the lab with a big smile on my face. We've had so much fun together and I am really grateful for that! You have taught me a lot at the start of my PhD and been an amazing friend throughout. Thank you so much for all that you have done for me!

Eris, working with you has been a truly unique experience! Thank you for all of those times you made me laugh (very hard) and for your never-ending willingness to discuss science with me. It's been great having you around!

Olga, I'm not sure how I would have made it through all those late nights without you! Thank you for always being a great friend, for all your tremendous help in the lab and for being a great person to work with.

Colette, it has been so amazing to have spent most of my PhD with a friend that's been there from the very start! Thank you for being the incredible human being that you are.

Rachael, thank you so much for all of the hard work you have contributed to my project! I really appreciate that you have taken the time away from your own research and I've really enjoyed working with you!

Dave, thank you for all that you have taught me over the years. This project has involved a fair amount of microscopy (and, unfortunately, analysis thereof…) and you have invested a great deal of your time teaching me virtually everything that I know now. And on top of that, your banter has made a lot of very long days down in COIL a lot more bearable! Thank you so much for all your help!

And to the rest of the Marston and Hardwick labs: there have been so many people coming and leaving the lab and all of you have been a joy to learn from and work with. I really appreciate all of your input, your help and all of the fun we've had in the past years. This time has been absolutely amazing and I am so glad I got to spend it with so many incredible people.

I would also like to thank the amazing team in our media and wash-up kitchen. I really do not want to think about what life would have been like without you guys, and how much longer my PhD would have taken if it wasn't for your hard work. You have been an absolute joy to work with and I am incredibly grateful for everything you have done for me!

I am also very grateful to the Wellcome Trust for their generous funding and to fellow scientists who have been so kind to share reagents, strains and plasmids with me. These include Angelika Amon, Nancy Hollingsworth, Wolfgang Zachariae, David Morgan and Kim Nasmyth.

Lastly, although mostly not involved in my scientific work, I would like to thank my family and friends. My PhD has at times been incredibly tough and I don't know what I would have done without all of you on my side to help me through when things didn't go as planned and to share a lot of incredible moments with me that I will never ever forget. Thank you for all your love, kindness, generosity and support!

ABSTRACT

Meiosis is a specialized form of cell division where homologous chromosomes are segregated in meiosis I before sister chromatids are segregated in meiosis II. To establish this pattern, a number of changes to the mitotic chromosome segregation machinery are put in place. Firstly, sister kinetochores orient towards the same pole in meiosis I (mono-orientation). Secondly, homologue recombination creates chiasmata, which link homologues together. And thirdly, cohesin, the molecule that holds sister chromatids together, is cleaved in a step-wise manner. This is achieved because the Shugoshin (Sgo1) protein recruits protein phosphatase 2A (PP2A) to centromeres to counteract cohesin phosphorylation, which is required for its cleavage. The work presented here has investigated two critical aspects of cohesin protection: firstly, how cohesin protection is deactivated in meiosis II and, secondly, how a meiosis-specific protein called Spo13 helps to set up cohesin protection in meiosis I.

Previously, our lab had shown that Sgo1 is removed from chromosomes when sister chromatids come under tension during mitosis. I therefore sought to investigate whether sister kinetochore mono-orientation allows Sgo1 to stay on centromeres during meiosis I and carry out its protective function. To this end, I modified meiosis I chromosomes to lack both chiasmata and mono-oriented kinetochores. Under these conditions, where sister chromatids are forced to be under tension in metaphase I, Sgo1 is undetectable on chromosomes. As a consequence, centromeric cohesin is largely lost in anaphase I leading to the premature separation of sister chromatids in a fraction of cells. Since mono-orientation of sister kinetochores is exclusive to meiosis I, these findings suggest that Sgo1 localisation is influenced by sister kinetochore tension in both mitosis and meiosis. Therefore, our findings suggest a mechanism that could contribute to the deprotection of cohesin in meiosis II. However, loss of cohesin protection upon bi-orientation is not complete, suggesting that other factors are involved in the efficient protection and deprotection of cohesin.

One such factor is the meiosis-specific protein Spo13, which had previously been shown to be required for cohesin protection as well as kinetochore monoorientation. Although it had been suggested that Spo13 regulates Sgo1

recruitment to centromeres, I could not find any evidence to support a loss of Sgo1, or PP2A, in *spo13Δ* cells. Additionally, even when Sgo1 is stabilised and clearly visible in anaphase I of *spo13Δ* mutants, pericentromeric cohesion is still defective. Therefore, I investigated the effect that polo kinase Cdc5, an interactor of Spo13, has on Sgo1. While cellular Sgo1 levels are increased in response to Cdc5 loss, this effect seems to be independent of Spo13. However, Spo13 is required for proper levels of Cdc5 at centromeres and the centromeric recruitment of Cdc5 by Spo13 is likely to be functionally important because tethering of Cdc5 to kinetochores rescued the mono-orientation phenotype of *spo13Δ* cells. In contrast, I found no evidence that the Spo13-Cdc5 interaction is required for cohesin protection. Meiotic overexpression of *SPO13* enhances cohesin protection in meiosis I, apparently independent of its robust interaction with Cdc5, and causes increased Sgo1 enrichment at centromeres. This suggested that Spo13 might recruit Sgo1 to cohesin itself to facilitate its protection. Although I could not detect a loss of Sgo1-cohesin interaction in *spo13Δ* cells, tethering of Sgo1 to cohesin restores pericentromeric Rec8 to *spo13Δ* mutants in anaphase I. Surprisingly, sister chromatids still segregate in this case, suggesting that pericentromeric cohesion is defective, despite maintenance of Rec8. Furthermore, inhibition of either one of the cohesin kinases, DDK and Hrr25, restores sister chromatid cohesion to *spo13Δ* cells. Therefore, the findings in this study suggest that Spo13 is at the centre of a complex regulatory network that coordinates cohesin protection and sister chromatid cohesion in meiosis I.

LAY SUMMARY

All living organisms are made up from cells. In order to grow and develop, cells need to multiply through a process called cell division. There are two different types of cell division. One of them is called mitosis and most cells in our body use this process when we grow or need to replace lost cells. The second process is called meiosis and is used exclusively to make sperm and egg cells.

Studying how meiosis works is of crucial importance. When meiosis goes wrong, the resulting embryos are likely to die. In some cases, errors in meiosis will lead to the birth of babies with severe disorders such as Down syndrome. Furthermore we now know that as women age, the chance of such diseases or miscarriages increases. Unfortunately, the incidence of errors in human meiosis is fairly high. Therefore, it is important to study the basic processes of meiotic cell division so that eventually scientists might identify why human meiosis is so error-prone and identify ways to combat this.

One limitation in studying meiosis, however, is that due to technical limitations and ethical considerations, working with human cells is very complicated. Instead, I have used yeast as a model organism because yeast readily undergo meiosis upon starvation and can easily be studied using genetic, biochemical and cell biological techniques. Furthermore, a lot of the key steps in the meiotic division programme are similar in yeast and human cells.

In my project, I have studied the regulation of a particular complex of proteins called cohesin. Each cell division process requires cells to equally divide up the DNA of the mother cell into the daughter cells. The cohesin complex is central to achieving this because it ensures that the equal partitioning of DNA among daughter cells in a timely manner. My project has investigated a couple of key proteins that allow cohesin to carry out its functions throughout meiosis, and what happens if these proteins are defective. Therefore, this thesis will contribute to our understanding of key meiotic processes and potentially serve to reducing the incidence of birth defects, miscarriages and infertility in the future.

TABLE OF CONTENTS

CHAPTER 1 – INTRODUCTION

The process of cell division underpins the development and reproduction of all forms of life. While the exact mechanisms for how cells divide may differ from organism to organism, it is absolutely essential for the survival of a species that this process occurs in a co-ordinated manner. Errors in this process will significantly impair an organism's ability to survive. Cancer, for example, is a disease that originates when cellular controls over the division process are lost (reviewed in Hartwell & Kastan, 1994). Therefore, an understanding of how cell division is executed in healthy cells is likely to provide us with a better understanding of how to tackle diseases that might arise from mistakes that occur during cell division.

Somatic cells reproduce by a process called mitosis, which allows the generation of two daughter cells from a single mother cell. Sexually reproducing organisms additionally have a second mode of cell division, called meiosis, allowing for the generation of gametes which, when they fuse, give rise to a new organism. The study of meiosis is important because errors during meiotic chromosome segregation may result in infertility, miscarriage or severe developmental disorders like Down's syndrome (reviewed in Hassold & Hunt, 2001). The meiotic division process generates four daughter cells from a single mother cell and the chromosomal content is halved. This requires an adaptation of normal mitotic cell division controls. The aim of this study is to shed light on how a particular aspect of meiosis – the protection of the cohesin protein complex – is regulated throughout meiosis to allow its timely cleavage.

1.1. Cell cycle of vegetative cells

Actively dividing cells will progress through a defined program of events that incorporates the replication of its DNA and eventually results in the formation of two daughter cells, which have retained the chromosomal content of the single mother cell (reviewed in Vermeulen *et al*, 2003). The cell cycle starts with a 'gap' phase called G1. The main aim of this phase is for cells to grow in size and prepare for DNA replication. The G1 phase also contains a checkpoint. In human cells, this is

referred to as the restriction point. At this time, the cell will commit itself to going into the cell cycle and will not require any further external positive growth factor signals to go through the cell cycle. If growth factor signals are missing, then cells may enter G0, or quiescence, a state where cells do not proliferate until external factors signal to do so. In budding yeast, this restriction point is referred to as 'Start' where cells will assess the nutritional environment as well as the presence of a mate. G1 phase is followed by S phase, in which the cell's DNA is replicated. This is followed by another gap phase (G2), which allows further cell growth and prepares the cell for M phase, or mitosis. The transition between these different stages is regulated through the action of cyclin-dependent kinases (CDKs). These kinases require proteins called cyclins for their activity. Cyclins, however, are differentially regulated within the cell cycle to turn their activity on and off at specific times. Cyclin-CDKs will in turn phosphorylate and thereby activate or inactivate a range of substrates to bring about activities specific to a particular cell cycle stage.

1.2. Mitosis

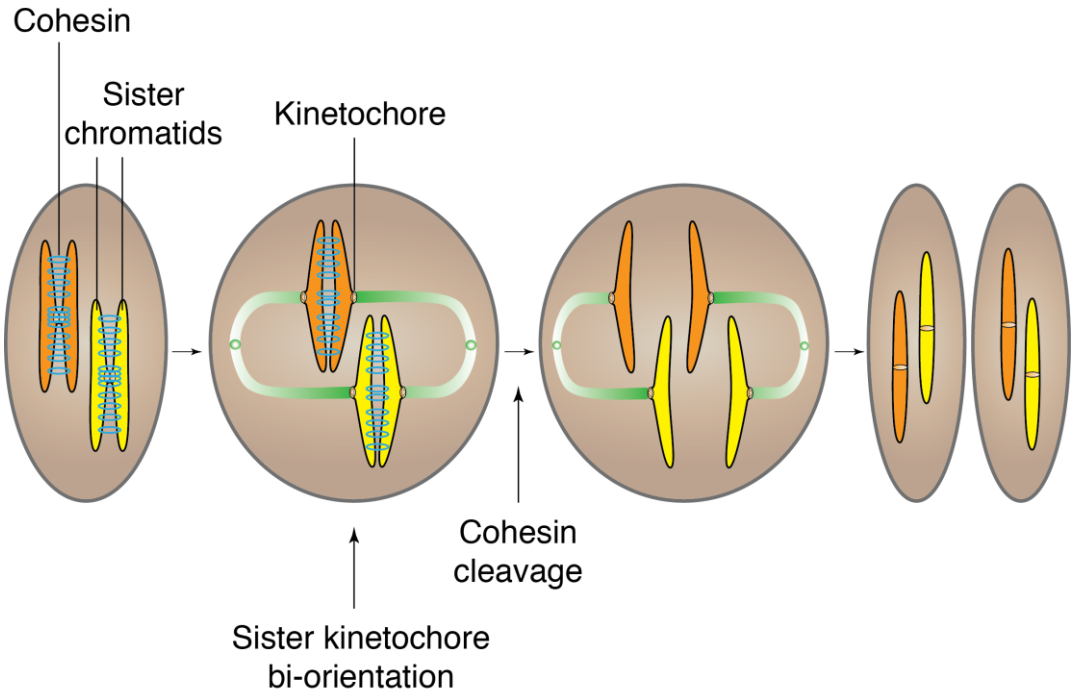

Figure 1.1: Chromosome segregation in mitosis. Mitotic chromosome segregation occurs in cells that have replicated their DNA. Chromosomes become attached by microtubules emanating from opposite poles and are aligned at the metaphase plate in the centre of the cell. Once all chromosomes have become aligned, the cohesin ring, which holds sister chromatids together, is cleaved to allow the segregation of sister chromatids. As a result, two identical daughter cells are formed.

After G2, the cell division and chromosome segregation process occurs in an orchestrated series of events (reviewed in Nasmyth, 2002). First, the nuclear envelope breaks down and chromosomes condense. In budding yeast, however, nuclear envelope breakdown does not occur and the mitotic spindle assembles within the nucleus. When chromosomes have condensed fully, they become attached by microtubules emanating from opposite spindle poles at a proteinacious structure on centromeres called the kinetochore. Chromosomes are then moved towards the centre of the mitotic spindle. Once all chromosomes are aligned, sister chromatids will be pulled towards opposite poles of the cell. A new nuclear envelope reforms around chromosomes and eventually two separate cells are formed in a process called cytokinesis.

1.3. Chromosome segregation in mitosis

A central aspect of mitotic chromosome segregation is that sister chromatids need to be able to resist the forces exerted upon them by the mitotic spindle. Otherwise, sister chromatids could be pulled apart randomly, leading to unequal partitioning of chromosomes so that daughter cells end up with abnormal numbers of chromosomes (aneuploidy). This function is mediated by the cohesin complex, a ring-shaped protein complex that topologically encircles sister chromatids.

1.3.1. Sister chromatid cohesion

Cohesin is a highly conserved protein complex. Originally, three core subunits were identified: two proteins from the SMC family, Smc1 and Smc3, as well as the kleisin subunit Scc1 (Michaelis *et al*, 1997; Losada *et al*, 1998). These three components form a tripartite complex that is thought to topologically enclose sister chromatids (Haering *et al*, 2002; Gruber *et al*, 2003). Later, a fourth subunit, called Scc3 was identified which is now considered part of the core cohesin complex (Tóth *et al*, 1999). Smc1 and Smc3 form rod-shaped molecules that fold up at a hinge domain which serves as interaction site between Smc1 and Smc3 (Haering *et al*, 2002; Hirano & Hirano, 2002). The regions in between the hinge and head domains form an intramolecular coiled-coil (Haering *et al*, 2002). The N-terminus and C-terminus of each Smc molecule form a globular head domain which interacts with Scc1 and contains ATPase activity (Haering *et al*, 2002).

Cohesin is loaded onto chromosomes in late G1 in budding yeast (Michaelis *et al*, 1997; Fernius *et al*, 2013) and during telophase in vertebrates (Gerlich *et al*, 2006). Cohesin loading requires the Scc2/Scc4 complex (Ciosk *et al*, 2000; Lengronne *et al*, 2006) and orthologs of this cohesin loader exist in a variety of model organisms, such as fission yeast, *Drosophila* and humans (Furuya *et al*, 1998; Krantz *et al*, 2004; Rollins *et al*, 2004; Tonkin *et al*, 2004). Cohesin loading occurs at specific sites on the chromosome and then spreads to adjacent regions, probably through the action of the transcriptional machinery, which is thought to push cohesin along the chromosomes so that it accumulates in regions of divergent transcription

(Lengronne *et al*, 2004; Bausch *et al*, 2007; Ocampo-Hafalla *et al*, 2007). How Scc2/Scc4 is recruited to chromosomes is largely unknown. At centromeres, however, Scc2/Scc4 association depends on the Ctf19 kinetochore complex (Fernius & Marston, 2009; Ng *et al*, 2009). Cohesin loading at and translocation away from centromeres establishes a 20-50 kb cohesin-rich domain around centromeres (Blat & Kleckner, 1999; Tanaka *et al*, 1999; Megee & Koshland, 1999; Glynn *et al*, 2004), called the pericentromere, which is important for accurate chromosome segregation in meiosis (Kiburz *et al*, 2005).

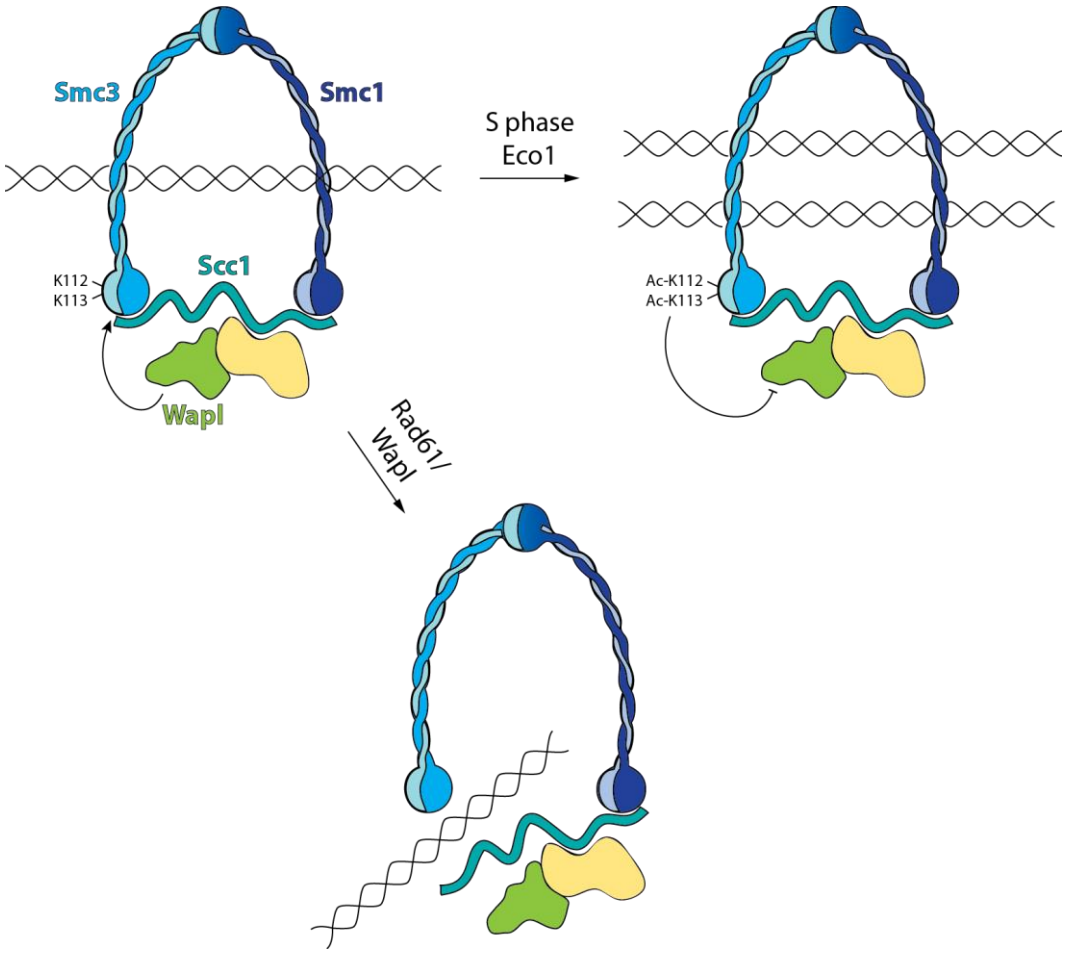

Figure 1.2: Cohesin establishment. During mitotic S phase, the cohesin acetylase Eco1 actylates Smc3 to prevent cohesin release by Wapl. For a detailed description, see text. The representation of the cohesin ring was adapted from Nasmyth & Haering (2009).

Once cohesin is loaded onto chromosomes it does not automatically hold sister chromatids together. Sister chromatid cohesion is only established during S phase, when sister chromatids are replicated. Cohesion establishment requires the acetyltransferase Eco1 (Tóth *et al*, 1999; Skibbens *et al*, 1999; Ivanov *et al*, 2002) whose main function is to protect cohesin from the destabilising activity of Wpl1/Rad61 through acetylation of Smc3 on K112 and K113 (Rowland *et al*, 2009; Sutani *et al*, 2009; Unal *et al*, 2008; Ben-Shahar *et al*, 2008; Zhang *et al*, 2008). The function of this acetylation is to prevent the opening of the cohesin ring at the Smc3-Scc1 interface, which is catalysed by Wpl1/Rad61 (Chan *et al*, 2012; Beckouët *et al*, 2016; Elbatsh *et al*, 2016). The cohesion establishment activity of Eco1 is restricted to S phase and it is thought that Eco1 travels with the replication fork to establish cohesion as DNA is replicated (Lengronne *et al*, 2006; Moldovan *et al*, 2006). Cohesin may be loaded onto chromosomes after S phase but does not hold sister chromatids together unless the function of Wpl1/Rad61 is abrogated (Lopez-Serra *et al*, 2013).

There are a number of models describing how cohesin might hold sister chromatids together. The predominant theory is that the cohesin ring of Smc1, Smc3 and Scc1 topologically embraces sister chromatids (Haering *et al*, 2002). The most convincing evidence demonstrating this comes from a study where the three protein-protein interfaces within the cohesin ring were crosslinked, which prevented dissociation of the cohesin complex from circular mini-chromosomes upon protein denaturation (Haering *et al*, 2008).

1.3.2. The mammalian prophase pathway

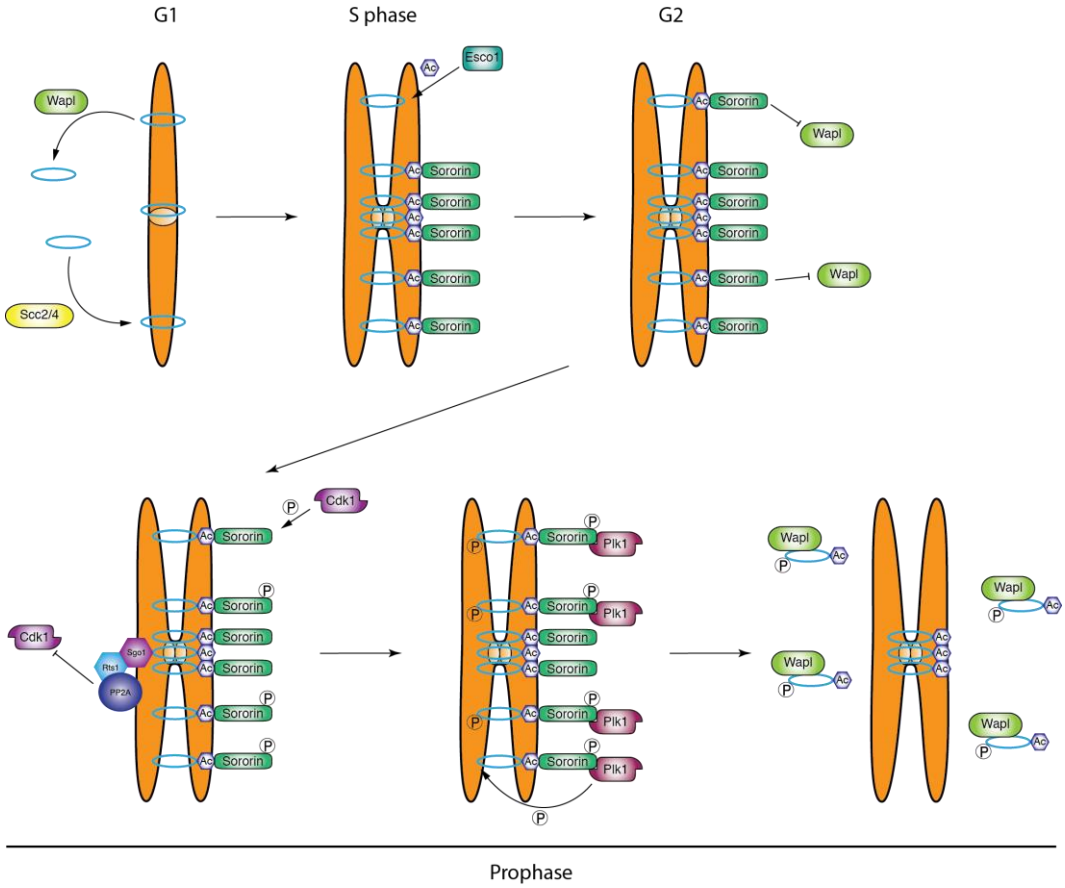

Figure 1.3: The mammalian prophase pathway. Wapl removes arm cohesin in prophase through a pathway independent of cohesin cleavage. This action is prevented in the pericentromere through the concerted action of Sgo1 and sororin. For a detailed description, see text.

While mitotic cohesin removal from chromosomes in budding yeast is thought to occur in a single step at the metaphase to anaphase transition (Michaelis *et al*, 1997), mammals remove cohesin from chromosomes in two steps. First, cohesin at chromosomes arms is lost in prophase by a cleavage-independent mechanism that requires the activity of Wapl (Gandhi *et al*, 2006; Kueng *et al*, 2006) before the remaining cohesin is cleaved by an enzyme called separase at the metaphase-anaphase transition. Prior to prophase, Wapl activity on cohesin is inhibited because acetylated cohesin recruits a protein called sororin (Rankin *et al*, 2005; Nishiyama *et al*, 2010; Lafont *et al*, 2010). Sororin competes with Wapl for binding to Pds5, a cohesin associated protein (Nishiyama *et al*, 2010), and prevents if from displacing

cohesin from chromosomes. In prophase, however, sororin is phosphorylated by Cdk1 and Aurora B (Dreier *et al*, 2011; Nishiyama *et al*, 2013). Cdk1-mediated phosphorylation of sororin allows it to interact with Plk1 (Zhang *et al*, 2011), which in turn hyperphosphorylates SA2, a cohesin subunit analogous to yeast Scc3, and subsequently allows Wapl-dependent cohesin removal (Zhang *et al*, 2011). How exactly SA2 phosphorylation allows cohesin removal is unknown, but phospho-null mutants of SA2 prevent cohesin removal in prophase (McGuinness *et al*, 2005) suggesting that regulation of the SA2 phosphorylation state is crucial.

In pericentromeric regions, prophase cohesin removal is prevented by the action of a protein called Sgo1, which recruits protein phosphatase 2A (PP2A) to chromosomes. In the absence of either protein, cohesin is lost along the length of the chromosome in prophase, which results in the premature segregation of sister chromatids (Kitajima *et al*, 2005; 2006; McGuinness *et al*, 2005; Salic *et al*, 2004; Tang *et al*, 2006). Sgo1-PP2A is thought to protect centromeric cohesin from premature removal by Wapl through at least two mechanisms. Firstly, Sgo1 binds to cohesin and recruits PP2A which dephosphorylates sororin (Liu *et al*, 2013b) and should thereby prevent its interaction with Plk1. Secondly, Sgo1 (which only localises to pericentromeric regions) also competes with Wapl for a binding site on SA2, and thereby prevents its association with cohesin around the centromere (Hara *et al*, 2014). Binding of Sgo1 to cohesin is regulated by Cdk1-mediated phosphorylation of Sgo1 at T346 (Liu *et al*, 2013b). Once sister chromatids successfully bi-orient in metaphase, Sgo1 relocalises from cohesin onto chromatin so that cohesin is no longer protected (Liu *et al*, 2013a).

1.4. Chromosome alignment at the metaphase plate

Before chromosomes can be segregated to opposite poles, they first become aligned at the metaphase plate. This requires the interaction of microtubules emanating from opposite spindle poles with a proteinacious structure that is assembled on centromeres, called the kinetochore. The kinetochore is a large protein complex consisting of multiple subcomplexes which connect the centromeric DNA to the kinetochore-microtubule interface (reviewed in Biggins, 2013). Kinetochore-

microtubule attachments first happen laterally; this means that the kinetochore attaches on the lateral surface of microtubules. In budding yeast, the Ndc80 complex is required for the initial attachment of kinetochores to the lateral surface of microtubules (Tanaka *et al*, 2005). Then chromosomes are actively transported along the microtubules towards the spindle pole body (the yeast equivalent of centrosomes) through the action of the motor protein Kar3 (Tanaka *et al*, 2005; 2007). Finally, the lateral attachment is converted into an end-on-attachment. Once each chromosome has formed end-on attachments between their sister kinetochores and opposing spindle poles, the cell is ready to go into anaphase.

1.5. Bi-orientation of sister chromatids

In order for sister chromatids to be segregated to opposite poles, sister kinetochores first need to become attached from microtubules emanating from opposite poles (amphitelic attachment). However, other forms of attachment may also occur, such as merotelic attachments, where one kinetochore becomes attached to microtubules from opposite poles, or syntelic attachments where both sister kinetochores become attached to the same pole. To prevent missegregation of sister chromatids, cells have evolved intricate mechanisms to ensure that such erroneous attachments are detected and corrected.

One factor contributing to achieving bi-orientation is kinetochore geometry. It is thought that sister kinetochores are positioned in a back-to-back orientation giving them an inherent tendency towards attaching to microtubules from opposite poles (Indjeian & Murray, 2007). In budding yeast, this property requires the pericentromeric adaptor protein Sgo1 (Indjeian & Murray, 2007). Although originally identified as a factor required for cohesin protection in mitosis and meiosis (section 1.12.3.), Sgo1 is also required for proper bi-orientation in a number of experimental systems (Indjeian *et al*, 2005; Huang *et al*, 2007; Kiburz *et al*, 2008). One of the ways in which Sgo1 aids bi-orientation is by recruitment of the condensin complex to centromeres (Verzijlbergen *et al*, 2014). A mutant of Sgo1 that is unable to interact with condensin, *sgo1-700*, lacks the bias towards sister kinetochore bi-

orientation (Verzijlbergen *et al*, 2014), indicating that condensin recruitment by Sgo1 is the critical requirement for establishing a bias towards bi-orientation.

If incorrect kinetochore-microtubule interactions have been made, the cell needs to correct these. This property, referred to as error correction, is carried out by a conserved protein complex called the chromosomal passenger complex (CPC), which consists of four subunits: Aurora B (Ipl1 in budding yeast), Survivin (Bir1), INCENP (Sli15) and Borealin (Nbl1). The key to successful bi-orientation is that cells can sense whether sister kinetochores are under tension. The predominant model for how this is achieved is referred to as the spatial separation model (Liu *et al*, 2009). Aurora B is a kinase that creates a phosphorylation gradient around the inner centromere, where the CPC is located (Wang *et al*, 2011a). Aurora B phosphorylates proteins of the KNL1-Mis12-Ndc80 (KMN) network of the outer kinetochore, which are responsible for contacting microtubules, to destabilise kinetochore-microtubule interactions (Welburn *et al*, 2010). However, when sister kinetochores are pulled apart by microtubules emanating from opposite poles (i.e. they are under tension), then Aurora B targets are pulled away from Aurora B and dephosphorylated, thereby stabilising kinetochore-microtubule interactions.

The CPC essentially consists of two modules, one of which is important for CPC localisation and the other is important for mediating error correction. The CPC is localised to centromeres because Survivin recognises histone H3 phosphorylated at T3 by Haspin kinase (Wang *et al*, 2010; Kelly *et al*, 2010; Yamagishi *et al*, 2010). Furthermore, phosphorylation of histone H2A at S120 is also likely to play a role since this modification recruits the pericentromeric adapter Sgo1 (Kawashima *et al*, 2010; Haase *et al*, 2012), which in turn recruits Aurora B to centromeres (Verzijlbergen *et al*, 2014). Aurora B regulates kinetochore-microtubule attachment in a number of ways; the most important, however, may be phosphorylation of the N-terminal tail of the kinetochore protein Ndc80/HEC1, which is adjacent to a calponin-homology domain thought to directly interact with microtubules (Ciferri *et al*, 2008; Wei *et al*, 2007). A recent model for how Aurora B regulates Ndc80/HEC1 binding to microtubules has suggested that phosphorylation of the N-terminal tail acts as a rheostat where each phosphorylation event, irrespective of its position, decreases the affinity of Ndc80/HEC1 for microtubules (Zaytsev *et al*, 2015).

Therefore, maximally phosphorylated Ndc80/HEC1 has the lowest affinity for microtubules but as tension is established across sister kinetochores Ndc80/HEC1 is pulled away from Aurora B and dephosphorylated in the process to increase its affinity for microtubules (Zaytsev *et al*, 2015). Interestingly, a study in budding yeast has suggested that Ipl1 (the yeast homologue of Aurora B) phosphorylation only affects end-on, and not lateral attachments of microtubules to kinetochores, thus enabling new kinetochore-microtubule attachments to be made even when sister kinetochores are not under tension (Kalantzaki *et al*, 2015). Ipl1 also regulates attachments by phosphorylating the budding yeast-specific Dam1 complex, which interacts with the Ndc80 complex upon formation of end-on attachments (Tien *et al*, 2010; Lampert *et al*, 2010). Similarly to Ndc80, Dam1 phosphorylation at its C-terminus by Ipl1 is thought to disrupt end-on kinetochore-microtubules interactions (Cheeseman *et al*, 2002; Kalantzaki *et al*, 2015). Therefore, the main function of Aurora B/Ipl1 is to generate unattached kinetochores when sister chromatids are not under tension. This acts as a signal to the cell to halt progression into anaphase due to the function of the spindle checkpoint.

1.6. The spindle checkpoint – sensing unattached kinetochores

In order to segregate sister chromatids of all chromosomes in a highly synchronised manner, cells need to prevent chromosome segregation until all sister kinetochores have bi-oriented successfully. Once this happens, an E3 ubiquitin ligase called the anaphase promoting complex/cyclosome (APC/C) is activated and degrades key substrates to initiate anaphase onset.

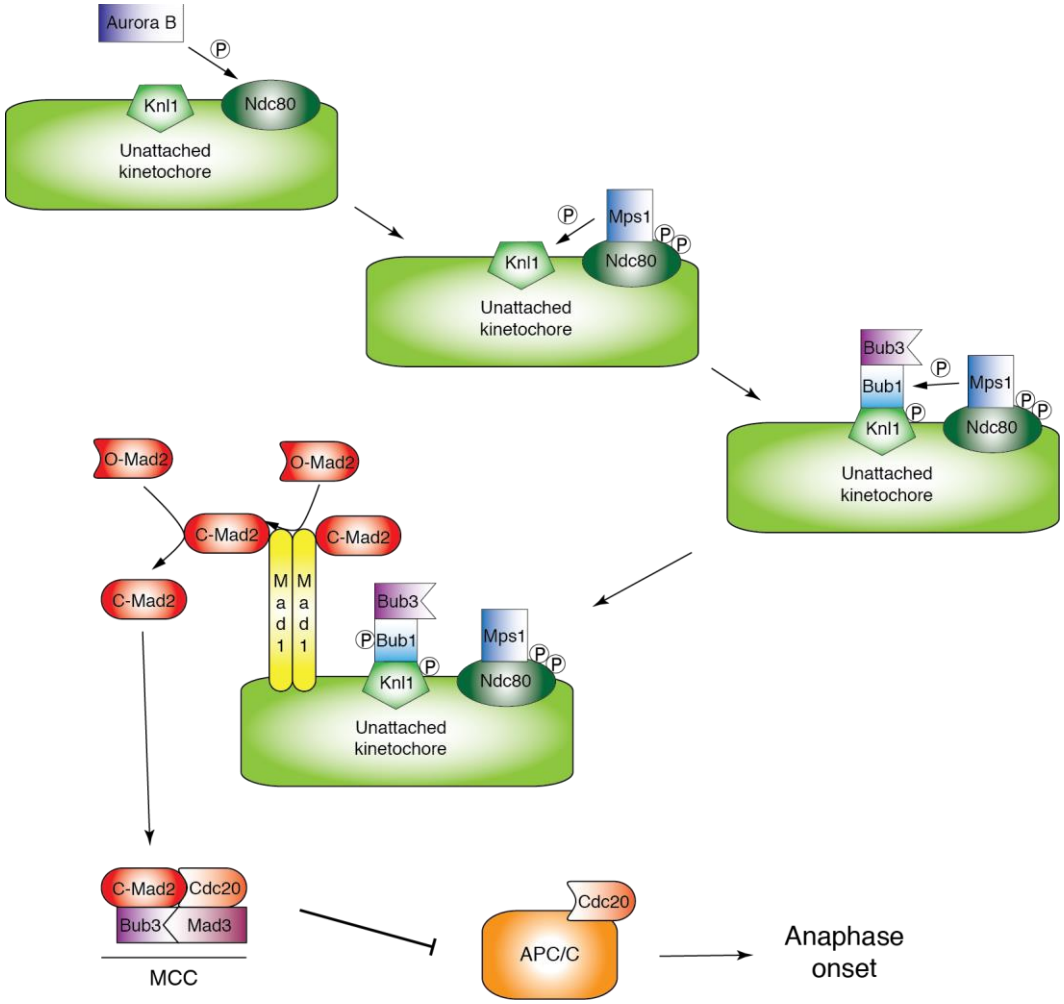

Figure 1.4: The spindle checkpoint. Through the sequential action of various kinases Mad1 is recruited to kinetochores. There, it converts Mad2 from an open to a closed conformation which allows the formation of the mitotic checkpoint complex (MCC) which acts as an inhibitor of the APC/C. For a detailed description, see text.

The function of the spindle checkpoint is to halt cell cycle progression until all chromosomes have bi-oriented. The checkpoint senses unattached kinetochores and prevents cells from entering anaphase. The components of the checkpoint were originally identified in screens searching for mutations capable of bypassing cell cycle arrests imposed through the presence of spindle poisons (Hoyt *et al*, 1991; Li & Murray, 1991). They include the conserved proteins Mad1, Mad2 and Mad3, as well as Bub1 and Bub3. Furthermore, two conserved kinases, Mps1 and Aurora B/Ipl1, are required for checkpoint activity. The spindle assembly checkpoint is initiated by recruitment of Mad1 to kinetochores. This requires the Aurora B-

dependent binding of Mps1 to Ndc80 (Jelluma *et al*, 2008; Saurin *et al*, 2011; Nijenhuis *et al*, 2013). Mps1 then phosphorylates KNL1 (London *et al*, 2012; Yamagishi *et al*, 2012) to allow binding of the Bub1-Bub3 complex (Shepperd *et al*, 2012; Overlack *et al*, 2015; Vleugel *et al*, 2013; Primorac *et al*, 2013). Studies in budding yeast and *C. elegans* have demonstrated that Mps1 then phosphorylates Bub1, which results in the recruitment of Mad1 to unattached kinetochores (Krenn *et al*, 2014; London & Biggins, 2014; Moyle *et al*, 2014). In metazoan cells, Mad1 recruitment additionally requires the RZZ complex (Chan *et al*, 2000; Basto *et al*, 2000; Buffin *et al*, 2005; Kops *et al*, 2005), although the exact mechanisms are poorly understood.

Kinetochore-bound Mad1 can interact with Mad2 and convert it from an open to a closed conformation (Luo *et al*, 2002; 2004; Sironi *et al*, 2002; Mapelli *et al*, 2006). Closed Mad2, bound to Mad1 at kinetochores, can then convert other Mad2 molecules into the closed conformation, allowing for amplification of the checkpoint signal (De Antoni *et al*, 2005; Vink *et al*, 2006). Closed Mad2 binds Cdc20 and forms a complex together with Bub1 and Mad3/BubR1 called the mitotic checkpoint complex (MCC) (Hardwick *et al*, 2000; Fraschini *et al*, 2001; Sudakin *et al*, 2001). How exactly the MCC inhibits the APC/C is not known but the predominant theory is that the MCC acts as a pseudosubstrate to inhibit APC/C activity (Burton & Solomon, 2007; Chao *et al*, 2012).

Once all sister kinetochores in the cell have become bi-oriented, the spindle checkpoint needs to be switched off. This primarily involves removal of spindle checkpoint proteins from kinetochores and reversal of phosphorylations that were put down by Aurora B and Mps1. In metazoans, the protein Spindly, which associates with the RZZ complex, recruits the motor protein Dynein (Griffis *et al*, 2007) which is thought to remove Mad1 and Mad2 from kinetochores (Howell *et al*, 2001). However, Mad1 and Mad2 are removed from kinetochores even in the absence of Spindly (Gassmann *et al*, 2010), suggesting additional mechanisms. These may involve the phosphatases protein phosphatase 1 (PP1) and protein phosphatase 2A (PP2A). PP1 is recruited to kinetochores through interaction with Knl1 (Liu *et al*, 2010; Rosenberg *et al*, 2011) and, at least in yeasts and *C. elegans*, PP1 is essential to spindle checkpoint silencing (Pinsky *et al*, 2009; Vanoosthuyse & Hardwick,

2009; Espeut *et al*, 2012; London *et al*, 2012). In human cells, PP1 association with kinetochores depends on PP2A, which was shown to counteract Aurora B phosphorylation on KNL1 and thereby mediate PP1 binding (Nijenhuis *et al*, 2014). Lastly, spindle checkpoint silencing in human cells also requires the protein $p31^{comet}$ (aka CMT2) (Habu *et al*, 2002; Xia *et al*, 2004). $p31^{comet}$ is thought to facilitate silencing by two distinct mechanisms: firstly, by preventing the formation of closed Mad2 at kinetochores (Xia *et al*, 2004; Mapelli *et al*, 2006) and, secondly, by causing disassembly of the MCC (Westhorpe *et al*, 2011; Eytan *et al*, 2014).

1.7. Entry into anaphase

Upon bi-orientation of sister chromatids, two key events lead to entry into anaphase: first the APC/C^{Cdc20} becomes active and then cohesin gets cleaved to allow sister chromatid segregation.

Cell cycle progression into anaphase is driven by the anaphase promoting complex/cyclosome (APC/C). However, APC/C activity relies on the availability of either Cdc20 or Cdh1, whose interaction with the APC/C causes its activation. Once the spindle checkpoint is silenced, high Cdk1 activity in metaphase promotes APC/C interaction with Cdc20 (Rudner & Murray, 2000). The APC/C causes anaphase onset by ubiquitination of securin/Pds1 (Cohen-Fix *et al*, 1996; Funabiki *et al*, 1996), an inhibitor of separase/Esp1 (Ciosk *et al*, 1998). Separase/Esp1 is a cysteine protease which targets the Scc1 subunit of cohesin and cleaves it (Uhlmann *et al*, 1999), leading to sister chromatid segregation. Similarly, if tobacco etch virus (TEV) protease is expressed in cells carrying a modified version of Scc1 that carries a TEV recognition site, cohesion is lost, indicating that Scc1 cleavage is sufficient for sister chromatid segregation (Uhlmann *et al*, 2000). This implies that regulation of securin/Pds1 destruction is critical to preventing anaphase onset. Recent evidence suggests that securin might act as a competitive inhibitor to prevent Scc1 cleavage by separase (Lin *et al*, 2016). However, in the absence of *PDS1*, cohesin cleavage does not occur prematurely (Alexandru *et al*, 2001a). Although Pds1 is also known to positively regulate Scc1 cleavage by Esp1 (Agarwal & Cohen-Fix, 2002; Hornig *et al*, 2002), this suggests that other factors also regulate timely Scc1 cleavage. One

such factor may be the PP2A regulatory subunit Cdc55. Conditional mutants of *PDS1* display premature Scc1 cleavage in *cdc55Δ* cells (Clift *et al*, 2009). Subsequent studies of cohesin cleavage using a separase biosensor have suggested that Cdc55 reverses polo kinase-mediated phosphorylation of Scc1, which is required for Scc1 cleavage (Alexandru *et al*, 2001b; Hornig & Uhlmann, 2004; Hauf *et al*, 2005), and thereby ensures its timely cleavage (Yaakov *et al*, 2012).

1.8. Anaphase progression and mitotic exit

Exit from mitosis requires two distinct processes: first, mitotic factors such as the mitotic cyclins need to be degraded or inactivated. Furthermore, phosphorylations laid down by mitotic kinases need to be reversed by a set of dedicated phosphatases.

Cyclin degradation occurs in two steps. Upon activation of APC/C^{Cdc20}, the S phase cyclin Clb5 as well as some of the mitotic cyclin Clb2 are degraded (Shirayama *et al*, 1999; Yeong *et al*, 2000). Later in anaphase, the phosphatase Cdc14 causes dephosphorylation of the APC/C activator Cdh1 (Visintin *et al*, 1998), and APC/C^{Cdh1} subsequently degrades mitotic cyclins to promote mitotic exit (Visintin *et al*, 1998; Zachariae *et al*, 1998). Furthermore, Cdc14 also dephosphorylates the Cdk1 inhibitor Sic1, thereby causing its accumulation (Visintin *et al*, 1998).

Cdc14 itself is sequestered in the nucleolus until anaphase, where it binds its inhibitor Cfi1/Net1 (Shou *et al*, 1999; Visintin *et al*, 1999). A complex signalling cascade known as the FEAR (Cdc14 early anaphase release) network governs the initial release of Cdc14 by regulating the phosphorylation state of Cfi1/Net1 (Stegmeier *et al*, 2002). Until anaphase, Cfi1/Net1 is kept in a dephosphorylated state by $PP2A^{Cdc55}$ (Queralt *et al*, 2006). In anaphase, however, the FEAR network downregulates $PP2A^{Cdc55}$. Moreover, Cdk1 bound to Clb1 and Clb2 phosphorylates Cfi/Net1 to disrupt its interaction with Cdc14 (Azzam *et al*, 2004; Queralt *et al*, 2006; Queralt & Uhlmann, 2008). Later on in anaphase, a second signalling cascade known as MEN (mitotic exit network) ensures prolonged activity of Cdc14 and

coordinates other events leading up to cytokinesis (reviewed in Hotz & Barral, 2014).

Similarly to budding yeast, mitotic exit in animal cells is also initiated by the degradation of cyclins. Cyclin B1 is destroyed immediately and completely upon anaphase onset (Clute & Pines, 1999), suggesting involvement of APC/C^{Cdc20}. Furthermore, they use a different set of phosphatases to drive mitotic exit, namely PP1 and PP2A bound to regulatory subunits of the B55 family (Wurzenberger & Gerlich, 2011). Together, these phosphatases reverse phosphorylations laid down by CDKs, PLK1 and Aurora B and thereby prepare the cell to exit mitosis.

1.9. The meiotic cell cycle

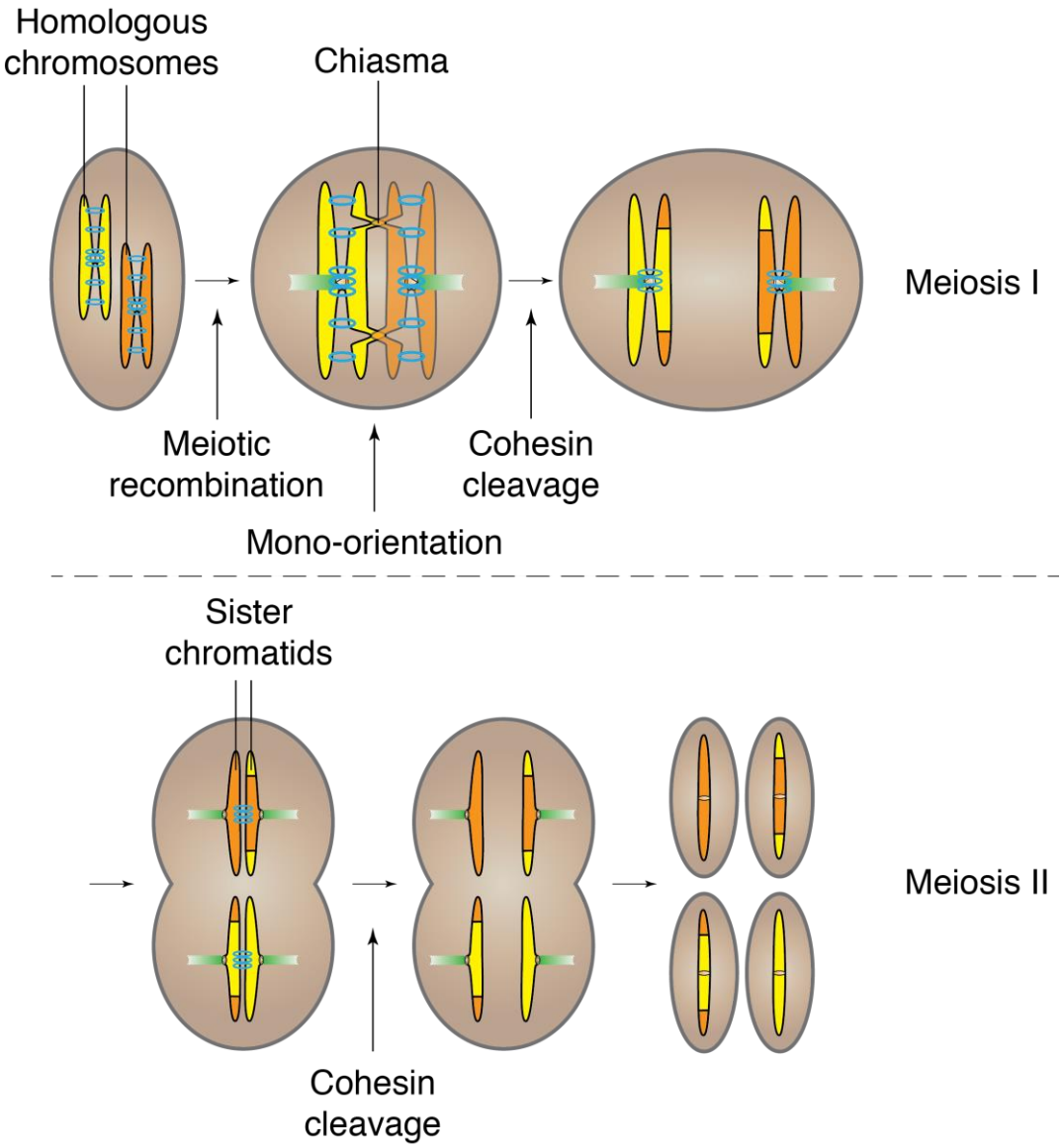

Figure 1.5: Chromosome segregation in meiosis. Meiotic chromosome segregation occurs in two steps. Following pre-meiotic DNA replication, an extended prophase occurs in which homologs recombine and establish linkages, called chiasmata. In contrast to mitosis, homologous chromosomes align at the metaphase plate and are segregated in meiosis I. Homolog segregation requires cohesin cleavage at chromosome arms in meiosis I to resolve chiasmata whereas centromeric cohesin is spared from cleavage until meiosis II. Meiosis II is a more mitosis-like division with sister chromatids bi-orienting in metaphase II. Cleavage of the remaining centromeric cohesin triggers sister chromatid segregation to opposite poles. As a result of meiotic division, four genetically distinct cells with reduced DNA content are formed from a single mother cell.

The key difference between the meiotic and mitotic cell cycle is that in meiosis a single round of DNA replication is followed by two rounds of chromosome segregation. This allows the generation of four haploid gametes from a single diploid progenitor cell. While meiosis in higher organisms mainly serves sexual reproduction, in yeast meiosis is induced in response to starvation.

1.10. Entry into meiosis

In budding yeast, meiotic entry only occurs if three key requirements are fulfilled (reviewed in van Werven & Amon, 2011). Firstly, cells need to be diploid with a *MATa*/*MATα* mating type. Secondly, they need to have mitochondria. And thirdly, they need to be in an environment devoid of nitrogen and fermentable carbon sources. Information about these states is integrated at the promoter of *IME1* (inducer of meiosis 1), which induces expression of early meiotic genes (Kassir *et al*, 1988), which govern pre-meiotic S phase and meiotic prophase. Interestingly, even when budding yeast have entered the meiotic programme, they may not complete it and instead carry out mitotic divisions. This phenomenon, called "return to growth", requires the absence of signals that promote meiosis (Honigberg & Esposito, 1994). However, once cells have passed meiotic prophase and express high levels of the transcription factor *NDT80*, which governs the expression of genes required for meiotic chromosome segregation, they are committed to dividing meiotically (Tsuchiya *et al*, 2014).

In fission yeast induction of meiosis follows similar principles to budding yeast. A key difference is that fission yeast do not vegetatively grow as diploids. Instead, in response to nutrient starvation, cells of opposite mating type are induced to mate, which is directly followed by initiation of the meiotic programme. Similarly to *IME1* in budding yeast, the signals for mating and sporulation converge at a single promoter, in this case for the *ste11+* gene (Sugimoto *et al*, 1991). Upon starvation, respiratory competent cells will induce the *ste11+* gene, which in turn causes expression of genes required for mating and early meiotic processes. To ensure that mating occurs before meiotic division, fission yeast prevent meiosis in haploid cells through Pat1 kinase. Pat1 phosphorylates Ste11, which allows binding of the

inhibitor Rad24 (Kitamura *et al*, 2001). Moreover, Pat1 also targets Mei2 and promotes its degradation (Kitamura *et al*, 2001). Mei2 is an inhibitor of the determinant of selective removal (DSR)-Mmi1 system, which degrades meiosis-specific mRNAs (Harigaya *et al*, 2006). In diploid cells, *ste11+* indirectly promotes the production of the Mei3 protein, which acts as an inhibitor of Pat1 (Li & McLeod, 1996), thereby allowing meiosis-specific genes to be expressed and cells to enter meiotic divisions.

In higher eukaryotes, future germ cells (which will eventually develop into sperm and egg cells) are determined in early embryogenesis. These primordial germ cells (PGCs) then move into the gonad where they will develop into cells proficient to undergo meiosis. While male PGCs do not enter gametogenesis before birth, female PGCs enter meiosis and arrest in prophase during embryonic development. Mammals appear to have a central transcription factor equivalent to Ime1 and Ste11, called STRA8 (Tedesco *et al*, 2009). *Stra8* expression is dependent on retinoic acid (RA), which, in females, stimulates Stra8 expression during embryonic stages in the ovaries (Bowles *et al*, 2006). In male embryonic testes, however, RA levels are kept low (Koubova *et al*, 2006) through a mechanism that may involve metabolisation of RA by the enzyme CYP26B (White *et al*, 2000). *Stra8* is then expressed in murine testes 10 days after birth (Zhou *et al*, 2008), allowing spermatogenesis to occur.

1.11. Pre-meiotic S phase and meiotic prophase

One of the key targets of Ime1 is a meiosis-specific Cdk1-like protein kinase called Ime2 (Smith & Mitchell, 1989). Ime2 is required for the initiation of pre-meiotic S phase as it inactivates the cyclin-Cdk1 inhibitor Sic1 (Dirick *et al*, 1998). Although DNA replication mechanisms are similar in pre-meiotic S phase and vegetative cells, meiotic cells possess a checkpoint that prevents the onset of meiotic recombination as long as chromosomes have not been replicated (Blitzblau & Hochwagen, 2013). Essentially, this checkpoint appears to prevent the loading of factors that cause double-strand breaks to initiate homologous recombination (Blitzblau & Hochwagen, 2013). Once DNA has been fully replicated, meiotic cells are ready to proceed into prophase.

1.11.1. Homolog pairing

Meiotic recombination requires that homologous chromosomes find each other and build certain structures that facilitate the recombination process. The first step, known as homolog pairing, is used to bring together a set of homologous chromosomes. A conserved process required for pairing is telomere clustering. In fission yeast, where this process was originally identified, telomeres cluster in the vicinity of spindle pole bodies (SPBs – yeast equivalent to centrosomes) (Chikashige *et al*, 1994). This is followed by rapid nuclear movement from one cell pole to the other, a phenomenon called horsetail movement (Chikashige *et al*, 1994). Telomere clustering and horsetail movement are thought to somehow allow homologs to identify each other since disruption of either of these processes prevents homolog pairing (Yamamoto *et al*, 1999; Niwa *et al*, 2000; Miki *et al*, 2002; Ding *et al*, 2004). Although horsetail movement appears to be a specific feature of fission yeast meiosis, telomere clustering has been identified both in budding yeast and mammalian cells (Trelles-Sticken *et al*, 2000; Scherthan *et al*, 1996; Morimoto *et al*, 2012). Although the mechanisms of telomere clustering show differences to fission yeast, this indicates that telomere clustering is a conserved process required for homolog pairing.

Homolog pairing additionally requires a process called centromere pairing. In budding yeast, this initially involves coupling of non-homologous centromeres and requires the Zip1 protein (Tsubouchi & Roeder, 2005). Although the exact function of centromere pairing in homolog pairing is unknown and the role of Zip1 in this process is elusive, centromere pairing by Zip1 supports the faithful segregation of homologs that did not form chiasmata in meiosis I (Gladstone *et al*, 2009; Newnham *et al*, 2010). Furthermore, the centromere serves as the initiation site for synapsis of homologs (Tsubouchi *et al*, 2008) suggesting that centromere pairing may facilitate synapsis formation.

1.11.2. Homolog synapsis

Once homologs have paired, they need to become physically connected through two different processes: homolog synapsis and meiotic recombination. Homolog synapsis involves the formation of a proteinacious structure, called the synaptonemal complex (SC), which connects homologous chromosomes along their entire length. During prophase, meiotic chromosomes adopt a particular structure where chromatin loops emanate from a protein-rich scaffold called the chromosome axis. Each homolog will form a single axis with DNA from both sister chromatids protruding from it (Page & Hawley, 2004). The SC essentially consists of proteins associated with the chromosome axis (lateral elements) as well as proteins that couple the lateral elements on homologous chromosomes (transverse filament).

Both homolog synapsis and meiotic recombination are initiated through double-strand break (DSB) formation by the Spo11 endonuclease (Keeney *et al*, 1997). In the absence of *SPO11*, recombination does not occur and cells enter the meiotic divisions without linking homologs (Klapholz *et al*, 1985), causing random segregation of homologs in meiosis I. Zip3, an E3 SUMO ligase, binds the Mre11-Rad50-Xrs2 (MRX) complex (Agarwal & Roeder, 2000), which recognises DSBs formed by Spo11. Zip3 will subsequently sumoylate the axis protein Red1, thereby allowing it to interact with the transverse filament protein Zip1 (Cheng *et al*, 2006; Eichinger & Jentsch, 2010). It has been suggested that poly-SUMO chains may then diffuse away from synapsis initiation sites to mediate Red1-Zip1 interactions close by (Lin *et al*, 2010) to facilitate SC assembly along the length of the chromosome.

Meiotic cohesin complexes form one important part of the SC chromosome axis. Budding yeast Rec8 and *C. elegans* REC-8 are both required for the formation of the SC (Klein *et al*, 1999; Pasierbek *et al*, 2001). Similarly REC8 has been found to localise to axial elements of the SC in rat spermatocytes (Eijpe *et al*, 2000; 2003). In mice, however, the absence of either REC8 or SMC1β does not preclude SC assembly, although SC structure is severely altered (Bannister *et al*, 2004; Revenkova *et al*, 2004; Xu *et al*, 2005). It is thought that cohesin complexes form a "core" which facilitates the assembly of other axial elements (Pelttari *et al*, 2001) together with the SYCP3 protein (Novak *et al*, 2008). Interestingly, a recent study in

Drosophila suggests that cohesin complexes involved in forming the SC may be different from those mediating sister chromatid cohesion (Gyuricza *et al*, 2016). The proteins Stromalin, Nipped-B and the kleisin-like C(2)M localise to chromosome arms in meiosis, are required for SC assembly and appear to be dynamically integrated and removed from the SC throughout the pachytene stage of prophase (Gyuricza *et al*, 2016). In contrast, cohesin proteins important for centromeric cohesion SUNN, SOLO and ORD show different dynamics, localise to centromeres and promote sister chromatid cohesion (Gyuricza *et al*, 2016). Interestingly, studies in mice have described the presence of at least three different cohesin kleisins, RAD21, RAD21L and REC8 with different spatiotemporal profiles of chromosome association (Ishiguro *et al*, 2011). Furthermore, mouse cohesin complexes may also incorporate a variety of different SMC subunits and accessory proteins (reviewed in Revenkova & Jessberger, 2006). This indicates that the presence of a variety of cohesin complexes with different meiotic functions may be conserved. While higher organisms usually have a variety of cohesin proteins that can mediate distinct functions, budding yeast is restricted to only a single meiotic kleisin, Rec8. However, Rec8 is heavily phosphorylated (Brar *et al*, 2006; Katis *et al*, 2010), which raises the intriguing possibility that Rec8 can adopt different conformations depending on its phosphorylation status and may therefore allow meiotic cohesin to perform distinct functions throughout the meiotic divisions. This point is illustrated by the fact that different mutants of *REC8*, namely *rec8-6A* and *rec8-29A*, display different defects in meiotic recombination (Brar *et al*, 2009). Importantly, although the *rec8-6A* mutant is defective for SC assembly, spore viability of the mutant is similar to wild type cells (Brar *et al*, 2009). Therefore, prophase cohesin functions are likely to be unrelated to cohesins ability to link sister chromatids and cohesin's SC functions are not required for faithful chromosome segregation.

1.11.3. Double strand break formation and repair during meiotic recombination

Meiotic recombination is an essential process for the accurate segregation of chromosomes since it creates linkages between homologs that allow tension to be generated across bivalents in meiosis I. This allows the cell to detect successful bi-orientation of homologs and initiates the first meiotic segregation. DSB formation is carried out by the Spo11 endonuclease but requires additional auxiliary factors. A chromosome axis protein called Mer2 links DNA replication with meiotic recombination. Mer2 is phosphorylated by Cdc28 and DDK (Henderson *et al*, 2006; Sasanuma *et al*, 2008; Wan *et al*, 2008), but phosphorylation, at least by DDK, is prevented until S phase is completed (Blitzblau & Hochwagen, 2013). Phosphorylated Mer2 then recruits Spo11 and other factors to the DSB site (Henderson *et al*, 2006; Sasanuma *et al*, 2008; Panizza *et al*, 2011). The MRX complex will then cleave the DNA strand bound by Spo11, resulting in Spo11 release from DNA (Neale *et al*, 2005). Free 5' ends are then resected by the action of the nucleases Exo1 and Mre11 (Mimitou & Symington, 2008; Zhu *et al*, 2008). This creates 3' overhangs, which are bound by Rad51 and the meiosis-specific Dmc1 protein, which are thought to bias DSB repair to occur through recombination with homologs rather than sister chromatids (Schwacha & Kleckner, 1997; Pittman *et al*, 1998; Yoshida *et al*, 1998; Cloud *et al*, 2012).

DSB repair can result in a number of outcomes. However, only crossover events will create linkages between homologous chromosomes that are required for faithful segregation of homologs in meiosis I. A phenomenon called crossover homeostasis ensures that a certain number of crossovers are formed even though the number of DSB events may vary (Martini *et al*, 2006). Therefore, the cell adjusts the ratio of crossover vs. non-crossover repair according to the amount of DSBs initiated. Furthermore, crossover formation is regulated by crossover interference, which prevents the formation of additional crossovers near crossover sites (reviewed in van Veen & Hawley, 2003). Lastly, crossover formation is also spatially controlled as certain areas of the chromosome, including centromeres, have a very low frequency of DSBs and make crossover formation unlikely (reviewed in Talbert & Henikoff, 2010).

1.11.4. Exit from prophase

One key requirement of meiotic recombination is that cell cycle progression into metaphase needs to be prevented until all DSBs have been repaired. In budding yeast, the so-called recombination checkpoint (RC; aka pachytene checkpoint) prevents Cdk1 activity through phosphorylation of Cdc28 at Y19 by Swe1 (Leu & Roeder, 1999) and inhibits transcription of *NDT80*, a transcription factor that is required for exit from prophase (Hepworth *et al*, 1998; Tung *et al*, 2000). Ndt80 binds to so-called middle sporulation elements (MSEs) in the promoter of its target genes to induce their transcription. One of Ndt80's targets is its own promoter. MSEs, however, are also recognised by Sum1, which competes with Ndt80 and represses Ndt80-mediated gene expression, including that of its own promoter (Lindgren *et al*, 2000; Pak & Segall, 2002; Pierce *et al*, 2003). Towards pachytene exit, however, Ime2 and Cdc28 phosphorylate Sum1 and inactivate it (Shin *et al*, 2010), allowing Ndt80 to activate its own transcription. Similarly DDK is also required to relieve Sum1-mediated transcription of MSEs (Lo *et al*, 2012) as expression of *NDT80* and its target genes is inhibited in the absence of Cdc7 or its kinase activity (Lo *et al*, 2008; Sasanuma *et al*, 2008). Furthermore, Ndt80 activity could also be regulated through its nuclear localisation (Wang *et al*, 2011b) and Ime2-dependent phosphorylation upon pachytene exit (Sopko *et al*, 2002; Benjamin *et al*, 2003; Shubassi *et al*, 2003). The fact that Ndt80 activates its own transcription creates a positive feedback loop upon pachytene exit. Once Ndt80 expression levels are high, this commits cells to meiotic divisions and they cannot return to vegetative growth (Tsuchiya *et al*, 2014).

1.11.5. Degradation of M phase factors in budding yeast

Meiotic prophase is a key difference between the mitotic and meiotic cell cycles in budding yeast because meiotic recombination extends the time span that prophase typically takes. Therefore, the production of factors that are normally expressed towards the end of G2 and prepare the cell for mitosis needs to be delayed until the end of prophase. This is particularly the case for budding yeast polo kinase Cdc5

because the expression of Cdc5 invariably forces cells to exit prophase (Sourirajan & Lichten, 2008). Cells solve this problem by degrading M phase factors in meiotic prophase through a meiosis-specific form of the APC/C with the activator Ama1 (APC/C^{Ama1}) (Okaz *et al*, 2012). In *ama1Δ* cells, mitotic factors such as the cyclins Clb1, Clb4 and Cdc5, which are otherwise only expressed upon prophase exit through Ndt80-mediated transcription, are stabilised after S phase (Okaz *et al*, 2012). Similarly, the mitotic transcription factor Ndd1 persists after S phase in *ama1Δ* mutants (Okaz *et al*, 2012). As a consequence of this, the meiotic spindle forms prematurely, SC assembly is inhibited and homologous chromosomes do not segregate correctly (Okaz *et al*, 2012). Therefore, degradation of mitotic factors is essential to proper execution of homologous recombination and chromosome segregation in meiosis. At the end of prophase, APC/C^{Ama1} is inhibited by Clb1-Cdc28 and at least one other currently unknown factor (Okaz *et al*, 2012). This allows exit from prophase and the rapid accumulation of proteins required for chromosome segregation. Whether these mechanisms are conserved in other model organisms is currently unknown. However, other organisms also possess a meiosis-specific form of the APC/C (Blanco *et al*, 2001; Chu *et al*, 2001), which might suggest that degradation of mitotic factors in prophase could be a conserved mechanism.

1.12. Adaptations in the meiosis I chromosome segregation machinery

Meiosis I is a specialised division because instead of segregating sister chromatids, as it occurs in meiosis II and mitosis, homologous chromosomes are segregated. Furthermore, cells need to prevent the complete destruction of cyclins at the end of meiosis I as it might otherwise lead to re-licensing of replication origins and induce DNA replication. The four key changes in the meiotic cell cycle are as follows. Firstly, regulation of cyclin-CDK complexes needs to be adapted in order to allow two consecutive rounds of chromosome segregation without an intervening replication phase. Secondly, homologous chromosomes become linked, by means of chiasmata, so as to allow homologs to bi-orient and tension between homologs to be generated. Thirdly, sister kinetochores need to mono-orient, which means they need

to face the same spindle pole in meiosis I. This is required for homolog segregation to opposite poles. Lastly, cohesin needs to be cleaved in two steps. Cohesin cleavage at the arms allows resolution of chiasmata in meiosis I. However, some cohesin is retained in the pericentromere until meiosis II, which allows tension to be generated between sister chromatids and therefore mediates their faithful segregation.

1.12.1. Control of meiotic divisions by cyclin-CDK

As in mitosis, progress through meiotic divisions requires the co-ordination of events by cyclin-CDK complexes. In budding yeast, there are 6 B-type cyclins Clb1-6 which regulate the function of the only CDK, Cdc28. As in mitosis, cyclins Clb5 and Clb6 are required for pre-meiotic DNA replication (Dirick *et al*, 1998; Stuart & Wittenberg, 1998). The remaining cyclins, however, are differentially regulated in meiosis compared to meiosis. The major mitotic cyclin, Clb2, is not expressed in meiosis (Grandin & Reed, 1993). Clb1 and Clb4 are both targets of the transcription factor Ndt80 and therefore expressed upon prophase exit; their activity, however, appears to be restricted to meiosis I (Carlile & Amon, 2008). Clb1 is considered the major meiotic cyclin as sporulation efficiency is strongly reduced in its absence (Grandin & Reed, 1993). Interestingly, Clb1-Cdc28 activity correlates with a post-translational modification of Clb1 (Carlile & Amon, 2008; Tibbles *et al*, 2013). Clb1 phosphorylation depends both on Cdc28 activity and Cdc5 (Tibbles *et al*, 2013). Inhibition of Cdc28 additionally prevents Clb1 localisation to the nucleus which is required for FEAR activation in meiosis I (Tibbles *et al*, 2013). This suggests that Clb1 activity may be restricted to meiosis I by dephosphorylation and subsequent export from the nucleus. Clb1 remains phosphorylated and retains nuclear localisation in the absence of the PP2A regulatory subunit Cdc55 (Bizzari & Marston, 2011), indicating that $PP2A^{Cdc55}$ could regulate meiotic Clb1 activity. Clb4 activity, on the other hand, appears to remain high until metaphase II, but rapidly declines afterwards (Carlile & Amon, 2008). Interestingly, *clb1Δ clb4Δ* double mutants only undergo a single meiotic division (Kiburz *et al*, 2008), indicating that Clb1 and Clb4 may complement the absence of the other cyclin in meiosis I. Lastly, Clb3 activity is restricted to meiosis II in a process that requires translational

repression of the *CLB3* transcript (Carlile & Amon, 2008). *CLB3* expression is prevented in meiosis I through binding of the meiosis-specific RNA binding protein Rim4 (Berchowitz *et al*, 2013). In meiosis II, however, Ime2 activity increases and leads to Rim4 phosphorylation, which relieves transcriptional repression of *CLB3* (Berchowitz *et al*, 2013). The restriction of cyclin-CDK activity in meiosis I is essential to proper chromosome segregation as pre-meiotic S phase expression of cyclins, particularly Clb1 and Clb3, leads to sister chromatid segregation in meiosis I (Miller *et al*, 2012). What exactly the function of restricting Clb3 to meiosis II is, however, remains unknown since there are no deleterious consequences to Clb3 expression upon prophase exit (Miller *et al*, 2012).

1.12.2. Sister kinetochore mono-orientation

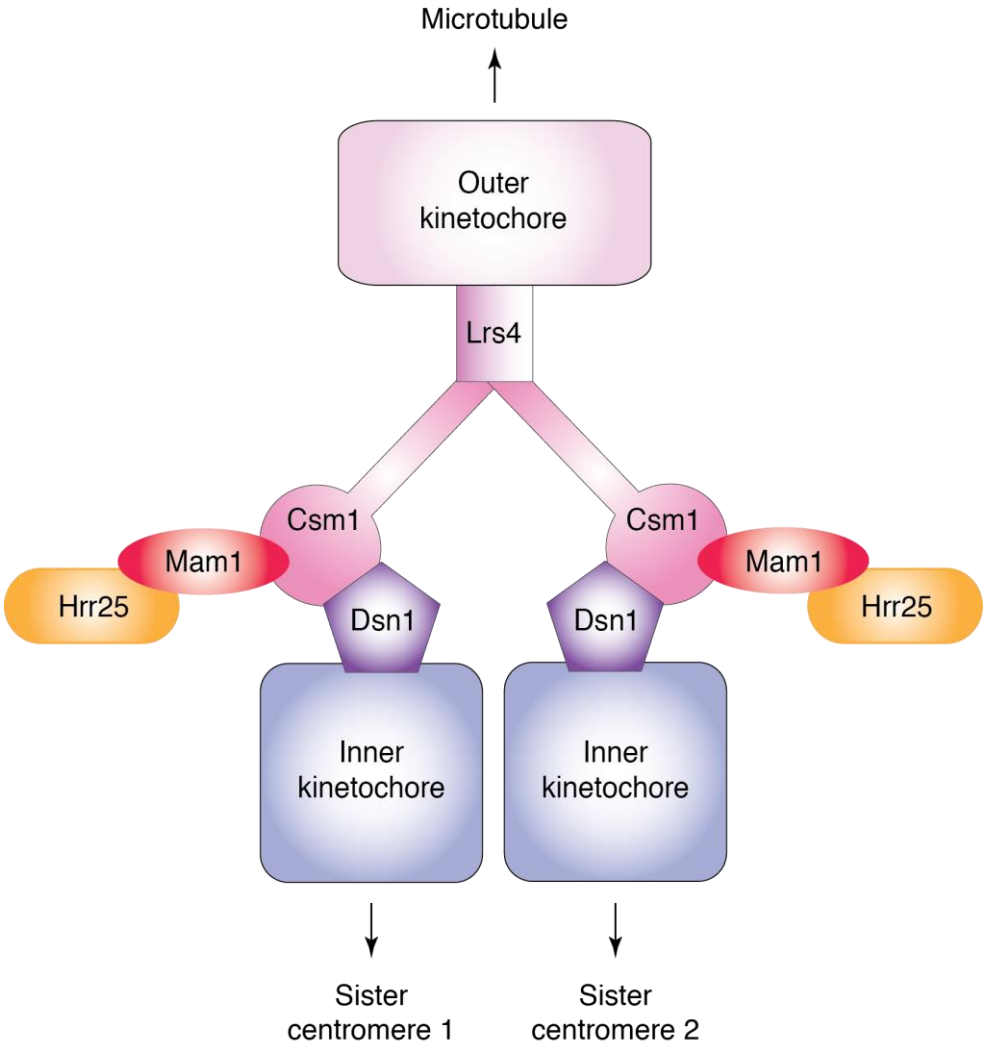

Figure 1.6: Mono-orientation through kinetochore fusion. Mono-orientation in budding yeast is brought about by the monopolin complex consisting of Mam1, Csm1, Lrs4 and Hrr25. Monopolin is thought to fuse sister kinetochores. The C-terminal globular domains of Csm1 contact two separate sister kinetochores via the inner kinetochore protein Dsn1. Furthermore, this portion of Csm1 also binds Mam1 which in turn recruits Hrr25. The N-terminus of Csm1 interacts with Lrs4. This area of the complex then somehow contacts the outer kinetochore so that one microtubule binding entity coordinates the segregation of two sister kinetochores.

The segregation of homologous chromosomes in meiosis I requires that sister chromatids are mono-oriented, i.e. they are facing towards the same spindle pole. Research in budding yeast has so far provided the most detail about how mono-orientation is regulated. Mono-orientation requires a protein complex called monopolin, which localises to kinetochores and is composed of four subunits: the meiosis-specific kinetochore protein Mam1 (Tóth *et al*, 2000), two nucleolar

proteins, Csm1 and Lrs4 (Rabitsch *et al*, 2003) and casein kinase Hrr25 (Petronczki *et al*, 2006). Mam1, Csm1 and Lrs4 are interdependent for their localisation to kinetochores (Rabitsch *et al*, 2003); Mam1 localisation additionally requires its interaction with Hrr25, but not Hrr25 kinase activity (Petronczki *et al*, 2006). Other factors required for mono-orientation are polo kinase Cdc5, Dbf4-dependent kinase Cdc7 (DDK) and the meiosis specific protein Spo13. The role of these auxiliary factors is largely unclear, although Cdc5 is known to be required for the release of Lrs4 and Csm1 from the nucleolus (Clyne *et al*, 2003). Spo13 and DDK are required for the localisation of monopolin to kinetochores as well as hyperphosphorylation of Lrs4 (Matos *et al*, 2008), although the role of this modification is currently still unclear. The crystal structure of monopolin subcomplexes has given clues as to how monopolin might bring about mono-orientation (Fig. 1.3). Csm1 exists as dimers with a long N-terminal coiled coil and globular C-terminal domains (Corbett *et al*, 2010). In the Csm1-Lrs4 complex, the N-termini of two Csm1 homodimers will form a V-shaped structure leaving the globular domains at the tips of the V, whereas the N-terminus of Lrs4 interacts with the N-terminal helices of Csm1 (Corbett *et al*, 2010). The C-terminal globular domains of Csm1 interact with the C-terminus of Mam1 (Corbett & Harrison, 2012) as well as the N-terminus of the kinetochore protein Dsn1 (Corbett *et al*, 2010; Corbett & Harrison, 2012; Sarkar *et al*, 2013). The core of Mam1 furthermore interacts with the N-terminus of Hrr25 (Corbett & Harrison, 2012). This arrangement has led to the suggestion that monopolin might fuse sister kinetochores as each C-terminus of Csm1 could in theory bind Dsn1 molecules on separate kinetochores (Corbett *et al*, 2010). This model is supported by biophysical data demonstrating that meiosis I kinetochores are able to resist stronger pulling forces from microtubules than mitotic kinetochores, a property that depends on the presence of Mam1 (Sarangapani *et al*, 2014). Furthermore, meiosis I kinetochores contain a higher ratio of Nuf2, a member of the microtubule-binding Ndc80 complex, over Mif2, an inner kinetochore component, than mitotic kinetochores (Sarangapani *et al*, 2014). This indicates that monopolin acts to fuse two sister kinetochores so that they act as a single microtubule-binding entity. The exact function of Mam1 and Hrr25 remain poorly understood, however. Interestingly, binding of Mam1 appears to cover up one of the Dsn1 binding sites on

Csm1 (Corbett & Harrison, 2012) but it is unclear whether constitutive binding of Mam1 to kinetochores is required for mono-orientation since meiotic kinetochores isolated for biophysical assays appear to be devoid of monopolin (Sarangapani *et al*, 2014). Therefore, Mam1 might only be required to localise Csm1 and Lrs4. Hrr25 function is also elusive but it is known that mono-orientation requires both its interaction with Mam1 as well as its kinase activity, although the latter is not required for the Mam1-Hrr25 interaction (Petronczki *et al*, 2006).

Although sister kinetochore fusion has been suggested to be important for mono-orientation in *Drosophila*, grasshoppers and maize (Goldstein, 1981; Paliulis & Nicklas, 2000; Li & Dawe, 2009), homologues of Mam1 have not been identified in other organisms. In fission yeast, mono-orientation relies on sister chromatid cohesion in the core centromere, a property conferred by cohesin containing the meiosis-specific kleisin subunit Rec8 (Watanabe & Nurse, 1999). Although meiotic chromosomes also contain cohesin with Rad21, the fission yeast equivalent of Scc1, Rad21-cohesin complexes only localise to the pericentromere, but not the core centromere (Tomonaga *et al*, 2000; Bernard *et al*, 2001; Nonaka *et al*, 2002; Sakuno *et al*, 2009). In contrast, Rec8-containing cohesin is enriched at the core centromere (Watanabe *et al*, 2001; Sakuno *et al*, 2009) where it binds Psc3, one of two Scc3-like proteins in fission yeast (Kitajima *et al*, 2003b). Replacement of Rec8 with Rad21 in meiosis leads to a reduction of cohesin in the core centromere and a loss of mono-orientation (Yokobayashi *et al*, 2003). Core centromere cohesion and, therefore, mono-orienation require the protein Moa1 (Yokobayashi & Watanabe, 2005; Sakuno *et al*, 2009; Kagami *et al*, 2011) but its exact functions remain elusive. Cohesin appears to facilitate mono-orientation simply bringing sister core centromere sequences in close proximity since artificial linkage of sister core centromere sequences significantly enhances sister chromatid co-segregation in *moa1Δ* mutants (Sakuno *et al*, 2009). Cohesin is also required for mono-orientation in *Arabidopsis* and *C. elegans* (Chelysheva *et al*, 2005; Severson *et al*, 2009), possibly indicating a conserved role for centromere cohesion in mono-orientation. In budding yeast, however, mono-orientation is intact when the meiosis-specific cohesin subunit Rec8 is replaced with its mitotic counterpart (Tóth *et al*, 2000). However, there is currently no evidence that Scc1 and Rec8 in budding yeast occupy distinct chromosomal

domains as is observed for Rad21 and Rec8 in fission yeast. *rec8Δ* cells, however, display a minor mono-orientation phenotype which is strongly elevated upon deletion of *MAM1* (Monje-Casas *et al*, 2007). Together, these results argue that mono-orientation in budding yeast mainly relies on monopolin and only to a lesser extent on cohesin.

1.12.3. Cohesin protection

A key feature of meiotic chromosome segregation is that cohesin cleavage needs to occur in two steps. Because of the lack of a replication phase between meiosis I and meiosis II, there is no opportunity for cells to load new cohesin and establish cohesion between the two meiotic divisions. Therefore, some cohesin needs to be retained until meiosis II to ensure faithful segregation of sister chromatids. However, due to the formation of chiasmata on chromosome arms during prophase, cohesin mediates the linkage between homologs, which need to be segregated in meiosis I. As a consequence, arm cohesin needs to be removed in the first meiotic division to allow chiasmata resolution. Cohesin in the pericentromere (where meiotic recombination does not occur), however, stays on chromosomes until the onset of anaphase II.

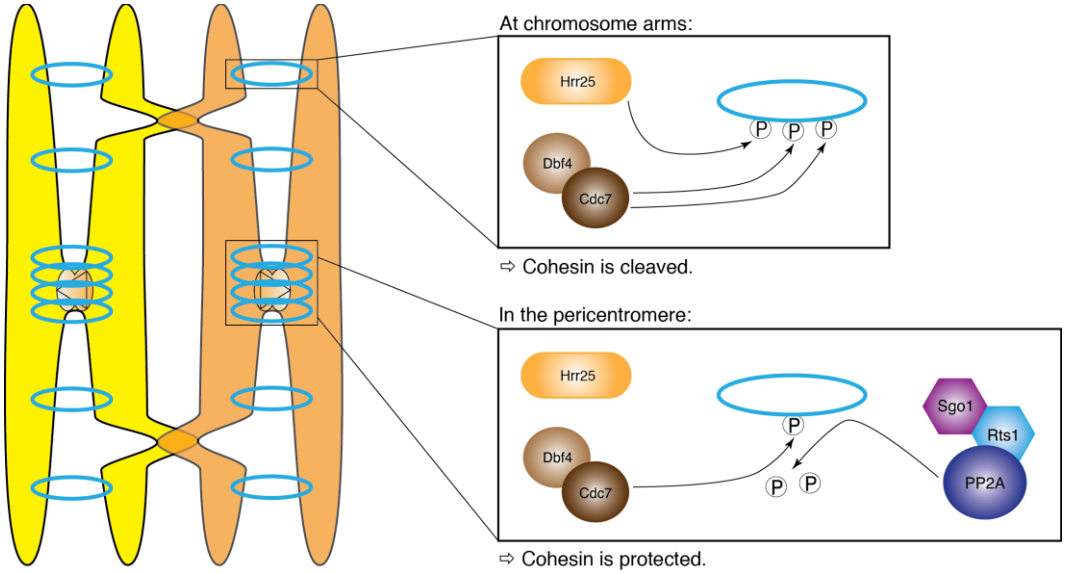

Figure 1.7: Cohesin protection in meiosis I. Along the length of the chromosome, two kinases, Hrr25 and Dbf4-Cdc7, phosphorylate the meiotic cohesin subunit Rec8. Rec8 phosphorylation renders cohesin susceptible to cleavage by separase. In order to protect centromeric cohesin, the pericentromeric adaptor protein Sgo1 recruits PP2A via its regulatory subunit Rts1. PP2A dephosphorylates cohesin and thereby prevents its cleavage. Because Sgo1 only localises to the pericentromere, cohesin protection is restricted to this area of the chromosome.

Similarly to mitosis, cohesin cleavage in meiosis requires the action of separase (Buonomo *et al*, 2000; Kitajima *et al*, 2003a). Several studies in budding yeast have shown that cohesin cleavage by separase depends on phosphorylation of Rec8 (Brar *et al*, 2006; Katis *et al*, 2010; Attner *et al*, 2013). Although full Rec8 phosphorylation is dependent on three kinases – Cdc5, Hrr25 and DDK – it is still debated which kinases are contributing to cohesin cleavage. Initially, polo kinase Cdc5 was suggested to be the crucial kinase as many phosphorylation events on Rec8 depend on the presence of Cdc5 (Brar *et al*, 2006). However, phospho-null mutants created in this study were either severely delayed in their prophase progression (indicating a loss of Rec8 function) or cohesin cleavage was not efficiently suppressed (Brar *et al*, 2006). Later, it was argued that DDK and Hrr25 are the kinases crucial for cohesin cleavage as inhibition of both kinases blocks Rec8 cleavage and chiasmata resolution (Katis *et al*, 2010). Although specific phosphorylation sites for these kinases on Rec8 were not identified, Katis *et al.* (2010) managed to generate Rec8 phospho-null mutants capable of preventing cohesin cleavage in meiosis I. Furthermore, they identified sites which, when

mutated to phospho-mimicking residues, allow Rec8 cleavage along the length of the chromosome in meiosis I (Katis *et al*, 2010). Curiously, the sites most important for cleavage are not located in the vicinity of the proposed separase recognition site (Katis *et al*, 2010) and many of them were previously identified to be Cdc5-dependent (Brar *et al*, 2006).

To faithfully segregate sister chromatids in meiosis II, pericentromeric cohesin needs to be protected from the action of separase in meiosis I. The requirement of cohesin phosphorylation for cohesin cleavage suggests that pericentromeric cohesin is dephosphorylated in meiosis I. This function is carried out by shugoshin (Sgo) proteins. Sgo1 was originally identified in a fission yeast screen that looked for proteins whose mitotic expression was lethal when combined with expression of the meiotic cohesin Rec8 (Kitajima *et al*, 2004). Shugoshin proteins are conserved in many model organisms (Marston *et al*, 2004; Katis *et al*, 2004a; Kerrebrock *et al*, 1992; Lee *et al*, 2008). Bub1 phosphorylation of histone H2A at serine 121 recruits Sgo1 specifically to the pericentromere (Tang *et al*, 2004; Kitajima *et al*, 2005; Kiburz *et al*, 2005; Fernius & Hardwick, 2007; Kawashima *et al*, 2010; Liu *et al*, 2013a). There Sgo1 recruits PP2A (Kitajima *et al*, 2006; Tang *et al*, 2006; Riedel *et al*, 2006; Lee *et al*, 2008) via its regulatory subunit Rts1, which is thought to dephosphorylate cohesin and thereby make it refractory to separase cleavage. Several lines of evidence suggest that $PP2A^{Rts1}$ acts directly on Rec8 to prevent its cleavage. Firstly, artificial tethering of fission yeast PP2A to arm cohesin prevents cohesin cleavage on chromosome arms (Riedel *et al*, 2006). Secondly, budding yeast depleted for the PP2A subunit Cdc55 show increased levels of $PP2A^{Rts1}$ on chromosomes, which leads to dephosphorylation and overprotection of Rec8 (Bizzari & Marston, 2011). Lastly, a separase biosensor containing the core part of Rec8, which is subject to phosphorylation by Cdc5, DDK and Hrr25, is not cleaved when Rts1 is fused to the biosensor (Yaakov *et al*, 2012). Taken together, these results suggest that pericentromeric cohesin is protected from cleavage in meiosis I because Sgo1 recruits PP2A to the pericentromere through Rts1. This leads to Rec8 dephosphorylation, which prevents proteolytic cleavage by separase. Further work should be aimed at understanding how phosphorylation of Rec8 makes it a substrate for separase.

1.12.4. Outer kinetochore disassembly and its role in mono-orienation and cohesin protection

One peculiar feature of the meiotic cell cycle is that in meiotic prophase outer kinetochores are disassembled and degraded. This phenomenon has been observed both in fission yeast and budding yeast (Asakawa *et al*, 2005; Miller *et al*, 2012; Meyer *et al*, 2015). Interestingly, mutants that affect the ability of cells to disassemble outer kinetochores in prophase show defects both in mono-orientation and cohesin protection. Cells that overexpress the cyclin *CLB3* from the copper-inducible *CUP1* promoter (*pCUP1-CLB3*) early in meiosis show defects both in mono-orientation and cohesin protection (Miller *et al*, 2012). Premature *CLB3* expression appears to induce spindle formation and allow kinetochore-microtubule interactions in pre-meiotic S phase and prophase, which is normally prevented through outer kinetochore disassembly in wild type cells. Consequently, *pCUP1-CLB3* cells fail to localise monopolin to kinetochores (Miller *et al*, 2012). However, transient disruption of kinetochore-microtubule interaction in *pCUP1-CLB3* cells restores sister kinetochore co-segregation in meiosis I (Miller *et al*, 2012) indicating that disengagement of kinetochore-microtubule interactions in early meiosis is required to set up the meiotic chromosome segregation pattern.

Similarly to *pCUP1-CLB3* cells, mutants lacking Ipl1 (budding yeast Aurora B) in meiosis also exhibit mono-orientation and cohesin protection defects (Monje-Casas *et al*, 2007; Yu & Koshland, 2007; Meyer *et al*, 2015). Recent evidence has suggested that cells lacking *IPL1* fail to disassemble their outer kinetochores and therefore kinetochores and microtubules are continuously engaged throughout meiosis (Meyer *et al*, 2013; 2015). Furthermore, Mam1 association with kinetochores is strongly reduced in the absence of *IPL1*; however, monopolin can be loaded if microtubules are transiently depolymerised through drug treatment (Meyer *et al*, 2015). Together, these results suggest that outer kinetochore disassembly in meiosis I is required to build a meiotic kinetochore that incorporates monopolin and potentially any other factors that facilitate mono-orientation.

How outer kinetochore disassembly impacts cohesin protection is currently still elusive. *pCUP1-CLB3* cells appear to successfully localise Sgo1 and Rts1 which has

led to the suggestion that they are either not functional or that the observed pools of these proteins do not represent the protective pool of Sgo1-PP2A^{Rts1} (Miller *et al*, 2012). The evidence for how depletion alleles of *IPL1* impact cohesin protection is currently somewhat contradictive. Whereas one study found a reduction in Sgo1 at centromeres in the absence of *IPL1* (Monje-Casas *et al*, 2007), another study suggested that Sgo1 is appropriately localised but instead Rts1 is not found at centromeres (Yu & Koshland, 2007). In the future, it would be interesting to determine whether it is indeed the failure to disassemble outer kinetochores that causes cohesion defects in *pCUP1-CLB3* or Ipl1 depletion mutants as this could reveal new clues as to how pericentromeric cohesion is set up in meiosis I.

1.12.5. Spo13 as a central regulator of meiosis I chromosome segregation

Although mechanistic models for both cohesin protection and mono-orientation exist, they fail to incorporate a protein that is required for both processes: Spo13. Spo13 was originally isolated as the nonsense mutant *spo13-1* which undergoes only a single division during meiosis resulting in diploid (or near-diploid) spores (Klapholz & Esposito, 1980a). While recombination occurs normally in *spo13-1* strains, the single round of chromosome segregation is largely equational (separating sister chromatids) rather than reductional (separating homologous chromosomes) (Klapholz & Esposito, 1980b). *SPO13* is expressed solely during meiosis (Wang *et al*, 1987) and expression depends on a region 170bp upstream of the *SPO13* start site (Buckingham *et al*, 1990). Mitotic repression of *SPO13* depends on the Ume6 and Sin3 proteins (Steber & Esposito, 1995; Rundlett *et al*, 1998), which are thought to mediate histone K4 lysine 5 deacetylation by Rpd3 that causes inactivation of the *SPO13* promoter in mitosis (Rundlett *et al*, 1998). Upon entry into meiosis, Ime1 expression is thought to counteract Sin3-mediated repression and convert Ume6 into a transcriptional activator (Washburn & Esposito, 2001). Consequently *SPO13* is classified as an early meiotic gene, which is expressed soon after induction of meiosis. Localisation studies of Spo13 show that Spo13 mainly associates with centromeres, but is also found in other regions of the chromosome (Lee *et al*, 2004). Upon anaphase onset, Spo13 is degraded, probably by the APC/C, and its

degradation depends on an atypical recognition motif at its N-terminus (Sullivan & Morgan, 2007). Stabilisation of Spo13, however, has no deleterious consequences on meiosis II division, indicating that additional pathways function to deactivate it (Sullivan & Morgan, 2007).

More detailed analyses of chromosome segregation in *spo13Δ* mutants showed that the ratio of equational/reductional segregation during the single meiotic division varied from chromosome to chromosome (Shonn *et al*, 2002). However, elimination of recombination causes all *spo13Δ* cells to divide chromosomes equationally (Klapholz *et al*, 1985; Shonn *et al*, 2002). This suggested defects in mono-orientation which is also supported by the splitting of heterozygous, centromere-proximal GFP foci in metaphase I of *spo13Δ* mutants (Shonn *et al*, 2002; Katis *et al*, 2004b). However, loss of mono-orientation is only complete in mutants that are also deleted for *MAM1* (Katis *et al*, 2004b; Lee *et al*, 2004). Spo13 is thought to contribute to mono-orientation in at least two ways: firstly, it is thought to either recruit or maintain monopolin components at the kinetochore (Katis *et al*, 2004b; Lee *et al*, 2004) and secondly, it is important for the hyperphosphorylation of Lrs4, which is hypothesised to be important for mono-orientation (Katis *et al*, 2004b). Spo13 was found to interact with polo kinase Cdc5 (Matos *et al*, 2008). A *SPO13* mutant that has reduced interaction with Cdc5, called *spo13-m2*, displays mono-orientation phenotypes similar to *spo13Δ* mutants (Matos *et al*, 2008), suggesting that the Cdc5 regulation by Spo13, or vice versa, is responsible for ensuring sister chromatids mono-orient in meiosis I.

In addition to mono-orientation, Spo13 also regulates cohesin protection. The first evidence of this was the observation that mitotic overexpression of Spo13 leads to protection of cohesin, although reports disagree whether Spo13 can only protect Rec8 (Shonn *et al*, 2002), or both Rec8 and Scc1 (Lee *et al*, 2002). Furthermore, cohesin protection by Spo13 overexpression in mitosis does not require Sgo1 (Lee *et al*, 2004). In meiosis, the presence of Spo13 is required for cohesin protection in meiosis I as indicated by a reduction in pericentromeric Rec8 in anaphase I (Lee *et al*, 2004; Katis *et al*, 2004b). Moreover, deletion of *SPO13* allows sister chromatid segregation upon anaphase onset in *mam1Δ* mutants, which is normally prevented due to protection of cohesin (Katis *et al*, 2004b). It is currently unclear whether

Spo13 regulates cohesin protection through the cohesin protector Sgo1. Initial studies suggested that Sgo1 localisation to centromeres is unaffected in *spo13Δ* cells (Lee *et al*, 2004) but it was later suggested that levels and maintenance of Sgo1 on centromeres are reduced in the absence of Spo13 (Kiburz *et al*, 2005).

Apart from errors in mono-orientation and cohesin protection, *spo13Δ* cells also display abnormalities in meiotic progression. *spo13Δ* cells only undergo a single meiotic division (Klapholz & Esposito, 1980a). This is characterised by a failure to re-accumulate Pds1 after its destruction in meiosis I (Katis *et al*, 2004b). However, the failure to undergo two chromosome segregation events can be partially overcome by deletion of the spindle checkpoint component *MAD2* (Shonn *et al*, 2000) or the APC/C activator *AMA1* (Katis *et al*, 2004b). Furthermore, *spo13Δ* single and *spo13Δ spo11Δ* double mutants are delayed in metaphase I progression (Shonn *et al*, 2002; Katis *et al*, 2004b), which may be a consequence of the loss of mono-orientation. Lastly, *spo13Δ* cells fail to arrest at metaphase I in cells depleted for the APC/C activator Cdc20 (Katis *et al*, 2004b). This has led to the suggestion that the APC/C might be hyperactive in *spo13Δ* mutants. However, there is currently no evidence to suggest how Spo13 affects APC/C activity and whether APC/C hyperactivity in *spo13Δ* cells is responsible for the failure to undergo a second meiotic division.

Spo13 does not have any obvious homologs in other organisms. However, there are proteins which show striking similarities to Spo13 and are likely to be functional homologs. In fission yeast, a protein called Moa1 was found to be required for mono-orientation (Yokobayashi & Watanabe, 2005). Moa1 localises to the central core region and this localisation depends on the kinetochore protein Cnp3 (CENP-C in humans) (Yokobayashi & Watanabe, 2005). Cnp3 point mutations that abolish Moa1 interaction show similar phenotypes to *moa1Δ* cells, indicating that Moa1 recruitment to kinetochores is essential for mono-orientation (Tanaka *et al*, 2009). Moa1 also interacts with Rec8 and is thought to be required for sister chromatid cohesion maintenance in the central core of the centromere (Yokobayashi & Watanabe, 2005; Kagami *et al*, 2011). Similarly to Spo13, Moa1 also interacts with polo kinase (Plo1 in fission yeast) (Kim *et al*, 2014). In the absence of Moa1, or in mutants that abolish this interaction, Plo1 does not localise to centromeres (Kim *et al*, 2014). Interestingly, depletion of Plo1 specifically at centromeres results in

defective mono-orientation, arguing that Plo1 recruitment to centromeres may be the core function of Moa1 (Kim *et al*, 2014).

Recent work has identified a mouse protein called MEIKIN which is thought to be analogous to Spo13 and Moa1 (Kim *et al*, 2014). Mice deficient in MEIKIN show defects in cohesin protection, which was attributed to decreased centromeric SGO2 (the meiotic cohesin protector in mice), and mono-orientation (Kim *et al*, 2014). Like its budding and fission yeast counterparts, MEIKIN is an interactor of the polo-like kinase PLK1, which itself is required for mono-orientation and cohesin protection (Kim *et al*, 2014). Together, these findings indicate that recruitment of polo kinases to centromeres may be a conserved property of meiotic cells, which is required for mono-orientation and, likely, cohesin protection.

1.13. Anaphase I and meiosis I-II transition

In contrast to mitotic exit, the transition from meiosis I to meiosis II poses the problem that CDK activity needs to be downregulated in order for anaphase I to occur and spindles to be disassembled; on the other hand, however, cells need to prevent the re-licensing of DNA replication origins which occurs in the context of low CDK activity.

Similarly to mitosis, exit from meiosis I in budding yeast is driven by Cdc14 phosphatase. Interestingly, however, only the FEAR network becomes activated at the meiosis I-meiosis II transition whereas MEN is inactive at this stage (Buonomo *et al*, 2003; Marston *et al*, 2003; Kamieniecki *et al*, 2005; Attner & Amon, 2012). In the absence of Cdc14 activity, cells undergo a single division, which may be either reductional or equational (Buonomo *et al*, 2003; Marston *et al*, 2003). Cdc14 is thought to aid SPB re-duplication between meiosis I and meiosis II (Connor & Marston, unpublished). In mitosis, Cdc14 reverses Cdk1-dependent phosphorylations on the SPB half-bridge component Sfi1 and thereby sets up SPBs for duplication (Elserafy *et al*, 2014). Recent evidence from our lab shows that this function is conserved in meiosis (Connor & Marston, unpublished), suggesting that Cdc14 is required to set up the meiosis II spindle.

Another mechanism to restrict Cdc14 activity between meiotic divisions may be by preventing substrate dephosphorylation. In meiosis, many CDK targets are instead phosphorylated by the meiosis-specific Cdk1-like kinase Ime2 (Holt *et al*, 2007). However, whereas Cdc14 is known to reverse phosphorylations laid down by cyclin-CDK, targets of Ime2 are immune to Cdc14 activity (Holt *et al*, 2007). Furthermore, Ime2 was shown to be capable of preventing nuclear import of the Mcm2-7 complex, which is required for replication initiation (Holt *et al*, 2007). Therefore, correct dosing of Cdc14 activity is a crucial mechanism to ensure proper transition from meiosis I to meiosis II.

In many organisms, restriction of APC/C activity is also required for the transition from meiosis I to meiosis II. In budding yeast, the activity of the meiosis specific APC/C activator Ama1 is restricted largely to prophase and exit from meiosis through the activity of the inhibitor Mnd2 (Oelschlaegel *et al*, 2005). Complete inhibition of Cdc28/Cdk1 in metaphase I-arrested cells promotes Pds1 degradation in the presence of Ama1 (Oelschlaegel *et al*, 2005). This indicates that careful balancing of CDK activity between meiosis I and meiosis II is required to keep the APC/C^{Ama1} in check and prevent untimely degradation of proteins required for meiosis II. In fission yeast, the APC/C inhibitor Mes1 prevents APC/C^{Slp1} (analogous to APC/C^{Cdc20}) from degrading the cyclin Cdc13, which is thought to be required to initiate meiosis II (Izawa *et al*, 2005). In *Xenopus*, CDKs are partially destroyed upon anaphase onset but low CDK activity is required to prevent entry into S phase after the first meiotic division (Iwabuchi *et al*, 2000). An APC/C inhibitor called Erp1 expressed towards the end of meiosis I is thought to prevent full CDK degradation and thereby allow progression into meiosis II (Ohe *et al*, 2007). In mice, the protein Emi2 operates very similarly to Erp1. Knockdown of Emi2 prevents assembly of the metaphase II spindle and this correlates with the permanent degradation of cyclin B1 (Madgwick *et al*, 2006). Expression of a non-degradable form of cyclin B, however, rescues the Emi2 knockdown phenotype and restores meiosis II spindles (Madgwick *et al*, 2006). Therefore, development of meiosis-specific APC/C inhibition is a conserved mechanism to prevent full cyclin degradation between meiotic divisions and ensure that DNA is not erroneously duplicated after cells exit meiosis I.

1.14. Cohesin deprotection in meiosis II

One key feature of meiosis II is that centromeric cohesin protection, which was in place during meiosis I, needs to be relieved in order to allow for sister chromatids to be segregated to opposite poles. However, the mechanisms for this remain largely elusive. Initial evidence from mouse oocytes has indicated that during meiosis II, SGO2 relocalises from the inner centromere towards kinetochores whereas Rec8 remains at the inner kinetochore (Lee *et al*, 2008). Therefore, tension exerted by microtubules pulling on kinetochores may cause SGO2 relocalisation and cohesin deprotection. A similar relocalisation of SGO1 in mitosis causes cohesin deprotection in metaphase after centromeric cohesin was protected from WAPL-dependent removal in prophase (Liu *et al*, 2013b; 2013a). Later studies, however, suggested that instead of sister chromatid tension, an inhibitor of PP2A, called I2PP2A, localises to centromeres of mouse oocytes specifically in meiosis II (Chambon *et al*, 2013). This is thought to cause cohesin phosphorylation and allow cleavage in meiosis II. How these processes are regulated, however, is currently unknown.

1.15. Aims of this study

As outlined previously, an understanding of the meiotic cell division processes is critical to understanding the causes of infertility, miscarriages, the maternal age effect and disorders such as Down's syndrome. One key aspect of the meiotic divisions is the stepwise removal of cohesin from chromosomes. Although we currently have a rough understanding of the key players involved in cohesin protection, much of the regulatory networks governing this process remain to be elucidated.

My first key aim is to understand the role of sister chromatid tension in cohesin deprotection. While previous research in mammalian cells has indicated that shugoshin localisation is regulated by sister chromatid tension, we do not know whether these mechanisms are conserved in budding yeast. Studies of Sgo1

regulation in mitosis have shown that even in budding yeast Sgo1 is depleted from chromosomes in response to tension (Nerusheva *et al*, 2014). Herein, I will test the effects of sister chromatid tension upon cohesin protection in meiosis I, which may allow us to extrapolate our findings to suggest a model for cohesin deprotection in meiosis II.

Secondly, I aim to understand the effect that the meiosis-specific protein Spo13 has on cohesin protection. Although Spo13 is known to be required for sister chromatid cohesion in meiosis, current evidence for how it functions mechanistically are scarce and, in parts, contradictory. Therefore, a thorough investigation of how Spo13 affects cohesin protection is required. In this study, I will provide evidence of the various ways in which Spo13 impacts cohesin and its protector Sgo1.

CHAPTER 2: COHESIN PROTECTION IN MEIOSIS I REQUIRES SISTER KINETOCHORE MONO-ORIENTATION

2.1. Introduction

One of the key adaptations of the meiotic chromosome segregation machinery is that cohesin, the protein complex that holds sister chromatids together, needs to be cleaved in two distinct steps. This allows the resolution of chiasmata on chromosome arms in meiosis I while maintaining cohesion in the pericentromere to ensure faithful segregation of sister chromatids in meiosis II. The stepwise cleavage of cohesin implies that the dynamics of the cohesin protector Sgo1-PP2A need to be differentially regulated throughout meiosis to allow cohesin protection in meiosis I and cohesin deprotection in meiosis II. The mechanisms of cohesin deprotection in *S. cerevisiae* are currently still elusive. Some clues, however, have been identified from studies on other model organisms. Immunofluorescence of mitotic chromosomes in HeLa cells showed that when sister chromatids come under tension, both Sgo1 and Sgo2 relocalise from cohesin onto kinetochores (Lee *et al*, 2008) and this allows deprotection of mitotic cohesin. In prophase, human Sgo1 is phosphorylated by CDK at T346 (Liu *et al*, 2013b) to allow its binding to cohesin (Liu *et al*, 2013a; 2013b). Upon tension establishment, Sgo1 gets dephosphorylated and relocalises to phosphorylated H2A binding sites near kinetochores (Liu *et al*, 2013a; 2013b). Similarly, a tension-dependent relocalisation of Sgo2 has been observed at metaphase II in mouse spermatocytes (Gómez *et al*, 2007). Later analysis of PP2A localisation in mouse oocytes, however, showed that PP2A co-localises with Rec8 until metaphase II (Chambon *et al*, 2013), implying that Sgo2 relocalisation is irrelevant for cohesin protection. Instead, an inhibitor of PP2A – I2PP2A – co-localises with PP2A specifically in meiosis II and its knockdown prevents sister chromatid segregation (Chambon *et al*, 2013). This suggests that, at least in mouse oocytes, cohesin deprotection depends on the inactivation of PP2A rather than Sgo1. In *Drosophila*, the Sgo1-homolog MEI-S332 is removed from centromeres when cells enter anaphase II in a manner that depends on POLO kinase (Clarke *et al*, 2005). However, even when Sgo1 dissociation is prevented, cells still successfully

segregate sister chromatids in meiosis II (Clarke *et al*, 2005), indicating that Sgo1 removal from chromosomes is not required for deprotection in meiosis II.

In mitotic budding yeast cells, Sgo1 localisation is also sensitive to sister kinetochore tension. When cells are arrested in metaphase with sister kinetochores under tension, Sgo1 is absent from chromosomes (Nerusheva *et al*, 2014). Addition of the microtubule-depolymerising drug nocodazole, however, restores Sgo1 localisation to centromeres (Nerusheva *et al*, 2014). The tension-dependent removal of Sgo1 from chromosomes in mitosis is key to the release of other proteins that promote bi-orientation at unattached kinetochores from the pericentromere, like Ipl1 (Aurora B) and condensin (Nerusheva *et al*, 2014).

In light of the mitotic regulation of Sgo1 localisation in *S. cerevisiae*, I wanted to determine whether sister kinetochore tension is an important factor in regulating Sgo1 in meiosis. One of the key differences between meiosis I and meiosis II cells is that in the first meiotic division sister kinetochores are mono-oriented so that homologues segregate to opposite poles. This means that in meiosis I sister kinetochores do not come under tension which, I hypothesised, should prevent Sgo1 removal from chromosomes when it is required for protecting cohesin, if tension is important. In meiosis II, however, when cohesin is deprotected, sister kinetochores bi-orient and the resultant tension may allow the cleavage of pericentromeric cohesin upon onset of anaphase II. The aim of this chapter is, therefore, to find out whether Sgo1 localisation to chromosomes is regulated by sister chromatid tension in meiosis and whether this is important for the protection of centromeric cohesion.

2.2. Results

2.2.1. Chiasmata inhibit proper sister-kinetochore bi-orientation in monopolin mutants

One of the limitations of studying meiosis in budding yeast is that there are currently no experimental manipulations that allow cells to be arrested in metaphase II, which would be the ideal system to study the effects of sister kinetochore tension on Sgo1 in meiosis. Therefore, I had to develop a system in which sister kinetochores bi-orient in meiosis I. Mutations that abolish mono-orientation, like deletion of the monopolin subunit, *MAM1*, cause bi-orientation in meiosis I. However, previous studies have detected biorientation in only approximately 25-30% of monopolin mutant cells (Katis *et al*, 2004b). I reasoned that this might be due to the presence of chiasmata in mono-orientation mutants, which allow for tension to be established across homologues, rather than sister chromatids. This would permit sister kinetochores to orient towards the same pole despite the lack of sister kinetochore fusion (Fig. 2.1). To test whether chiasmata limit successful bi-orientation in monopolin mutants, I deleted *SPO11*, the endonuclease required for initiation of meiotic recombination (Keeney *et al*, 1997), in *mam1Δ* mutants. Deletion of *SPO11* causes cells to undergo meiosis without creating linkages between homologs (Klapholz *et al*, 1985). Due to the lack of chiasmata, *spo11Δ mam1Δ* mutants should be more efficient at bi-orienting sister chromatids. To test this hypothesis, I used strains which have an array of bacterial Tet operators (*tetO*) integrated close to the centromere of one copy of chromosome V. When GFP fused to Tet repressor (TetR) is expressed in these cells, a single GFP focus can be detected using fluorescence microscopy. In cells with bi-oriented sister chromatids, the GFP signal will resolve into two foci since the *tetO* arrays are pulled away from each other (Fig. 2.2A). Additionally, I have arrested cells in metaphase I by putting the APC/C activator *CDC20* under control of the *CLB2* promoter, which is inactive in meiosis and thereby causes depletion of Cdc20.

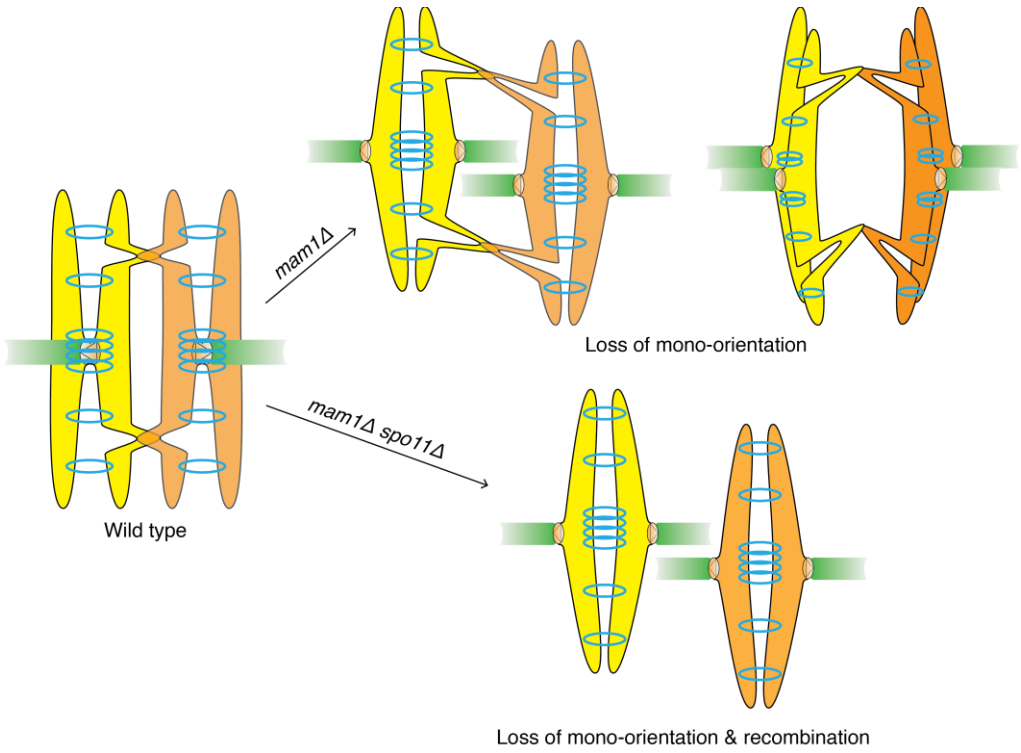

Figure 2.1: Constructing a strain with bi-oriented sisters in meiosis I. Deletion of the mono-orientation factor *MAM1* prevents sister kinetochore fusion in meiosis I and sister chromatids should bi-orient. However, due to the presence of chiasmata, other arrangements within the bivalent may allow tension to be generated across homologs so that sister chromatids face towards the same pole although their kinetochores are not fused. Additional deletion of *SPO11* prevents formation of chiasmata and, hence, *spo11Δ mam1Δ* double mutants can only bi-orient in meiosis I.

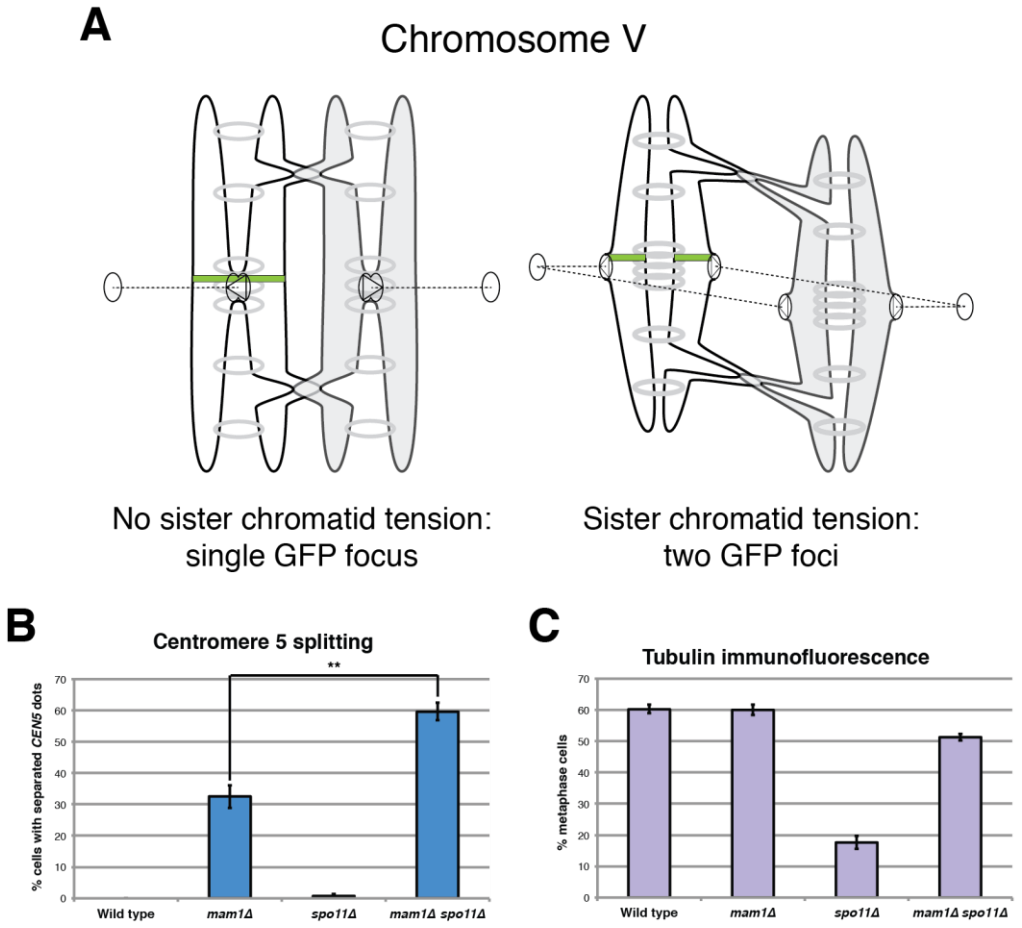

Figure 2.2: Bi-orientation is enhanced by abolishing chiasmata in mono-orientation mutants. (A) Schematic representation of the assay carried out in B. If sister chromatids are not under tension, GFP bound in the vicinity of the centromere on one copy of chromosome V will resolve into a single focus. Upon bi-orientation, this focus will split into two distinct foci. (B and C) Deletion of *SPO11* significantly increases bi-orientation in *mam1Δ* mutants. (B) Wild type (AMy5310), *mam1Δ* (AMy5892), *spo11Δ* (AMy13362) and *mam1Δ spo11Δ* (AMy13363) cells were arrested in metaphase I for 6hrs in SPO media by depletion of Cdc20. The separation of Tet operators integrated near the centromere of one homolog of chromosome V as visualised through expression of TetR-GFP was scored in 200 cells. Error bars represent standard error of the mean for 3 independent experiments (**p < 0.01). (C) Metaphase spindle staining was scored for strains described in B (n = 200). Error bars represent standard error for 3 independent experiments.

As expected, metaphase I-arrested wild type and *spo11Δ* do not split *CEN5*-GFP foci (Fig. 2.2B). In contrast, *mam1Δ* cells bi-orient in 33% of cases (Fig. 2.2B). Strikingly, the number of cells that successfully bi-orient is increased to 60% in *spo11Δ mam1Δ* mutants. To confirm that the observed differences are not due to a failure of *mam1Δ* cells to enter meiosis or arrest in metaphase I, I performed tubulin immunofluorescence. Given that both *mam1Δ* and *mam1Δ spo11Δ* cells arrested with similar numbers of metaphase I spindles, I can conclude that more efficient bi-orientation in *mam1Δ spo11Δ* is not due to differences in their efficiency to arrest in metaphase I. It should be noted that the low number of metaphase I cells in *spo11Δ* single mutants is due to the fact that homologs are not linked and can therefore separate prematurely, giving rise to spindle morphologies different from metaphase I arrested cells. This is caused by the lack of linkages between homologs in *spo11Δ* mutants, which allows homolog segregation and spindle elongation in the absence of APC/C activity (Shonn *et al*, 2000). Taken together, these findings suggest that *mam1Δ spo11Δ* cells provide a better system to study Sgo1 dynamics in meiosis when sister chromatids are under tension than *mam1Δ* mutants alone do.

2.2.2. Sister kinetochore bi-orientation in meiosis I leads to loss of Sgo1 from kinetochores

Having established a system in which sister chromatids largely bi-orient in meiosis I, I next wanted to test whether meiotic bi-orientation of sister kinetochores affects Sgo1 localisation to chromosomes. To this end, I performed chromatin immunoprecipitation followed by qPCR (ChIP-qPCR) of a 9Myc-tagged allele of Sgo1 in metaphase I-arrested cells. Analysis of Sgo1-9Myc localisation to centromere 4 shows that Sgo1 recruitment to this centromere in *mam1Δ* is very similar to that of wild type cells (Fig. 2.3A). Interestingly, however, Sgo1 enrichment at *CEN4* is significantly reduced in *mam1Δ spo11Δ* double mutants to levels similar to those observed in an untagged strain (Fig. 2.3A). This observation is replicated at a pericentromeric site on chromosome IV, whereas Sgo1 levels on chromosome arms are unaffected (Fig. 2.3A). To ensure that the differences observed at chromosome IV are not the result of a decline in cellular Sgo1 levels, I

performed western blot analysis of the samples analysed by ChIP. This clearly shows that Sgo1 levels are unaltered in any of the mutants analysed (Fig. 2.3B). Taken together, these findings suggest that Sgo1 localisation to centromeres may be regulated by sister chromatid tension, as was previously observed in mitotic cells (Nerusheva *et al*, 2014).

To determine whether the observations on chromosome IV hold true for other chromosomes, I decided to image GFP-tagged Sgo1 in metaphase I-arrested cells. Whereas wild type and *spo11Δ* cells display clear foci of Sgo1-GFP, which localise in the vicinity of kinetochores, both *mam1Δ* and *mam1Δ spo11Δ* mutants show a dispersed nuclear signal of Sgo1 and lack distinct foci (Fig. 2.4). The extent to which this is observed is larger in *mam1Δ spo11Δ* double mutants (88% of cells) than in *mam1Δ* single mutants (42% of cells), presumably due to more efficient bi-orientation in *mam1Δ spo11Δ* double mutants (Fig. 2.2B). Taken together, these results suggest that, upon sister chromatid bi-orientation in meiosis, Sgo1 detaches from chromosomes and relocalises to the nucleoplasm.

2.2.3. Spindle tension reduces the levels of Sgo1 at centromeres in meiosis I

One interesting observation from my ChIP experiments was that the average enrichment of Sgo1 on centromere 4 is increased in *spo11Δ* mutants (Fig. 2.3A). Although the enrichment is not statistically significant, it led me to hypothesise that tension across homologs may also, in part, be able to remove Sgo1 from centromeres. In *spo11Δ* mutants, due to the lack of chiasmata, homologs will be pulled towards one of the cell's poles as soon as they become stably attached by microtubules. This means that no tension will be exerted across the bivalent, as would be the case for wild type cells, and this may be the reason for the increased enrichment of Sgo1 at centromere 4.

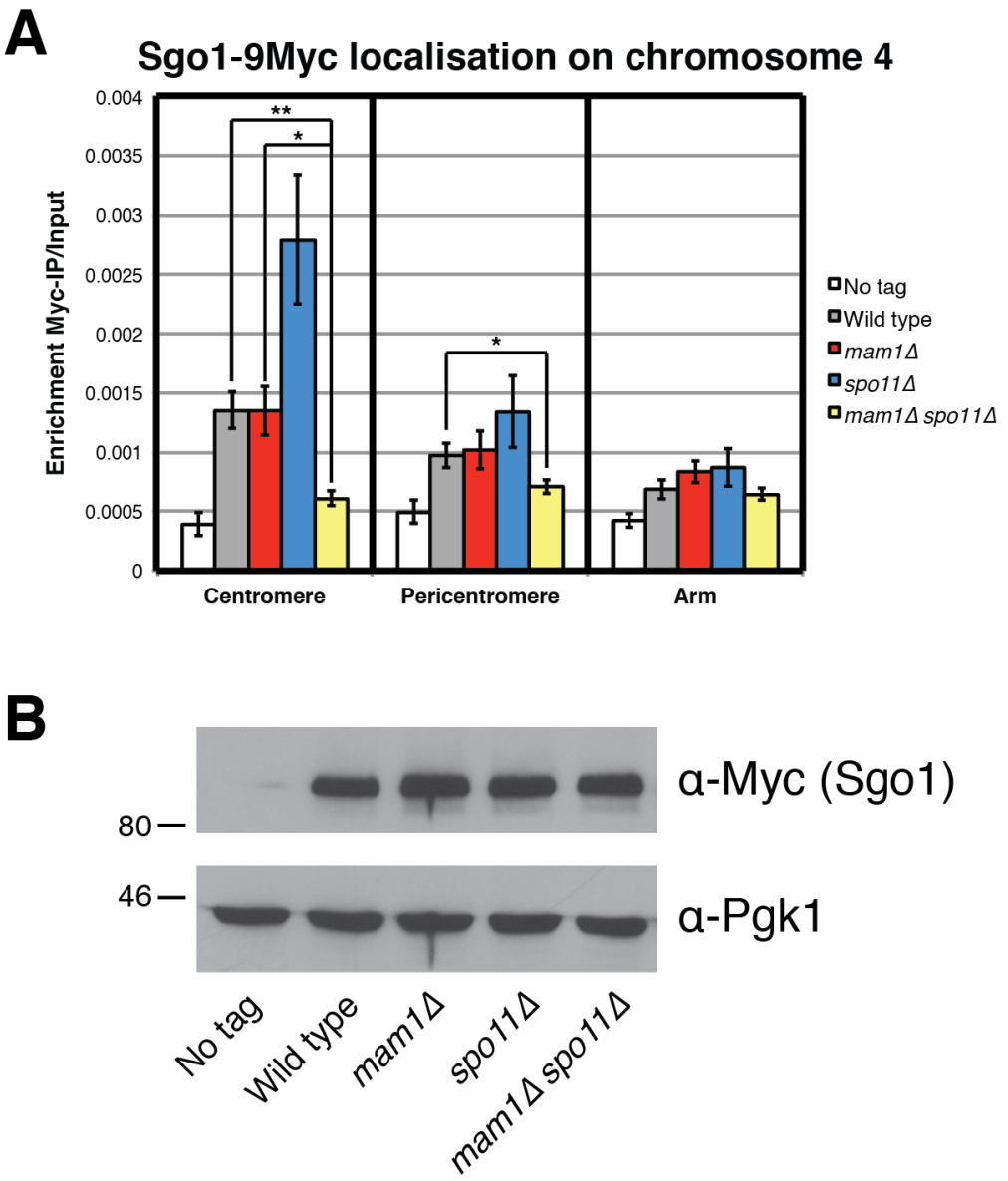

Figure 2.3: Sgo1 localisation to centromere 4 is lost when sister chromatids are under tension. (A) ChIP-qPCR of Sgo1-9Myc at different locations on chromosome IV. No tag (AMy10617), wild type (AMy9102), *mam1Δ* (AMy9210), *spo11Δ* (AMy10618) and *mam1Δ spo11Δ* (AMy11226) cells were arrested in SPO media for 6 hours before fixing cells for α-Myc ChIP-qPCR. Error bars represent standard error of the mean for 6 independent experiments (*p < 0.05, **p < 0.01). (B) Cellular levels of Sgo1 remain unaffected when sister chromatids bi-orient. TCA fixed samples were collected for western blot analysis just prior to fixing cells for ChIP. A representative blot is shown.

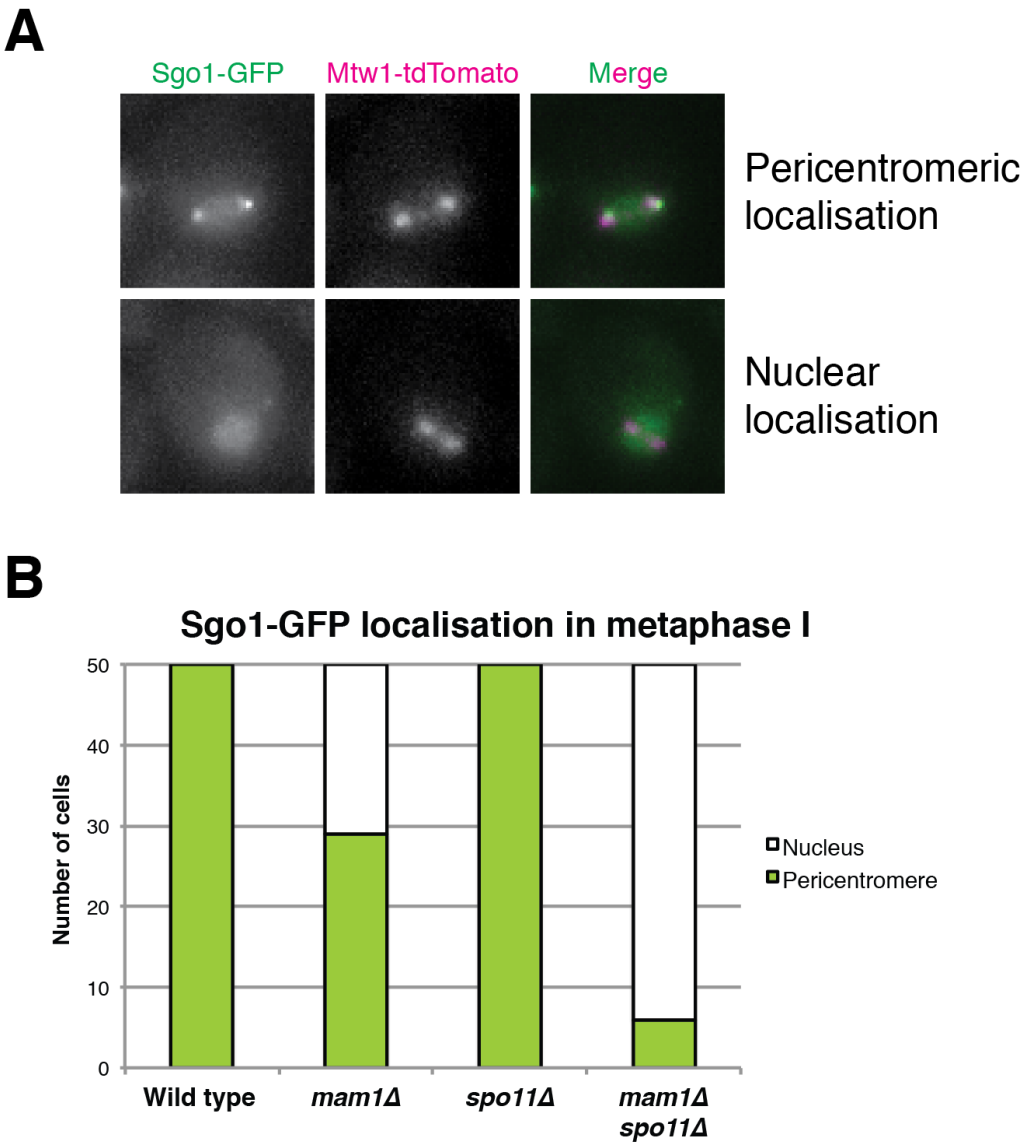

Figure 2.4: Sgo1 relocates from the pericentromere to the nucleus upon bi-orientation in meiosis. (A and B) Live cell imaging of Sgo1-GFP tagged strains in metaphase I arrested cells. Wild type (AMy15137), *mam1Δ* (AMy15138), *spo11Δ* (AMy15139) and *mam1Δ spo11Δ* (AMy15140) cells were arrested in SPO media for 4 hours and transferred onto a microfluidics plate for imaging at 15 min intervals. (A) Representative images of different Sgo1 localisations with separated kinetochores (visualised through tdTomato-tagged Mtw1) are shown. (B) Sgo1 localisation was scored at the first observed splitting of kinetochores in all mutants and categorised as either pericentromeric (focus area < 2μm^2) or nuclear (absence of distinct foci with an area > 2μm^2 and signal intensity larger than three times the background signal).

To further test the hypothesis that homolog tension leads to partial depletion of Sgo1 from chromosomes, I sought to abolish tension by treating meiotic cells with the microtubule depolymerising drug benomyl. In order to prevent a premature arrest of cells before entering meiotic divisions (Hochwagen *et al*, 2005), I first arrested cells in metaphase I by depletion of the APC/C activator Cdc20 and subsequently depolymerised microtubules in arrested cells by pulse-treating them with benomyl for 30 mins. I then performed ChIP-qPCR analysis of Sgo1-9Myc to determine its association with centromere 4. Interestingly, benomyl-treated wild-type cells have significantly higher enrichment of Sgo1 at *CEN4* and levels are comparable to those seen in *spo11Δ* cells (Fig. 2.5A). Additionally, I used western blotting of whole cell meiotic extracts to confirm that the observed increase on centromeres is not due to an increase in overall Sgo1 levels (Fig. 2.5B). In fact, cellular Sgo1-9Myc is decreased in benomyl-treated cells, an effect which may be attributed to a decline in transcription, which has previously been observed in meiotic cells subjected to high concentrations of benomyl (Hochwagen *et al*, 2005). In summary, these results suggest that tension across homologs may lead to a partial loss of Sgo1 from centromeres.

2.2.4. Sister kinetochore bi-orientation in meiosis I causes a premature reduction in pericentromeric cohesin

The finding that Sgo1 is removed from chromosomes when sister chromatids are under tension suggests that cohesin may no longer be protected if sister kinetochore bi-orientation occurs prematurely. In order to address this question, I imaged a GFP-tagged allele of the meiotic kleisin Rec8 in live meiotic cells. I further utilised a kinetochore marker, Mtw1-tdTomato, as a reference point because protected cohesin should persist until meiosis II in an area around kinetochores. Furthermore, I used Pds1-tdTomato as a marker for anaphase I onset since Pds1 gets degraded at the end of metaphase I.

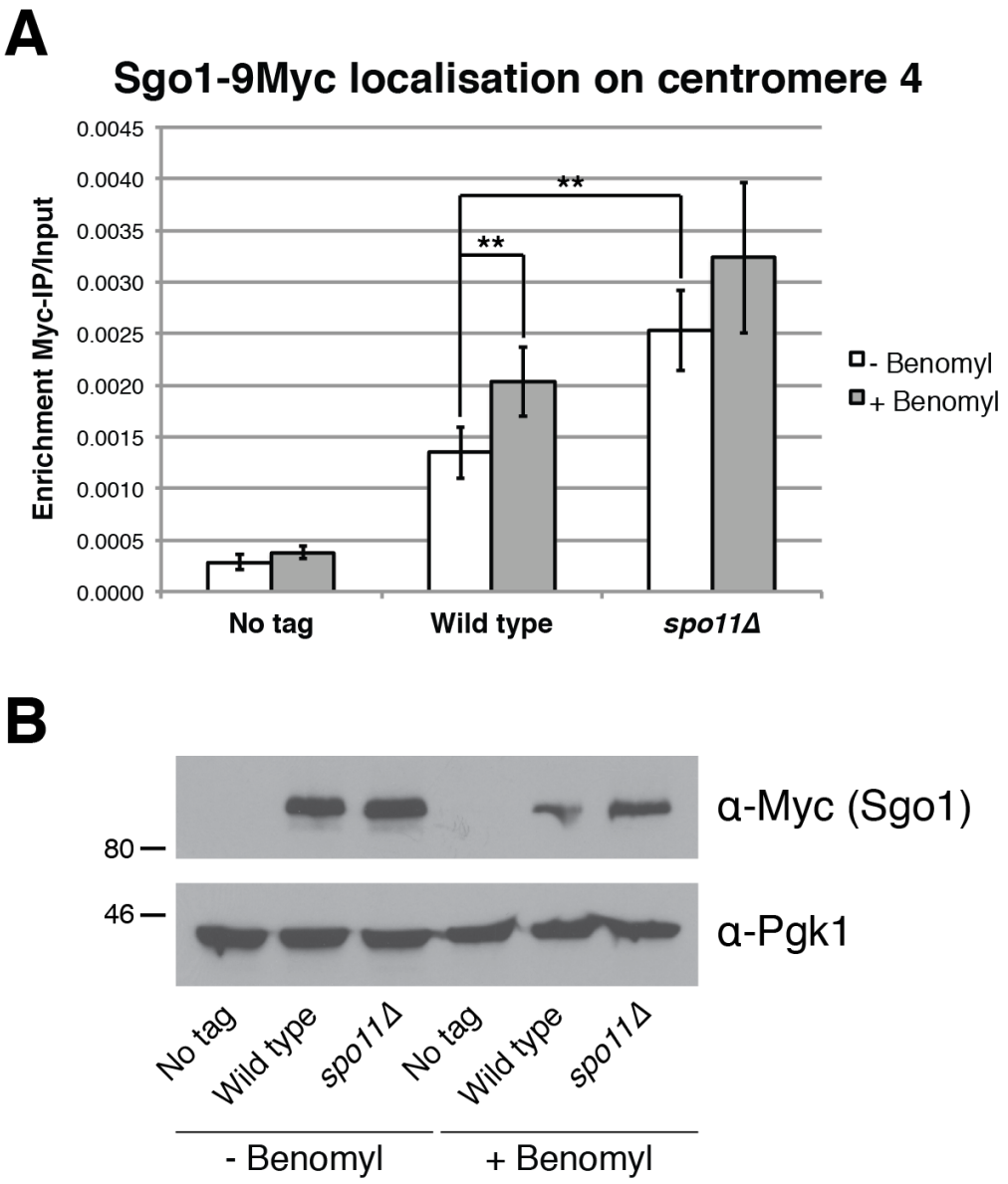

Figure 2.5: Sgo1 responds to tension across homologous chromosomes. (A) ChIP-qPCR of Sgo1-9Myc at centromere 4. No tag (AMy10617), wild type (AMy9102) and *spo11Δ* (AMy10618) cells were arrested in SPO media for 6 hours before fixing cells for α-Myc ChIP-qPCR. Benomyl-treated cells were sporulated for 5.5 hours, pelleted, resuspended in SPO containing 90μg/ml benomyl and sporulated for a further 30 minutes. Error bars represent standard error of the mean for 6 independent experiments (*$p < 0.05$, **$p < 0.01$). (B) Cellular levels of Sgo1 are decreased in benomyl-treated cells. TCA fixed samples were collected for western blot analysis just prior to fixing cells for ChIP. A representative blot is shown.

As expected, when wild type cells enter anaphase, the bulk of Rec8 is cleaved (Fig. 2.6). However, Rec8-GFP foci remain in the area occupied by kinetochores until meiosis II (Fig. 2.6). *mam1Δ* cells behave in a similar manner. However, after kinetochores stretch at anaphase onset, they often snap back together with cohesin found in the area between kinetochores (Fig. 2.6). This behaviour is most likely due to sister kinetochores bi-orienting but being prevented from separation because cohesin in the pericentromere is protected and holding sister chromatids together. *spo11Δ* mutants differ from other strains in that they segregate chromosomes before proceeding into anaphase I (Fig. 2.6). Due to the lack of chiasmata, homologs are pulled to the cell's poles as soon as they become attached by microtubules. Pds1 degradation and cleavage of arm cohesin only occur later. However, Rec8-GFP is still cleaved in two steps and is retained in an area around kinetochores after anaphase I until meiosis II (Fig. 2.6). Lastly, in *mam1Δ spo11Δ* cells, only a single round of cohesin cleavage can sometimes be detected, implying that these cells may have a cohesin protection defect (Fig. 2.6).

To gain a better understanding of this defect, I first subjectively scored whether cells retained Rec8-GFP after Pds1 degradation. Interestingly, 26% of *mam1Δ* cells appear to lose all cohesin in the first meiotic division (Fig. 2.7A), indicating that loss of mono-orientation impacts cohesin protection even in the presence of chiasmata. Deletion of *SPO11* in *mam1Δ* strains slightly increases the proportion of cells which lose centromeric cohesin after metaphase I to 34%. To better quantify this loss of cohesin, I measured the intensity of Rec8-GFP in anaphase I cells (as judged by the disappearance of Pds1-tdTomato signal). In accordance with the scoring data, *mam1Δ* and *mam1Δ spo11Δ* cells show a significant decrease of Rec8-GFP signal in anaphase I (Fig. 2.7B). Additionally, deletion of *SPO11* in the *mam1Δ* background aggravates the loss of cohesin observed in *mam1Δ* mutants significantly (Fig. 2.7B). Taken together, these results suggest that cohesin protection may be impaired when sister kinetochores bi-orient in meiosis I.

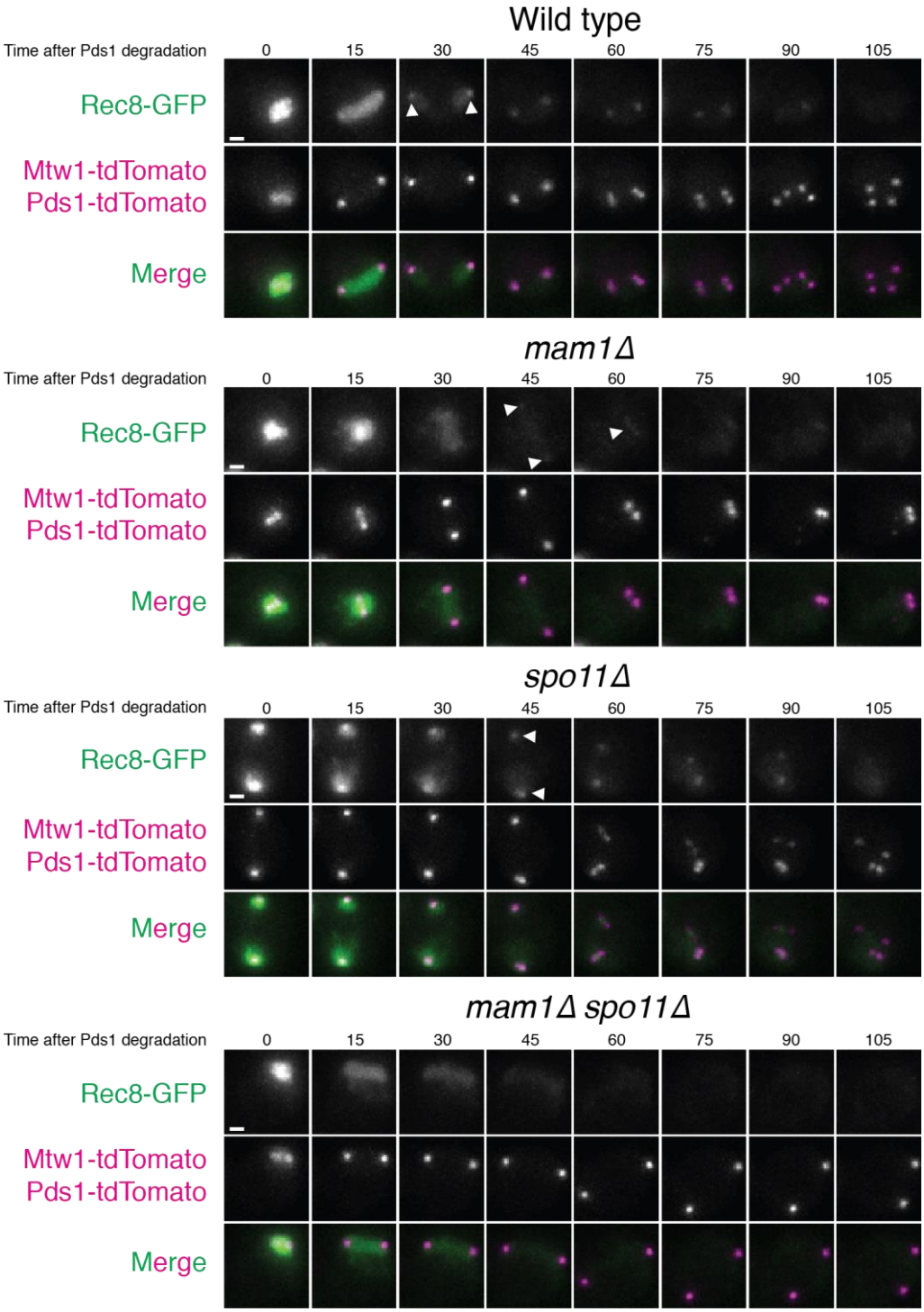

Figure 2.6: Comparison of Rec8-GFP cleavage in mono-oriented and bi-oriented cells. Whereas Rec8-GFP persists within the pericentromere in wild type and *spo11Δ* cells, it is detected only weakly or not at all in mutants where sister kinetochores bi-orient. Wild type (AMy13716), *mam1Δ* (AMy13717), *spo11Δ* (AMy13718) and *mam1Δ spo11Δ* (AMy13719) cells were induced to sporulate for 2 hours and transferred onto a microfluidics plate for imaging at 15 min intervals. Representative movies are shown. Scale bars represent 1μm. Arrows highlight pericentromeric cohesin retained after the first round of cohesin cleavage.

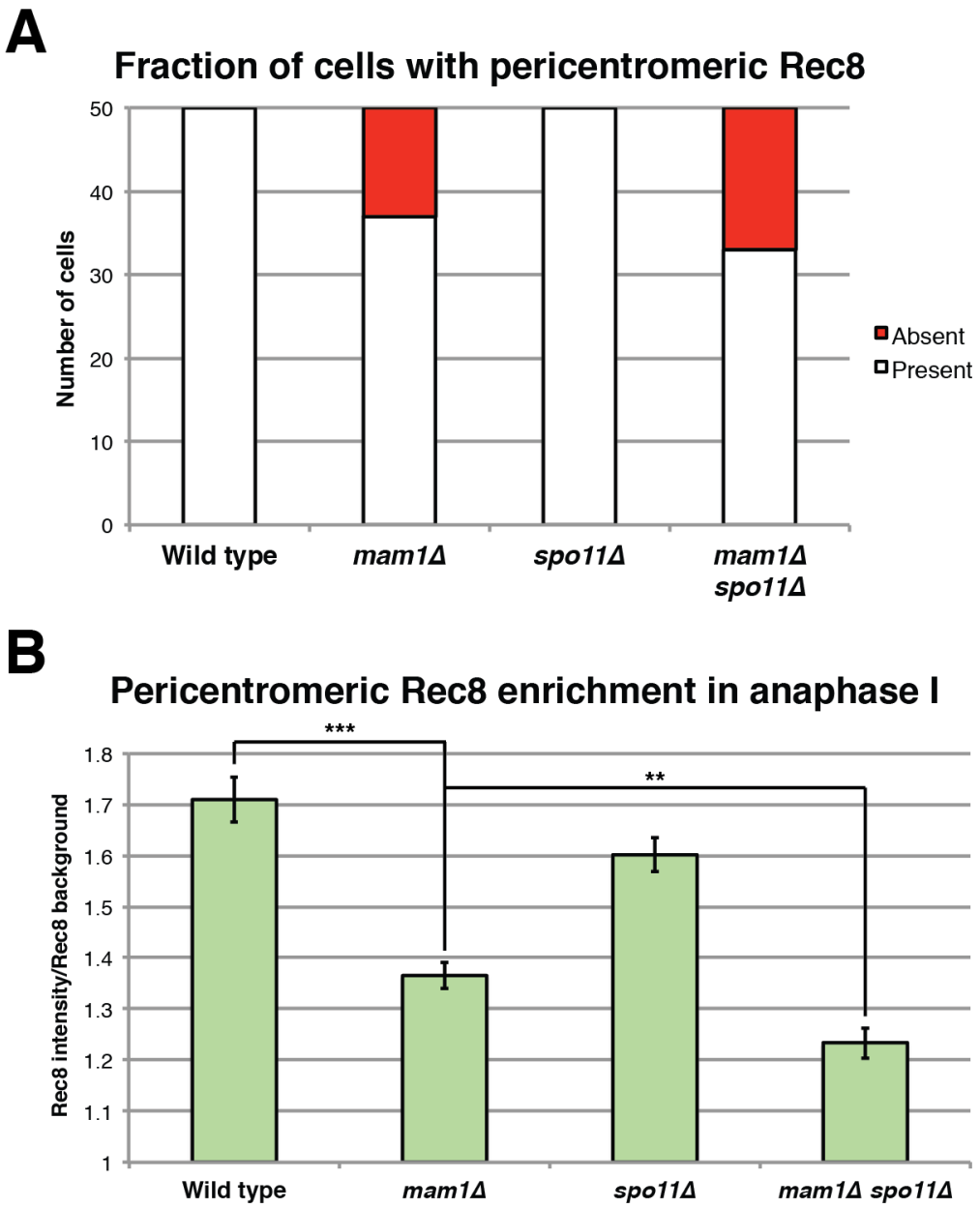

Figure 2.7: Cohesin is reduced when meiosis I cells lose mono-orientation. (A) Cells from movies shown in Fig. 2.6 were subjectively scored for the presence of pericentromeric cohesin after Pds1 degradation (n = 50). (B) The average intensity of Rec8 was measured in the area occupied by kinetochores in anaphase I (first or second time frame after Pds1 degradation). Alternatively, Rec8-GFP intensity was measured in the area in between kinetochores when Rec8-GFP was found to localise in this area (which may occur in mono-orientation mutants, as previously described (Matos *et al*, 2008)). The intensity values for 50 cells per strain were divided by an average background intensity, which was obtained by measuring fluorescence intensity in the green channel in the area occupied by kinetochores in anaphase II, when Rec8 should have been degraded. Error bars show standard error of the mean (**p < 0.01, ***p < 0.001).

2.2.5. Sister chromatid cohesion is impaired when sister kinetochores bi-orient in meiosis I

The fact that the amount of cohesin at pericentromeres is reduced in anaphase I when sister chromatids have bi-oriented in meiosis I suggests that the loss of Sgo1 observed previously may have led to an impairment of cohesin protection. To test this hypothesis, I sought to find out whether sister chromatid cohesion is lost in meiosis I when sister kinetochores have been under tension. To study this, I needed a system to test whether pericentromeric cohesion is lost in anaphase I (Fig. 2.8). I used strains carrying a *tetO* array close to *CEN5* on one copy of chromosome V and expressing TetR-GFP. When wild type cells go into anaphase I, only one GFP focus will be visible and will segregate to one of the cell poles (as judged by the spindle pole marker Cnm67-3mCherry). Only in meiosis II, when sister kinetochores bi-orient and cohesin gets cleaved in the pericentromere will the GFP focus split in two (Fig. 2.9A). In contrast, if sister kinetochores were to bi-orient in metaphase I already, then splitting of *CEN5* dots could be detected before anaphase I onset (as judged by degradation of Pds1-tdTomato). However, due to intact cohesin protection, *CEN5* dots could only split a certain distance as pericentromeric cohesion restricts how far they can be pulled apart (Fig. 2.9A). In contrast, a strain which had lost mono-orientation, but which is also defective for cohesin protection, should show segregation of *CEN5* dots a great distance because they are no longer held together by cohesin (Fig. 2.9A).

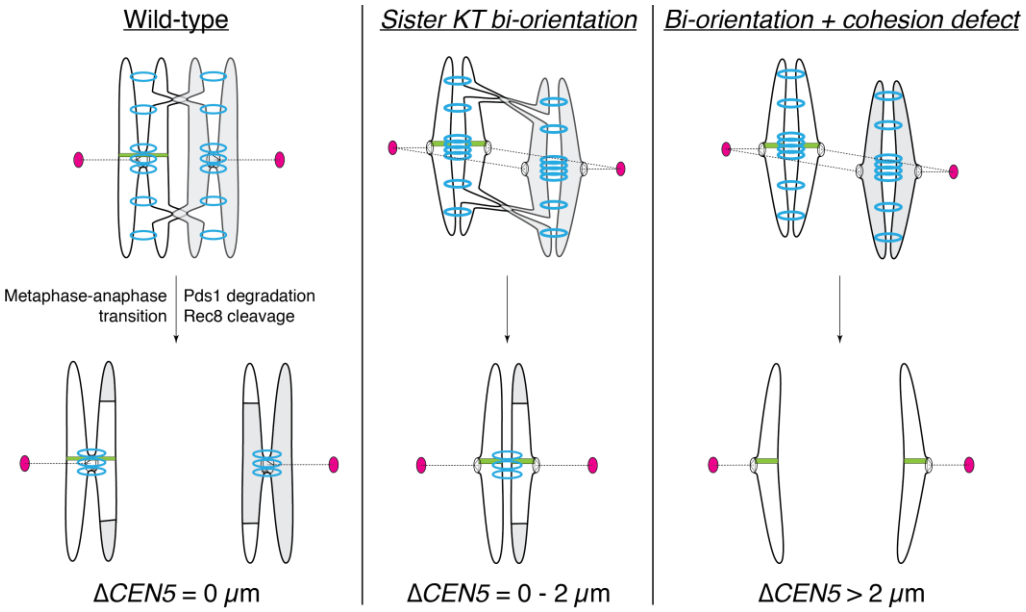

Figure 2.8: An assay to detect loss of pericentromeric cohesion. TetR-expressing cells have a *tetO* array integrated near the centromere of one copy of chromosome V. In wild type cells, only a single GFP focus will be visible near one of the spindle pole bodies (SPBs) in anaphase I (left panel). When sister kinetochores bi-orient in metaphase I, the *CEN5-GFP* signal can be detected as two foci which can only separate a certain distance (a cut-off of 2 µm was chosen) because cohesin holds sister centromere sequences close together. If a bi-orientation mutant also has a cohesin protection defect, however, then *CEN5-GFP* foci will be able to split a great distance (i.e. further than 2 µm) upon anaphase onset.

To assess the loss of cohesion in mono-orientation mutants, I imaged heterozygous *CEN5* foci in *mam1Δ* and *mam1Δ spo11Δ* mutants. As expected, the majority of *mam1Δ* cells will bi-orient sister chromatids but retain cohesion, leading to *CEN5* separation distances between 0 and 2 μm in 58% of cases (Fig. 2.9B). Interestingly, *CEN5* foci separate by more than 2 μm in 18% of cells even when chiasmata are still present. In *mam1Δ spo11Δ* strains, this number is increased to 52% (Fig. 2.9B), indicating that cohesin protection is defective in more than half of the cells. Taken together, these results support a model in which premature sister kinetochore bi-orientation leads to Sgo1 removal from chromosomes that subsequently results in the deprotection of cohesin in meiosis I. However, the fact that some cells still protect cohesin even when sister kinetochores bi-orient, suggests that other mechanisms are also important for efficient deprotection in meiosis II.

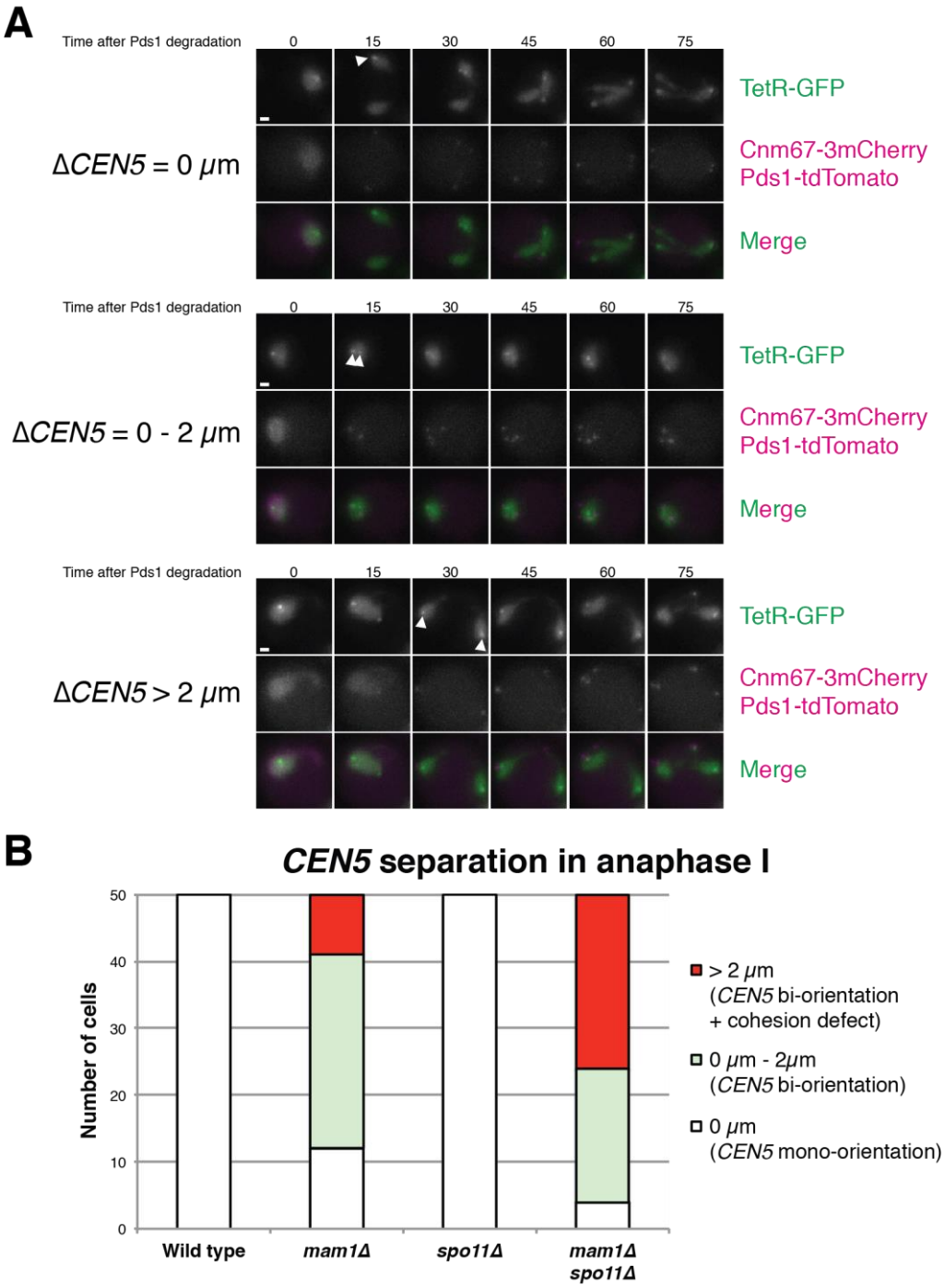

Figure 2.9: Pericentromeric cohesion is impaired when sister kinetochores bi-orient in meiosis I. (A and B) Live-cell imaging of mono-orientation mutants in meiosis. Wild type (AMy13431), *mam1Δ* (AMy13978), *spo11Δ* (AMy13979) and *mam1Δ spo11Δ* (AMy13980) were induced to sporulate and transferred to a microfluidics device after 2 hours in SPO media. Images were taken at 15 min intervals. (A) Example sequences of cells going through meiosis with the different phenotypes outlined in Fig. 2.8. Scale bars represent 1μm. Arrows highlight *CEN5*-GFP foci. (B) Sister chromatids segregate in anaphase I in a portion of mono-orientation mutants. The distance between *CEN5*-GFP foci was measured in 50 cells after Pds1 degradation but prior to SPB re-duplication for the mutants indicated.

2.3. Discussion

The data shown in this chapter support a model by which sister kinetochore tension, as it occurs when sister chromatids bi-orient, leads to the removal of Sgo1 from chromosomes. This subsequently causes a partial failure to protect cohesin and eventually leads to a premature loss of sister chromatid cohesion in anaphase I.

2.3.1. Studying the effects of bi-orientation in meiosis

The basis of these conclusions is the identification of a system where sister chromatids are more efficiently bi-oriented in meiosis I. The genetic modification of meiotic cells to achieve this was necessary because there are currently no methods to arrest cells at metaphase II. The first step was to delete the mono-orientation factor *MAM1*. This, however, leads to detection of biorientation in only ~30% of metaphase I-arrested cells (Fig. 2.2B), which is in line with previously published data (Katis *et al*, 2004b). Surprisingly, the number of bi-oriented cells is still well below what could theoretically be expected as the maximum amount of bi-oriented cells – in the presence of chiasmata, this should be 50%. However, when examining how heterozygous *CEN5* dots separate in anaphase I in *mam1Δ* mutants (Fig. 2.9), it becomes apparent that just under 80% of *mam1Δ* cells attempt to separate sister chromatids in anaphase I. This is unexpected because in theory, even when sister kinetochores are not fused, the presence of chiasmata linking homologs should allow for sister kinetochores to be oriented towards the same pole as tension is created across homologous chromosomes. Therefore, it is tempting to speculate that tension across sister chromatids is favourable over homolog tension. One likely reason for the small amount of bi-oriented sister chromatids in metaphase I arrested *mam1Δ* cells is that only about 60% of cells have efficiently arrested (Fig. 2.2C). This, however, does not fully explain the low amount of bi-oriented cells. One further clue comes from studies measuring the binding efficiency of purified meiotic kinetochores to microtubules on a laser trap (Sarangapani *et al*, 2014). This investigation showed that meiosis I kinetochores devoid of Mam1 are actually much less efficient at binding microtubules (Sarangapani *et al*, 2014). If kinetochores

lacking monopolin are actually worse at achieving proper kinetochore-microtubule attachment, then this might explain the low efficiency of bi-oriented kinetochores in metaphase I arrested *mam1Δ* cells because cells may simply spend a longer amount of time to form stable kinetochore-microtubule attachments. In an attempt to at least partially circumvent these problems, I deleted *SPO11* in *mam1Δ* cells because in the absence of chiasmata, sister kinetochore bi-orientation is the only way for cells to establish tension. This increases the fraction of cells that efficiently bi-orient in a metaphase I arrest to 60%. Therefore, this strain was significantly more promising to study Sgo1 dynamics upon bi-orientation in meiosis. Ultimately, however, it will be necessary to identify a way to efficiently arrest cells in metaphase II, as this is the only stage of meiosis that sister chromatids would normally bi-orient. Since the biochemical state of meiosis II cells is likely to be very different from meiosis I cells, a metaphase II arrest will be a more representative system to study what happens to Sgo1 when sister chromatids bi-orient in meiosis II.

2.3.2. Sgo1 removal from chromosomes upon sister kinetochore bi-orientation in meiosis

After successfully establishing a system to study the dynamics of Sgo1 when sister chromatids come under tension, I first performed ChIP-qPCR to study what happens to Sgo1 at different locations along chromosome IV. The finding that Sgo1 is absent at *CEN4* when sister chromatids bi-orient mirrors previous observations in mitotic cells (Nerusheva *et al*, 2014). Interestingly, however, Sgo1 is not reduced at all in *mam1Δ* single mutants, although bi-orientation occurs in at least a third of cells. This may be explained by the fact that this ChIP assay looks at a population of cells, some of which are bi-oriented, but some of which may not be attached at all, in which case the lack of tension would cause an increase of Sgo1 levels (discussed below). Overall, Sgo1 levels in the population may simply average out at approximately wild type levels. In *mam1Δ spo11Δ* double mutants, on the other hand, the population of bi-oriented cells is likely to be large enough to allow detection of a decrease in Sgo1 levels at *CEN4*. To gain a better understanding of how Sgo1 association with centromeres may be affected on a more global level, I

performed live cell imaging of Sgo1-GFP in metaphase I-arrested cells. This very clearly showed that pericentromeric foci of Sgo1 are lost in a significant portion of cells in mono-orientation mutants. A clear limitation of this analysis, however, is the fact that labelling kinetochores did not allow me to determine if Sgo1 is indeed removed in response to bi-orientation since, when kinetochores split, they may be either oriented towards the same or opposite poles. An improvement of this experiment would therefore be to perform three-colour imaging where one of the centromeres is labelled in addition to kinetochores and Sgo1. This would give a better indication of whether Sgo1 loss from pericentromeres occurs directly in response to establishment of bi-orientation.

The discovery that Sgo1 is removed from centromeres upon bi-orientation raises the question about how this may be regulated. In many model organisms, Sgo1 recruitment relies on Bub1-mediated phosphorylation of histone H2A at serine 121 (Kawashima *et al*, 2010; Haase *et al*, 2012; Nerusheva *et al*, 2014). However, at least in budding yeast, Bub1 also has additional functions in recruiting Sgo1 to centromeres because H2A S121 phosphomimetic mutations are not sufficient to enrich Sgo1 at centromeres in the absence of Bub1 (Nerusheva *et al*, 2014). The maintenance of Sgo1 at centromeres also requires Bub1 (Nerusheva *et al*, 2014). This may indicate that Bub1 phosphorylation of an unknown target is required to lock Sgo1 at centromeres. An alternative explanation is that Sgo1 association with chromosomes is highly dynamic and that Bub1 is required to allow Sgo1 to continually re-associate with kinetochores. Fluorescence recovery after photobleaching (FRAP) studies of Sgo1 at centromeres should allow us to distinguish between these two scenarios. Another factor that is important for the association of Sgo1 with centromeres is the PP2A subunit Rts1 (Nerusheva *et al*, 2014). In the absence of Rts1, Sgo1 levels at centromeres are significantly increased (Nerusheva *et al*, 2014). Interestingly, preliminary data from our lab has shown that Sgo1-3A, a mutant that cannot associate with Rts1 (Xu *et al*, 2009), is increased at centromeres in meiotic metaphase I arrested cells (A. Dowbaj & C. Barnard, personal communication). This makes it tempting to suggest that PP2A-Rts1 is important for the removal of Sgo1 from chromosomes. However, upon deletion of *RTS1* in mitotic cells, Sgo1 is still removed from centromeres when sister chromatids

bi-orient (Nerusheva *et al*, 2014). This implies that either tension-dependent removal of Sgo1 is not a function of Rts1 at all and that Rts1's ability to affect Sgo1 localisation is temporally restricted to times when sister kinetochores are not bi-oriented. Alternatively, other proteins may be involved in Sgo1 removal and their function may compensate for the lack of Rts1. In any case, it seems likely that Sgo1's tension-dependent association with centromeres is regulated by a balance of kinases and phosphatases, but the exact targets remain to be identified in the future.

In mitotic HeLa cells, Sgo1 also responds to tension establishment. In prometaphase, Sgo1 is phosphorylated at T346 and this allows its binding to cohesin as well as histone H2A (Liu *et al*, 2013a; 2013b). Only when sister chromatids come under tension is Sgo1 dephosphorylated and fully re-localises from centromeres to kinetochores (Liu *et al*, 2013a). Whether budding yeast Sgo1 exists in two distinct pools as well is unclear. Live cell imaging in mitosis (Nerusheva *et al*, 2014) and meiosis (Fig. 2.4), however, indicates that in budding yeast Sgo1 dissociates from chromosomes rather than re-distributing from one chromosomal localisation to another. However, it cannot be excluded that there is still a small amount of Sgo1 retained on chromosomes after dissociation that may not be detectable given the background of Sgo1 in the nucleus. Analysis of mono-orientation mutants by ChIP-seq is likely to provide a better picture of whether Sgo1 is completely removed from chromosomes upon successful bi-orientation in mitosis and meiosis or whether some Sgo1 is retained at specific sites.

A curious aspect of Sgo1 regulation was the finding that even tension across homologs appears to cause partial Sgo1 removal from chromosomes (Fig. 2.5). Although this phenomenon has only been analysed for a single centromere here, it suggests that Sgo1 centromere binding is intimately linked to tension applied on chromosomes. However, ChIP-seq studies should be carried out to determine whether this is a global phenomenon. Taken together, these findings support a model where Sgo1 association with centromeres in meiosis is highest at unattached kinetochores, which are not under tension. The disassembly of outer kinetochores in prophase (Asakawa *et al*, 2005; Miller *et al*, 2012; Meyer *et al*, 2015) which leads to the dissociation of kinetochore-microtubule attachments may therefore facilitate

efficient recruitment of Sgo1 to centromeres at the end of prophase and aid the protection of pericentromeric cohesin.

2.3.3. Tension-dependent Sgo1 regulation and cohesin protection

Having found that upon sister chromatid bi-orientation, Sgo1 is removed from centromeres, it seemed obvious to test the impact of this on cohesin protection in meiosis I. I first investigated cohesin retention at centromeres in anaphase I directly by imaging Rec8-GFP. This analysis showed that Rec8 is significantly reduced when sister chromatids bi-orient in meiosis I (Fig. 2.7B). For *mam1Δ* and *mam1Δ spo11Δ* mutants the reduction in Rec8-GFP intensity may partly be caused by the fact that the presence of bioriented kinetochores in anaphase I causes protected cohesin to be spread out in the area between, rather than concentrated at, centromeres, thereby lowering the average intensity of the Rec8 signal. However, when subjectively scoring for the presence of Rec8-GFP in anaphase I, I found that for a number of cells Rec8 could not be detected above background levels (Fig. 2.7A). It was therefore necessary to measure whether centromeres are still cohesed in anaphase I when sister chromatids have bi-oriented. As expected from previously published data, the large majority of *mam1Δ* cells will attempt to separate sisters and therefore split GFP dots in anaphase. However, since cohesin protection is mostly intact, GFP foci are restricted in how far they move apart (Fig. 2.9). In contrast, about 50% of *mam1Δ spo11Δ* cells will split *CEN5* dots to a distance greater than 2 µm, indicating that cohesion is lost.

An obvious conundrum is the existence of anaphase I cells with closely opposed, split (< 2µm) GFP foci. These cells have clearly bi-oriented *CEN5* and yet cohesion has not been lost, contradicting the idea that bi-orientation should lead to loss of Sgo1 from centromeres. One possible explanation for this is that Sgo1 removal may be temporally regulated such that it requires factors that may only be present or active in metaphase I. Therefore, if Sgo1 has not been removed in time, its removal and, consequently, cohesin deprotection may be delayed until meiosis II. Similarly, it is currently unclear what the activity window of separase in meiotic cells is. In mitotic cells, separase is active from the onset of anaphase until G1 (Uhlmann *et al*,

1999) but during the meiosis I to meiosis II transition separase may only be active and cleave cohesin in a short window of time before the APC/C is shut off and separase gets bound by newly synthesised Pds1. Therefore, successful bi-orientation in anaphase may not cause cleavage of cohesin even if Sgo1 were to be removed at this stage. Another possible explanation for the above conundrum may lie in that fact that in my analysis I have only looked at a single centromere. Given that in 24% of cases *CEN5* is not mono-oriented at all in *mam1Δ* mutants, it is possible that within each cell there is a mixture of mono-oriented and bi-oriented chromosomes. Since budding yeast kinetochores cluster together after meiotic prophase, it is not inconceivable that the segregation of one chromosome may influence that of another. Therefore, sister chromatid segregation may only occur successfully when all (or the large majority) of sister kinetochores within a cell have bi-oriented and therefore lost both Sgo1 and cohesin protection.

Taken together the data here provide an extension to our current understanding of the importance of sister chromatid mono-orientation in ensuring efficient protection of cohesin. Previously, it was argued that due to the failure to separate sisters in anaphase I, *mam1Δ* mutants and cells defective for the activity of DDK (which resemble *mam1Δ spo11Δ* mutants in their chromosome segregation pattern), bi-orientation does not affect cohesin protection (Tóth *et al*, 2000; Matos *et al*, 2008). The data presented here, on the other hand, provide a more thorough analysis of the effects of losing mono-orientation than previous observations. However, since a significant proportion of cells in both *mam1Δ* and *mam1Δ spo11Δ* double mutants still succeed in protecting cohesin and preventing sister chromosome segregation in meiosis I, the findings shown here should be considered an extension, rather than a contradiction to previously published observations. Furthermore, the ability of some cells to protect cohesin when sister chromatids bi-orient and, consequently, dissociate Sgo1 from chromosomes, indicates that successful deprotection of cohesin in meiosis II requires additional mechanisms than simply sister kinetochore tension.

CHAPTER 3: SPO13 REGULATES COHESIN PROTECTION WITHOUT AFFECTING SGO1 LOCALISATION OR DEGRADATION TIMING

3.1. Introduction

In our current model of cohesin protection, Sgo1 binding within the pericentromere recruits PP2A through its regulatory subunit Rts1. PP2A in turn removes phosphate groups on the meiotic cohesin Rec8, which have been laid down by cohesin-phosphorylating kinases. Since dephosphorylated Rec8 cannot be cleaved, pericentromeric cohesin will not be removed from chromosomes in meiosis I. Although a lot of evidence supports this model, there are a number of proteins that have been linked to cohesin protection which currently have no place in the above model.

One of these proteins is budding yeast Spo13. *SPO13* is exclusively expressed in meiosis and gets degraded in anaphase I (Katis *et al*, 2004b; Sullivan & Morgan, 2007). Cells in which *SPO13* is deleted have been reported to lose Rec8 at centromeres in anaphase I (Klein *et al*, 1999; Katis *et al*, 2004b; Lee *et al*, 2004). Although it was initially reported that *spo13Δ* cells are unaffected for the localisation and protein levels of Sgo1 (Lee *et al*, 2004), it was later argued that pericentromeric Sgo1 levels are reduced in the absence of *SPO13* (Kiburz *et al*, 2005). Henceforth, it had been assumed that the cohesion defect of *spo13Δ* mutants is due to a failure to recruit and maintain Sgo1 at centromeres (Kiburz *et al*, 2005) but how Spo13 affects Sgo1 association with chromosomes mechanistically has never been investigated.

Although *SPO13* does not appear to be conserved in other eukaryotes, a number of proteins with similar functions have been identified. In fission yeast, a protein called Moa1 is required for mono-orientation of sister kinetochores in meiosis I as well as for cohesion of sister chromatids in the central core region of fission yeast chromosomes (Yokobayashi & Watanabe, 2005). In mice, a protein called MEIKIN was found to have functions analogous to Spo13. Mice deficient in MEIKIN are defective for mono-orientation and cohesin protection (Kim *et al*, 2014). Therefore, identification of mechanisms by which Spo13 affects cohesin protection may provide clues as to the function of conserved proteins in higher organisms.

The overall aim of this chapter is to determine the role Spo13 plays in cohesin protection. The main focus will be to analyse whether Spo13 regulates the cohesin protector Sgo1. However, *spo13Δ* mutants display a complex pleiotropic phenotype, which, apart from defects in cohesin protection and mono-orientation, also include an overactive APC/C and the lack of a second meiotic division (Katis *et al*, 2004b). Therefore, I decided to investigate Spo13's function in cohesion protection on a variety of levels, particularly localisation and degradation of Sgo1.

3.2. Results

3.2.1. Loss of Spo13 causes a cohesion defect despite apparently normal Sgo1 localisation

3.2.1.1. Sister chromatid cohesion is prematurely lost in *spo13Δ* mutants

Although the premature loss of cohesin in *spo13Δ* mutants was previously reported (Klein *et al*, 1999; Katis *et al*, 2004b; Lee *et al*, 2004), reports have been inaccurate as to the degree of the cohesion defect. Therefore, I decided to investigate the severity of the cohesin loss phenotype. Initially, I decided to image Rec8-GFP in live meiotic cells. However, due to the fact that *spo13Δ* cells are defective for mono-orientation, I reasoned that some of the reported cohesin phenotype might be due to bi-orientation of sisters in meiosis I (Fig. 2.9). Therefore, as a control, I included the *mam1Δ* strain, which is defective for mono-orientation, in my analysis of the *spo13Δ* cohesion phenotype for comparison.

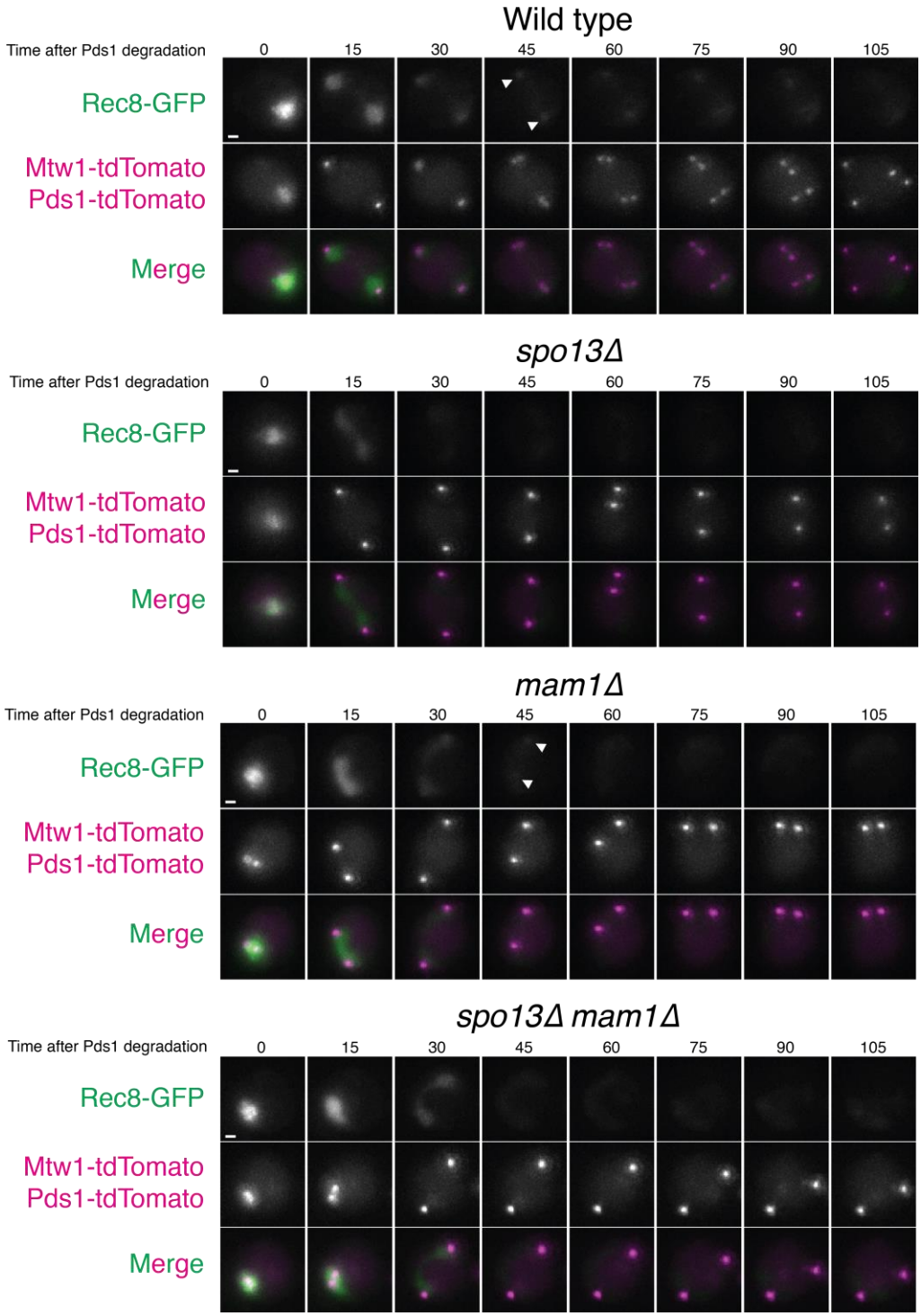

Figure 3.1: Rec8 disappears after metaphase I from pericentromeric regions in *spo13Δ* cells. Wild type (AMy13716), *spo13Δ* (AMy15133), *mam1Δ* (AMy15134) and *spo13Δ mam1Δ* (AMy15135) cells were induced to sporulate for 2.5 hours and transferred onto a microfluidics plate for imaging at 15 min intervals. Representative movies are shown. Scale bars represent 1µm. Arrows highlight pericentromeric cohesin retained after the first round of cohesin cleavage.

As described previously in chapter 2, both wild type cells and *mam1Δ* cells retain cohesin in the pericentromere at anaphase I. In *spo13Δ* cells and *spo13Δ mam1Δ* double mutants, on the other hand, Rec8-GFP rapidly disappears along the length of the chromosome upon anaphase I onset so that pericentromeric foci of Rec8-GFP cannot be detected in anaphase (Fig. 3.1). When subjectively scoring cells for the presence of pericentromeric Rec8 foci in anaphase, it became clear that all *spo13Δ* and *spo13Δ mam1Δ* cells appear to lose cohesin along the entire length of chromosomes in anaphase I (Fig. 3.2A). Accordingly, the intensity of Rec8-GFP in anaphase I in *spo13Δ* and *spo13Δ mam1Δ* cells is reduced almost to background levels. I therefore conclude that *SPO13* deletion causes loss of cohesin along the length of the chromosome in anaphase I.

To test whether the loss of detectable cohesin translates into a loss of functional cohesion in *spo13Δ* mutants, I subjected *spo13Δ* and *spo13Δ mam1Δ* cells to the *CEN5* cohesion assay (Fig. 2.8) using Spc42-tdTomato as SPB marker. Whereas wild type and *mam1Δ* cells behaved as previously observed (Fig. 2.9), *spo13Δ* cells displayed a mixed mono-orientation and cohesion phenotype (Fig. 3.3). Approximately half of *spo13Δ* cells segregate homologs, preventing an assessment of cohesion. However, the other half bi-orient sister chromatids and successfully segregate them to opposite poles in anaphase I, indicating a complete loss of cohesion in these cells. In *spo13Δ mam1Δ* cells, on the other hand, mono-orientation is almost completely lost (Fig. 3.3). Because deletion of *SPO13* allows *mam1Δ* cells to segregate sister chromatids to opposite poles, I conclude that cohesion is almost completely defective in the absence of *SPO13*. Taken together, these results suggest that cohesin protection is strongly impaired in *spo13Δ* cells.

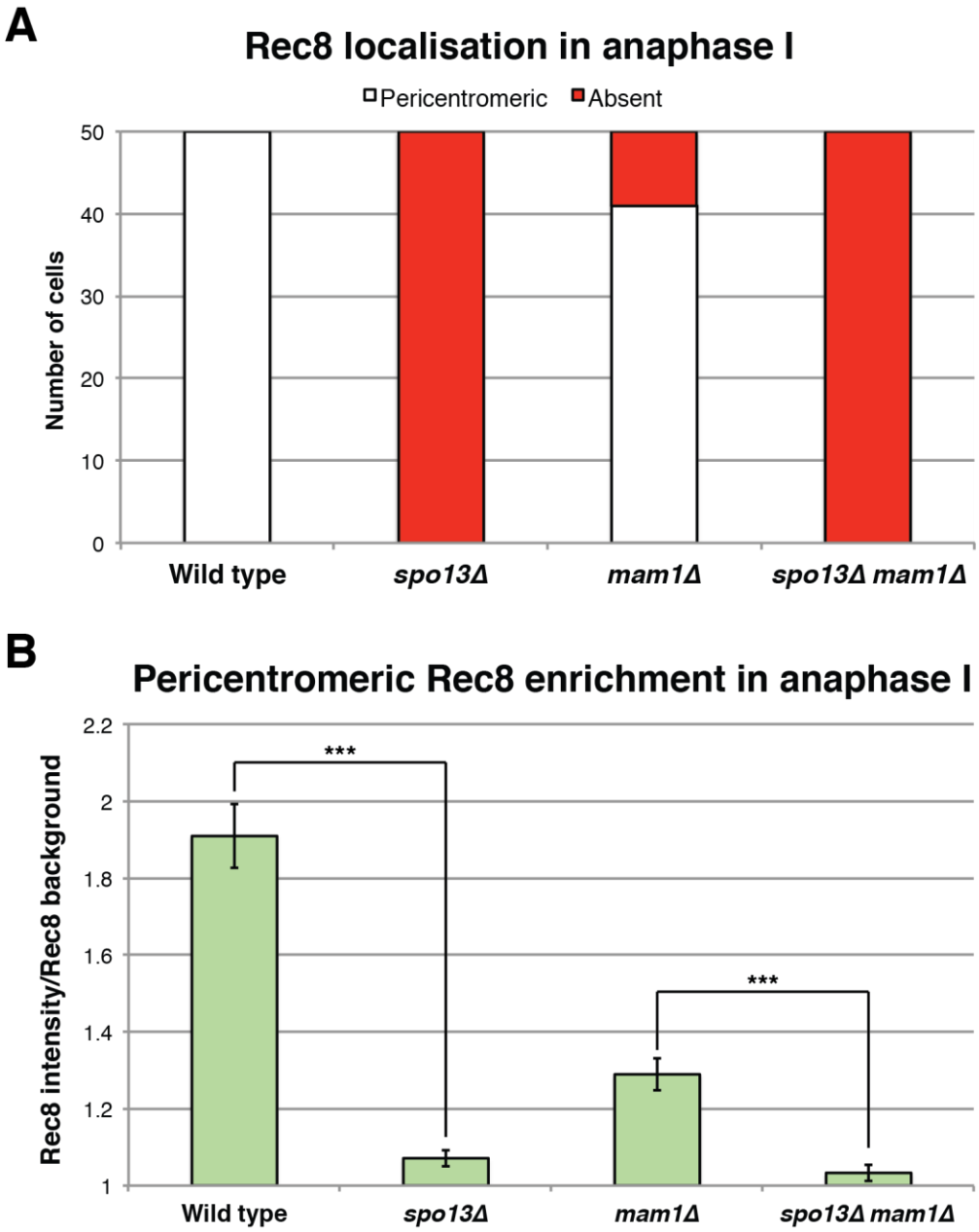

Figure 3.2: Rec8 disappears after metaphase I from pericentromeric regions in *spo13Δ* cells. (A) Cells from movies shown in Fig. 3.1 were subjectively scored for the presence of pericentromeric cohesin after Pds1 degradation (n = 50). (B) The average intensity of Rec8 was measured in the area occupied by kinetochores in anaphase I as described in Fig. 2.7. Error bars show standard error of the mean (***p < 0.001).

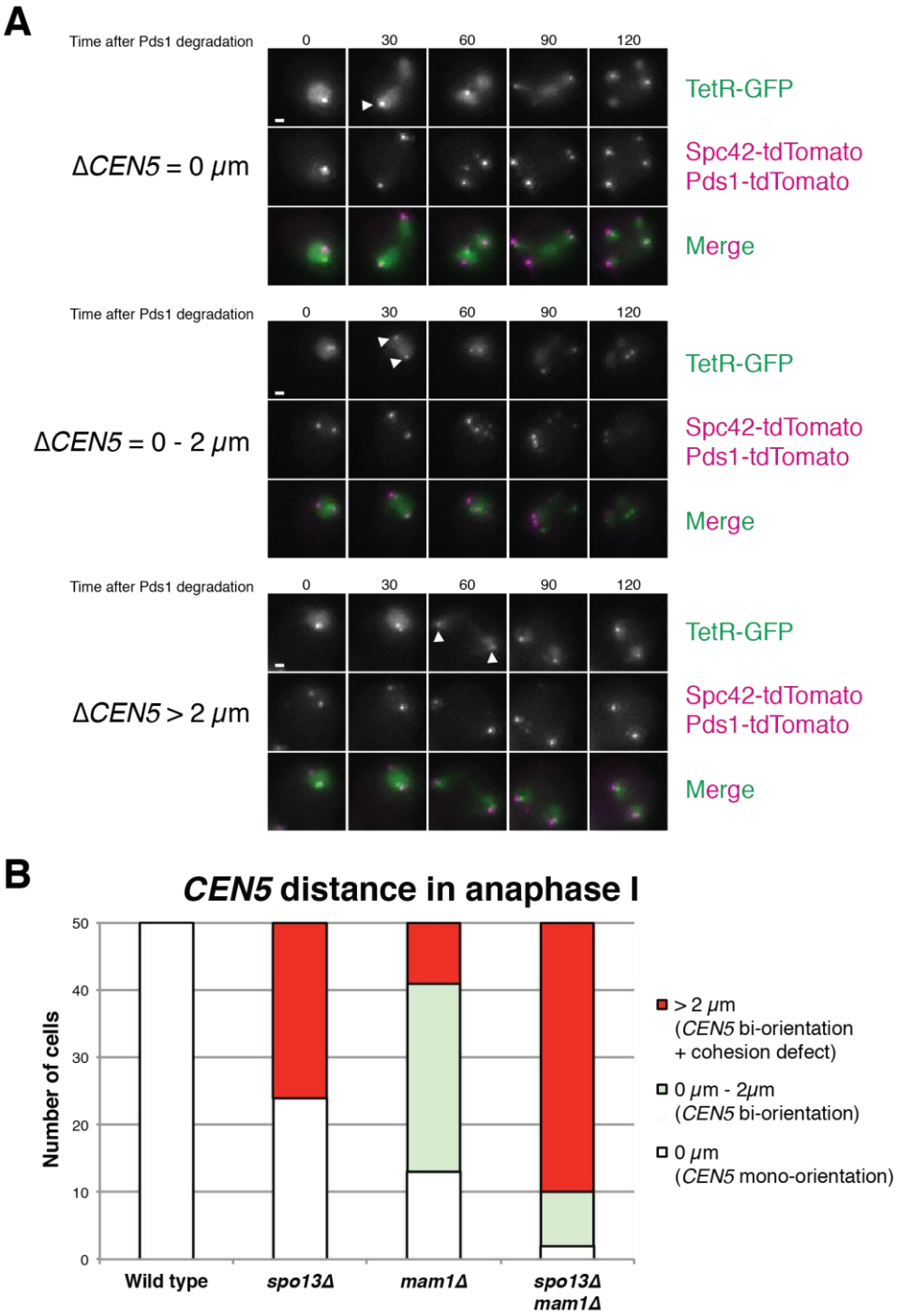

Figure 3.3: *spo13Δ* cells have a severe cohesion defect. (A and B) Live-cell imaging of heterozygous *CEN5*-GFP dots in meiosis. Wild type (AMy15190), *spo13Δ* (AMy15118), *mam1Δ* (AMy15119) and *mam1Δ spo11Δ* (AMy15120) were induced to sporulate and transferred to a microfluidics device after 2 hours in SPO media. Images were taken at 15 min intervals. (A) Example sequences of cells going through meiosis. Scale bars represent 1μm. Arrows highlight *CEN5*-GFP foci. (B) The distance between *CEN5-GFP* foci was measured in 50 cells after Pds1 degradation but prior to SPB re-duplication for the mutants indicated.

3.2.1.2. Cohesin loading is unaffected in *spo13Δ* mutants

One possible explanation for the cohesin phenotype of *spo13Δ* cells is that cohesin may not be loaded appropriately in the pericentromere. Mutants that are defective for centromeric cohesin loading, like mutations in the Ctf19 kinetochore complex, have previously been shown to suffer from cohesion defects in meiosis II (Marston *et al*, 2004; Fernius & Marston, 2009). Therefore, I sought to test whether cohesin association with centromeres is reduced in *spo13Δ* cells. To this end, I performed ChIP-qPCR of Rec8-3Ha in cells that were arrested at the end of prophase by deletion of the transcription factor *NDT80*, which is required for cells to exit from prophase. Analysis of Rec8 binding to centromeres 3 and 4, as well as an arm site on chromosome 4, showed no indication of a change in Rec8 levels in *spo13Δ* mutants or a mono-orientation mutant (*mam1Δ*) alone. I therefore conclude that Rec8 loading to centromeres appears to be unperturbed in *spo13Δ* mutant cells and that this is unlikely to be the reason for the cohesion defect in these cells.

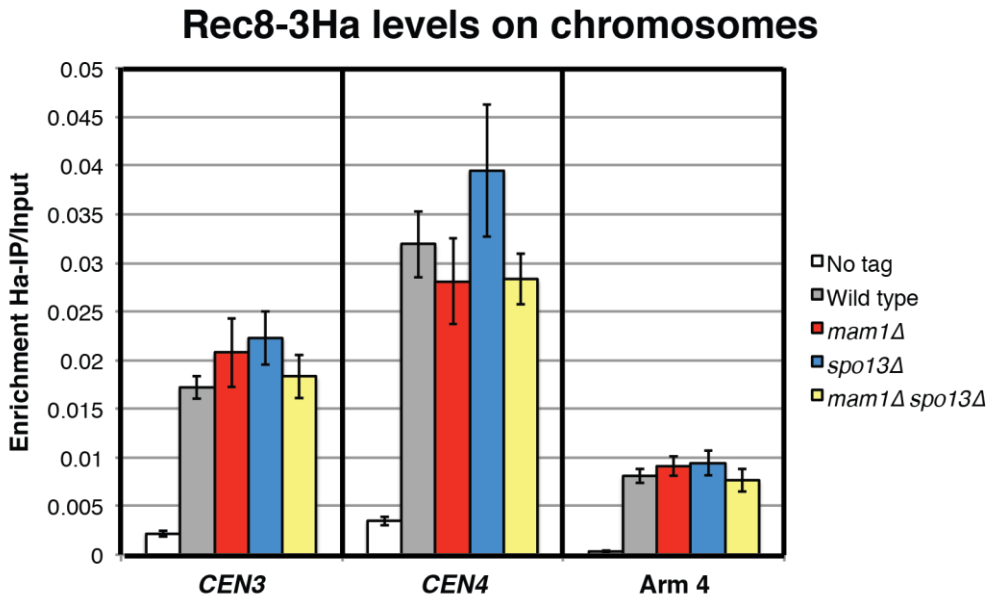

Figure 3.4: Rec8 loading to centromeres is unaffected in *spo13Δ* cells. (A) ChIP-qPCR of Rec8-3Ha at different locations. No tag (AMy11633), wild type (AMy4015), *mam1Δ* (AMy15342), *spo13Δ* (AMy15343) and *mam1Δ spo13Δ* (AMy15344) cells carrying *pCLB2-CDC20* were arrested in SPO media for 5 hours before fixing cells for α-Ha ChIP-qPCR. Error bars represent standard error of the mean for 3 independent experiments.

3.2.1.3. Sgo1-PP2A appear to be localised appropriately in metaphase I *spo13Δ* mutants

The loss of cohesion in *spo13Δ* mutants suggested that the ability of Sgo1-PP2A to protect cohesin might be impaired. Indeed, previous reports have argued that Spo13 affects the recruitment and maintenance of Sgo1 at centromeres (Kiburz *et al*, 2005). However, these results contradict earlier observations and reports that could not find a reduction of Sgo1 on chromosomes (Lee *et al*, 2004; Katis *et al*, 2004b). Therefore, I wanted to determine whether cohesin protection is properly set up in metaphase I by correctly localising Sgo1 and Rts1. First, to clarify whether Sgo1 recruitment to centromeres is indeed dependent on *SPO13*, I performed ChIP-qPCR of Sgo1-6Ha in cells arrested in metaphase I by depletion of the APC/C activator Cdc20. Once again I used *mam1Δ* mutants as a control to allow comparison to a mutant, which, like *SPO13* deletion, causes mono-orientation defects.

Analysis of Sgo1 binding to *CEN3* and *CEN4* showed that levels of Sgo1 are unchanged in *spo13Δ* or *spo13Δ mam1Δ* cells (Fig. 3.5A) whereas Sgo1-binding to a chromosomal arm site on chromosome 4 is close to background levels in both wild type and mutant cells (Fig. 3.5A). Interestingly, I observed a small but statistically significant increase in centromeric Sgo1 levels in *mam1Δ* mutants. To compare chromosomal association with cellular Sgo1 levels, I also performed western blot on whole cell extracts from ChIP cultures. This showed an increase in global Sgo1 levels in Sgo1 in the *mam1Δ* mutant, which likely explains the increased association of Sgo1 with *CEN3* and *CEN4* in this strain. The reasons for the increased Sgo1 levels are currently unclear, as this finding was not reproducible in other experiments. Interestingly, Sgo1 levels are markedly reduced in the absence of *SPO13*. This is likely due to the fact that *spo13Δ* mutants fail to arrest efficiently in metaphase I (Katis *et al*, 2004b), a time when Sgo1 levels decrease (see below). Given that Sgo1 binding to *CEN3* and *CEN4* is still comparable to wild type cells despite a decrease in global Sgo1, I conclude that *SPO13* deletion does not affect Sgo1 recruitment to these sites negatively.

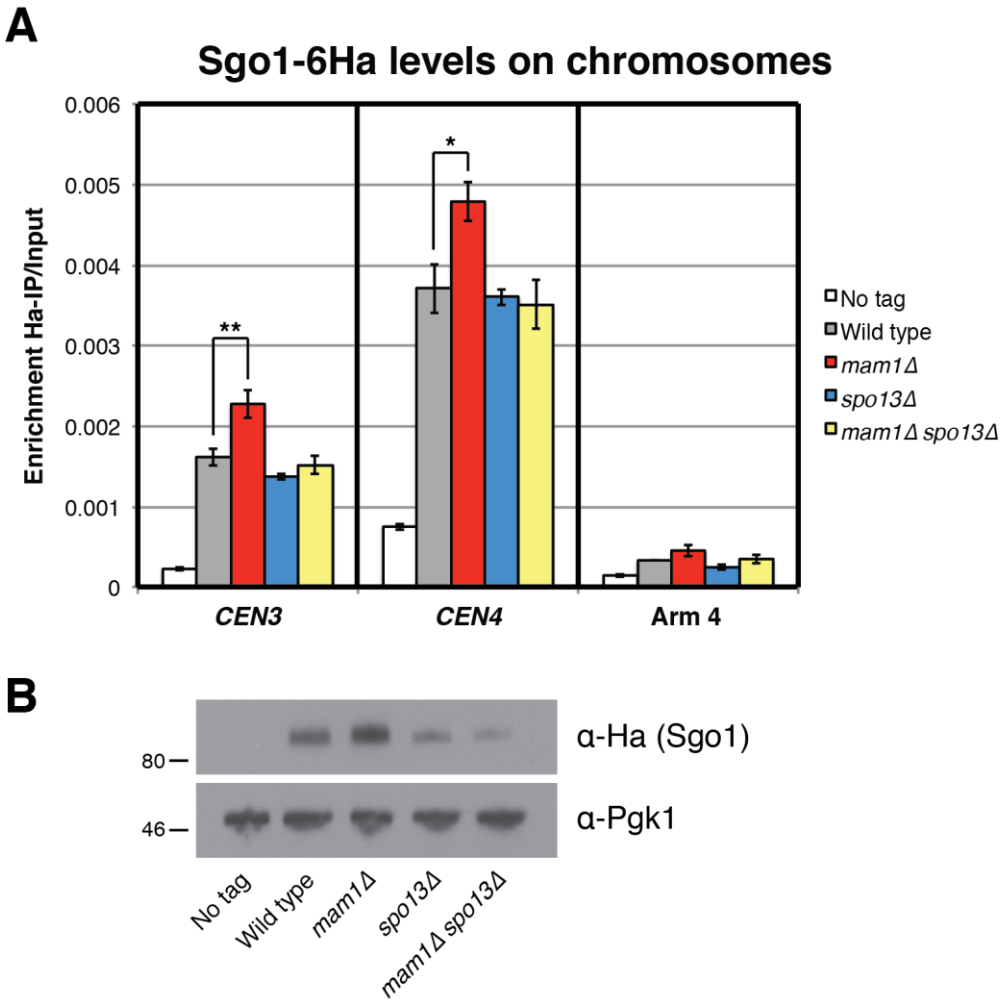

Figure 3.5: Sgo1 levels at *CEN3* and *CEN4* are unaltered in *spo13Δ* cells. (A) ChIP-qPCR of Sgo1-6Ha at different locations on chromosome IV. No tag (AMy8067), wild type (AMy2261), *mam1Δ* (AMy8068), *spo13Δ* (AMy9464) and *mam1Δ spo13Δ* (AMy9456) cells carrying *pCLB2-CDC20* were arrested in SPO media for 6 hours before fixing cells for α-Ha ChIP-qPCR. Error bars represent standard error of the mean for 4 independent experiments (*$p < 0.05$, **$p < 0.01$). (B) Cellular levels of Sgo1 are reduced in *spo13Δ* mutants. TCA fixed samples were collected for western blot analysis just prior to fixing cells for ChIP. A representative blot is shown.

To gain a better understanding of how lack of *SPO13* may affect the Sgo1-PP2A protector, I decided to image both Sgo1 and the PP2A subunit Rts1 in meiosis. Firstly, I followed GFP-tagged Sgo1 in metaphase I arrested cells. In wild type cells, Sgo1 is present from the end of prophase and will localise as foci proximal to kinetochores in metaphase I (Fig. 3.6A). Interestingly, Sgo1-GFP shows a very similar localisation pattern in *spo13Δ* mutants, indicating that its localisation is not altered majorly. However, cohesin protection also requires proper localisation of PP2A. Therefore, I imaged Rts1-GFP throughout meiosis. In wild type cells, Rts1 localises around kinetochores in meiosis I (Fig. 3.6B). In anaphase, it appears as diffuse signal before concentrating again around kinetochores (Fig. 3.6B; 30 min after Pds1 degradation). In *spo13Δ* cells, Rts1 localisation strongly mirrors that of Sgo1: it localises as distinct foci around kinetochores (Fig. 3.6B). However, after anaphase onset it can no longer be detected in the vicinity of kinetochores. I therefore conclude that the localisation of Sgo1 and Rts1 in metaphase I appears largely unaffected in *spo13Δ* mutants. It therefore seems unlikely that the cohesion defect of *spo13Δ* cells is caused by the inability of either Sgo1 or Rts1 to be recruited to the pericentromere.

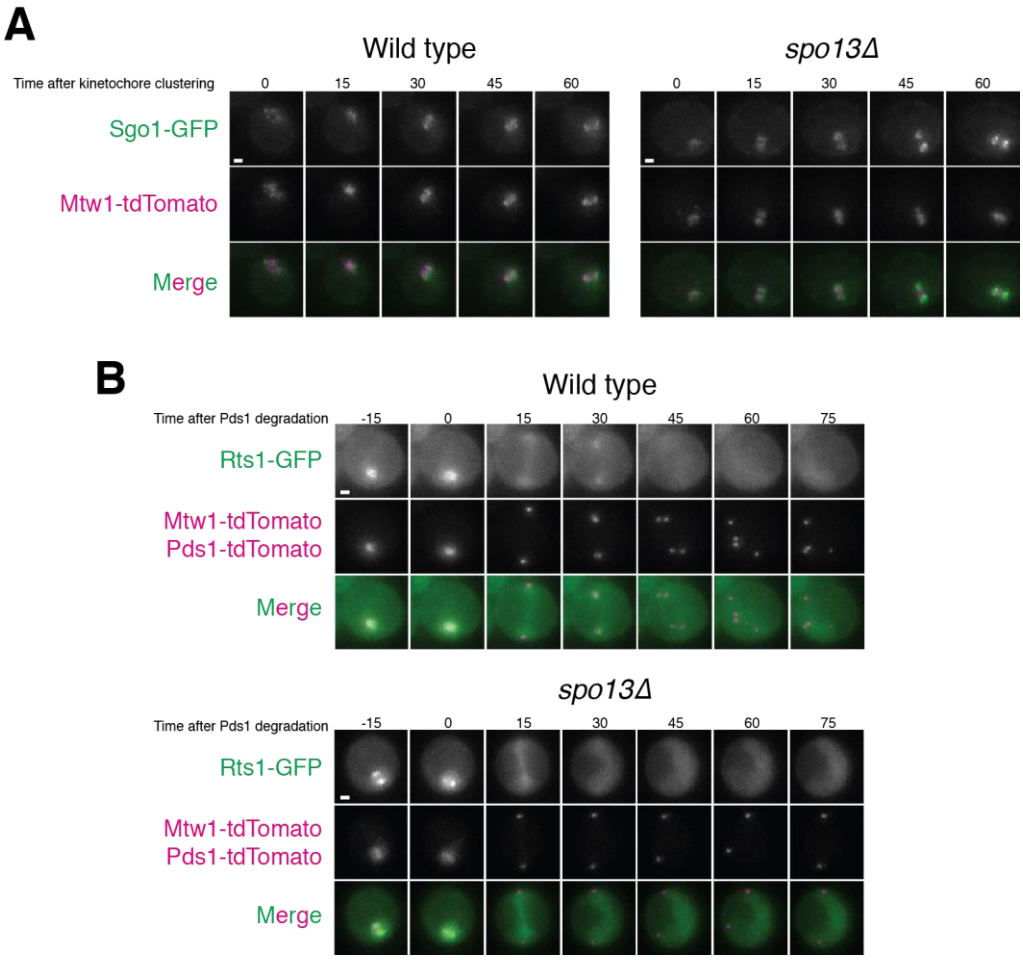

Figure 3.6: The Sgo1-PP2A protector localises in proximity to centeromeres in *spo13Δ* mutants. (A) Live cell imaging of Sgo1-GFP in metaphase I arrested cells. Wild type (AMy16001) and *spo13Δ* (AMy16059) cells carrying *pCLB2-CDC20* were sporulated for 2.5 hours before transferring to a microfluidics device and imaging at 15 min intervals. Kinetochore clustering indicates exit from meiotic prophase. Representative movies are shown. (B) Live cell imaging of Rts1-GFP in meiotic cells. Wild type (AMy20218) and *spo13Δ* (AMy20219) were sporulated for 2.5 hours before transferring to a microfluidics device and imaging at 15 min intervals. Representative movies are shown. Scale bars represent 1μm.

3.2.2. Premature Sgo1 degradation is not responsible for defective cohesion in *spo13Δ* mutants

3.2.2.1 Deletion of Sgo1's destruction box stabilises Sgo1 in *spo13Δ* cells

Surprised by the finding that both Sgo1 and PP2A appear to localise correctly in *spo13Δ* mutants during metaphase I, I reasoned that the cohesion defect of these cells may be due to loss of Sgo1 at anaphase I onset, the time at which separase becomes active and Sgo1-PP2A would be expected to play its critical role in protection of pericentromeric cohesin. One possibility was that Sgo1 might be degraded upon entry into anaphase I so that it can no longer protect cohesin at this stage. Indeed, mitotic Sgo1 is degraded by the APC/C bound to Cdc20 (Eshleman & Morgan, 2014) and whole cell extracts from meiotic cells indicated a reduction of Sgo1 protein levels in *spo13Δ* cells (Fig. 3.5B). Therefore, I sought to test whether Sgo1 stabilisation in meiosis rescues the cohesion defect of *spo13Δ* mutants.

Firstly, however, I tried to establish how Sgo1 degradation is regulated in meiosis. Although it has been argued that the APC/C bound to its Cdc20 activator causes Sgo1 degradation in mitotic anaphase (Eshleman & Morgan, 2014), for meiotic cells it was shown that the meiosis-specific APC/C activator Ama1 can cause degradation of Sgo1 as well (Oelschlaegel *et al*, 2005; Okaz *et al*, 2012). Therefore, I decided to image Sgo1 in meiotic cells in various mutants with the aim of identifying a mutant that stabilises Sgo1 in wild type and *spo13Δ* cells. Firstly, I used the *sgo1Δdb* mutant, which lacks Sgo1's destruction box – 5 highly conserved C-terminal residues that were proposed to be important for APC/C^{Cdc20}-mediated degradation in mitosis (Eshleman & Morgan, 2014). Secondly, I used a deletion mutant of *AMA1*. However, *ama1Δ* cells are biochemically very different from normal meiotic cells because deletion of *AMA1* prevents the destruction of the transcription factor *NDD1* and the cyclin *CLB4*, causing a variety of meiotic defects (Okaz *et al*, 2012). Therefore, to minimise the biochemical alterations of *AMA1* deletion (which may indirectly affect Sgo1 dynamics), I carried out my analysis in a strain background where *NDD1* is put under control of the mitosis-specific *SCC1* promoter, thereby precluding its expression in meiosis, and which carries a deletion

of *CLB4*. The *pSCC1-NDD1 clb4Δ* background was previously shown to restore normal meiotic chromosome segregation to *ama1Δ* cells (Okaz *et al*, 2012).

Analysis of Sgo1-GFP localisation in wild type cells showed that, surprisingly, Sgo1 seems to delocalise from chromosomes in anaphase I as distinct Sgo1-GFP foci in the vicinity of kinetochores are no longer visible by live cell imaging. However, earlier studies in fixed cells indicate that Sgo1 is still present at centromeres in anaphase I cells (Marston *et al*, 2004), indicating that live cell imaging may not be sensitive enough to detect Sgo1 in anaphase I. Later, Sgo1 can be again observed at pericentromeres, where it continues to be detectable until the end of metaphase II when it eventually disappears (Fig. 3.6). While Sgo1 still associates with chromosomes in metaphase I in *spo13Δ* cells, it becomes undetectable upon anaphase onset and does not return afterwards (Fig. 3.6). Interestingly, Sgo1Δdb is stable throughout meiosis. However, unlike wild type Sgo1 protein, Sgo1Δdb-GFP is clearly visible at pericentromeres in both anaphase I and anaphase II as indicated by the presence of distinct foci in the vicinity of the kinetochore (Fig. 3.6). In contrast, *ama1Δ* cells do not appear to have altered Sgo1 dynamics in meiosis. Equally, *AMA1* deletion also does not prevent degradation of Sgo1 in a *spo13Δ* background (Fig. 3.6). However, the *sgo1Δdb* mutant causes stabilisation of Sgo1 throughout meiosis in *spo13Δ* cells and this effect is not enhanced by additional deletion of *AMA1*.

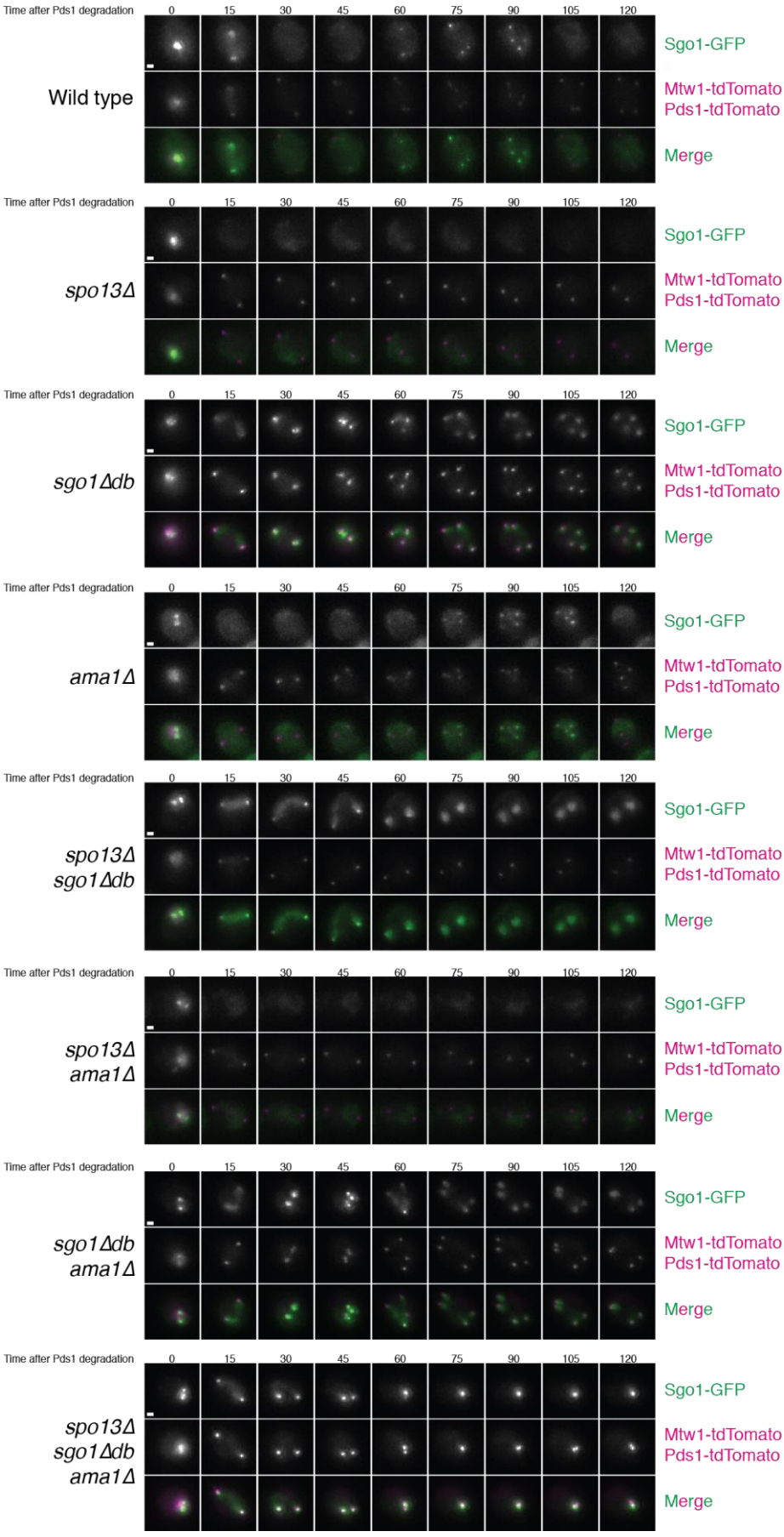
Time after Pds1 degradation
0
15
30
45
60
75
90
105
120
Wild type
spo13Δ
sgo1Δdb
ama1Δ
spo13Δ sgo1Δdb
spo13Δ ama1Δ
sgo1Δdb ama1Δ
spo13Δ sgo1Δdb ama1Δ
Sgo1-GFP
Mtw1-tdTomato
Pds1-tdTomato
Merge

In order to quantify these phenotypes, I subjectively categorised the localisation of Sgo1 in these mutants as either pericentromeric, diffuse or undetectable in 50 cells for 2.5 hours after Pds1 degradation (Fig. 3.8). This analysis reinforced the major conclusions stated above. Firstly, Sgo1 is undetectable in anaphase I and anaphase II in wild type cells. Secondly, in *spo13Δ* mutants Sgo1 permanently disappears after anaphase I in the large majority of cells. Thirdly, Ama1 does not appear to regulate Sgo1 degradation after metaphase I. And lastly, deletion of Sgo1's destruction box allows it's stabilisation in meiosis and association of Sgo1 with pericentromeres in anaphase I of *spo13Δ* mutants. Taken together, these findings suggest that *SPO13* deletion prevents re-accumulation of Sgo1 after anaphase I. However, deletion of the Sgo1 destruction box allows Sgo1 to associate with the pericentromere in anaphase I *spo13Δ* mutants.

Figure 3.7: Sgo1Δdb is stable in anaphase I in *spo13Δ* mutants. Live cell imaging of Sgo1-GFP or Sgo1Δdb-GFP in live meiotic cells. Wild type (AMy17483), *spo13Δ* (AMy17485), *sgo1Δdb* (AMy17487), *ama1Δ* (AMy17484), *spo13Δ sgo1Δdb* (AMy17734), *spo13Δ ama1Δ* (AMy17486), *sgo1Δdb ama1Δ* (AMy17488) and *spo13Δ sgo1Δdb ama1Δ* (AMy17735) cells were sporulated for 2.5 hours before transferring to a microfluidics device and imaging at 15 min intervals. Representative movies are shown. Scale bars represent 1μm.

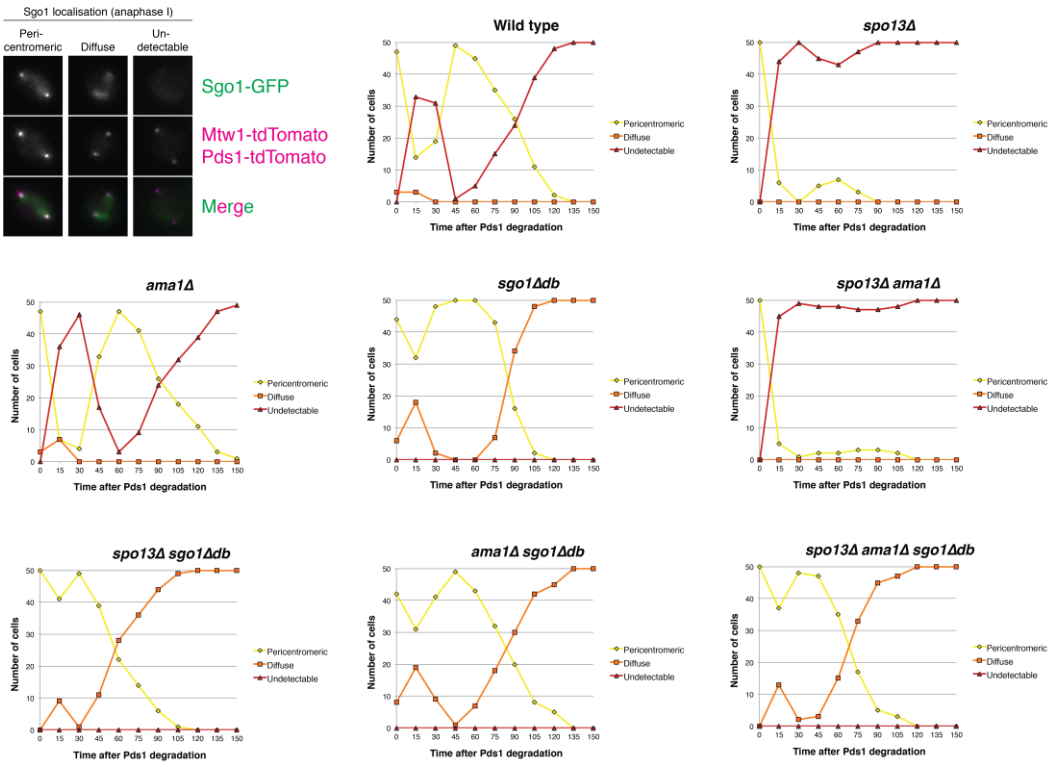

Figure 3.8: Sgo1Δdb associates with the pericentromere in anaphase I in *spo13Δ* mutants. 50 cells for each strain in Fig. 3.6 were followed for 2.5 hours after Pds1 degradation and Sgo1 localisation subjectively scored as either pericentromeric (distinct foci near kinetochores), diffuse (absence of distinct foci) or undetectable (no signal above background). Example images are shown in the top left.

3.2.2.2. Sgo1 stabilisation does not rescue the cohesion defect of *spo13Δ* cells

Having established a condition in which Sgo1 is clearly localised to the pericentromere in anaphase I of *spo13Δ* cells, I wanted to test whether deletion of Sgo1's destruction box would rescue the cohesion defect of these mutants. Therefore, I first imaged Rec8-GFP throughout meiosis to see whether pericentromeric cohesin is retained in anaphase I in *spo13Δ sgo1Δdb* cells. While *sgo1Δdb* cells mimic the wild type pattern of Rec8 loss (Fig. 3.9), additional deletion of *SPO13* causes the disappearance of pericentromeric Rec8, although sometimes very faint remnants of Rec8 can be detected near the pericentromere in anaphase I (Fig. 3.9). To further illustrate this phenotype, I scored anaphase I cells for the presence of Rec8 near pericentromeres and measured the intensity of Rec8-GFP at this stage (Fig. 3.10). Interestingly, while wild type and *sgo1Δdb* cells behave identically in terms of cohesin protection and *spo13Δ* cells completely lose cohesin, faint pericentromeric Rec8-GFP can be detected in 38% of *spo13Δ sgo1Δdb* cells (Fig. 3.10A). Analysis of Rec8-GFP intensity in anaphase I, however, showed that there is only a very minor (albeit significant) increase of pericentromeric Rec8-GFP in the *spo13Δ sgo1Δdb* mutant compared to the *spo13Δ* single mutant (Fig. 3.10B). I then wanted to find out whether the mild increase in Rec8 is sufficient to at least partially rescue the cohesion phenotype of *spo13Δ* mutants. To this end, I carried out the *CEN5* cohesion assay (Fig. 2.8) for *spo13Δ sgo1Δdb* mutants. While deletion of Sgo1's destruction box does not affect its ability to protect cohesin (Fig. 3.10C), it also does not enhance cohesin protection in *spo13Δ* mutants (Fig. 3.10C). I therefore conclude that although there is a very minor increase in cohesin in anaphase I, this cohesin is not sufficient to hold sister chromatids together in *sgo1Δdb spo13Δ* cells.

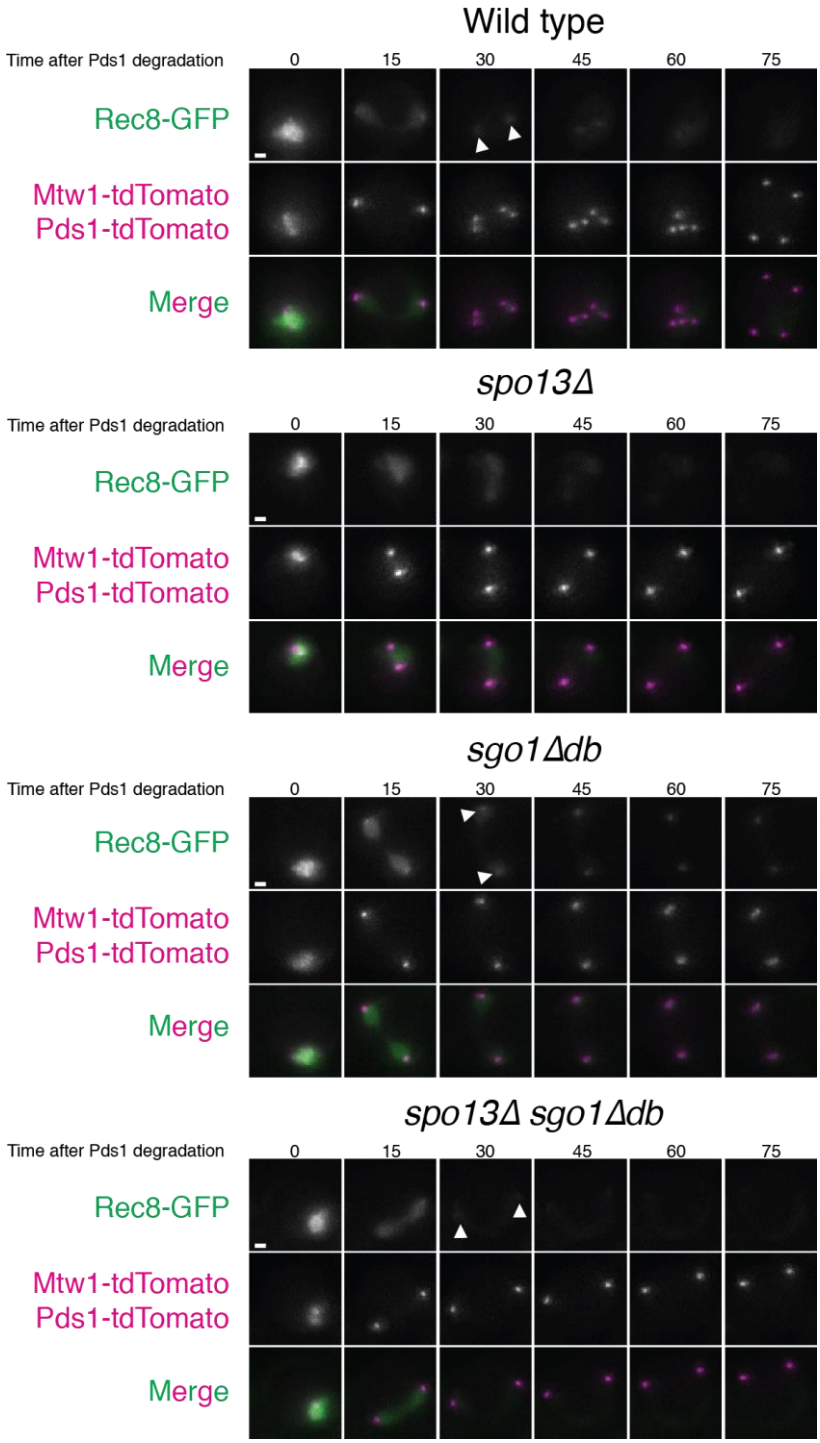

Figure 3.9: Faint foci of Rec8-GFP remain around kinetochores in *spo13Δ sgo1Δdb* double mutants. Wild type (AMy13716), *spo13Δ* (AMy20033), *sgo1Δdb* (AMy19994) and *spo13Δ sgo1Δdb* (AMy19995) cells were induced to sporulate for 2.5 hours and transferred onto a microfluidics plate for imaging at 15 min intervals. Representative movies are shown. Scale bars represent 1µm. Arrows highlight pericentromeric cohesin retained after the first round of cohesin cleavage.

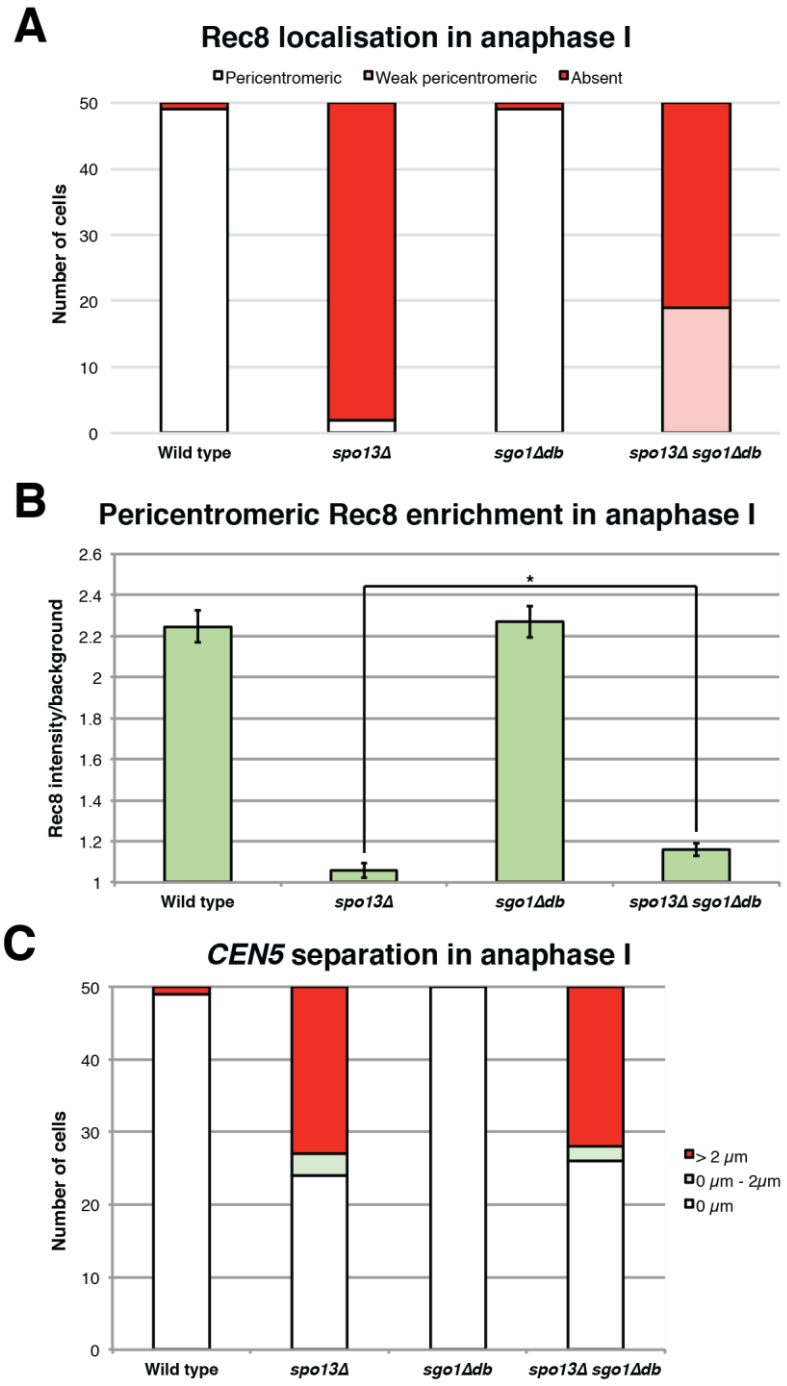

Figure 3.10: *sgo1Δdb* does not rescue the cohesion defect of *spo13Δ* mutants. (A and B) Rec8 is present at pericentromeres only weakly in *spo13Δ sgo1Δdb* mutants. (A) 50 cells of the strains in Fig. 3.9 were subjectively scored for the presence of Rec8 around pericentromeres in anaphase I. (B) Intensity measurements of Rec8-GFP signal at kinetochores in anaphase I for cells analysed in A. (C) Wild type (AMy15190), *spo13Δ* (AMy20146), *sgo1Δdb* (AMy20147) and *spo13Δ sgo1Δdb* (AMy20148) cells were induced to sporulate and transferred to a microfluidics device after 2.5 hours in SPO media. The distance between *CEN5-GFP* foci was measured in 50 cells after Pds1 degradation but prior to SPB re-duplication for the mutants indicated.

3.2.3. Cdc5 regulates cellular Sgo1 levels

3.2.3.1. Sgo1 levels are increased in the absence of Cdc5

Since I could not find any evidence as to how Spo13 might directly regulate cohesin protection through Sgo1, I wanted to investigate other factors that might be regulated by Spo13 or which may affect Spo13 function. An obvious candidate was the budding yeast polo kinase Cdc5. Spo13 was found to be an interactor of Cdc5 (Matos *et al*, 2008) and functional homologues of Spo13 are thought to regulate cohesin protection and mono-orientation by recruiting polo kinase to centromeres (Kim *et al*, 2014). Therefore, I first wanted to test what the effect of depleting Cdc5 on Sgo1 is. To this end, I performed ChIP of Sgo1-6Ha in metaphase I arrested cells. To deplete Cdc5, I put *CDC5* under the control of the meiosis-specific *CLB2* promoter (Lee & Amon, 2003). Additionally, I used a *spo13Δ* strain and the *spo13-m2* mutant (Matos *et al*, 2008) as a control. *spo13-m2* has two mutations in the proposed polo-binding domain of *SPO13* and this interferes with the Spo13-Cdc5 interaction, although there is residual binding between these two proteins in the mutant (Matos *et al*, 2008). Together, this set of mutants should allow me to distinguish whether effects on Sgo1 localisation are due to the absence of Cdc5 itself or due to the loss of Cdc5 binding to Spo13.

Surprisingly, *pCLB2-CDC5* cells show a significant increase of Sgo1-6Ha levels at four different sites on chromosome IV (Fig. 3.11) – the centromere, an arm site as well as the boundary sites between the pericentromere and chromosome arm, which are highly enriched for cohesin. In contrast, the *spo13-m2* mutant shows similar levels of Sgo1 to wild type and *spo13Δ* cells at each of the locations tested. Therefore, the enrichment of Sgo1 along chromosomes is not a consequence of losing the Spo13-Cdc5 interaction but instead due to a loss of Cdc5 itself. Next, I wanted to determine whether the increase in chromosomal levels might be due to increased levels of Sgo1 in the cell. Therefore, I performed western blot on the cultures used for ChIP analysis. Interestingly, Sgo1 levels are clearly increased compared to wild type in *pCLB2-CDC5* cells. The fact that Sgo1 levels are higher in the *spo13-m2* mutant than in *spo13Δ* cells is likely explained by the failure of *spo13Δ*

mutants to arrest in metaphase (Katis *et al*, 2004b). Taken together these results suggest that Cdc5 affects Sgo1 localisation to chromosomes by regulating cellular protein levels.

3.2.3.2. Cdc5 controls Sgo1 levels independently of the APC/C

Given the increased protein levels of Sgo1 in *pCLB2-CDC5* cells, I wondered how Cdc5 might affect Sgo1 levels mechanistically. Cdc5 has long been suggested to be an activator of the APC/C (Charles *et al*, 1998), although exact mechanisms remain elusive to this date. Because my previous ChIP experiment used a depletion allele of the APC/C activator Cdc20, I excluded the possibility that Cdc5 regulates APC/C^{Cdc20}. Instead, I reasoned that Cdc5 depletion may instead decrease the activity of APC/C^{Ama1}. If this were the case, then deletion of *AMA1* could be expected to replicate the phenotype of *pCLB2-CDC5* cells and a *pCLB2-CDC5 ama1Δ* mutant would be expected not to have additive effects. To test this, I performed ChIP-qPCR and western blot analysis of these mutants in a metaphase I arrest. In contrast to *pCLB2-CDC5* cells, *ama1Δ* mutants show a similar enrichment of Sgo1 at *CEN3* and *CEN4* to wild type cells (Fig. 3.12A). Consequently, there is also no additional enrichment of Sgo1 in *pCLB2-CDC5 ama1Δ* double mutants (Fig. 3.12A). Similarly, western blot analysis showed that there is no global increase in Sgo1 levels in *ama1Δ* mutants compared to wild type or in *pCLB2-CDC5 ama1Δ* double mutants compared to *pCLB2-CDC5* single mutants (Fig. 3.12B). Therefore, I conclude that Cdc5 controls Sgo1 levels in meiosis independently of the APC/C.

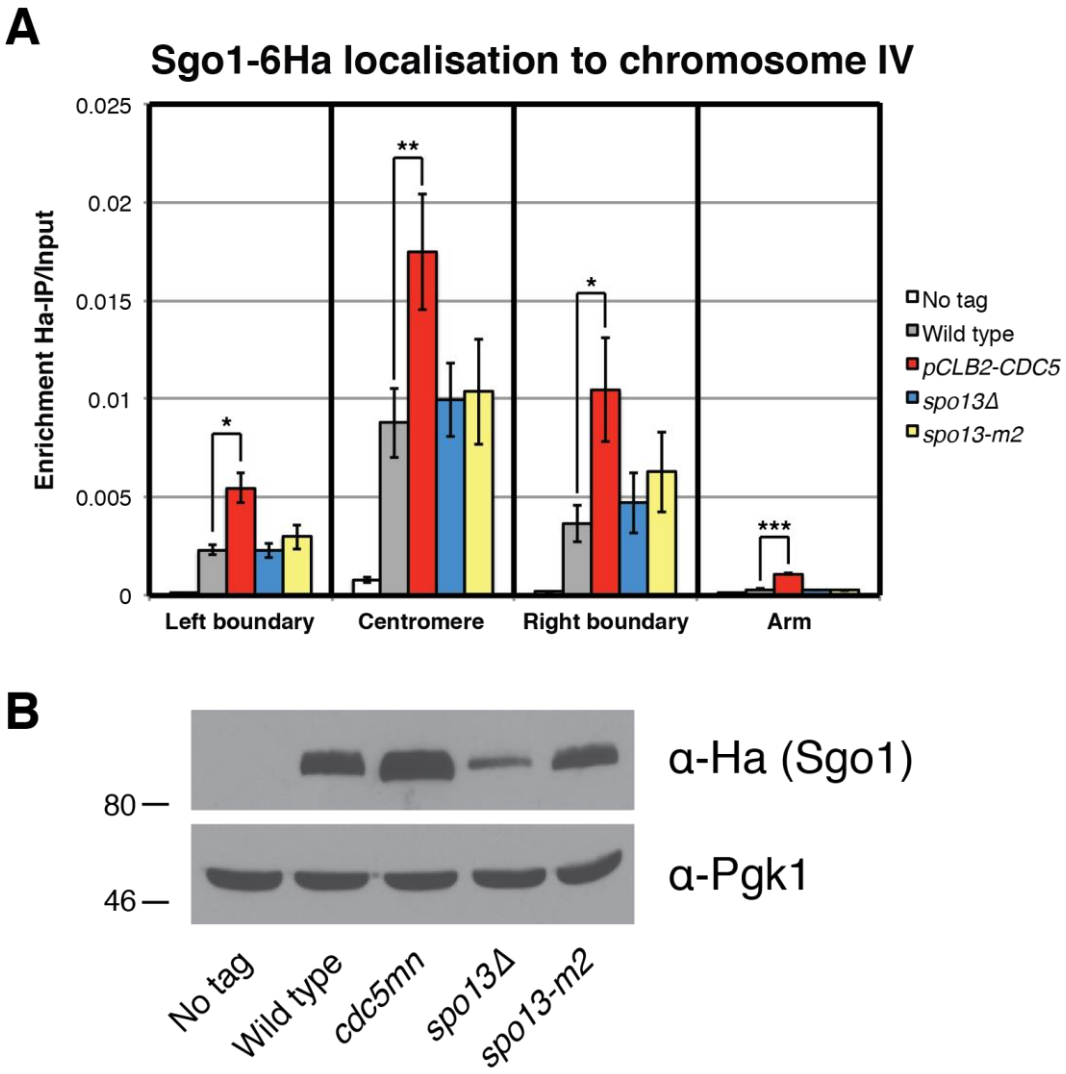

Figure 3.11: Cdc5 controls Sgo1 stability. (A) Sgo1 levels along chromosome IV are increased in *pCLB2-CDC5* cells. ChIP-qPCR of Sgo1-6Ha at different locations on chromosome IV. No tag (AMy8067), wild type (AMy14542), *pCLB2-CDC5* (AMy14544), *spo13Δ* (AMy15123) and *spo13-m2* (AMy15124) cells carrying *pCLB2-CDC20* were arrested in SPO media for 6 hours before fixing cells for α-Ha ChIP-qPCR. Error bars represent standard error of the mean for 4 independent experiments (*p < 0.05, **p < 0.01). (B) Cellular levels of Sgo1 are increased in *pCLB2-CDC5* mutants. TCA fixed samples were collected for western blot analysis just prior to fixing cells for ChIP. A representative blot is shown.

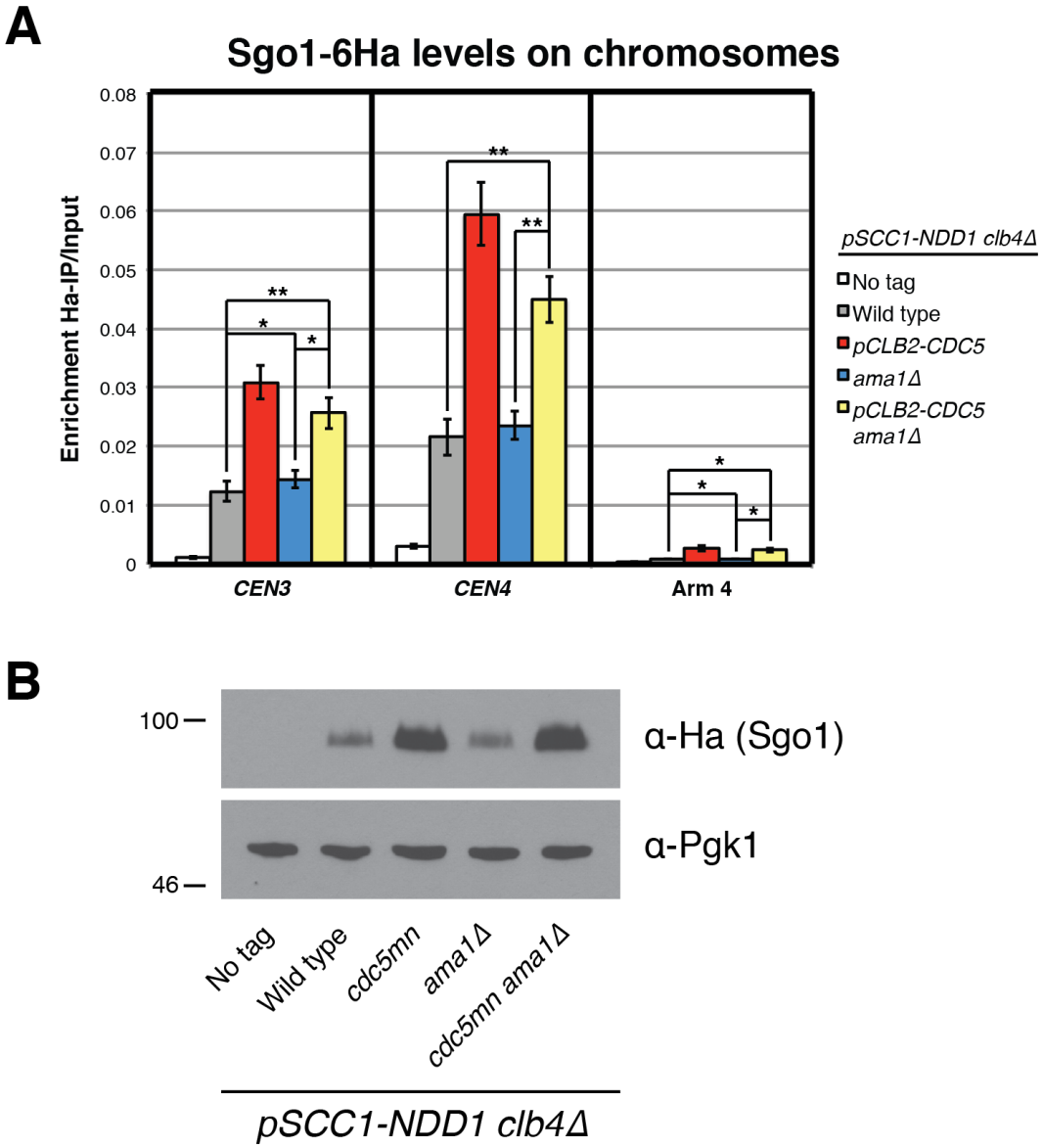

Figure 3.12: Cdc5 controls Sgo1 stability independently of the APC/C. (A) Sgo1 levels at *CEN3* and *CEN4* in *ama1Δ* cells are comparable to wild type. ChIP-qPCR of Sgo1-6Ha. No tag (AMy16886), wild type (AMy16811), *pCLB2-CDC5* (AMy16812), *ama1Δ* (AMy16813) and *pCLB2-CDC5 ama1Δ* (AMy16814) cells carrying *pCLB2-CDC20* were arrested in SPO media for 6 hours before fixing cells for α-Ha ChIP-qPCR. Error bars represent standard error of the mean for 4 independent experiments (*p < 0.05, **p < 0.01). (B) Cellular levels of Sgo1 are not increased in *ama1Δ* mutants. TCA fixed samples were collected for western blot analysis just prior to fixing cells for ChIP. A representative blot is shown.

3.2.3.3. Increased chromosomal levels of Sgo1 in *pCLB2-CDC5* cells depend on *BUB1*

Given the global increase of Sgo1 levels in *pCLB2-CDC5* cells, I wondered whether the increased association of Sgo1 with centromeres is due to unspecific binding of Sgo1 to chromosomes or whether *CDC5* may actually regulate the specific association of Sgo1 with chromosomes. To distinguish between these possibilities, I decided to test Sgo1 association with centromeres in *pCLB2-CDC5* cells in which Bub1 is also depleted by placement of its gene under control of the mitosis-specific *CLB2* promoter. Bub1 is the kinase responsible for localising Sgo1 at centromeres through phosphorylation of histone H2A (Kitajima *et al*, 2005; Fernius & Hardwick, 2007; Haase *et al*, 2012; Liu *et al*, 2013a). If increased Sgo1 association with chromosomes in *pCLB2-CDC5* occurs at specific binding sites, then decreasing the levels of Bub1 should also lead to depletion of centromeric Sgo1 levels in *pCLB2-CDC5* mutants. Indeed, when testing Sgo1-6Ha levels at *CEN3* and *CEN4*, I found that *pCLB2-CDC5 pCLB2-BUB1* double mutants exhibit a significantly reduced enrichment of Sgo1 compared to a *pCLB2-CDC5* single mutant (Fig. 3.13). Given that *pCLB2-BUB1* mutants do not cause a complete loss of Sgo1 in cells that are otherwise wild type, it is unlikely that the *pCLB2-BUB1* allele causes complete depletion of Bub1. This may explain why the drop in centromeric Sgo1 is not more pronounced. Taken together, however, these results argue that Cdc5 controls the specific association of Sgo1 with centromeres.

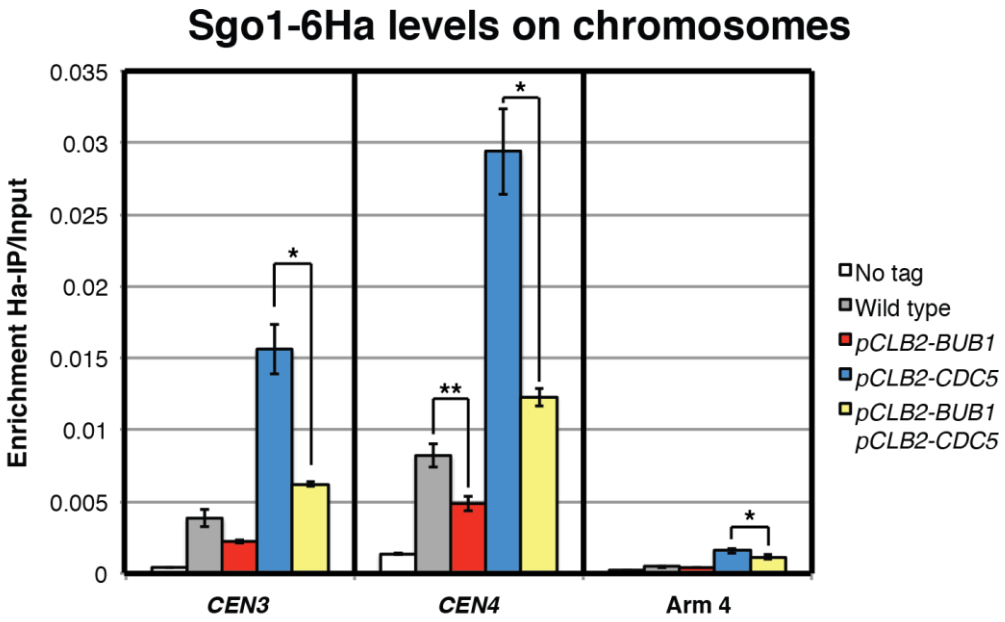

Figure 3.13: Cdc5 controls specific association of Sgo1 with chromosomes. *BUB1* is required for the increased association of Sgo1 with *CEN3* and *CEN4* in *pCLB2-CDC5* cells. ChIP-qPCR of Sgo1-6Ha. No tag (AMy8067), wild type (AMy2261), *pCLB2-BUB1* (AMy18331), *pCLB2-CDC5* (AMy10157) and *pCLB2-BUB1 pCLB2-CDC5* (AMy18332) cells carrying *pCLB2-CDC20* were arrested in SPO media for 6 hours before fixing cells for α-Ha ChIP-qPCR. Error bars represent standard error of the mean for 4 independent experiments (*p < 0.05, **p < 0.01).

3.2.3.4. Overexpression of *CDC5* is not detrimental to cohesin protection

The fact that depletion of Cdc5 causes increased levels of Sgo1 suggested that overexpression of *CDC5* might deplete cellular Sgo1 levels and, thus, impair cohesin protection. Interestingly, previous studies have found that cohesin protection is indeed diminished when *CDC5* is overexpressed in meiosis (Attner *et al*, 2013). However, this study found that Spo13 is degraded prematurely as a result of *CDC5* overexpression and cohesion defects were therefore attributed to a lack of Spo13 (Attner *et al*, 2013). To test this idea further, I decided to overexpress *CDC5* from the copper-inducible promoter *CUP1* promoter in a strain expressing a stable allele of *SPO13, spo13(L26A)* (Sullivan & Morgan, 2007). If *CDC5* overexpression causes cohesin deprotection as a result of Spo13 degradation, then stabilisation of Spo13 should rescue the observed phenotype. To assess cohesin protection, I imaged Rec8-GFP in cells released synchronously from a prophase I block (Carlile & Amon, 2008). These cells have *NDT80*, the transcription factor required for exit from meiotic prophase, under the control of the *GAL1* promoter. Expression from this promoter in turn requires Gal4 which is fused to a portion of the estrogen receptor (*GAL4.ER*) in this strain. This causes Gal4 to be cytoplasmic until the addition of β-estradiol upon which it translocates into the nucleus to mediate *NDT80* expression and exit from prophase. I chose this method because it allowed me to simultaneously induce overexpression of *CDC5*, which is a target of *NDT80*, and release cells from the prophase block. This ensured that any of the observed effects are caused by *CDC5* overexpression rather than its untimely expression. Additionally, I only included cells in my analysis that had dispersed kinetochores at the start of imaging (which is a marker of the prophase stage), thereby excluding cells in which Cdc5 overexpression was induced prior to prophase.

When scoring the effects of *CDC5* overexpression on cohesin protection, I noticed that increased levels of Cdc5 do not impact cohesin protection in my hands because all cells retain pericentromeric cohesion in anaphase I (Fig. 3.14). Interestingly, although all spo13(L26A) cells retain visible pericentromeric Rec8-GFP in anaphase I (Fig. 3.14B), there is a significant overall reduction the intensity of pericentromeric Rec8-GFP in anaphase (Fig. 3.14C). Together, these results

suggest that *CDC5* overexpression does not impact cohesin protection and, thus, excess Cdc5 is unlikely to deplete Sgo1 sufficiently enough to cause cohesin deprotection. However, I cannot not exclude that CDC5 overexpression was less efficient than in previous studies (Attner *et al*, 2013), which may explain the different observations.

3.2.3.5. Spo13 counteracts Cdc5 in controlling Sgo1 levels

Given the interaction of Spo13 and Cdc5 and the opposite effect of deleting or depleting these proteins upon Sgo1 levels (Fig. 3.5), I wondered whether Spo13 might simply function as an inhibitor of Cdc5 such that deletion of Spo13 causes Cdc5 hyper-activity. Although regulation of Sgo1 levels is unlikely to be the mechanism by which Spo13 might maintain proper cohesin protection through Cdc5, I reasoned that the opposing effects of Spo13 and Cdc5 on Sgo1 levels could provide a useful readout of whether Spo13 acts as a Cdc5 inhibitor. Therefore, I sought to test the effect of combining *SPO13* mutants with the *pCLB2-CDC5* allele on Sgo1 localisation to chromosomes and overall cellular levels. If Spo13 acts as an inhibitor of Cdc5 so that *spo13Δ* phenotypes are due to Cdc5 hyper-activity, I predict that a *pCLB2-CDC5 spo13Δ* double mutant should behave similarly to a *pCLB2-CDC5* single mutant. Additionally, I investigated the *spo13-m2* and *pCLB2-CDC5 spo13-m2* mutants to assess whether Spo13 may have roles independently of its Cdc5 interaction.

Interestingly, I found that when combining *pCLB2-CDC5* and *spo13Δ*, Sgo1 was reduced to wild type levels at *CEN3*, *CEN4* and *CEN5* but the minor increase of Sgo1 at an arm site on chromosome 4 upon *pCLB2-CDC5* was not dependent on *SPO13* (Fig. 3.15A). In *pCLB2-CDC5 spo13-m2* mutants, the recruitment of Sgo1 to centromeres is only partially restored indicating that the Spo13 Polo-binding domain (PBD) is necessary for full association of Sgo1 with centromeres in *pCLB2-CDC5* mutants and that the PBD might have Cdc5-independent functions. When examining the effects of these mutants on global Sgo1 levels, it became apparent that the increase in Sgo1 levels observed in *pCLB2-CDC5* cells is lost upon additional deletion of *SPO13* (Fig. 3.15B). However, the PBD of Spo13 is not required to

stabilise Sgo1 in *pCLB2-CDC5* cells, since Sgo1 levels are elevated in *spo13-m2 pCLB2-CDC5* mutants to similar levels as observed in the *pCLB2-CDC5* single mutant. Therefore, Spo13 regulates Sgo1 levels independently of its interaction with Cdc5. This data does not support the model that Spo13 acts as a Cdc5 inhibitor. Instead it suggests that Cdc5 modulates Sgo1 association with centromeres largely by regulating its cellular levels and that Spo13 operates either downstream of or in a separate pathway to Cdc5 to control the levels of Sgo1.

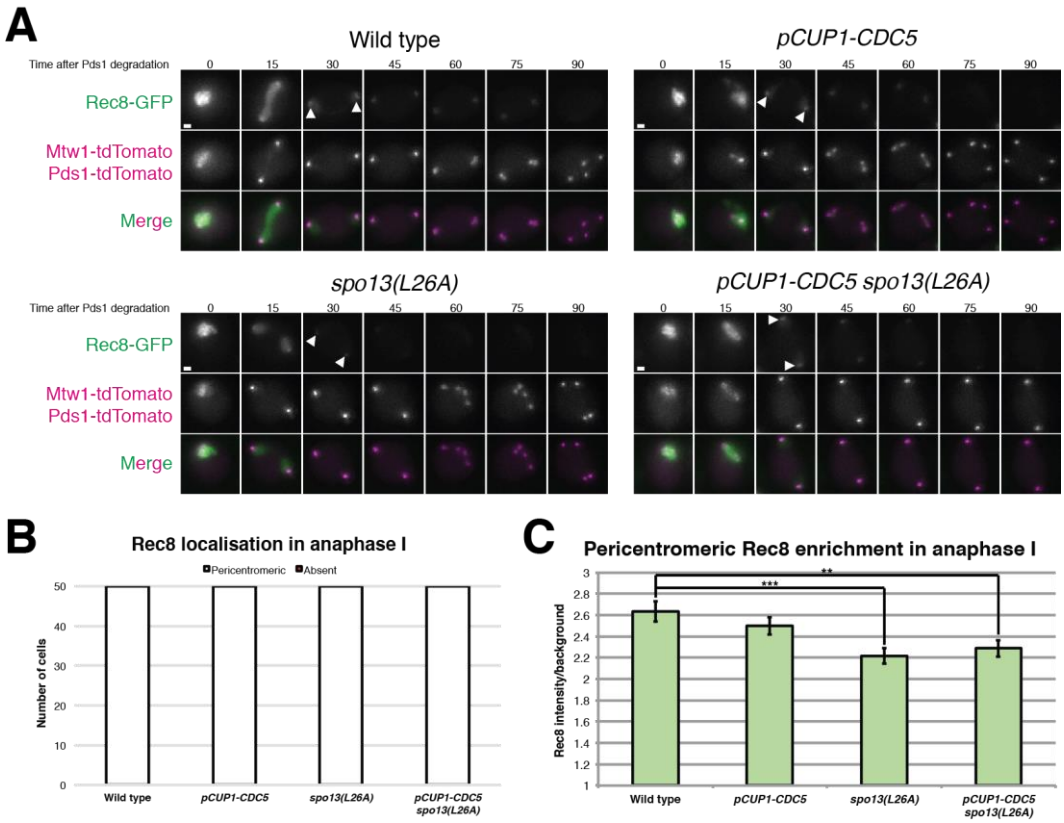

Figure 3.14: Cdc5 overexpression has no impact on cohesin protection. (A-C) Wild type (AMy18507), *pCUP1-CDC5* (AMy19290), *spo13(L26A)* (AMy19291) and *pCUP1-CDC5 spo13(L26A)* (AMy19292) cells were induced to sporulate for 5 hours before adding 1µM β-estradiol and 25µM $CuSO_4$ to cultures. Strains were shaken in flask for 15 minutes and then transferred onto a microfluidics plate for imaging at 15 min intervals. (A) Representative movies are shown. Scale bars represent 1µm. Arrows highlight pericentromeric cohesin retained after the first round of cohesin cleavage. (B) Cells were subjectively scored for the presence of pericentromeric cohesin after Pds1 degradation (n = 50). (C) The average intensity of Rec8 was measured in the area occupied by kinetochores in anaphase I as described in Fig. 2.7. Error bars show standard error of the mean (**p < 0.01, ***p < 0.001).

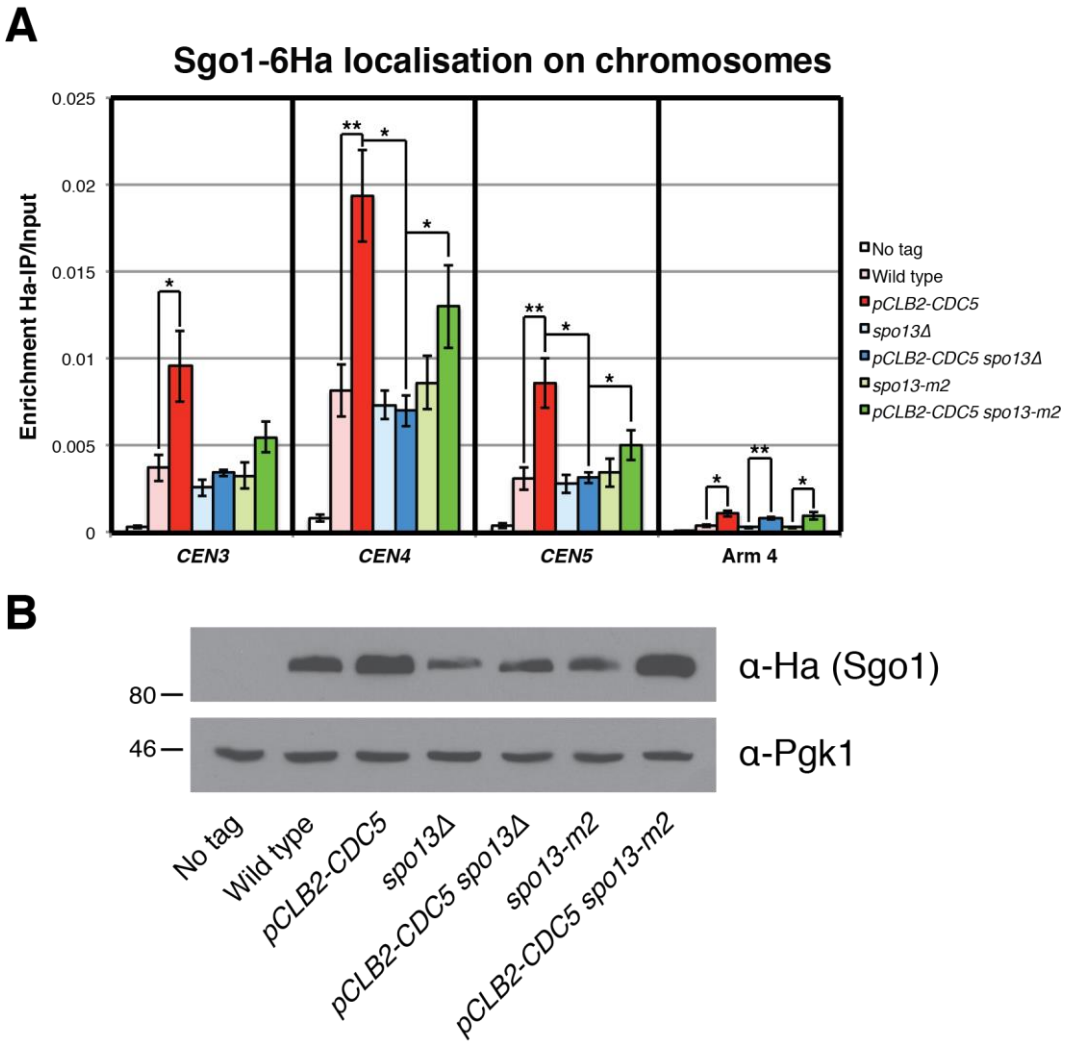

Figure 3.15: Spo13 counteracts Cdc5 in regulating Sgo1 stability. (A) Sgo1 levels at *CEN3*, *CEN4* and *CEN5* are comparable to wild type in *pCLB2-CDC5 spo13Δ* double mutants. ChIP-qPCR of Sgo1-6Ha. No tag (AMy8067), wild type (AMy2261), *pCLB2-CDC5* (AMy10157), *spo13Δ* (AMy12700), *pCLB2-CDC5 spo13Δ* (AMy12701), *spo13-m2* (AMy18077) and *pCLB2-CDC5 spo13-m2* (AMy15132) cells *carrying pCLB2-CDC20* were arrested in SPO media for 6 hours before fixing cells for α-Ha ChIP-qPCR. Error bars represent standard error of the mean for 4 independent experiments (*p < 0.05, **p < 0.01). (B) *SPO13* deletion decreases Sgo1 levels in *pCLB2-CDC5* cells. TCA fixed samples were collected for western blot analysis just prior to fixing cells for ChIP. A representative blot is shown.

3.3. Discussion

The data in this chapter provide a comprehensive analysis of the effect of *SPO13* deletion upon cohesin protection and Sgo1. While *spo13Δ* mutants exhibit a very strong cohesion defect, Sgo1 appears to be localised appropriately. However, after anaphase I, Sgo1 can no longer be observed in *spo13Δ* cells. However, even when degradation of Sgo1 is prevented and Sgo1 appears at centromeres in anaphase, cohesion is lost.

3.3.1. Cohesion is lost in *spo13Δ* mutants, although Sgo1 is appropriately localised

The initial step in my analysis was to characterise the cohesion phenotype of *spo13Δ* mutants. This was necessary because previous studies showed some disagreement to the severity of the phenotype (Klein *et al*, 1999; Katis *et al*, 2004b; Lee *et al*, 2004). This is probably due to the fact that previous studies used immunofluorescence of fixed cells to study cohesin maintenance. However, this technique makes it difficult to accurately stage cells. Therefore, I decided to carry out live cell imaging of Rec8 in *spo13Δ* cells, which allowed me to assess cohesin retention at centromeres right after Pds1 degradation. Interestingly, I could not detect pericentromeric foci of Rec8 in *spo13Δ* mutants (Figs. 3.1 and 3.2), indicating a complete loss of cohesin during anaphase I. Additionally, Rec8-GFP intensity was close to background (Fig. 3.3). Therefore, the loss of cohesin in *spo13Δ* mutants is much more severe than previously described (Katis *et al*, 2004b). This is also illustrated by the results of the *CEN5* cohesion assay I carried out for *spo13Δ* and *spo13Δ mam1Δ* mutants. In *spo13Δ* cells loss of sister chromatid cohesion can be detected in all cells that lose mono-orientation and deletion of *SPO13* allows the large majority of *mam1Δ* cells to split sister chromatids upon Pds1 degradation (Fig. 3.3B). To explain the lack of sister chromatid cohesion, I first wanted to investigate whether cohesin itself was appropriately loaded onto chromosomes, particularly in the pericentromere. My ChIP-qPCR analysis indicated that Rec8 levels were unaltered at the end of prophase at *CEN3* and *CEN4* (Fig. 3.4). While this is not a comprehensive analysis of cohesin association with chromosomes and ChIP-seq

analysis would provide a more detailed picture, it indicates that cohesin loading in the pericentromere is intact as mutants that fail to appropriately load cohesin at centromeres, like those that affect the function of the Ctf19 kinetochore complex, show a decrease in centromeric cohesin in prophase-arrested cells (Vincenten *et al*, 2015). Therefore, it seemed more likely that *SPO13* deletion affects the maintenance or protection of cohesin in meiosis I rather than its loading onto centromeres.

The possibility that Spo13 may be required for cohesin protection was supported by a previous study which suggested that Sgo1 is decreased on chromosomes in the absence of Spo13 (Kiburz *et al*, 2005), though earlier studies observed Sgo1 at centromeres in *spo13Δ* cells (Lee *et al*, 2004; Katis *et al*, 2004b). Furthermore, Sgo1 localisation to centromeres is diminished in mice lacking the functional Spo13 homolog MEIKIN (Kim *et al*, 2014). I therefore analysed Sgo1 localisation in *spo13Δ* cells by ChIP-qPCR. Surprisingly, Sgo1 in *spo13Δ* mutants localised normally to both *CEN3* and *CEN4* with the same enrichment as in wild type cells (Fig. 3.5A). However, western blot analysis revealed that Sgo1 levels in the cell are decreased in *spo13Δ* mutants, suggesting that Sgo1 enrichment at centromeres may actually be increased. One potential cause of the decrease in Sgo1 levels is the ability of *spo13Δ* cells to bypass the metaphase I arrest caused by depletion of Cdc20 (Katis *et al*, 2004b). As observed later, *spo13Δ* mutants fail to re-accumulate Sgo1 after its degradation in anaphase I (Figs. 3.7 and 3.8) and therefore, the decrease in Sgo1 levels observed in *spo13Δ* mutants may, at least partially, be due to a fraction of cells entering anaphase I. This difficulty in staging *spo13Δ* cells could explain the contradictory results regarding Sgo1 localization in previous studies. To more globally assess whether Sgo1 recruitment to centromeres is affected, I carried out live cell imaging of Sgo1-GFP in metaphase I-arrested cells. This showed that the localisation of Sgo1 in *spo13Δ* mutants appears normal when compared to wild type cells (Fig. 3.6A). Therefore, my data are consistent with the earlier studies (Katis *et al*, 2004b; Lee *et al*, 2004) and I conclude that Spo13 does not affect the recruitment or maintenance of Sgo1 on chromosomes, at least during metaphase I.

Despite normal Sgo1 localization, it was possible that cohesin protection fails in *spo13Δ* due to inproper recruitment of PP2A. Imaging of GFP-tagged Rts1, the relevant PP2A regulatory subunit, throughout meiosis indicated that Rts1 is indeed

present near kinetochores in meiosis I of *spo13Δ* cells (Fig. 3.6B). However, while Rts1-GFP is briefly detected near kinetochores after anaphase onset in wild type cells, it does not return to the pericentromeric region in *spo13Δ* cells (Fig. 3.6B). It is currently unclear whether the inability to maintain or re-accumulate Rts1 near centromeres contributes to the cohesion phenotype of *spo13Δ* mutants but this data indicates that Rts1 is at least present near centromeres in metaphase I, which should allow for cohesin protection to be set up. Unfortunately, it is difficult to make a detailed comparison of Rts1-GFP localisation in metaphase I because wild type cells spend very little time with split kinetochores in meiosis I, which precludes an analysis of Rts1 localisation at the time when homologs have come under tension. In the future, assessing Rts1-GFP localisation in metaphase I-arrested cells should provide a more detailed picture of Rts1 localisation with respect to kinetochores once homologs have bi-oriented and how this might be changed in *spo13Δ* mutants. Taken together, these results indicate that, firstly, *spo13Δ* mutants exhibit a very severe cohesion defect in meiosis I. Secondly, the cohesion protection machinery appears to be set up correctly during metaphase I in *spo13Δ* cells, indicating that the defect may occur at the transition into anaphase or later.

3.3.2. Regulation of Sgo1 degradation in meiosis

Because cohesin protection was apparently set up properly in *spo13Δ* mutants, I reasoned that cells might prematurely cleave pericentromeric cohesin because cohesin protection is lost at the metaphase I to anaphase I transition. Because I had observed decreased levels of Sgo1 in *spo13Δ* mutants (Fig. 3.5B) I first investigated the effects of *SPO13* deletion on Sgo1 levels and localisation by live cell imaging. The first intriguing observation was that, in wild-type cells, Sgo1 is degraded upon anaphase I onset and reaccumulates on chromosomes in meiosis II (Fig. 4.7). This is surprising because according to the current model of cohesin protection, Sgo1 should be required in anaphase to prevent Rec8 from being cleaved by separase. Although this disappearance of Sgo1 in anaphase I in live cells had been noted previously (Katis *et al*, 2010), Sgo1 can be detected near kinetochores in fixed anaphase I cells by chromosome spreads (Marston *et al*, 2004). This discrepancy may simply be

explained by the decreased sensitivity of live cell imaging. This would mean that a small pool of Sgo1 is retained on chromosomes to allow cohesin protection whereas the bulk of Sgo1 is degraded upon anaphase I entry. Furthermore, this theory implies that there must be distinct mechanisms that prevent the degradation of the protective Sgo1 pool and therefore allow cohesin protection in anaphase I. Alternatively, one could hypothesise that all Sgo1 is degraded upon anaphase onset and that cells analysed in previous studies had reached later stages in anaphase where Sgo1 has already started to re-accumulate. This theory, however, poses major implications for cohesin protection as it would indicate that the presence of Sgo1 in anaphase is not required to prevent cohesin cleavage. To distinguish between these two possibilities, it would be best to look at Sgo1 localisation to centromeres by chromosome spreads or ChIP in a time course of synchronous meiotic cultures. If all Sgo1 were indeed degraded upon anaphase entry, then at least some cells should lack Sgo1 near kinetochores shortly after they have gone into anaphase.

The second important point is that in *spo13Δ* mutants Sgo1 disappears upon anaphase entry and does not re-accumulate. Similarly to wild type cells, previous analysis of Sgo1 localisation in *spo13Δ* cells by chromosome spreads showed that Sgo1 is actually still present in binucleate cells (Lee *et al*, 2004). This, once more, suggests that live cell imaging is not sensitive enough to detect small amounts of Sgo1 at pericentromeres. In this case, however, Sgo1 that is retained at centromeres must be incapable of protecting cohesin. Therefore, the main phenotype of *spo13Δ* mutants is that re-accumulation of Sgo1 in meiosis II does not occur. However, this phenomenon has been described for other proteins like Pds1 (Katis *et al*, 2004b) and it is likely that proteins that are normally degraded by the APC/C at anaphase I onset do not re-accumulate because most *spo13Δ* cells only undergo a single division (Klapholz & Esposito, 1980b).

Lastly, the analysis of the *sgo1Δdb* and *ama1Δ* mutants showed that Ama1 does not regulate Sgo1 degradation after prophase (Figs. 3.7 and 3.8) although previous studies indicated that Sgo1 can be a substrate for the APC/C^{Ama1} (Oelschlaegel *et al*, 2005; Okaz *et al*, 2012). In contrast, deletion of the destruction box within Sgo1 prevented degradation of Sgo1 both in anaphase I and anaphase II (Figs. 3.7 and 3.8). While this confirms that Sgo1 is actively degraded in anaphase I, it, importantly,

prevented degradation of Sgo1 in *spo13Δ* mutants. This allowed me to detect Sgo1 near kinetochores even in anaphase I of *spo13Δ* cells (Fig. 3.8). Therefore, I had established a situation where Sgo1 is associated with chromosomes throughout meiosis in *spo13Δ* mutants, allowing me to test whether retaining Sgo1 near kinetochores is sufficient to protect cohesin.

Imaging Rec8-GFP in *spo13Δ sgo1Δdb* cells revealed faint pericentromeric foci of Rec8 during anaphase I (Fig. 3.9). However, the intensity of these foci was barely above background levels and much lower than in wild type cells (Fig. 3.10B), indicating that cohesin protection is not fully restored despite presence of Sgo1 near kinetochores in anaphase. Nevertheless, I tested whether the weak foci of Rec8 are sufficient to hold sister chromatids together using the *CEN5* cohesion assay. This revealed that *spo13Δ sgo1Δdb* double mutants lose cohesion similar to *spo13Δ* single mutants (Fig. 3.10C). Taken together, these findings show that preventing Sgo1 degradation does not rescue the cohesion defect of *spo13Δ* cells.

3.3.3. Regulation of Sgo1 protein levels by Cdc5

Because Sgo1 localisation to centromeres appeared normal in *spo13Δ* cells, I wanted to investigate how potential effectors of Spo13 might affect Sgo1 behaviour in meiosis. An obvious candidate was Cdc5 because it was reported to interact with Spo13 (Matos *et al*, 2008). I first decided to investigate Sgo1 enrichment at centromeres in the absence of Cdc5 and in the *spo13-m2* mutant, where the Spo13-Cdc5 interaction is disrupted. This analysis showed that Sgo1 is significantly enriched at centromeres when Cdc5 is depleted (Fig. 3.11A). This phenotype is independent of its interaction with Spo13 because both *spo13Δ* and *spo13-m2* mutants show a wild type-like enrichment of Sgo1 (Fig. 3.11A). Interestingly, *pCLB2-CDC5* cells also show a significant enrichment of Sgo1 compared to wild type on chromosome arms (Fig. 3.11A). It is tempting to speculate that the increase of Sgo1 at chromosome arms leads to protection of cohesin on chromosome arms. This might explain why some studies have reported Cdc5 as being required for cohesin cleavage (Brar *et al*, 2006; Attner *et al*, 2013) whereas other studies, which used a different allele for Cdc5 depletion, did not (Katis *et al*, 2010). Furthermore,

western blot analysis revealed that cellular levels of Sgo1 are increased compared to wild type in *pCLB2-CDC5* cells (Fig. 3.11B). Cdc5 was previously reported to be required for APC/C activation in mitosis (Charles *et al*, 1998) and depletion of Cdc5 in meiosis causes a metaphase arrest in which the APC/C target Pds1 is stabilised (Lee & Amon, 2003), suggesting that Cdc5 also regulates the APC/C in meiosis. However, my ChIP experiments used a depletion allele of *CDC20* and, therefore, it is unlikely that Cdc5 interferes with the APC/C^{Cdc20} to bring about this phenotype. Although I had previously found that APC/C^{Ama1} does not seem to regulate Sgo1 in meiosis, I wanted to test if this form of the APC/C might be responsible for the observed increase in Sgo1 levels in the absence of Cdc20. However, both the analysis of Sgo1 localisation to centromeres as well as western blot analysis, demonstrated that *ama1Δ* cells do not replicate the phenotype of *pCLB2-CDC5* cells in the *pCLB2-CDC20* background (Fig. 3.12). Therefore, it remains unclear whether Cdc5 regulates Sgo1 stability through the APC/C or any other means. It is possible that Cdc5 might affect APC/C^{Cdh1}. However, so far no meiotic roles for Cdh1 have been described and it is unclear whether Cdh1 is even expressed in meiosis (W. Zachariae, personal communication). Comparison of the effect of *pCLB2-CDC5* and *cdh1Δ* cells have on Sgo1 localisation and protein levels will be useful in determining whether Cdc5 regulates Sgo1 levels though Cdh1.

Next, I wanted to understand whether the increased enrichment of Sgo1 with chromosomes in *pCLB2-CDC5* mutants occurred at specific or unspecific binding sites. Therefore, I chose the *pCLB2-BUB1* allele to decrease levels of Bub1, the protein required to localise Sgo1 to chromosomes (Tang *et al*, 2004; Kiburz *et al*, 2005). Depletion of Bub1 caused a significant decrease of centromere-associated Sgo1 in *pCLB2-CDC5* mutants (Fig. 3.13) and this indicates that Sgo1 indeed binds to specific binding sites in cells without Cdc5. The most likely model for the increased association of Sgo1 with chromosomes in *pCLB2-CDC5* cells is that the increase in Sgo1 levels within the cell allows more Sgo1 molecules to bind to H2A that has been primed through phosphorylation by Bub1. One caveat to the analysis presented here is that the *pCLB2-BUB1* allele does not cause complete loss of Sgo1 at centromeres (Fig. 3.13), even in cells that are otherwise wild type. This suggests that either residual amounts of Bub1 remain in the cell or that there is a pool of Sgo1

that localises independently of Bub1. The former seems more likely since there is currently no evidence that Sgo1 can localise to centromeres in the absence of Bub1. Therefore, using a *bub1Δ* strain in combination with *pCLB2-CDC5* should give insight into whether Sgo1 can localise to centromeres, at least partially, independently of Bub1 in the absence of Cdc5.

The fact that Cdc5 regulates Sgo1 association with chromosomes by controlling its protein levels was interesting because *CDC5* overexpression has been reported to be detrimental to cohesin protection, although it was argued that this resulted from premature degradation of Spo13 (Attner *et al*, 2013). I therefore wanted to determine whether *CDC5* overexpression also impairs cohesin protection even when Spo13 is stabilised by introduction of the L26A mutation (Sullivan & Morgan, 2007). However, in contrast to previously published data, overexpression of *CDC5* did not disrupt cohesin protection in my hands (Fig. 3.14), One possible explanation for this is that the expression levels of *CDC5* in my experiments were lower than in previous experiments (Attner *et al*, 2013). However, the degree of overexpression would be difficult to assess for cells in a microfluidics device and *CDC5* expression levels have not been quantified previously (Attner *et al*, 2013). The findings of my study, however, argue that *CDC5* overexpression does not negatively impact cohesin protection and, consequently, that Sgo1 is not downregulated to a degree that would interfere with its function in meiosis.

Lastly, I wanted to investigate the possibility that Spo13 might act as a Cdc5 inhibitor. In *Drosophila*, a protein called Matrimony (Mtrm) has previously been identified as an inhibitor of Polo kinase (Xiang *et al*, 2007). Interestingly, Mtrm and Spo13 share similar expression patterns in meiosis (Xiang *et al*, 2007) and have a similar destruction box near the N-terminus (Whitfield *et al*, 2013). Given the opposing effects of *spo13Δ* and *pCLB2-CDC5* on Sgo1 levels, I considered the possibility that Spo13 might also function as a Cdc5 inhibitor. In this case, the cohesion defect of *spo13Δ* cells could be a consequence of Cdc5 hyperactivity. Although premature degradation of Sgo1 is unlikely to be the mechanism by which Cdc5 hyperactivity could regulate cohesin protection in *spo13Δ* cells, I reasoned that investigating the effects of *SPO13* deletion on Sgo1 levels and chromosomal association in *pCLB2-CDC5* cells would prove a useful readout of whether Spo13

acts as a Cdc5 inhibitor. If this were the case, then *pCLB2-CDC5 spo13Δ* cells should behave similarly to *pCLB2-CDC5* single mutants. Instead, however, *pCLB2-CDC5 spo13Δ* double mutants showed similar enrichment of Sgo1 to wild type at centromeres by ChIP-qPCR as well as similar protein levels by western blot (Fig. 3.15). One potential explanation for this is that *pCLB2-CDC5 spo13Δ* double mutants still bypass the metaphase I arrest, allowing degradation of Sgo1 and thereby counteracting the absence of Cdc5. To test this, it would be useful to monitor another APC/C substrate, like Pds1, by western blot to determine if it mirrors the patterns observed for Sgo1. While this illustrates that Spo13 does not merely act as an inhibitor of Cdc5, it also highlights that at least the effect of *SPO13* deletion on Sgo1 protein levels is Cdc5-independent. This is further illustrated by the fact that centromeric enrichment and cellular levels of Sgo1 are increased in *pCLB2-CDC5 spo13-m2* mutants when compared to *pCLB2-CDC5 spo13Δ* cells (Fig. 3.15).

Taken together, these results suggest that depletion of Cdc5 results in an increase of cellular Sgo1 levels that is independent of APC/C^{Cdc20} and APC/C^{Ama1}. As a consequence, Sgo1 association with chromosomes increases. However, it is unlikely that Cdc5 or the Spo13-Cdc5 interaction regulate cohesin protection by altering cellular levels of Sgo1.

CHAPTER 4: SPO13 REGULATES COHESIN KINASES CDC5, HRR25 AND DDK FOR MONO-ORIENTATION AND COHESIN PROTECTION

4.1. Introduction

Our current understanding of proteins that regulate, and those that are regulated by Spo13 is very limited. In budding yeast, mono-orientation depends on the interaction of Spo13 and polo kinase Cdc5 (Matos *et al*, 2008). However, whether this interaction is also important for cohesin protection is currently unknown. The functional homolog of Spo13 in mice, MEIKIN, also interacts with Polo-like kinase PLK1 (Kim *et al*, 2014) and it is thought that its main function is to recruit PLK1 to the pericentromere as PLK1 inhibition causes phenotypes similar to deletion of *Meikin* (Kim *et al*, 2014). Intriguingly, fission yeast Moa1 interacts with Polo-like kinase Plo1 as well (Kim *et al*, 2014). When the polo-binding domain (PBD) of *moa1* is mutated to prevent binding of Plo1, cells will undergo equational segregation similarly to *moa1Δ* mutants (Kim *et al*, 2014).

The aim of this chapter is to identify novel pathways by which Spo13 regulates cohesin protection. I will investigate the importance of the Spo13-Cdc5 interaction for cohesin protection, how Spo13 may impact the Sgo1-cohesin interaction and analyse the interplay of Spo13 and the cohesin kinases Hrr25 and DDK.

4.2. Results

4.2.1. Spo13 recruits Cdc5 to kinetochores for proper mono-orientation but not cohesin protection

4.2.1.1. Spo13 is required for full association of Cdc5 with centromeres

Since I could not find any evidence that the Spo13-Cdc5 interaction regulates either Sgo1 stability or its recruitment to centromeres, I decided to investigate the impact that loss of Spo13 or mutation of its PBD might have on Cdc5 itself. Previous studies in mice had suggested that Spo13's functional homologue MEIKIN recruits

PLK1 to centromeres and that this was crucial to its role in cohesin protection and mono-orientation (Kim *et al*, 2014). Therefore, I first wanted to test the effect mutation or deletion of *SPO13* has on Cdc5 recruitment to chromosomes. I pulled down Cdc5-3V5 in metaphase I-arrested cells in wild type, *spo13Δ* and *spo13-m2* cells and assessed its chromosomal association by ChIP-qPCR. Interestingly, Cdc5 association with both *CEN3* and *CEN4* is significantly reduced similarly in *spo13Δ* and *spo13-m2* mutants (Fig. 4.1A). On an arm site on chromosomal 4, however, Cdc5 recruitment is unaffected by *SPO13* mutants (Fig. 4.1A). To ensure that these differences are not caused by a reduction in global Cdc5 levels, I performed western blotting on cells from the ChIP cultures. Since Cdc5-3V5 levels are approximately equal in wild type and mutant strains, these results suggest that *SPO13* and the Spo13-Cdc5 interaction are required for full recruitment of Cdc5 to centromeres, but not to chromosome arms.

4.2.1.2. Overexpression of *SPO13* causes enhanced recruitment of Cdc5 to centromeres

Given the reduction in centromeric Cdc5 levels in *spo13Δ* and *spo13-m2* mutants, I wanted to know whether Spo13 might be able to directly recruit Cdc5 to centromeres. I reasoned that overexpression of *SPO13* might cause Spo13 to accumulate at centromeres and, subsequently, recruit more Cdc5. However, if other factors are involved in Cdc5 localisation to centromeres then these might limit the amount of Cdc5 that associates with centromeres even when Spo13 is in excess. As a control, I also overexpressed the *spo13-m2* mutant in which additional Cdc5 recruitment should be prevented due to the loss of the Spo13-Cdc5 interaction. To assay Cdc5 association with chromosomes I performed ChIP-qPCR of Cdc5-3V5 and Spo13-3Flag in metaphase I arrested cells. As expected, overexpression of *SPO13* led to a signficant increase in Cdc5 levels at *CEN3*, *CEN4* and *CEN5* (Fig. 4.2A). Additionally, Cdc5's recruitment to an arm site on chromosome 4 is also enhanced. In contrast, an excess of Spo13-m2 did not alter Cdc5 localisation to chromosomes when compared to endogenous Spo13-m2 levels (Fig. 4.2A). Next, I wanted to determine whether overexpression of *SPO13* or *spo13-m2* indeed caused

stronger association of the corresponding proteins to chromosomes. Suprisingly, Spo13 levels were only increased at an arm site on chromosome 4, albeit very modestly. At centromeres, however Spo13 levels remained roughly the same (Fig. 4.2B), indicating that Spo13 binding sites at centromeres are saturated in wild type cells already. Furthermore, Spo13-m2 exhibited significantly decreased association with centromeres compared to wild type cells, even under overexpression conditions (Fig. 4.2B). This suggests that the mutant is inherently compromised in its ability to bind to centromeres. To confirm that *SPO13* overexpression led to an increase in Spo13 protein and to test the effect of overexpression on Cdc5 levels, I performed western blotting on the ChIP cultures. This confirmed that both *SPO13* and *spo13-m2* had been overexpressed successfully and revealed lower amounts of the *spo13-m2* allele compared to wild type (Fig. 4.2C), suggesting decreased stability. Cdc5 levels were largely unaffected, although there was a modest increase in Cdc5 levels in *pCUP1-SPO13* cells, which may account for the modest increases of Cdc5 association with chromosomes. Taken together, these results suggest that (i) *SPO13* overexpression causes increased association of Cdc5 with chromosomes and (ii) reduced centromere-associated Spo13 leads to decreased localisation of Cdc5 to centromeres in *spo13-m2* cells. Furthermore, loss of the Spo13-Cdc5 interaction is likely to contribute to the reduction in centromeric Cdc5 enrichment in *spo13-m2* mutants.

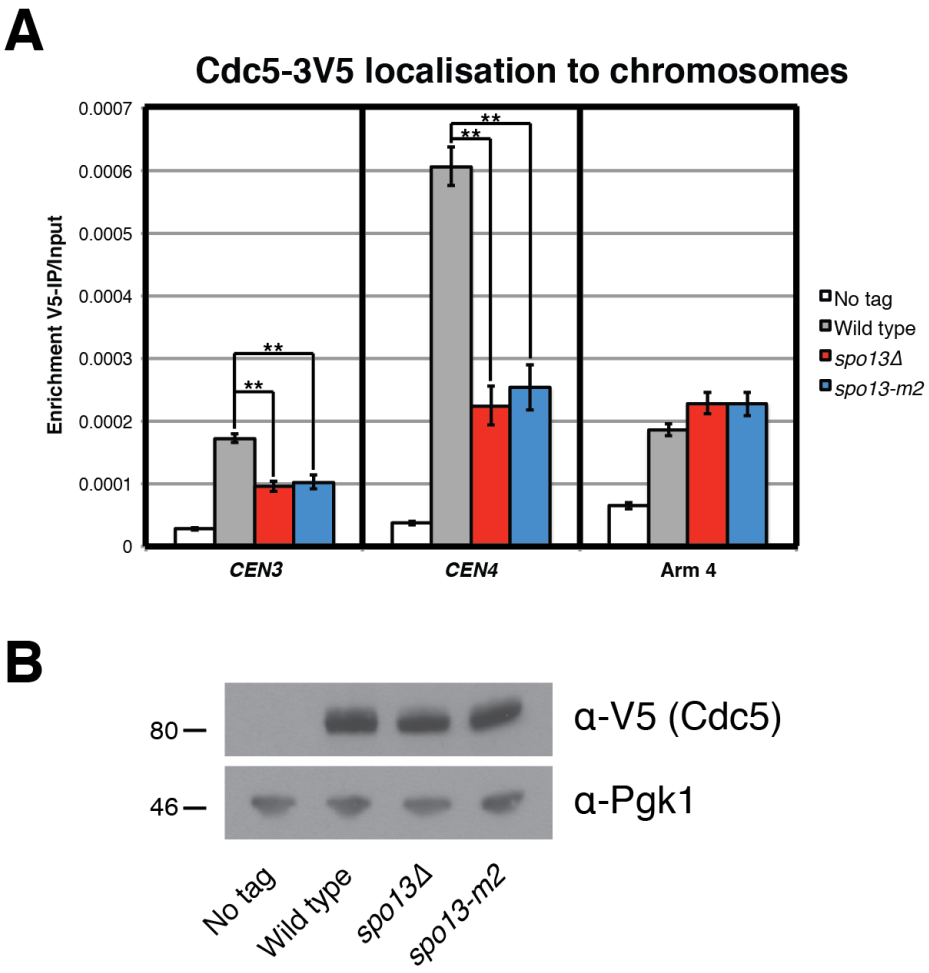

Figure 4.1: Full recruitment of Cdc5 to centromeres requires Spo13. (A) Cdc5 levels at *CEN3* and *CEN4* are reduced in *SPO13* mutants. ChIP-qPCR of Cdc5-3V5. No tag (AMy8067), wild type (AMy14051), *spo13Δ* (AMy14052) and *spo13-m2* (AMy15128) cells carrying *pCLB2-CDC20* were arrested in SPO media for 6 hours before fixing cells for α-V5 ChIP-qPCR. Error bars represent standard error of the mean for 4 independent experiments (**p < 0.01). (B) *SPO13* deletion does not affect Cdc5 stability. TCA fixed samples were collected for western blot analysis just prior to fixing cells for ChIP. A representative blot is shown.

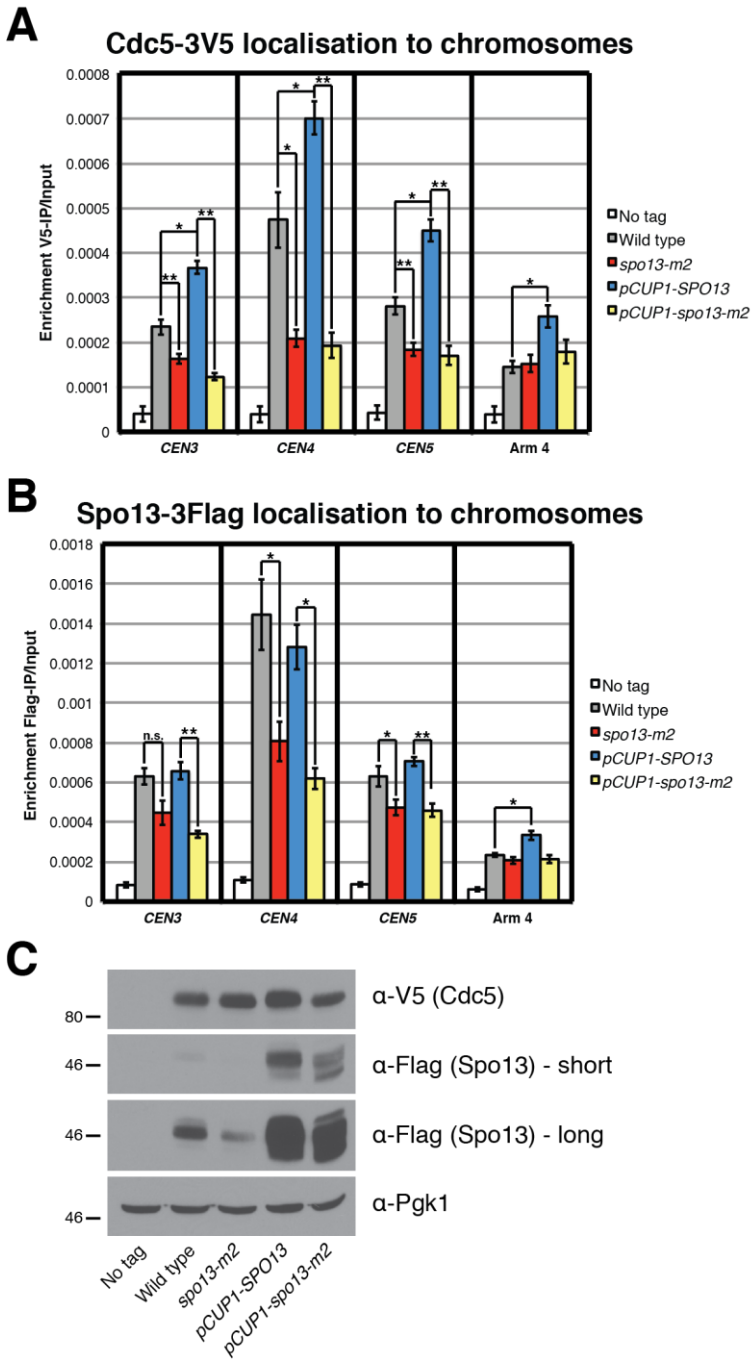

Figure 4.2: Overexpression of *SPO13* enhances Cdc5 recruitment to chromosomes. (A and B) No tag (AMy8067), wild type (AMy15717), *spo13-m2* (AMy15718), *pCUP1-SPO13* (AMy15797) and *pCUP1-spo13-m2* (AMy15798) cells carrying *pCLB2-CDC20* were arrested in SPO media for 4.5 hours before adding 50μM $CuSO_4$. After a further 1.5 hours cells were fixed for α-V5 and α-Flag ChIP-qPCR. Error bars represent standard error of the mean for 4 independent experiments (*p < 0.05, **p < 0.01, n.s. = not significant). (A) Cdc5 levels at centromeres and an arm site are increased when *SPO13* is overexpressed. ChIP-qPCR of Cdc5-3V5. (B) Spo13-m2 fails to associate fully with centromeres. ChIP-qPCR of Spo13-3Flag. (C) *SPO13* overexpression stabilises Cdc5. TCA fixed samples were collected for western blot analysis just prior to fixing cells for ChIP. A representative blot is shown.

4.2.1.3. Reduction of centromeric Cdc5 is specific to *SPO13* mutants

Although I found Cdc5 levels to be reduced in both *spo13Δ* and *spo13-m2* mutants, I was concerned that this effect may not be specific and rather a consequence of the mono-orientation defect of these two mutants. Previously, it was shown that sister kinetochore bi-orientation can reduce the enrichment of proteins localising to centromeres when assayed by ChIP-qPCR, even when such proteins are not tension-regulated (Nerusheva *et al*, 2014). Therefore, I wanted to test whether the decreased enrichment of Cdc5 at centromeres is specific to mutants of *SPO13* or whether this is generally observed in mono-orientation mutants. I decided to perform ChIP-qPCR of Cdc5-3V5 and Spo13-3Flag in metaphase I arrested cells and compare the *spo13-m2* mutant to a *mam1Δ* strain, which is defective for mono-orientation only. When assaying *CEN3*, *CEN4* and *CEN5* I observed that the average enrichment of Cdc5-3V5 is similar in wild type and *mam1Δ* cells whereas it is reduced in *spo13-m2* cells (Fig. 4.3A). At *CEN4* and *CEN5* Cdc5-3V5 is significantly enriched in *mam1Δ* cells over *spo13-m2* cells. Similarly, Spo13-3Flag enrichment at centromeres is significantly higher in *mam1Δ* mutants than in *spo13-m2* mutants (Fig. 4.3B). Together, these data demonstrate that the reduction in centromeric Cdc5 in mutants of *SPO13* is not a consequence of mono-orientation defects.

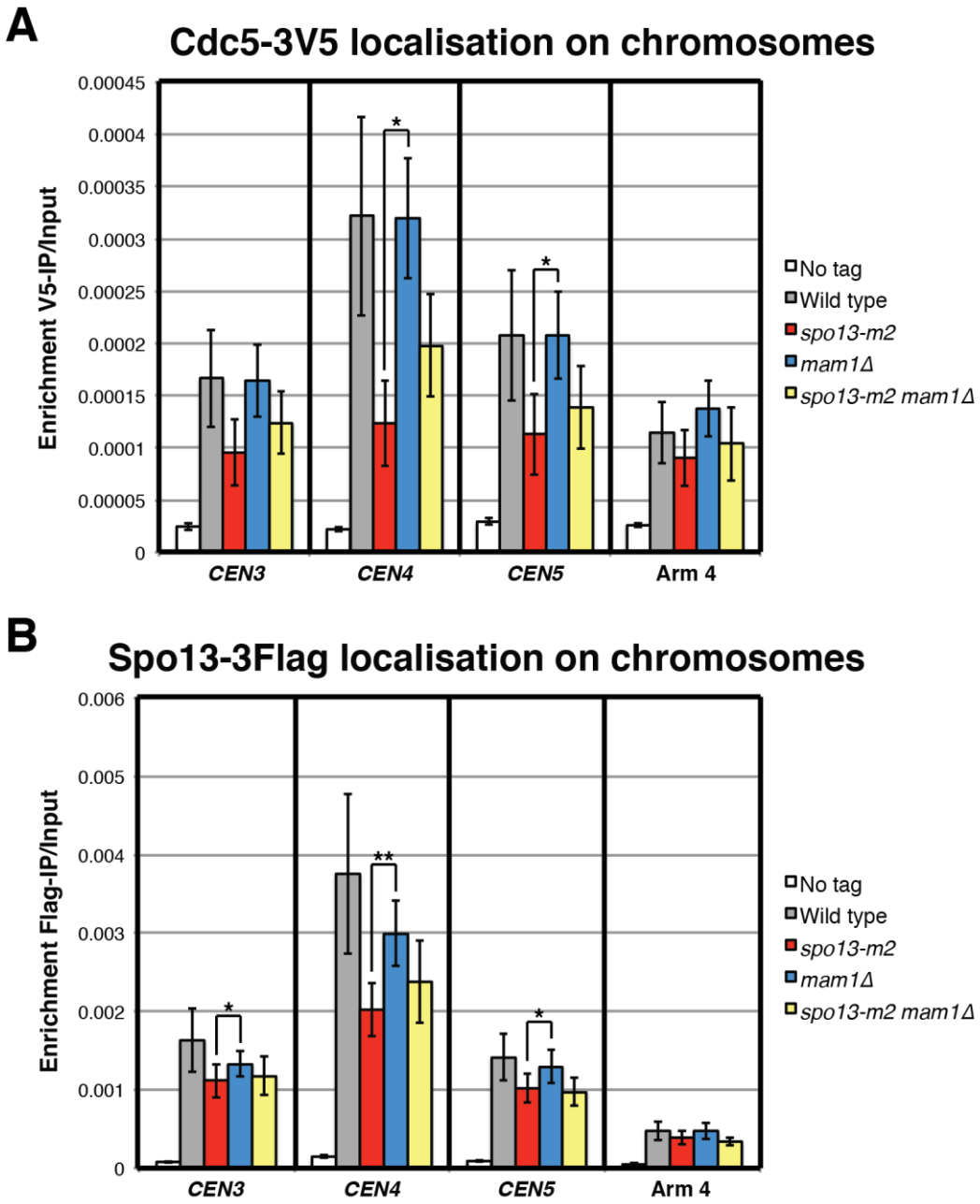

Figure 4.3: Reduction in centromeric Cdc5 is specific to *SPO13* mutants. (A and B) No tag (AMy8067), wild type (AMy15717), *spo13-m2* (AMy15718), *mam1Δ* (AMy17492) and *spo13-m2 mam1Δ* (AMy17493) cells carrying *pCLB2-CDC20* were arrested in SPO media for 6 hours before fixing for α-V5 and α-Flag ChIP-qPCR. Error bars represent standard error of the mean for 4 independent experiments (*p < 0.05, **p < 0.01). (A) Cdc5 levels at centromeres are comparable to wild type in *mam1Δ* cells. ChIP-qPCR of Cdc5-3V5. (B) Spo13 association with centromeres is higher in *mam1Δ* mutants than in *spo13-m2* cells. ChIP-qPCR of Spo13-3Flag.

4.2.1.4. Cdc5 tethering to kinetochores rescues the mono-orientation defect of *spo13Δ* mutants

Given the specific reduction of Cdc5 levels in *spo13Δ* and *spo13-m2* mutants, I wanted to test the significance of recruiting Cdc5 to centromeres. Therefore, I decided to tether Cdc5 to centromeres in the absence of *SPO13* and determine whether this rescues the *spo13Δ* cohesion defect using the *CEN5* cohesion assay (Fig. 2.8). To allow tethering of Cdc5 to kinetochores (Fig. 4.4), I tagged Mtw1, an essential kinetochore protein within the Dsn1 complex, with GFP-binding protein (GBP), a nanobody derived from a GFP-chromobody (Rothbauer *et al*, 2006). Additionally, I tagged Cdc5 with GFP. However, to allow imaging of *CEN5* dots in the green channel without disturbance from the Cdc5-GFP signal, I introduced the G67A mutation on the GFP tag to make it non-fluorescent (nfGFP) (Kutrowska *et al*, 2007). When trying to combine *CDC5-nfGFP* and *MTW1-GBP* into the same strain, however, I found that this combination is often synthetically lethal (data not shown). Therefore, I put *CDC5-nfGFP* under the meiosis-specific *SPO21* promoter. This promoter is, like the *CDC5* promoter, responsive to *NDT80* and closely mirrors the expression pattern of the *CDC5* promoter in meiosis (Chu *et al*, 1998). Choosing the *SPO21* promoter therefore allowed me to tether Cdc5 to kinetochores only in meiosis without disturbing its normal expression pattern. In order to compensate for the lack of *CDC5* expression in mitosis (which is lethal), I introduced an additional copy of *CDC5* under the mitosis-specific *CLB2* promoter at the *URA3* locus, which allows viability of *pSPO21-CDC5-nfGFP* strains. To avoid Cdc5 being tethered away from other important substrates in meiosis, I only used one copy of *pSPO21-CDC5-nfGFP* in tethering strains while the second copy was untagged *CDC5* under its native promoter. Lastly, I had to modify the *CEN5* dot system. Previously, I had used TetR-GFP to visualise *CEN5* dots but I reasoned that the presence of another GFP tagged protein was likely to interfere with efficient tethering of Cdc5-nfGFP. Instead, I created a version of TetR that was tagged with a yeast expression optimised version of mEos3.2 (Zhang *et al*, 2012), a monomeric version of Eos, a photo-switchable protein that normally fluoresces in the green channel until exposed to UV light (Wiedenmann *et al*, 2004). mEos3.2 was an ideal choice for this experiment because

it fluoresces in the green channel with high brightness (Zhang *et al*, 2012), but is not a GFP-derivative and will therefore not interfere with the tethering assay.

I first analysed the segregation of *CEN5* dots in wild type and *spo13Δ* cells to ensure that the complex strain background does not interfere with the expected segregation patterns. Indeed, the large majority of wild type cells still mono-orient in meiosis I whereas *spo13Δ* mutants display an approximate 50:50 ratio of cells that segregate *CEN5* dots reductionally or equationally (Fig. 4.5B). When tethering Cdc5 to kinetochores in wild type cells, the pattern of *CEN5* segregation in meiosis I does not change (Fig. 4.5B). Interestingly, however, when tethering Cdc5 to kinetochores in *spo13Δ* cells, over 90% of cells will now segregate *CEN5* dots to the same pole after Pds1 degradation. While this makes it difficult to assess the importance of kinetochore-associated Cdc5 in cohesin protection, it indicates that one of the key functions of Spo13 is to recruit Cdc5 to kinetochores to allow mono-orientation.

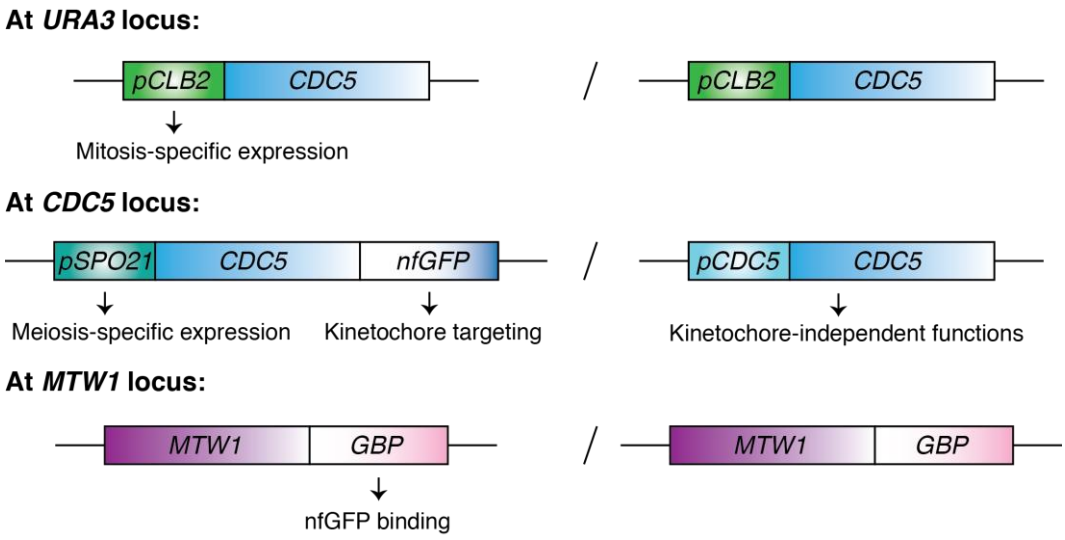

Figure 4.4: Cdc5 tethering to kinetochores. At the *URA3* locus, an additional copy of *CDC5* is inserted under control of the *CLB2* promoter to drive expression in mitosis. This facilitates propagation of the *pSPO21-CDC5-nfGFP* construct, which is meiosis-specific, during strain construction. Expression from the *SPO21* promoter prevents kinetochore-targeting of Cdc5-nfGFP in mitosis, which is usually lethal. nfGFP is a non-fluorescent version of GFP which allows visualisation of other proteins fused to a non-GFP-derived fluorescent protein in the green channel. The GBP tag on Mtw1 allows binding of Cdc5-nfGFP and thereby recruits it to kinetochores. However, cells only contain one copy of *CDC5-nfGFP*; the other copy is untagged *CDC5* under its own promoter and this allows Cdc5 to carry out functions within other compartments of the cell.

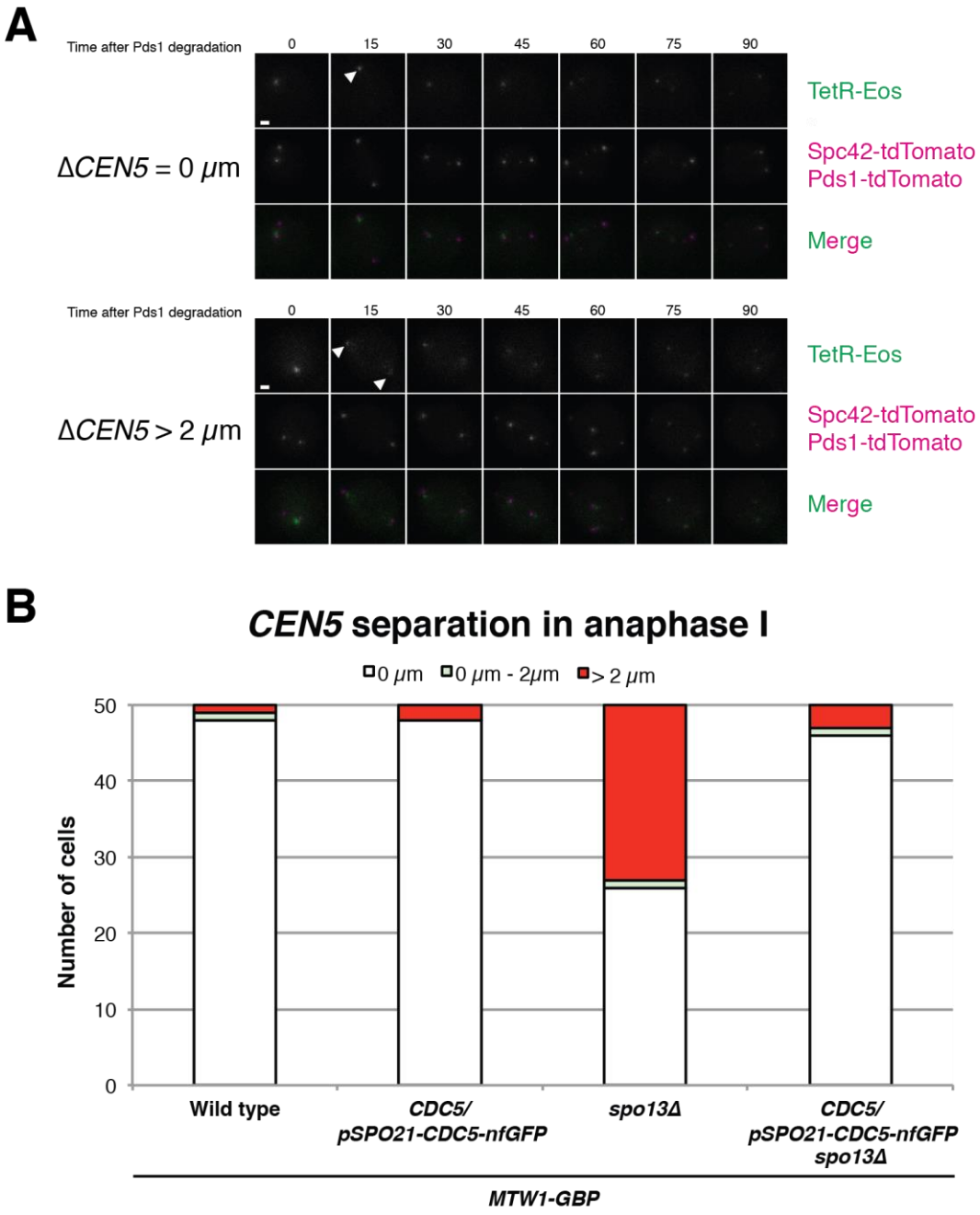

Figure 4.5: Cdc5 tethering to centromeres rescues mono-orientation in spo13Δ mutants. (A and B) Wild type (AMy19286) and *spo13Δ* (AMy19288) cells, or corresponding strains heterozygously expressing *CDC5-nfGFP* (AMy19287 and AMp19289, respectively) were grown in SPO media for 2.5 hours before imaging at 15 min intervals. (A) Example sequences of cells going through meiosis. Scale bars represent 1μm. Arrows indicate *CEN5*-Eos foci. (B) The distance between *CEN5*-Eos foci was measured in 50 cells after Pds1 degradation but prior to SPB re-duplication for the mutants indicated.

4.2.1.5. Cdc5 recruitment to kinetochores is not required for cohesin protection

Because tethering of Cdc5 to kinetochores rescued mono-orientation and thereby precluded an analysis of cohesion at this stage, I looked for an alternative way to determine whether Cdc5 recruitment to kinetochores is important for cohesin protection. The *spo13-m2* mutant was ideal for this as Spo13 is still present in cells, allowing it to carry out Cdc5-independent functions, but Cdc5 recruitment to kinetochores is impaired (Fig. 4.1A). Therefore, I carried out the *CEN5* cohesion assay on the *spo13-m2* mutant. Additionally, I combined it with a *mam1Δ* mutant because cohesion defects are more obvious in this background (*cf.* Fig. 3.3B). Although *spo13-m2* mutants were published to have a mono-orientation defect (Matos *et al*, 2008), 78% of cells successfully segregated homologs in the first meiotic division in the *CEN5* dot assay (Fig. 4.6), precluding strong conclusions about its cohesion phenotype. However, when combined with the *mam1Δ* mutant, it became apparent that the *spo13-m2* mutant did not allow *mam1Δ* cells to split *CEN5* dots a great distance (Fig. 4.6) which is in stark contrast to *spo13Δ mam1Δ* mutants (Fig. 3.3). Therefore, I conclude that Spo13's role in cohesin protection is distinct from its interaction with Cdc5 and that the centromeric pool of Cdc5 that is recruited by Spo13 is not required for cohesin protection. However, I cannot exclude the possibility that residual Spo13-Cdc5 interaction in the *spo13-m2* mutant (Matos *et al*, 2008) is sufficient to mediate cohesin protection.

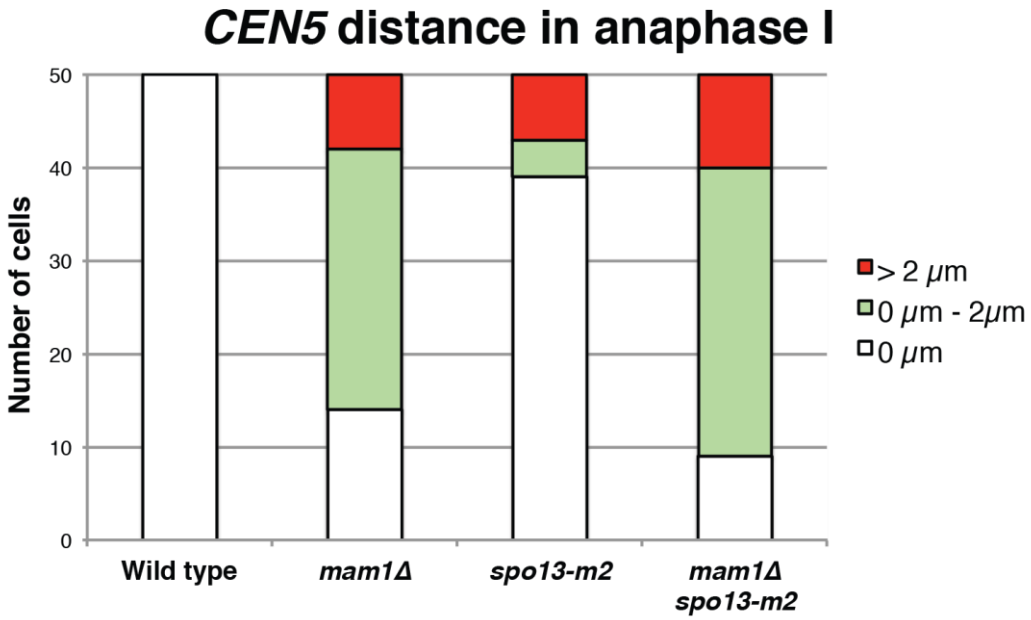

Figure 4.6: Centromeric Cdc5 is not required for cohesin protection. Wild type (AMy15190), *mam1Δ* (AMy15119), *spo13-m2* (AMy17494) or *mam1Δ spo13-m2* (AMy17544) cells were induced to sporulate and transferred to a microfluidics device after 2.5 hours in SPO media. The distance between *CEN5-GFP* foci was measured in 50 cells after Pds1 degradation but prior to SPB re-duplication for the mutants indicated.

4.2.2. Meiotic *SPO13* overexpression causes overprotection of cohesin by recruiting additional Sgo1 to centromeres

4.2.2.1. Overexpression of *SPO13* enhances cohesin protection

Since I could not find any evidence that Spo13 regulates Sgo1 for cohesin protection, I considered the possibility that Spo13 may be able to protect cohesin independently of Sgo1. This idea had been proposed previously since mitotic overexpression of *SPO13* prevented cleavage of cohesin even in the absence of Sgo1 (Lee *et al*, 2004). However, due to technical limitations the effect of *SPO13* overexpression in meiosis has not been investigated previously (Lee *et al*, 2002). Therefore, I decided to investigate the effect of *SPO13* overexpression on cohesin protection by putting it under the control of the copper-inducible *CUP1* promoter. First, I wanted to investigate the pattern of cohesin localisation in meiosis I. Previously, it was shown that mitotic overexpression of *SPO13* can inhibit cohesin cleavage, although there is an argument about whether it can prevent cleavage of both Scc1 and Rec8 (Lee *et al*, 2002) or Rec8 only (Shonn *et al*, 2002). I decided to image Rec8-GFP in cells released from an *NDT80* prophase block (Carlile & Amon, 2008) and overexpressing *SPO13* from the exit of prophase onwards. Additionally, I compared overexpression of *SPO13* to overexpression of *spo13-m2* to assess whether any phenotypes are independent of its association with Cdc5.

When analysing the pattern of Rec8 localization, I firstly noticed that overexpression of *SPO13* does not prevent loss of arm cohesin (Fig. 4.7A) although this was previously reported for *SPO13* overexpression in mitosis (Lee *et al*, 2002; Shonn *et al*, 2002). Secondly, a small fraction of *spo13-m2* and *pCUP1-spo13-m2* cells did not display pericentromeric Rec8 foci in anaphase I, indicating that cohesin protection was impaired (Fig. 4.7A/B). I then measured the intensity of Rec8 in the pericentromere in anaphase I to determine whether *SPO13* overexpression had any effect on protection of cohesin. Interestingly, *pCUP1-SPO13* cells displayed a significant increase in Rec8-GFP levels in the pericentromere in anaphase I (Fig. 4.7C), indicating that cohesin protection is more efficient. *spo13-m2* mutants, on the other hand, showed a significant decrease in pericentromeric cohesin in anaphase I

(Fig. 4.7C), although the effect is much less severe than that of a *spo13Δ* mutant (*cf.* Fig. 3.2B). Overexpression of *spo13-m2* restores anaphase I cohesin levels to wild type, indicating that the loss of cohesin in *spo13-m2* cells may be due to decreased stability of *spo13-m2* (Fig. 4.2C) rather than the loss of the Spo13-Cdc5 interaction. Taken together, these results suggest that overexpression of *SPO13* enhances cohesin protection in the pericentromere but does not extend cohesin protection to chromosome arms.

4.2.2.2. Cohesin overprotection upon *SPO13* overexpression requires Sgo1

Previously, mitotic overexpression of *SPO13* was found to protect cohesin independently of Sgo1 (Lee *et al*, 2004). To test whether the same is true for the overprotection of pericentromeric cohesin that I observed in meiosis, I depleted Sgo1 in cells overexpressing *SPO13* by putting it under the control of the mitosis-specific *CLB2* promoter and assessed cohesin protection by imaging Rec8-GFP in meiotic cells. As expected, cohesin is cleaved along the length of chromosomes in *pCLB2-SGO1* cells (Fig. 4.8A/B). Although *SPO13* overexpression once again led to an increase in pericentromeric Rec8 in anaphase (Fig. 4.8C), depletion of Sgo1 completely abolished cohesin protection in *pCUP1-SPO13* cells (Fig. 4.8). Therefore, I conclude that the increased protection of cohesin upon *SPO13* overexpression requires Sgo1 and that *SPO13* overexpression in meiosis is insufficient for cohesin protection in the absence of Sgo1.

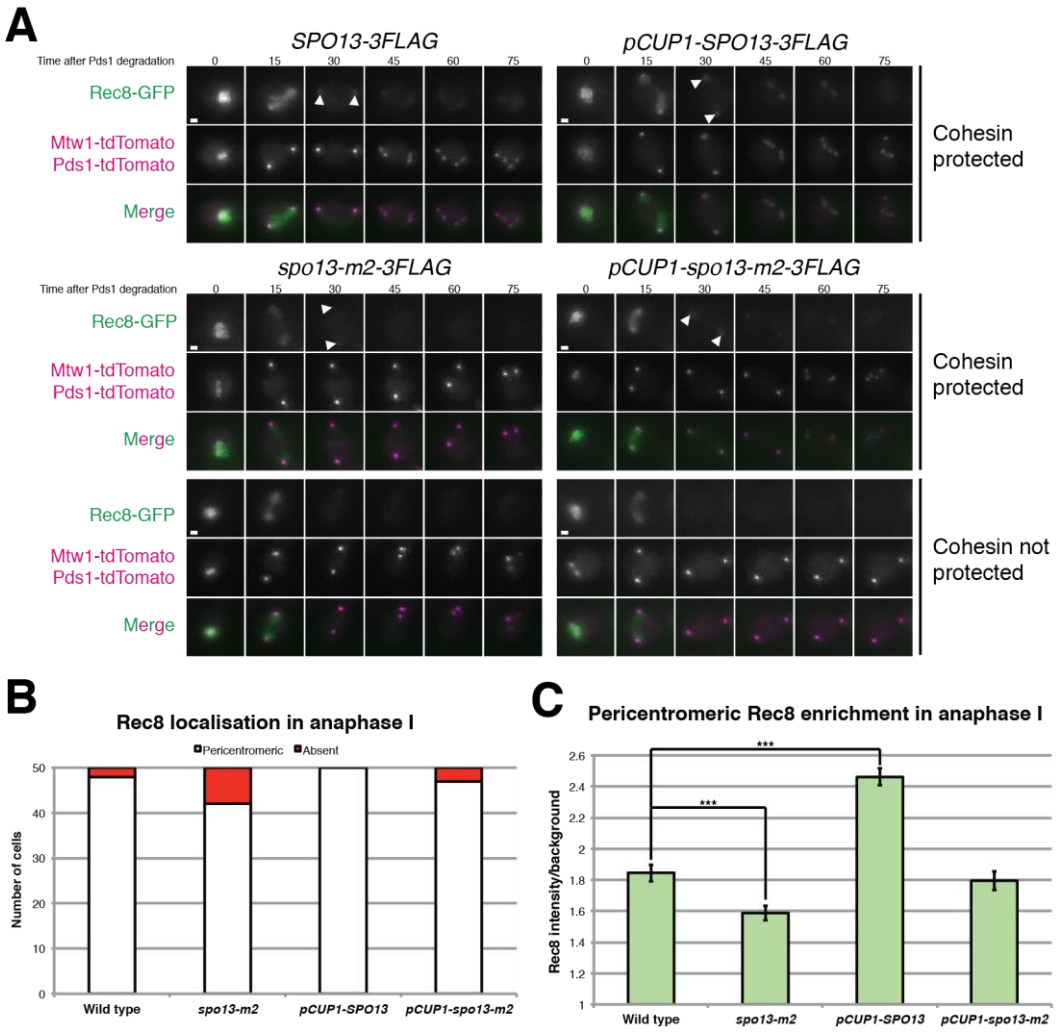

Figure 4.7: *SPO13* overexpression leads to overprotection of pericentromeric cohesin. (A-C) *SPO13-3FLAG* (AMy16378), *spo13-m2-3FLAG* (AMy16379), *pCUP1-SPO13-3FLAG* (AMy16520) or *pCUP1-spo13-m2-3FLAG* (AMy16521) cells were induced to sporulate and 25μM $CuSO_4$ added after 4.5 hours in SPO media. Cells were released from prophase by addition of 1μM β-estradiol after 5 hours and transferred onto a microfluidics plate 15 minutes later. Images were taken at 15 min intervals. (A) Representative movies are shown. Scale bars represent 1μm. Arrows highlight pericentromeric cohesin retained after the first round of cohesin cleavage. (B) Cells were subjectively scored for the presence of pericentromeric cohesin after Pds1 degradation (n = 50). (C) The average intensity of Rec8 was measured in the area occupied by kinetochores in anaphase I as described in Fig. 2.7. Error bars show standard error of the mean (***p < 0.001).

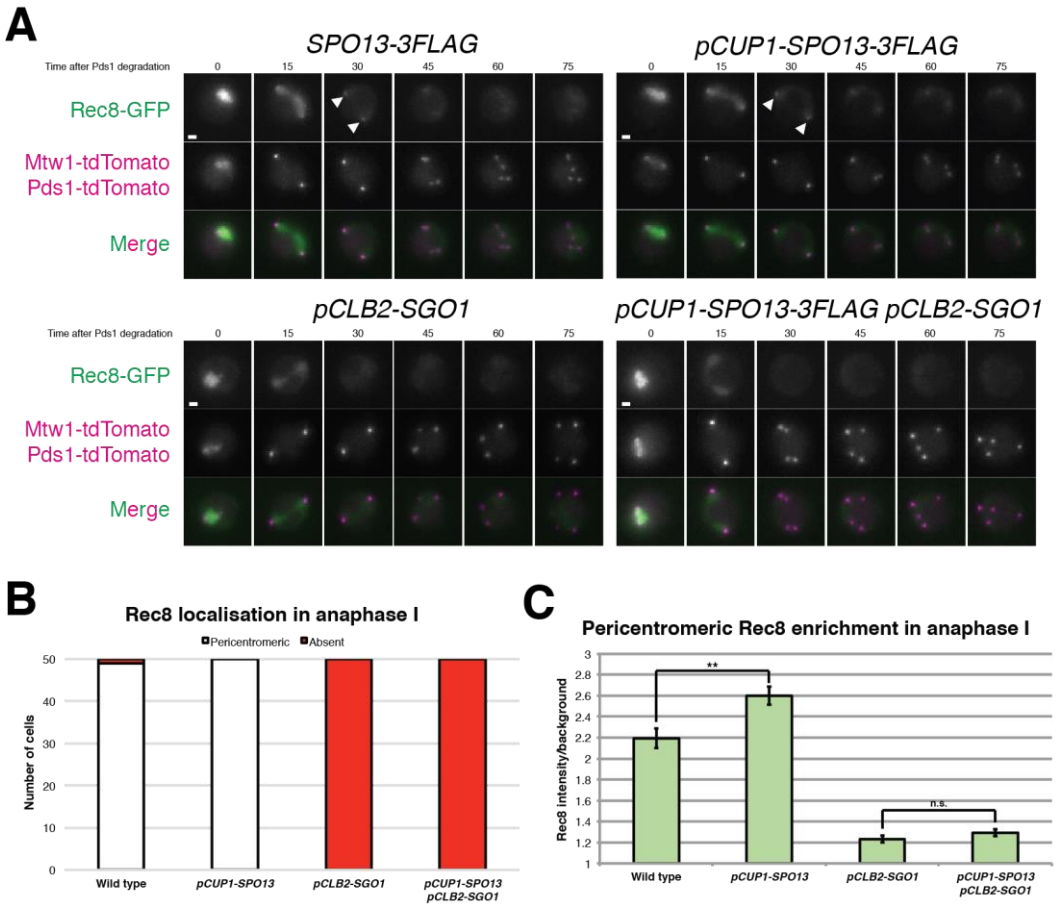

Figure 4.8: Overprotection of pericentromeric cohesin depends on Sgo1. (A-C) *SPO13-3FLAG* (AMy16378), *pCUP1-SPO13-3FLAG* (AMy16520), *pCLB2-SGO1* (AMy17481) or *pCUP1-SPO13-3FLAG pCLB2-SGO1* (AMy17482) cells were induced to sporulate and 25μM $CuSO_4$ added after 4.5 hours in SPO media. Cells were released from prophase by addition of 1μM β-estradiol after 5 hours and transferred onto a microfluidics plate 15 min later. Images were taken at 15 min intervals. (A) Representative movies are shown. Scale bars represent 1μm. Arrows highlight pericentromeric cohesin retained after the first round of cohesin cleavage. (B) Cells were subjectively scored for the presence of pericentromeric cohesin after Pds1 degradation (n = 50). (C) The average intensity of Rec8 was measured in the area occupied by kinetochores in anaphase I as described in Fig. 2.7. Error bars show standard error of the mean (***p < 0.001).

4.2.2.3. Overexpression of *SPO13* increases Sgo1 recruitment to centromeres

Because cohesin overprotection under *SPO13* overexpression conditions relies on Sgo1, I decided to investigate whether overexpression of *SPO13* affects chromosomal levels of Sgo1. To test this, I performed ChIP-qPCR of Sgo1-6Ha in metaphase I arrested cells overexpressing either *SPO13* or *spo13-m2* (to determine whether any effects depend on the Spo13-Cdc5 interaction). At three centromeres – *CEN3*, *CEN4* and *CEN5* – overexpression of *SPO13* causes a significant increase of Sgo1 levels compared to wild type cells (Fig. 4.9A). Surprisingly, the same effect is observed when *spo13-m2* is overexpressed (Fig. 4.9A). In contrast, Sgo1 localisation to an arm site on chromosome IV is not affected. To determine whether these effects might be explained by Sgo1 stabilisation under *SPO13* overexpression conditions, I performed western blot on the ChIP cultures. Although overexpression of *SPO13* and *spo13-m2* was successful, cellular Sgo1 levels were comparable in all strains (Fig. 4.9B). Therefore, I conclude that *SPO13* overexpression can recruit additional Sgo1 to centromeres largely independently of Cdc5 (given the residual interaction of Spo13-m2 and Cdc5), which allows more efficient protection of cohesin in meiosis I.

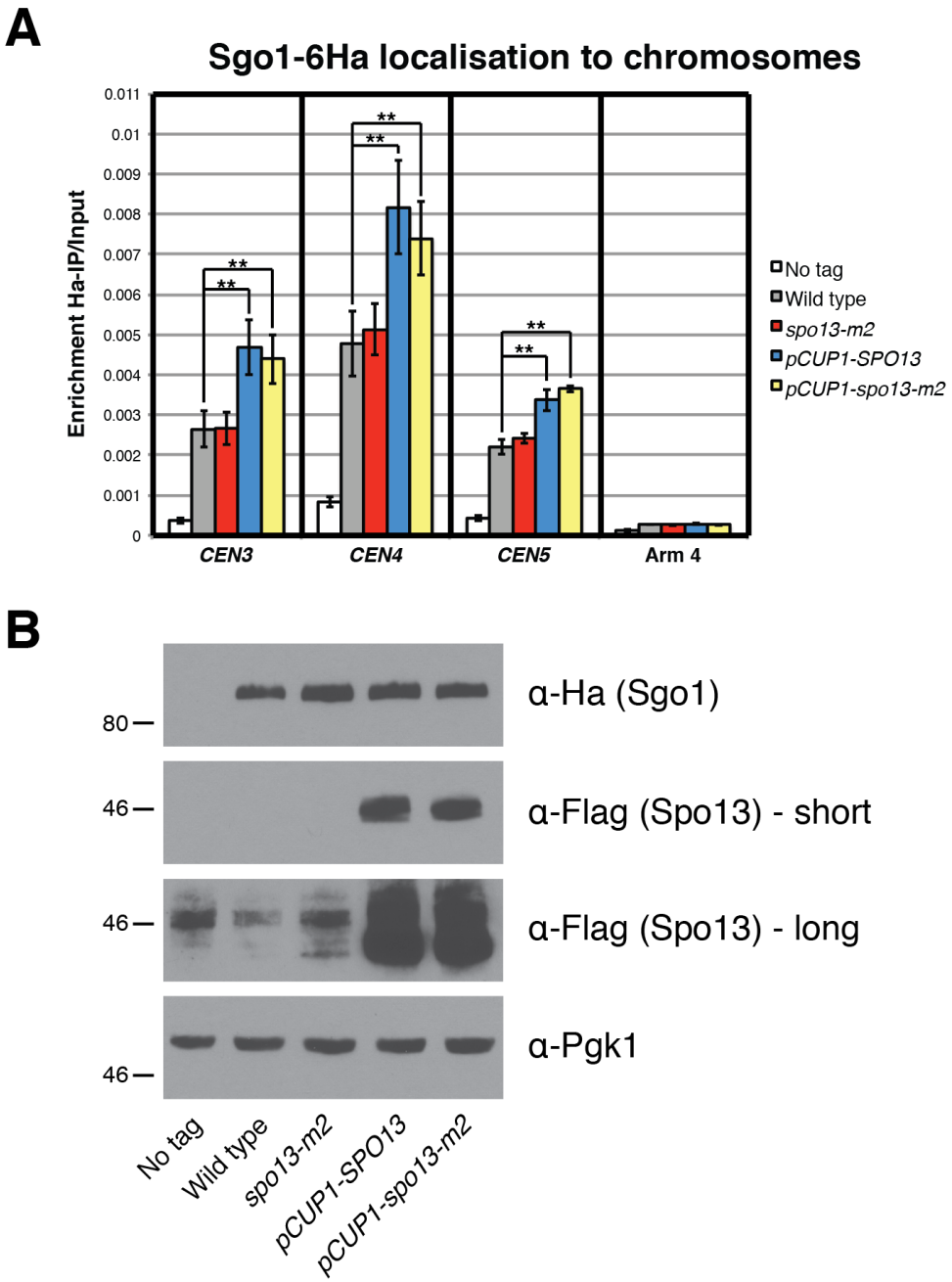

Figure 4.9: *SPO13* overexpression recruits additional Sgo1 to centromeres. (A and B) No tag (AMy11699), wild type (AMy15719), *spo13-m2* (AMy15790), *pCUP1-SPO13* (AMy15996) and *pCUP1-spo13-m2* (AMy15997) cells carrying *pCLB2-CDC20* were induced to sporulate and 25μM $CuSO_4$ added after 4.5 hours in SPO media. After a further 1.5 hours cells were fixed for α-Ha ChIP-qPCR. (A) Sgo1 is increased at centromeres when *SPO13* or *spo13-m2* are over-expressed. ChIP-qPCR of Sgo1-6Ha. Error bars represent standard error of the mean for 4 independent experiments (**p < 0.01). (B) *SPO13* and *spo13-m2* overexpression do not affect Sgo1 stability. TCA fixed samples were collected for western blot analysis just prior to fixing cells for ChIP. A representative blot is shown.

4.2.3. Cohesin is protected in *spo13Δ* mutants when Sgo1 and Rec8 interact

4.2.3.1. Sgo1 and cohesin are in close proximity in *spo13Δ* mutants

The fact that *SPO13* overexpression caused recruitment of additional Sgo1 to centromeres posed a conundrum because deletion of *SPO13* had no effect on Sgo1 centromere localisation despite a decrease in cellular Sgo1 levels (Fig. 3.5). One possible explanation for this is that there are two different pools of Sgo1 in the cell, only one of which relies on *SPO13* for proper localisation. This would mean that the majority of Sgo1 at centromeres, which is detected by ChIP and live cell imaging, localises independently of *SPO13*. However, a much smaller pool is localised through *SPO13* so that overexpression of *SPO13* causes additional recruitment of Sgo1 to centromeric regions. Given that *SPO13* overexpression causes overprotection of cohesin, it seems likely that *SPO13* affects the pool of Sgo1 that is involved in cohesin protection. The idea that two distinct Sgo1 pools exist at centromeres has been proposed previously because some mutants, like cells overexpressing the cyclin *CLB3*, are defective for cohesion although Sgo1 and PP2A are appropriately localised (Miller *et al*, 2012). In human cells, the presence of two distinct Sgo1 pools is important to protect pericentromeric cohesin from removal in mitotic prophase (Liu *et al*, 2013a; 2013b). However, only the pool of Sgo1 that interacts with cohesin in human cells is capable of protecting cohesin whereas the chromatin bound Sgo1 pool cannot carry out this function (Liu *et al*, 2013a; 2013b). I reasoned that in budding yeast meiosis, cohesin protection may occur in a similar way – there may be a pool of Sgo1 which binds to cohesin and is required for protection and another, chromatin-bound pool that carries out other functions. Importantly, *SPO13* may only influence localisation of Sgo1 to the cohesin-bound pool.

To test the idea that Spo13 allows the interaction of cohesin and Sgo1, I utilised a proximity assay called M-track that tests for protein-protein interaction *in vivo* (Zuzuarregui *et al*, 2012). I tagged the cohesin subunit Rec8 with a histone lysine methyl transferease (HKMT) and Sgo1 with two copies of the N-terminal 21 amino acids of histone H3 as well as two Ha tags. When Rec8-HKMT and Sgo1-2H3-2Ha

interact, then the HKMT tag on Rec8 will tri-methylate the histone tag on Sgo1 and this methylation can be detected by western blot (Fig. 4.10A). I performed M-track on cultures released from a prophase block to determine whether the Sgo1-cohesin interaction is impaired in *spo13Δ*, *spo13-m2* or *pCLB2-CDC5* mutants.

In wild type cells, the Sgo1-cohesin interaction can be detected already in the prophase block (Fig. 4.10B – time 0). Upon release from prophase, the M-track signal gets stronger and declines somewhat with the onset of anaphase. A similar pattern is observed in all mutants (Fig. 4.10B). In fact, Sgo1-2H3-2Ha is tri-methylated in all mutants. Analysis of meiotic spindles by tubulin immunofluorescence revealed that wild type, *spo13Δ* and *spo13-m2* cells released from the prophase block with similar kinetics (Fig. 4.10C). *pCLB2-CDC5* cells exhibit a delay in forming metaphase I spindles but this defect has been observed previously (Clyne *et al*, 2003; Lee & Amon, 2003) and is therefore unlikely to be a problem specific to this experiment. Given that M-track is, strictly speaking, not able to distinguish whether two proteins interact directly or whether they are just in close proximity (Zuzuarregui *et al*, 2012), I conclude that Sgo1 and Rec8 should at least be close enough for Rec8 dephosphorylation by PP2A-Rts1 to occur, assuming that the Sgo1-Rts1 interaction is not disrupted in the absence of *SPO13*. However, because methylation by M-track is not reversible, I cannot exclude the possibility that *spo13Δ* mutants exhibit defects in maintaining the Sgo1-cohesin interaction.

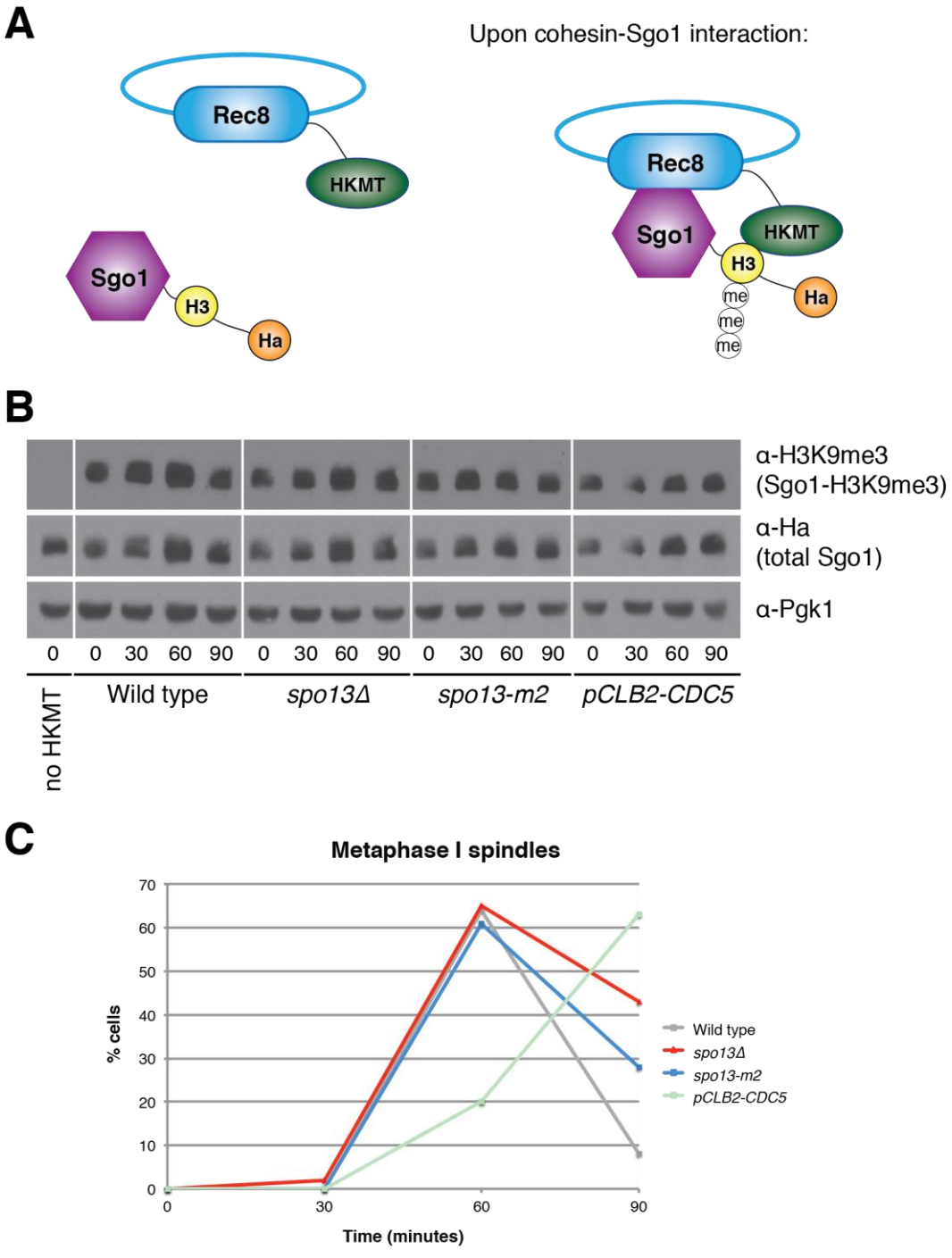

Figure 4.10: Sgo1 and Rec8 are in physical proximity. (A) Principle of M-track. Rec8 is tagged with a histone lysine methyl transferase (HKMT) and Sgo1 with a histone H3 tag. When the proteins interact, HKMT will tri-methylate the H3 tag which can be detected by western blot. (B and C) No tag (AMy19999), wild type (AMy20000), *spo13Δ* (AMy20001), *spo13-m2* (AMy20002), and *pCLB2-CDC5* (AMy20003) cells were induced to sporulate for 5 hours before adding 1μM β-estradiol. Samples for TCA whole cell extracts and tubulin immunofluorescence were taken at the indicated times (in min) after β-estradiol addition. (B) A representative western blot is shown. (C) 100 cells per time point were scored for the presence of metaphase I spindles by tubulin immunofluorescence.

4.2.3.2. Tethering of Sgo1 to Rec8 restores cohesin protection in *spo13Δ* cells

Given the drawbacks of M-track in determining whether the cohesin-Sgo1 interaction might be defective in *spo13Δ* mutants, I wanted to find a more conclusive way to identify whether the inability of Sgo1 to bind cohesin may be the reason for defective cohesin protection in *spo13Δ* cells. I reasoned that if this were the case, then restoring the interaction between Sgo1 and Rec8 artificially would allow cohesin protection in these mutants. Therefore, I tagged Sgo1 with GBP and imaged Rec8-GFP throughout meiosis in these strains. The GBP tag should allow Sgo1 to constitutively bind to Rec8-GFP, even in the absence of *SPO13*. *SGO1-GBP* strains still manage to cleave arm cohesin upon Pds1 degradation and pericentromeric cohesin protection is still intact (Fig. 4.11A). Furthermore, pericentromeric cohesin is cleaved in meiosis II, indicating that tethering Sgo1 to cohesin does not prevent cohesin deprotection. Interestingly, however, pericentromeric foci of Rec8-GFP can be observed in *spo13Δ* mutants when Sgo1 is tethered to Rec8 (Fig. 4.11A/B). The intensity of these foci is significantly stronger than those of wild type cells (Fig. 4.11C), indicating that cohesin is protected more efficiently in *spo13Δ SGO1-GBP* strains. Taken together, these results suggest that forcing the interaction between Sgo1 and cohesin is sufficient to restore cohesin protection in *spo13Δ* cells.

4.2.3.3. Tethering Sgo1 to cohesin does not rescue loss of sister chromatid cohesin in *spo13Δ* mutants

The discovery that pericentromeric cohesin is maintained in *spo13Δ SGO1-GBP* mutants raised the question of whether tethering Sgo1 to Rec8 would also restore sister chromatid cohesion. If this were the case, one would expect *spo13Δ SGO1-GBP* cells to behave similarly to *mam1Δ* strains in anaphase – bi-orientation should be lost but if pericentromeric cohesin is protected, centromeres should split apart by only a short distance. Therefore, I decided to carry out the *CEN5* cohesion assay (Fig. 2.8) for *spo13Δ*, *mam1Δ, SGO1-GBP* and combination mutants. Because Rec8-GFP was required for tethering, I used TetR fused to tdTomato to visualise *CEN5*.

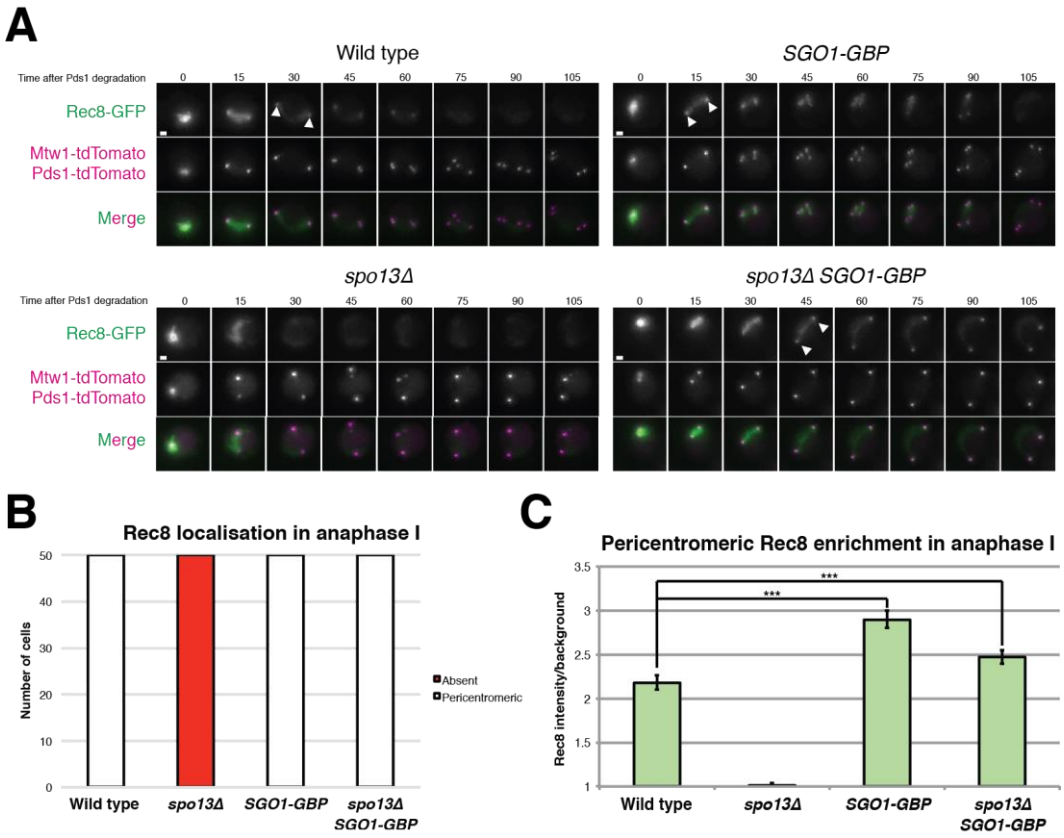

Figure 4.11: Tethering of Sgo1 to Rec8 rescues the cohesion phenotype of *spo13Δ* mutants. (A-C) Pericentromeric foci of cohesin are restored in anaphase stage *spo13Δ* mutants when Sgo1 is tethered to Rec8. Wild type (AMy13716), *spo13Δ* (AMy15133), *SGO1-GBP* (AMy17888), and *spo13Δ SGO1-GBP* (AMy17889) cells were induced to sporulate and transferred onto a microfluidics plate after 2.5 hours in SPO. Images were taken at 15 min intervals. (A) Representative movies are shown. Scale bars represent 1μm. Arrows highlight pericentromeric cohesin retained after the first round of cohesin cleavage. (B) Cells were subjectively scored for the presence of pericentromeric cohesin after Pds1 degradation (n = 50). (C) The average intensity of Rec8 was measured in the area occupied by kinetochores in anaphase I as described in Fig. 2.7. Error bars show standard error of the mean (***p < 0.001).

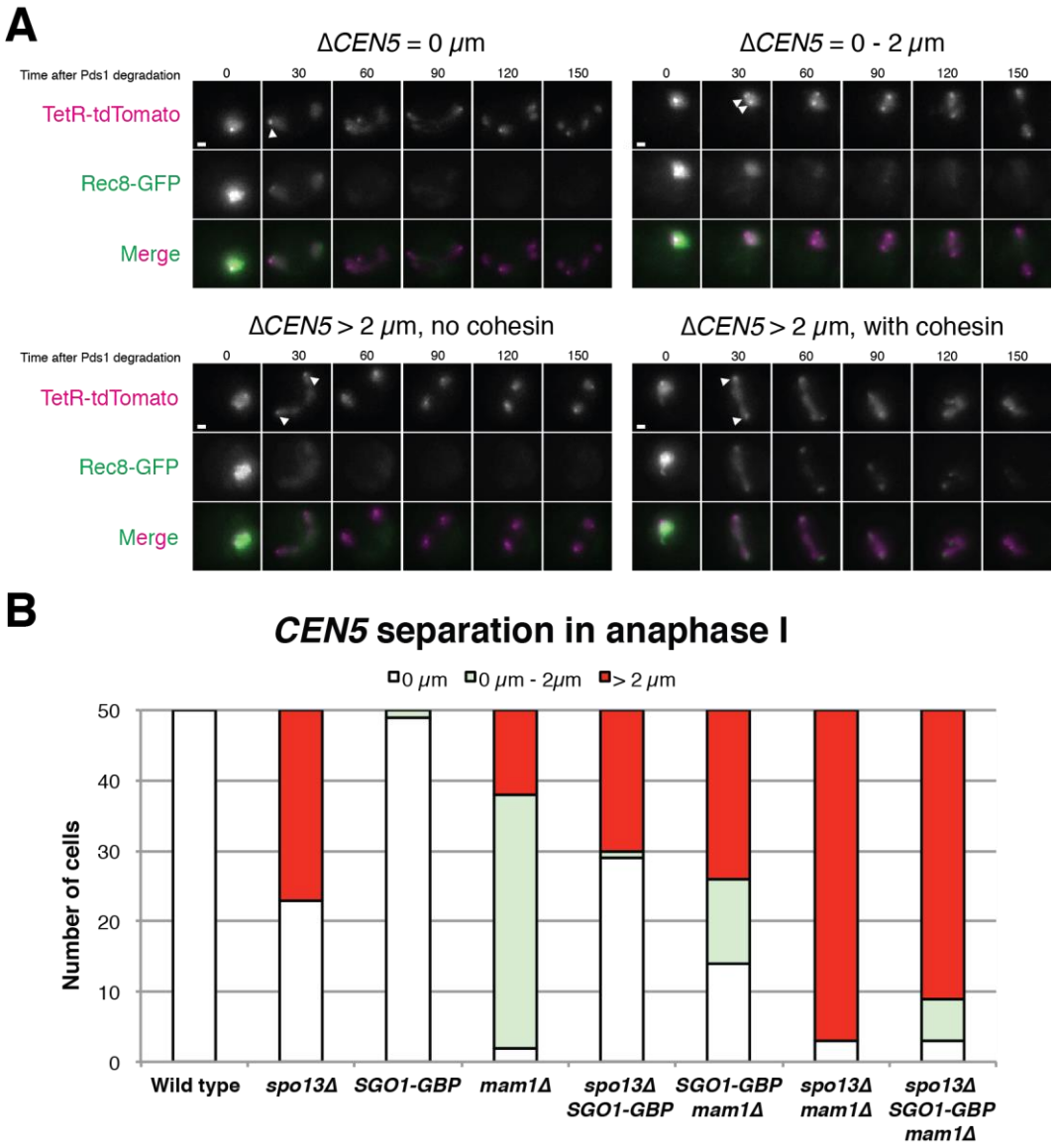

Figure 4.12: Tethering of Sgo1 to Rec8 does not restore sister chromatid cohesion in *spo13Δ* mutants. (A and B) Wild type (AMy19273), spo13Δ (AMy19274), *SGO1*-GBP (AMy19275), *mam1Δ* (AMy19276), *spo13Δ SGO1-GBP* (AMy19282), *SGO1-GBP mam1Δ* (AMy19283), *spo13Δ mam1Δ* (AMy19284) or *spo13Δ SGO1-GBP mam1Δ* (AMy19285) cells were induced to sporulate and transferred to a microfluidics device after 2.5 hours in SPO media. (A) Representative movies are shown. Scale bars represent 1μm. Arrows indicate *CEN5*-tdTomato foci. (B) The distance between *CEN5*-GFP foci was measured in 50 cells after Pds1 degradation but prior to SPB re-duplication for the mutants indicated.

While wild type, *spo13Δ*, *mam1Δ* and *spo13Δ mam1Δ* strains behaved similarly to what I had observed previously (Fig. 4.3), *SGO1-GBP* alone did not affect *CEN5* segregation in meiosis I (Fig. 4.12B). Unexpectedly, however, the fraction of cells that split *CEN5* dots further than 2 µm doubled in *SGO1-GBP mam1Δ* cells when compared to *mam1Δ* single mutants (Fig. 4.12B). Strains that had Sgo1 tethered to Rec8 in *spo13Δ* mutants displayed a previously unseen phenotype: while Rec8-GFP foci were clearly retained in anaphase, sister centromeres were associated with the pericentromeric GFP signal (Fig. 4.12A), indicating that sisters still separated in both *spo13Δ SGO1-GBP* double mutants and *spo13Δ SGO1-GBP mam1Δ* triple mutants. Taken together, these results indicate that although Rec8-GFP is seemingly protected upon tethering of Sgo1 to cohesin in *spo13Δ* mutants, sister chromatid cohesion is not intact.

4.2.3.4. Tethering of Sgo1 to kinetochores in meiosis does not rescue sister chromatid cohesion in *spo13Δ* mutants

The fact that sister chromatid cohesion is lost even when Sgo1 is tethered to cohesin suggested that Sgo1 might not be tethered in the correct place to allow maintenance of sister chromatid cohesion. Therefore, I wanted to investigate whether Sgo1 tethering to kinetochores may be able to restore sister chromatid cohesion in *spo13Δ* mutants. I therefore chose to use the GFP-GBP tethering system to tether Sgo1 to the kinetochores protein Nkp1 (fused to nfGFP) and monitor *CEN5* segregation using TetR-Eos. Nkp1 is one of the outer components of the Ctf19 kinetochore complex which localises to kinetochores throughout meiosis (Marston *et al*, 2004; Meyer *et al*, 2015). I chose Nkp1 for tethering, mainly because tethering of Sgo1 to kinetochore proteins in mitosis is lethal (data not shown). However, *NKP1* is non-essential and this allowed me to put it under control of the meiosis-specific *IME2* promoter without deleterious effects on mitotic or meiotic chromosome segregation (Fernius & Marston, 2009). Analysis of *CEN5* segregation when Sgo1 was tethered to Nkp1 showed that kinetochore tethering of Sgo1 does not significantly alter the pattern of *CEN5* segregation when compared *spo13Δ* cells

(Fig. 4.13). Therefore, tethering of Sgo1 to kinetochores does not rescue the cohesion defect of *spo13Δ* mutants.

4.2.4. Cohesin kinases are required for sister chromatid separation in *spo13Δ* mutants

4.2.4.1. *spo13Δ* cells exhibit a decrease in centromeric Hrr25 similar to mono-orientation mutants

Despite the fact that sister chromatid cohesion was not restored by tethering Sgo1 to cohesin in meiosis, I was intrigued by the fact that pericentromeric foci were retained in this situation. While a lack of the cohesin-Sgo1 interaction in *spo13Δ* cells may explain the cohesin defect in these cells, an alternative hypothesis may be that tethering Sgo1 to Rec8 shifts the balance of kinases and phosphatases on cohesin. This would imply that *spo13Δ* cells have impaired cohesin protection either because the cohesin kinases localise to the centromere in excess or they are overactive. In this case, tethering of Sgo1 to cohesin may simply restore the balance between kinases and phosphatases on cohesin.

To test this idea, I first wanted to investigate whether localisation of either one of the two kinases that are required for cohesin cleavage, Hrr25 and Dbf4-Cdc7 (DDK), display increased localisation at the pericentromere. To this end, I carried out ChIP-qPCR of Hrr25-3Flag and 6Ha-Dbf4 in metaphase-arrested cells. I compared *spo13Δ, spo13-m2* and *pCLB2-CDC5* cells with *mam1Δ* cells because all of these mutants are known to affect mono-orientation and, therefore, I wanted to determine whether either of these mutants affects centromeric recruitment of cohesin kinases independently of mono-orientation functions.

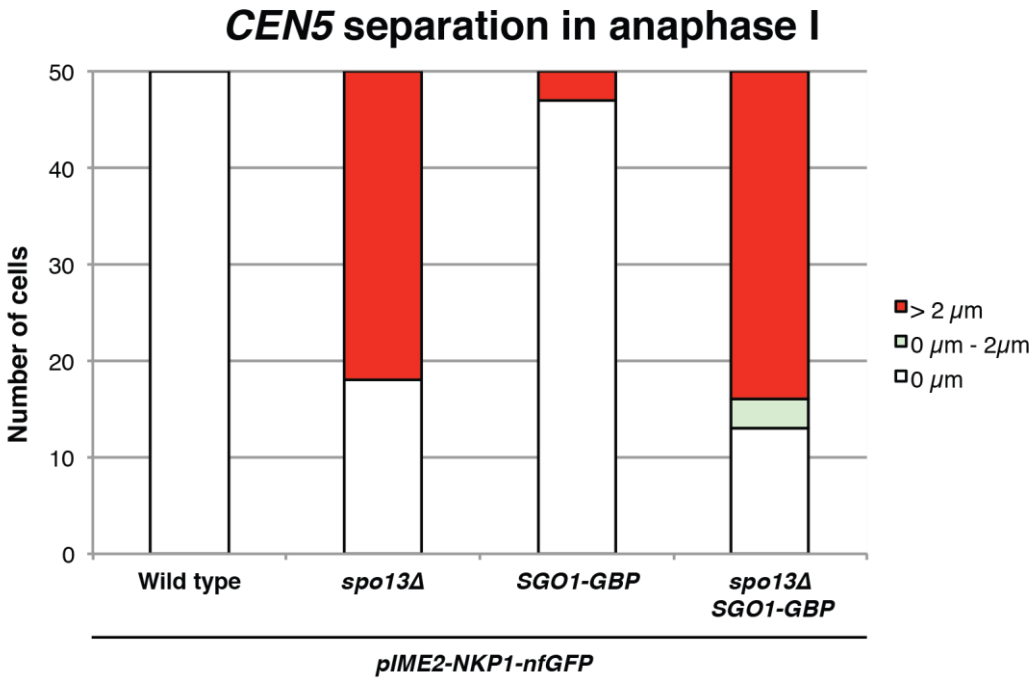

Figure 4.13: Tethering of Sgo1 to Nkp1 does not restore sister chromatid cohesion in *spo13Δ* mutants. Wild type (AMy19560), spo13*Δ* (AMy19561), *SGO1*-GBP (AMy19562) and *spo13Δ SGO1-GBP* (AMy19563) cells were induced to sporulate and transferred to a microfluidics device after 2.5 hours in SPO media and imaged at 15 min intervals. The distance between *CEN5*-Eos foci was measured in 50 cells after Pds1 degradation but prior to SPB re-duplication for the mutants indicated.

When analysing the localisation of Hrr25 at four different sites on chromosome IV, I found that Hrr25 is reduced to a similar degree at *CEN4* in *mam1Δ*, *pCLB2-CDC5*, *spo13Δ* and *spo13-m2* mutants (Fig. 4.14A). This indicates that centromeric Hrr25 is reduced upon loss of mono-orientation rather than as a consequence of losing Spo13 or Cdc5 function. Further away from the centromere, at the boundaries between the pericentromere and chromosome arms, as well as on an arm site, the reduction in Hrr25 levels is only very mild. At all three sites, there is a significant decrease in the *spo13-m2* mutant but for *spo13Δ* cells the reduction is only significant at the right boundary (Fig. 4.14A).

For Dbf4, on the other hand, I first noticed that wild type cells do not have a significant enrichment of Dbf4 at any of the investigated sites compared to an untagged strain (Fig. 4.14B). At *CEN4*, however, *pCLB2-CDC5* and *spo13-m2* mutants show a significant enrichment over no tag whereas *spo13Δ* cells have a very modest but significant increase of Dbf4 at the investigated boundary and arm sites (Fig. 4.14B). The reasons for higher Dbf4 enrichment in these strains are currently unclear. Western blot analysis of whole cell extracts revealed that protein levels of Hrr25 and Dbf4 are largely unchanged in all mutants I investigated. From this data I firstly conclude that Spo13 and Cdc5 are required for Hrr25 to associate with centromeres but this is likely related to mono-orientation functions of Hrr25. Secondly, although Dbf4 association is increased at particular sites in some mutants the increase is only very mild and the enrichment is barely above that observed in the untagged strain. Therefore, these data suggest that Dbf4 may not normally be associated with chromosomes in metaphase I-arrested cells.

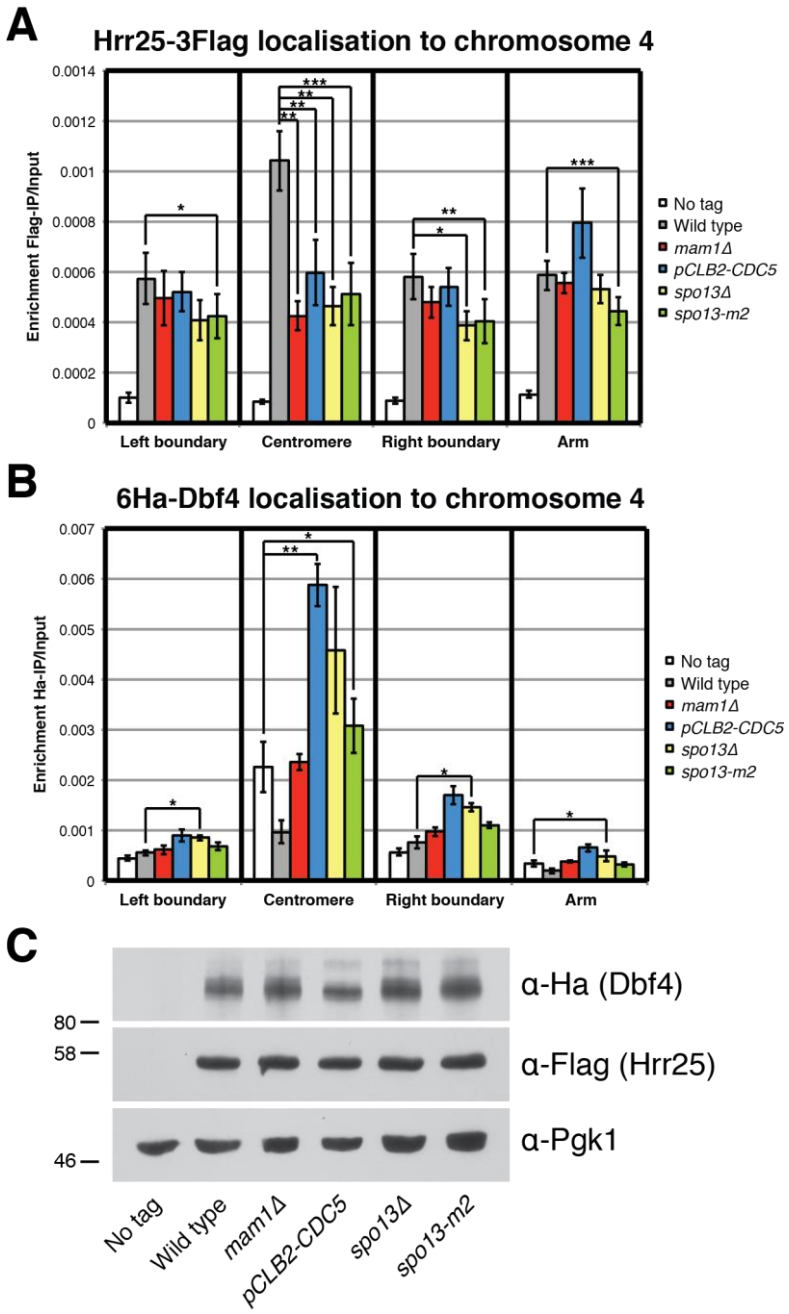

Figure 4.14: *spo13Δ* mutants exhibit decreased Hrr25 and slightly increased Dbf4 levels at *CEN4*. No tag (AMy8067), wild type (AMy16887), *mam1Δ* (AMy16888), *pCLB2-CDC5* (AMy16889), *spo13Δ* (AMy16890) and *spo13-m2* (AMy16891) cells carrying *pCLB2-CDC20* were arrested in SPO media for 6 hours before fixing for α-Flag and α-Ha ChIP-qPCR. Error bars represent standard error of the mean for 4 independent experiments (*p < 0.05, **p < 0.01, ***p < 0.001). (A) Hrr25 levels at *CEN4* are decreased as a result of defective mono-orientation. ChIP-qPCR of Hrr25-3Flag. (B) Dbf4 is mildly increased over no tag levels in *spo13Δ* mutants. ChIP-qPCR of 6Ha-Dbf4. (C) Levels of Hrr25 and Dbf4 are unchanged in *pCLB2-CDC5*, *spo13Δ* and *spo13-m2* mutants. TCA fixed samples were collected for western blot analysis just prior to fixing cells for ChIP. A representative blot is shown.

4.2.4.2. Inhibition of either DDK or Hrr25 prevents sister chromatid segregation in *spo13Δ* mutants

Although I could not find any evidence that either Hrr25 or DDK show a strong enrichment at centromeres in *spo13Δ* cells, it was still possible that either kinase is over-active in *spo13Δ* mutants causing a shift in the kinase phosphatase balance that eventually leads to phosphorylation and cleavage of Rec8. Therefore, I decided to inhibit these kinases in *spo13Δ* cells and assess the effect on cohesion protection using the *CEN5* cohesion assay (Fig. 2.8). To interfere with the activity of the cohesin kinases, I used analogue sensitive versions of Hrr25 and Cdc7, namely Hrr25-as1 (Petronczki *et al*, 2006) and Cdc7-as3 (Wan *et al*, 2006), because deletion mutants of either kinase are inviable. I decided to arrest cells in prophase and inhibit both kinases only upon release from the prophase block because, at least for Cdc7, premature kinase inhibition may have effects that prevent meiotic progression (Wan *et al*, 2006).

While inhibition of Cdc7 interferes with mono-orientation as previously reported (Matos *et al*, 2008) and subsequently prevents homologue segregation in 60% of cells, cells with inactive Hrr25 segregated homologs in the large majority of cells (Fig. 4.15). Inhibition of both kinases disrupted mono-orientation in nearly all cells and sister chromatids were not able to separate further than 2 µm, probably because cohesin cleavage is inhibited globally (Katis *et al*, 2010). Inhibition of either kinase exaggerated the mono-orientation phenotype of *spo13Δ* mutants. In contrast to *spo13Δ mam1Δ* mutants (Fig. 3.3), however, sister chromatids separate to more than 2 µm in only approximately 20% of *spo13Δ* cells upon inhibition of Cdc7 or Hrr25 (Fig. 4.15). Moreover, inhibition of both Hrr25 and Cdc7 in *spo13Δ* cells almost completely prevents separation of sister centromeres to further than 2 µm, indicating that sister chromatid cohesion is preserved (Fig. 4.15). Taken together, these results suggest that both Cdc7 and Hrr25 are required for the untimely loss of cohesion in *spo13Δ* cells.

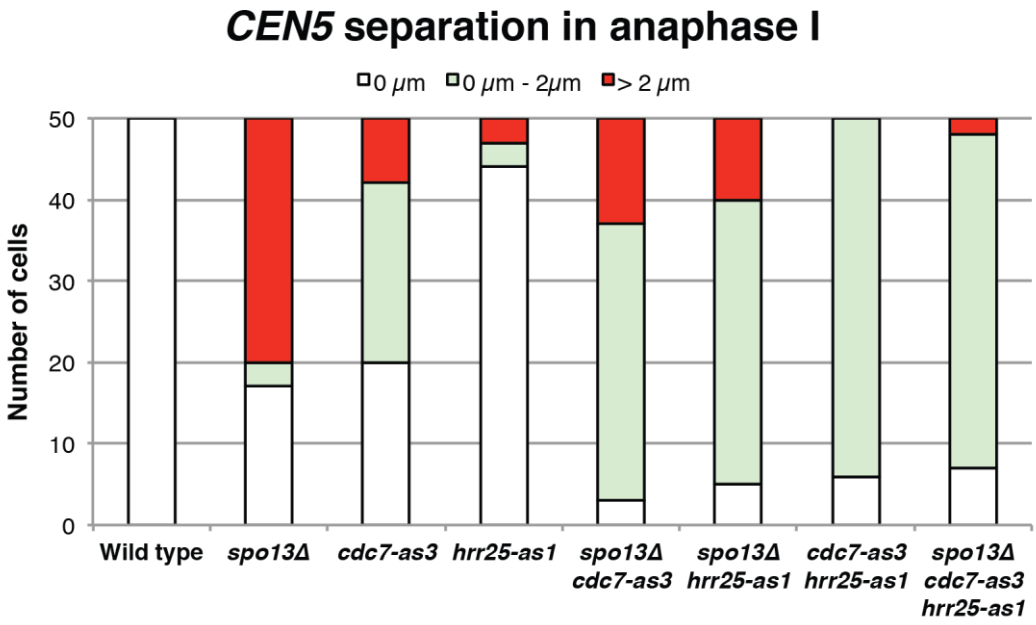

Figure 4.15: Inhibition of either cohesin kinase is sufficient to rescue sister chromatid cohesion in *spo13Δ* mutants. Wild type (AMy19944), *spo13Δ* (AMy19945), *cdc7-as3* (AMy20317), *hrr25-as1* (AMy20318), *spo13Δ cdc7-as3* (AMy19946), *spo13Δ hrr25*-as1 (AMy19947), *cdc7-as3 hrr25-as1* (AMy20319) or *spo13Δ cdc7-as3 hrr25-as1* (AMy19948) cells were induced to sporulate for 5 hours before addition of 1μM estradiol, 20μM PP1 and 5μM 1-NMPP1. 15 minutes later, cells were transferred to a microfluidics device and imaged at 15 min intervals. The distance between *CEN5-GFP* foci was measured in 50 cells after Pds1 degradation but prior to SPB re-duplication for the mutants indicated.

4.3. Discussion

In this chapter, I have analysed functional interactions of Spo13 with various kinases and identified potential mechanisms for how Spo13 regulates mono-orientation and cohesin protection. First, I tested whether the Spo13-Cdc5 interaction may be important for cohesion establishment or maintenance. While the Spo13-Cdc5 interaction is important for mono-orientation, I could not find evidence that Spo13 regulates cohesion through Cdc5. Instead, *SPO13* overexpression causes Sgo1-dependent cohesin overprotection in the pericentromere, which led me to hypothesise that Spo13 regulates a potential Sgo1-cohesin interaction. Although tethering of Sgo1 to cohesin restores pericentromeric Rec8 foci in anaphase I, sister chromatids are not held together. Instead, inhibition of either of the cohesin kinases, Hrr25 or Cdc7, can restore pericentromeric sister chromatid cohesion in *spo13Δ* mutants.

4.3.1. The importance of centromere-associated Cdc5

Although the Spo13-Cdc5 interaction did not have any obvious effects on Sgo1 localisation to centromeres or cellular levels, I wanted to investigate the effect of *SPO13* loss on Cdc5 further. Previously, it was shown that MEIKIN, the functional homolog of Spo13 in mice, and Moa1, the functional homolog in fission yeast, are important for the recruitment of Polo-like kinases to centromeres (Kim *et al*, 2014). Importantly, centromere localisation of Polo-like kinases is thought to be important for cohesin protection and mono-orientation in these systems (Kim *et al*, 2014). Therefore, I wanted to test whether Spo13 also recruits Cdc5 to centromeres. Analysis of Cdc5 localisation in *spo13Δ* and *spo13-m2* mutants in metaphase I arrested cells showed that these mutants show a significantly decreased enrichment of Cdc5 at centromeres, however, not at a chromosomal arm site (Fig. 4.1). Although it would be useful to carry out ChIP-seq of Cdc5 in these mutants to assess whether these observations hold true on a genomic level, it is interesting that Spo13 only affects the recruitment of Cdc5 at the centromere, but not at chromosome arms. This suggests that there is a pool of Cdc5 that is recruited to chromosomes independently of Spo13 and that the pool of Cdc5 that remains at centromeres in *spo13Δ* and *spo13-*

m2 cells is recruited, or maintained, similarly to Cdc5 on arms. It is tempting to speculate that this pool of Cdc5 is bound to cohesin since Cdc5 was reported to interact with cohesin (Matos *et al*, 2008; Katis *et al*, 2010). However, my preliminary data (not shown) indicates that in the absence of *REC8*, Cdc5 localisation to chromosomes is unchanged. Therefore, recruitment of Cdc5 to chromosome arms and to Spo13-independent centromeric sites may not depend on cohesin. How Cdc5 is recruited to chromosomal sites independently of Spo13 should be subject of future investigation.

Next, I wanted to know whether Spo13 directly recruits Cdc5 to centromeres. I chose to overexpress *SPO13* and *spo13-m2* in the hope that this would increase association of these proteins with chromosomes and, consequently, recruit additional Cdc5. Although Cdc5 levels on chromosomes were significantly increased upon *SPO13* overexpression (Fig. 4.2A), I cannot exclude that this is a result of increased Cdc5 levels in this condition (Fig. 4.2C). Furthermore, Spo13 enrichment at centromeres is not increased under overexpression conditions, indicating that the increase of Cdc5 on chromosomes does not result from direct recruitment by Spo13. Interestingly, however, analysis of the Spo13-m2 mutant protein showed that this mutant is not fully associated with centromeres, although its arm localisation is not affected (Fig. 4.2B). This finding mirrors the localisation of Cdc5 in *spo13-m2* mutants. Therefore, Spo13 and Cdc5 may be co-dependent for their association with centromeres. Preliminary data from our lab, however, indicate that Spo13 localisation to centromeres is unchanged in *pCLB2-CDC5* cells (R. Barton, personal communication). Therefore, modification of Spo13 in the polo-binding domain, potentially by cyclin-dependent kinase Cdc28, may be required for its association with centromeres and subsequent recruitment of Cdc5. Analysis of point mutants within Spo13's PBD by ChIP-qPCR might reveal which residues of Spo13 are critical for its localisation to centromeres.

A further possibility that I considered was that the decrease of Spo13 and Cdc5 enrichment at centromeres results from a ChIP-qPCR artefact that may occur when sister chromatids come under tension (Nerusheva *et al*, 2014). Because both deletion of *SPO13* as well as the *spo13-m2* mutant are known to be defective for mono-orientation (Katis *et al*, 2004b; Matos *et al*, 2008), I wanted to compare association

of Spo13 and Cdc5 with centromeres in a *mam1Δ* mutant, which is defective for mono-orientation but which has no known involvement in localising Cdc5. This analysis revealed that Spo13 and Cdc5 enrichment at centromeres in *mam1Δ* cells is comparable to wild type (Fig. 4.3). Therefore, loss of mono-orientation does not affect Spo13 and Cdc5 association with centromeres. Further research should investigate how Spo13 is recruited to centromeres. In mice, the kinetochore subunit CENP-C was identified as an interactor of MEIKIN (Kim *et al*, 2014). Therefore, budding yeast Mif2, which is orthologous to CENP-C, may be required for Spo13 centromere recruitment. The establishment of mutants that allow conditional depletion of Mif2 in meiosis would aid greatly in understanding whether Spo13 is recruited to centromeres in a similar manner as MEIKIN is in mice. If this function is conserved, then it could be used as an additional tool to study the downstream effects of losing Cdc5 recruitment to centromeres. Furthermore, it would clarify whether there are two distinct pools of Spo13 at centromeres, as is likely the case for Cdc5. The fact that Spo13-m2 still displays residual association with centromeres (Figs. 4.2B & 4.3B) supports this idea. However, very little is known about proteins that may allow Spo13 association with chromosomes. One candidate could be cohesin, because in my ChIP-qPCR analysis Spo13 associates not only with centromeres (which are rich in cohesin), but also with a cohesin-rich arm site on chromosome IV (Figs. 4.2B & 4.3B). However, genome-wide analysis of Spo13 localisation by ChIP-seq is required to compare localisation patterns of Spo13 and cohesin. Furthermore, analysis of Spo13 localisation in *rec8Δ* cells could reveal if cohesin is required for Spo13 association with chromosomes.

Having established that Spo13 recruits Cdc5 to centromeres, I wanted to determine the functional significance of Cdc5 association with kinetochores. To test this, I tethered Cdc5 to kinetochores in meiosis in both wild type and *spo13Δ* cells. Interestingly, tethering Cdc5 to Mtw1 allows the large majority of *spo13Δ* cells to segregate homologs in the first meiotic division (Fig. 4.5B). Wild type cells with kinetochore-tethered Cdc5, however, still segregate sister chromatids in meiosis II, indicating that the presence of Cdc5 at kinetochores alone is not sufficient to force segregation of homologs. Instead, it is likely that additional factors like Mam1, which gets degraded upon anaphase I entry, are required to achieve mono-orientation

and homolog segregation. A crucial question to answer in the future is whether tethering of Cdc5 also rescues mono-orientation and not simply the segregation of homologs. As seen for *spo13-m2* (Fig. 4.6) and *hrr25-as1* (Fig. 4.15), both mutants that were previously reported to be defective for mono-orientation (Petronczki *et al*, 2006; Matos *et al*, 2008), homolog separation can still occur fairly successfully even when mono-orientation may be impaired. This suggests that fusing kinetochores may be a distinct function of the monopolin complex (Corbett *et al*, 2010; Sarangapani *et al*, 2014). Other proteins, like Spo13 and Cdc5, may simply support this function, for example by recruiting monopolin subunits (Katis *et al*, 2004b; Lee *et al*, 2004) or by posttranslationally modifying monopolin subunits, such as hyperphosphorylation of Lrs4 (Matos *et al*, 2008). Therefore, it is necessary to investigate whether tethering of Cdc5 to kinetochores rescues mono-orientation in metaphase I arrested cells. If this is the case, then it would be interesting to test whether tethering of Cdc5 also restores the recruitment of monopolin subunits to kinetochores, which are known to be defective in *spo13Δ* cells (Katis *et al*, 2004b; Lee *et al*, 2004), and whether Lrs4 hyperphosphorylation, which is thought to be required for mono-orienation, can be rescued in *spo13Δ* cells upon tethering of Cdc5 to kinetochores.

Lastly, I wanted to determine whether centromeric Cdc5 is also required for sister chromatid cohesion. To do this, I combined the *spo13-m2* mutant, which shows reduced Cdc5 recruitment to centromeres similar to *spo13Δ* (Fig. 4.1A), with the *mam1Δ* mutation. If centromeric Cdc5 is required for cohesin protection, then cohesion should be defective in *spo13-m2* mutants and *spo13-m2 mam1Δ* double mutants are expected to separate *CEN5* dots to a distance larger than 2 µm as observed in *spo13Δ mam1Δ* cells (Fig. 3.3B). However, this was not the case and *spo13-m2 mam1Δ* double mutants behave very similarly to *mam1Δ* single mutants (Fig. 4.6). Surprisingly, *spo13-m2* mutants segregated homologous chromosomes in the large majority of cells (Fig. 4.6), although they were previously published to be defective for mono-orientation (Matos *et al*, 2008). Additionally, preliminary data from our lab shows that *spo13-m2* mutants have a similar fraction of bi-oriented cells in a metaphase I arrest as *mam1Δ* mutants (C. Dixon, personal communication). This raises the question of why so few cells actually attempt to segregate sister chromatids. As mentioned above, there may be a difference between loss of mono-

orientation in metaphase I and the final segregation of chromosomes in anaphase which may, despite loss of mono-orientation, be biased towards homolog segregation. Therefore, a more detailed understanding of the role of Spo13 and Cdc5 in mono-orientation is required to support this discussion. An alternative explanation is that *spo13-m2* mutants retain a residual amount of their Cdc5 interaction (Matos *et al*, 2008), which may be sufficient for mono-orientation to occur and therefore account for their failure to attempt sister chromatid segregation in anaphase I. However, according to my own ChIP data (Fig. 4.1) Cdc5 is similarly reduced at centromeres in *spo13Δ* and *spo13-m2* mutants. To clarify the question of whether loss of centromeric Cdc5 is the cause of the cohesion phenotype of *spo13Δ* mutants, I would tether Cdc5 to centromeres in *spo13Δ mam1Δ* double mutants in the hope that Cdc5 kinetochore tethering does not compensate for the lack of monopolin. Analysis of *CEN5* dot segregation should give a clear indication of whether kinetochore-tethered Cdc5 prevents sister chromatid segregeation in *spo13Δ mam1Δ*. If this were the case, then Spo13's main function in cohesin protection would be to recruit Cdc5 to centromeres and an investigation of downstream targets of Cdc5 would be required to understand its role in maintaining cohesion in meiosis I.

4.3.2. Overprotection of cohesin upon *SPO13* overexpression

Because I could not find any evidence that Spo13 regulates cohesin protection through Sgo1 or Cdc5, I investigated the possibility that Spo13 may be able to protect cohesin independently of Sgo1. This was indicated by a previous study that showed that Spo13 overexpression in mitosis causes cohesin protection independently of Sgo1 (Lee *et al*, 2002). Therefore, I decided to overexpress *SPO13* in meiosis using the *CUP1* promoter and determine how this affects cohesin protection. Interestingly, investigation of Rec8-GFP in meiosis showed that overexpression of *SPO13* results in increased pericentromeric levels of Rec8 in anaphase, although cohesin at chromosome arms is still cleaved (Figs. 4.7A & 4.7C). This is in contrast to previous studies which found that overexpression of *SPO13* in mitosis can protect both Rec8 (Shonn *et al*, 2002; Lee *et al*, 2002) and Scc1 (Lee *et al*, 2002). The most likely reason for this are differences in the levels of *SPO13*

overexpression. Mitotic studies have used the *GAL1* promoter to overexpress *SPO13*, which causes stronger overexpression than the *CUP1* promoter (Romanos *et al*, 1992). Additionally, Shonn et al. (2002) found that upon transformation of their *GAL-SPO13* construct they obtained transformants with three different phenotypes, which is likely due to different copy numbers of *GAL-SPO13* in those strains. I therefore suggest that the degree of *SPO13* overexpression is very important to how it affects cohesin protection. Nevertheless, the fact that overexpression of *SPO13* from the *CUP1* promoter increases cohesin protection in the pericentromere in meiosis I indicates that even lower levels of overexpression are sufficient to enhance the protective effects of Spo13 on cohesin.

Next, I wanted to find out whether the overprotection of cohesin in meiosis observed upon *SPO13* overexpression is independent of Sgo1, as was seen for *SPO13* overexpression in mitotic cells (Lee *et al*, 2002). To test this, I depleted Sgo1 in cells overexpressing *SPO13*. Analysis of Rec8 localisation revealed that pericentromeric cohesin cannot be detected in anaphase I when *SPO13* is overexpressed in *pCLB2-SGO1* cells (Fig. 4.8). Therefore, Sgo1 is still required for cohesin protection when *SPO13* is overexpressed. This indicates that Spo13 cannot protect cohesin in the absence of Sgo1. Furthermore, it is likely that Spo13 regulates cohesin protection through Sgo1. This led me to investigate the effect that *SPO13* overexpression has on localisation of Sgo1 to chromosomes. Interestingly, overexpression of both *SPO13* and *spo13-m2* leads to accumulation of Sgo1 at centromeres (Fig. 4.9A). This suggests that Spo13 can recruit additional Sgo1 to centromeres and that this function is independent of its ability to bind Cdc5. However, it also represents a conundrum because deletion of Spo13 does not affect Sgo1 localisation to chromosomes (Fig. 3.5A). This suggests that there may be two distinct pools of Sgo1, only one of which is affected by Spo13. This would imply that the Spo13-regulated pool is very small (because *SPO13* deletion does not allow detection of a drop in Sgo1 enrichment at centromeres); however, this pool is expected to be crucial for cohesin protection given the severe cohesion defect of *spo13Δ* cells. Taken together, these results argue that Spo13 acts through Sgo1 to protect cohesin in meiosis I.

4.3.3. Spo13 and the Sgo1-cohesin interaction

Because the overexpression data indicated that there may be two distinct pools of Sgo1, I tested whether Sgo1 might bind to cohesin itself. In human mitotic cells, Sgo1 binds both cohesin and chromatin at phosphorylated H2A. However, it is only the cohesin bound pool of Sgo1 that protects cohesin from Wapl-dependent removal in prophase (Liu *et al*, 2013b). I reasoned that meiotic cohesin protection might work in a similar manner and that Sgo1 binding to cohesin in meiosis may be required for cohesin protection. I used the M-track system (Zuzuarregui *et al*, 2012) as it has been proposed to be able to detect protein-protein interactions *in vivo*. While I detected methylated Sgo1-2H3-2Ha in wild type cells, indicating that Rec8 and Sgo1 interact, I also detected this interaction with similar intensity in *spo13Δ*, *spo13-m2* and *pCLB2-CDC5* cells (Fig. 4.10B). Although this suggests that the Sgo1-cohesin interaction may be maintained in these mutants, one potential problem to this analysis is that, potentially, the second (non-protective) pool of Sgo1 still associates with centromeres and may be in sufficient proximity to pericentromeric cohesin to be methylated.

Therefore, I wanted to look for a way to more definitively determine whether loss of the Sgo1-cohesin interaction is the cause of the cohesion phenotype in *spo13Δ* mutants. I decided to utilise the GFP-GBP tethering system to force the interaction between Rec8 and Sgo1 in meiotic *spo13Δ* cells, hypothesising that this would restore cohesin protection. Interestingly, tethering of Sgo1 to cohesin did restore pericentromeric foci of Rec8 to anaphase I *spo13Δ* cells (Fig. 4.11A & 4.11B) with an intensity that was similar to wild type cells (Fig. 4.11C). These findings led me to test whether sister chromatid cohesion is restored upon tethering Sgo1 to cohesin in *spo13Δ* mutants. Surprisingly, I observed that despite the retention of pericentromeric Rec8 foci in anaphase I, *spo13Δ* cells still separate sister chromatids so that each of the Rec8 foci is associated with a *CEN5* tdTomato dot (Fig. 4.12).

In principle, there are two different explanations for this observation. The first is that the observed GFP foci do not actually represent protected cohesin. One concern with the tethering assay is that tethering of proteins does not have a predetermined directionality. This means that while Sgo1 and Rec8 are forced to interact, this

interaction may occur at native Rec8 binding sites (i.e. Sgo1 is tethered to Rec8) or at native Sgo1 binding sites (i.e. Rec8 is tethered to Sgo1). Although I did not observe Sgo1-GFP in anaphase I *spo13Δ* cells (Figs. 3.7 & 3.8), it may be possible that Sgo1 is retained in anaphase, as previously indicated (Lee *et al*, 2004). This would allow free (i.e. not chromatin-bound) Rec8-GFP, or even cleaved Rec8-GFP particles to bind chromatin-associated Sgo1-GBP and therefore show up as pericentromeric foci. To test whether this is the case, it would be useful to repeat the tethering experiment with a GBP-tagged version of *sgo1-3A*, a mutant which cannot bind PP2A (Xu *et al*, 2009) and therefore should not be able to protect cohesin. I hypothesise that if the pericentromeric foci observed upon tethering of Sgo1 to Rec8 are indeed protected cohesin, then these foci should disappear when tethering Sgo1-3A instead. It is crucial to determine whether the GFP foci observed in this tethering experiment actually represent Rec8-GFP. If this turns out not to be the case, then it is possible that Spo13 might affect the interaction between Sgo1 and PP2A, a possibility that I have not investigated so far. However, if the GFP foci are indeed protected Rec8, then this indicates that Sgo1-PP2A are fully capable of protecting Rec8 in *spo13Δ* mutants.

An alternative hypothesis for the segregation of sister chromatids while pericentromeric Rec8-GFP foci are protected in *spo13Δ SGO1-GBP* strains is that sister chromatids are never actually cohesed at the pericentromere in *spo13Δ* cells. This would imply that *SPO13* is not only required for cohesin protection but also for the establishment or maintenance of cohesion in the pericentromere, independently of the Sgo1-PP2A-dependent protection mechanism superimposed on it. Since cohesion establishment happens during S phase and must be maintained until at least metaphase I, this would require investigation of the early meiotic functions of Spo13, which are completely elusive to date.

Lastly, I wanted to investigate the possibility that Sgo1 tethering to kinetochores instead of Rec8 may rescue the cohesin phenotype of *spo13Δ* cells. I tethered Sgo1 to the kinetochore component Nkp1 in wild type and *spo13Δ* cells. However, the presence of Sgo1 at kinetochores was not sufficient to restore cohesin protection to *spo13Δ* mutants (Fig. 4.13). This provides further evidence to the fact that Sgo1's presence at centromeres is not sufficient to allow cohesin protection in *spo13Δ* cells.

Taken together, these results suggest that Spo13 may impact cohesin protection by facilitating the cohesin-Sgo1 interaction and/or by ensuring the establishment or maintenance of functional pericentromeric cohesion. Although further experiments are required to verify this, the latter hypothesis would suggest that Spo13 might function very similarly to Moa1 in fission yeast, which was proposed to establish sister chromatid cohesion in the central core of the centromere.

4.3.4. Interplay between Spo13 and cohesin kinases

After discovering that pericentromeric foci of Rec8-GFP persist in *spo13Δ* cells when Sgo1 is tethered to Rec8, I considered the possibility that Spo13 may cause a shift in the phosphatase-kinase balance on Rec8, which could be re-balanced by tethering of Sgo1 to cohesin. This would suggest that Spo13 might either reduce the association of cohesin kinases with cohesin or that the kinases are hyperactive in *spo13Δ* mutants. Firstly, I considered the possibility that either kinase may be recruited to centromeres in excess in *spo13Δ* cells. However, ChIP analysis of Hrr25 and Dbf4 association with chromosomes showed that, firstly, Hrr25 is significantly reduced at centromeres in *spo13Δ* cells and, secondly, Dbf4 shows only a very slight increase over no tag levels. The finding that Hrr25 is reduced in *spo13Δ* and other mutants (Fig. 4.14A) is not surprising because levels are similar to *mam1Δ* cells, suggesting that centromeric Hrr25 is depleted in response to loss of mono-orientation, as previously observed (Petronczki *et al*, 2006). This is likely a direct consequence of loss of centromeric Mam1 in these mutants (Lee & Amon, 2003; Katis *et al*, 2004b; Matos *et al*, 2008), which is required for Hrr25 association with kinetochores (Petronczki *et al*, 2006). In contrast, Dbf4 does not seem to localise to chromosomes in wild type cells and there is only a very mild increase in some of the mutants tested (Fig. 4.14B). The finding that Dbf4 does not appear to associate with chromosomes is surprising because it was previously reported to interact with the cohesin subunit Rec8 (Katis *et al*, 2010), although earlier studies did not detect any cohesin subunits in a mass spectrometry analysis of Cdc7 purified from meiotic cells (Matos *et al*, 2008). Furthermore, live cell imaging of Dbf4 in meiotic cells does not show any distinct centromeric foci (Bonnie Alver, personal communication),

although these can be observed in telophase/G1 of mitotic cells (Natsume *et al*, 2013). To confirm that DDK does indeed not associate with chromosomes, ChIP of tagged Cdc7 should be performed because it is conceivable that we cannot detect Dbf4 on chromosomes for technical reasons. However, if DDK does indeed fail to associate with chromosomes in meiosis I, then this has implications for our current model for cohesin phosphorylation and subsequent cleavage, which postulates that DDK is one of the kinases that phosphorylates Rec8. In terms of cohesin protection in meiosis I though, it seems unlikely that the minor increase in centromeric Dbf4 is the cause for the severe cohesion defect of *spo13Δ* cells.

Instead, I considered the possibility that either Hrr25 or DDK might be hyperactive in the absence of *SPO13*. I hypothesised that if this were true then inhibition of the affected kinase would prevent sister chromatid segregation in *spo13Δ* mutants. Surprisingly, inhibition of either Hrr25 or Cdc7 largely prevented sister chromatid segregation. The simplest model that would explain this observation is that in *spo13Δ* cells, Rec8 phosphorylation is favoured such that Sgo1-PP2A dephosphorylating activity cannot compensate for the hyperphosphorylation of Rec8 in the pericentromere. However, inhibition of either kinase restores the kinase-phosphatase balance so that Rec8 can be protected from cleavage. How exactly Spo13 affects cohesin phosphorylation remains unclear and should be a subject of future investigations.

CHAPTER 5 – FINAL DISCUSSION AND FUTURE DIRECTIONS

Meiosis is one of the two key cell division processes. Ensuring that chromosomes are faithfully segregated during meiosis is key in the production of gametes with the correct number of chromosomes. Errors in this process will give rise to aneuploid gametes and may thus result in miscarriage or developmental disorders such as Down's syndrome.

A central component of the meiotic segregation machinery is the cohesin complex that holds sister chromatids together. According to current thinking, a failure to maintain sister chromatid cohesion may be a contributor to the maternal age effect – the observation that the probability for having an aneuploid foetus increases with maternal age. Therefore, understanding the regulation of cohesin maintenance is crucial in targeting foetal aneuploidy and its consequences.

In contrast to mitosis, meiotic cohesin gets cleaved in two steps. This requires a number of adaptations. Firstly, meiotic cohesin usually contains a specialised cohesin subunit, which mediates its meiotic functions. Importantly, however, the cohesin cleavage pattern is altered so that in meiosis I only cohesin on chromosome arms gets cleaved. Pericentromeric cohesin is spared from cleavage until meiosis II. This is achieved through the action of the conserved shugoshin family of proteins, which recruits PP2A to centromeres. PP2A in turn dephosphorylates cohesin to protect it from the action of separase. While these basic mechanisms for cohesin protection are generally well accepted, there is very little information on how cohesin protection is regulated so that cohesin protection only occurs in meiosis I and not meiosis II.

Two key aspects which may regulate cohesin protection are sister chromatid tension and other proteins like the meiosis-specific Spo13. Sister chromatid tension has been proposed as a method to regulate Sgo1 localisation in meiosis II. Interestingly, since homologs are bi-oriented in meiosis I (meaning sister kinetochores face the same pole), regulating Sgo1 localisation through sister tension would prevent Sgo1 removal from chromosomes in meiosis I, when cohesin needs to be protected. Therefore, I first investigated the consequences of sister chromatid bi-orientation when it is artificially induced in meiosis I.

However, cohesin protection is known to require other factors than Sgo1. Possibly the most important factor in budding yeast is Spo13, and similar proteins have been described in other organisms. Intriguingly, Spo13 is only present in meiosis I. Therefore, if Spo13 is involved in cohesin protection, its degradation at the end of meiosis I should ensure that cohesin is not protected in meiosis II. However, since little is known about how Spo13 facilitates cohesin protection, I decided to study its function in more detail.

5.1. Tension-dependent Sgo1 regulation in meiosis

Previous research in our lab had indicated that in mitosis, Sgo1 is removed from chromosomes in response to sister kinetochore tension. To test whether the same holds true for meiotic cells, I first created a strain in which sister chromatids are predominantly bi-oriented in meiosis I. This required the deletion of both *MAM1*, which is required for mono-orientation, as well as *SPO11*, which induces chiasmata formation. Although this allows the majority of cells to bi-orient, future research should focus on establishing a way to arrest cells in meiosis II. A key aspect of this research is to identify whether cohesin deprotection in meiosis II occurs via the removal of Sgo1 from chromosomes in response to tension. Therefore, it would be ideal to test this hypothesis directly in metaphase II arrest cells, where chromosomes bi-orient naturally. Nevertheless, analysis of Sgo1 localisation both by ChIP-qPCR as well as live cell imaging showed that Sgo1 is absent from chromosomes when sister chromatids come under tension. This is a strong indication that meiotic Sgo1 regulation is similar to mitosis and that Sgo1 is likely to be removed from chromosomes in response to tension in meiosis II. Therefore, I went on to test whether cohesin protection is defective upon induction of sister chromatid bi-orientation. Indeed, I found that pericentromeric cohesion is impaired upon successful bi-orientation. However, my analysis also showed that in about 50% of cells cohesion remains intact. This indicates that further factors ensure cohesin protection in meiosis I. Many other proteins have been linked to cohesin protection, such as Ipl1 (Aurora B), Cdc5 (polo kinase) and cyclins (particularly Clb3), but the prime candidate is certainly the meiosis I-specific factor Spo13. It would be essential

to study the mechanisms by which these proteins influence cohesin protection as this will certainly prove useful in understanding the requirements for cohesin deprotection in meiosis II. Another interesting question is whether Sgo1 removal from chromosomes is actually required for cohesin protection. Tethering of Sgo1 to Rec8 did not prevent cohesin removal and sister chromatid segregation in meiosis II (chapter 4). Although it is not clear that Sgo1 is appropriately localised to protect cohesin in this situation, it is certainly a strong indication that multiple pathways are engaged to ensure cohesin deprotection in meiosis II. However, without a clear understanding of how cohesin protection is set up in the first place, deciphering cohesin deprotection is likely to prove a difficult task in the future.

5.2. The influence of Spo13 on cohesin protection

One of the key factors involved in sister chromatid cohesion, which our current model of cohesin protection fails to incorporate, is the meiosis I-specific Spo13. Although earlier studies had demonstrated Spo13's importance for cohesin protection and suggested a reduction in centromeric Sgo1 as the reason for defective cohesion, little was known about the mechanisms by which Spo13 would regulate Sgo1. In an attempt to gain a deeper understanding of Spo13's functions, I first wanted to quantify the degree of the cohesion defect in Spo13 and confirm its effect on Sgo1 localisation. Although I did find that *spo13Δ* cells exhibit a severe cohesion defect, I surprisingly could not detect any change in Sgo1 localisation by ChIP-qPCR or live cell imaging. Although ChIP-seq studies are required to confirm that genome-wide Sgo1 localisation is indeed unaffected in the absence of *SPO13*, this finding indicated that Spo13 regulates other aspects of cohesin protection than Sgo1 localisation.

I subsequently turned my attention to Sgo1 degradation. Previous research indicated that Sgo1 is a target of APC/C^{Cdc20} and Spo13 had previously been implicated as a negative regulator of the APC/C. It therefore seemed possible that Spo13 prevents full degradation of Sgo1 upon entry into anaphase. Interestingly, I observed that Sgo1 disappears upon anaphase onset even in wild type cells and reaccumulates in meiosis II. As discussed earlier, it is not clear whether some Sgo1

remains at centromeres but is undetectable by live cell imaging. However, successful cohesin protection and degradation of Sgo1 in anaphase may not be mutually exclusive. However, this model predicts that the function of cohesin kinases is also impaired in anaphase. While DDK is known to be inactive due to degradation of the Dbf4 subunit, little is known about the regulation of Hrr25. Understanding Hrr25 regulation is therefore an interesting subject for future study and will provide further insight into when Sgo1's protective function is required. The reaccumulation of Sgo1 in meiosis II does not occur in the majority of *spo13Δ* cells, suggesting that Sgo1 is permanently degraded in this mutant. However, deletion of Sgo1's destruction box allows detection of Sgo1 near kinetochores in anaphase I. Despite this clear centromeric Sgo1 localisation, cohesin protection was still impaired in the *spo13Δ* mutant.

Another factor that regulates Sgo1 levels is polo kinase Cdc5. Interestingly, depletion of Cdc5 not only causes accumulation of Sgo1 in the cell, but also increases localisation of Sgo1 to chromosomes. It will be interesting to determine whether decreased cohesin phosphorylation in the absence of Cdc5 may be a consequence of increased Sgo1 binding. Although Cdc5 was shown to bind cohesin, it is unclear whether it directly phosphorylates cohesin or whether full cohesin phosphorylation indirectly requires Cdc5. Given my findings on cohesin protection in cells with stabilised Sgo1, however, it seems unlikely that Cdc5 regulates cohesin protection through Sgo1 levels alone.

Next, I wanted to investigate whether the interaction between Spo13 and Cdc5 may be required for cohesin protection. When investigating Cdc5 localisation to chromosomes, I found that full enrichment of Cdc5 at kinetochores requires both Spo13 as well as the Spo13-Cdc5 interaction. Furthermore, tethering of Cdc5 to kinetochores in *spo13Δ* cells restores homolog segregation in these mutants. This suggests that the presence of Cdc5 at kinetochores is actually functionally relevant. When considering the requirement of Moa1 and MEIKIN for Cdc5-dependent homolog segregation in fission yeast and mice, respectively, these findings argue that polo kinase recruitment to kinetochores is a conserved feature of mono-orientation. An obvious follow-up question is what the targets of Cdc5 in mono-orientation are. While it is tempting to speculate that Cdc5 phosphorylates monopolin subunits

(indeed, Lrs4 hyperphosphorylation depends on Cdc5), the fact that polo kinase recruitment to kinetochores is conserved in fission yeast and mice, which lack monopolin, suggests that the key target of Cdc5 is a different one. One possible effector is the cohesin subunit Rec8, which is thought to be phosphorylated by Cdc5. However, current evidence suggests that Rec8 itself is not required for mono-orientation but this does not exclude the possibility that cohesin supports mono-orientation irrespective of the associated kleisin. It will also be interesting to determine which aspects of the mono-orientation defect in *spo13Δ* cells are restored by tethering back Cdc5. This may include kinetochore recruitment of monopolin subunits and hyperphosphorylation of Lrs4. However, whereas kinetochore-associated Cdc5 restores homolog segregation in *spo13Δ* mutants, I could not find any evidence that cohesin protection is restored in this situation. An investigation of cohesin localisation in anaphase I and an analysis of sister chromatid cohesion will provide conclusive evidence as to whether kinetochore-associated Cdc5 also aids cohesin protection.

I next considered the possibility that Spo13 might affect cohesin protection independently of Sgo1 and Cdc5. Indeed, overexpression of *SPO13* causes an Sgo1-dependent increase of pericentromeric Rec8 in anaphase, which coincides with increased Sgo1 recruitment. Although the accumulation of Sgo1 indicates that Rec8 is overprotected upon *SPO13* overexpression, I cannot exclude the possibility that Spo13 actually causes recruitment or maintenance of additional cohesin in the centromere. Given that the Sgo1-Rec8 interaction appears intact in *spo13Δ* cells, higher enrichment of Sgo1 upon *SPO13* overexpression could be a consequence of additional cohesin in the pericentromere. Therefore, it would be interesting to test cohesin levels within the pericentromere in cells overexpressing *SPO13*, and whether increased Sgo1 association in these cells is cohesin-dependent.

Another surprising observation was that tethering of Sgo1 to cohesin restored pericentromeric cohesin levels in anaphase I although sister chromatids were still able to segregate. A key experiment to carry out next is to test whether tethering of the Sgo1-3A mutant, which cannot associate with PP2A-Rts1, abolishes the cohesin protection phenotype. If this were the case, then it seems likely that the cohesin protection machinery is actually fully functional in *spo13Δ* cells. To further validate

this, I would use the separase biosensor (Yaakov *et al*, 2012) to test whether Sgo1 can protect the biosensor from cleavage in a *spo13Δ* background. The outcomes of these experiments could demonstrate whether Spo13 is required to establish sister chromatid cohesion in the pericentromere rather than being required for cohesin protection.

Lastly, I investigated the possibility that Spo13 regulates the cohesin kinases Hrr25 and Dbf4-Cdc7. While the localisation of these kinases to centromeres is reduced in the absence of Spo13, inhibition of either kinase prevented sister chromatid segregation in *spo13Δ* mutants. A simple explanation is that Spo13 affects the balance of kinases and phosphatase on cohesin. However, given that kinase levels on cohesin are not increased, this model implies that Spo13 somehow restricts the kinase activity of Hrr25 and DDK. If this were the case, then sister chromatid cohesion may be restored in *spo13Δ* cells either by overexpressing Sgo1 or by introducing a number of phospho-null mutations into Rec8.

Overall, the findings presented in this thesis indicate that Spo13 is at the centre of a complex network of protein kinases and phosphatases that regulate both cohesin protection and mono-orientation in meiosis I. In order to obtain a more mechanistic understanding of Spo13's functions, it will be essential to carry out a thorough analysis of Spo13 itself, particularly its expression patters, temporal regulation of chromosomal association, post-translational modifications and binding partners. Understanding these aspects of Spo13 and its regulation will provide the basis to understanding the many functions this protein exhibits in ensuring accurate chromosome segregation in meiosis.

CHAPTER 6 – MATERIALS AND METHODS

6.1. General information

6.1.1. Supplier information

Reagents for liquid growth media and agar plates were provided by Difco, Formedium and Sigma. Chemicals and other consumables were supplied through Sigma, Melford, Scientific Laboratory Supplies, Boehringer Mannheim, Fisher and Gibco BRL unless otherwise stated.

6.1.2. Sterilisation

Growth media were autoclaved at 120˚C and pressure of 15 pounds/inch^2 for 15 minutes. Solutions were sterilised using 0.22µm bottle top filters (Nalgene) or 0.22µm syringe filters (Milipore). Glassware and plating beads were sterilised by baking at 250˚C for 16 hours.

6.1.3. Buffers and solutions

Buffers and solutions used in this study are listed in Table 7.2 in the appendix with an indication of techniques they were used for.

6.2. Microbiology

6.2.1. Bacterial methods

6.2.1.1. Bacterial strain

The DH5α *E. coli* strain was used for cloning and propagation of plasmids. The genotype of this strain is as follows: F^- φ80lacZΔM15 Δ(lacZYA-argF)U169 deoR recA1 endA1 hsdR17(rk^-, mk^+) phoA supE44 thi-1 gyrA96 relA1 λ^-.

6.2.1.2. Bacterial media

Media	Composition	Concentration
Luria Bertani (LB)	Bacto-tryptone Bacto-yeast extract NaCl Agar (solid media only) (pH adjusted to 7.2 with NaOH)	1% (w/v) 0.5% (w/v) 0.5% (w/v) 2% (w/v)
SOC	Bacto-tryptone Bacto-yeast extract NaCl Glucose $MgCl_2$ $MgSO_4$ KCl	2% (w/v) 0.5% (w/v) 20mM 20mM 10mM 10mM 10mM

Table 6.1: Bacterial growth media

6.2.1.3. Transformation by electroporation

Electro-competent DH5α were removed from storage at -80˚C and thawed on ice. Per transformation, 40µl were pipetted into pre-chilled electroporation cuvettes (Cell Project, 2mm gap). 0.5µl of plasmid DNA from mini-prep or midi-prep was added and cells electroporated using a Bio-Rad Gene Pulser II at 2.5V, 200Ω and 2.5µF. Cells were immediately resuspended in 1ml LB media and incubated at 37˚C for 1 hour. Cells were spun at 3000rpm, resuspended in 200µl LB media and plated onto LB + ampicillin plates and incubated at 37˚C for 16 hours.

6.2.1.4. Growth conditions

Bacteria were grown in LB media or on LB plates containing ampicillin at 100 µg/ml at 37˚C. Liquid cultures were shaken at 200rpm.

6.2.2. Yeast methods

6.2.2.1. Yeast strains

All *S. cerevisiae* strains used in this study are derivatives of SK1. All strains are diploids. Strains in this study are listed in table 7.1 in the appendix. The origins of alleles used in this study are as follows:

Allele	**Source**
Previously published alleles and gifted strains	
ndt80Δ::LEU2	Xu *et al* (1995)
spo11Δ::URA3	Klein *et al* (1999)
mam1Δ::KanMX6	Gift from Angelika Amon
mam1Δ::TRP1	Lee *et al* (2004)
spo13Δ::hisG	Shonn *et al* (2002)
spo13Δ::KanMX6	Brar *et al* (2009)
REC8-3HA::URA3	Klein *et al* (1999)
PDS1-18MYC::LEU2	Shirayama *et al* (1999)
SGO1-6HA::TRP1 *SGO1-9MYC::TRP1*	Marston *et al* (2004)
RTS1-3PK::TRP1	Riedel *et al* (2006)
SPC42-tdTomato::NatMX6	Fernius & Hardwick (2007)
REC8-GFP::URA3 *PDS1-tdTomato::KITRP1* *CNM67-3mCherry::NatMX4*	Matos *et al* (2008)
RTS1-EGFP::KanMX4	Katis *et al* (2010)
cdc20::pCLB2-3HA-CDC20::KanMX6 *cdc5::pCLB2-CDC5::KanMX6*	Lee & Amon (2003)
cdc20::pCLB2-CDC20::KanMX6	Brar *et al* (2006)
hrr25-as1::HIS3::hrr25Δ::KanMX4	Petronczki *et al* (2006)
leu2::pURA3-TetR-GFP::LEU2	Michaelis *et al* (1997)
leu2::pURA3-TetR-tdTomato::LEU2	Katis *et al* (2010)
CEN5::tetOx224::HIS3	Tanaka *et al* (2000)
pGAL1-NDT80::TRP1 *ura3::pGPD1-GAL4(848).ER::URA3*	Benjamin *et al* (2003)

Allele	**Source**
Modifications of published alleles	
cdc7::cdc7-as3::KanMX6	published as *cdc7-as3-9MYC* (Wan *et al*, 2006) *9MYC* tag was removed by replacement with *ADH1* terminator and *KanMX6* cassette from AMp968
spo13::spo13-(L26A)::HphMX6	published as *spo13-(L26A)-3HA::TRP1* (Sullivan & Morgan, 2007) *3HA* tag and *TRP1* marker removed by replacement with *ADH1* terminator and *HphMX6* cassette from AMp969
Gene deletions	
spo11Δ::NatMX6	PCR-based deletion (Longtine *et al*, 1998) using AMp683
ama1Δ::NatMX6	PCR-based deletion (Longtine *et al*, 1998) using AMp683
clb4Δ::His3MX6	PCR-based deletion (Longtine *et al*, 1998) using AMp190
spo13Δ::LEU2	PCR-based deletion (Longtine *et al*, 1998) using AMp1077
spo13Δ::HphMX6	*KanMX6* marker in *spo13Δ::KanMX6* strain was replaced with *HphMX6* marker using AMp969
Tagged genes	
loxp-6HA-Dbf4	PCR-based tagging (Gauss *et al*, 2005) using AMp1041 Creator: Bonnie Alver
MTW1-tdTomato::NatMX6	PCR-based tagging (Longtine *et al*, 1998) using AMp751 Creator: Nadine Vincenten
HRR25-3FLAG::NatMX6	PCR-based tagging (Longtine *et al*, 1998) using AMp680 Creator: Eris Duro
SPO13-3FLAG::KanMX6	PCR-based tagging (Longtine *et al*, 1998) using AMp894 Creator: Eris Duro
spo13::spo13-m2-3FLAG::KanMX6	PCR-based tagging (Longtine *et al*, 1998) using AMp894
CDC5-3V5	PCR-based tagging (Moqtaderi & Struhl, 2008) using AMp729

Allele	**Source**
SGO1-yEGFP::KanMX6	PCR-based tagging (Knop *et al*, 1999) using AMp476
SGO1-GBP::His3MX6	PCR-based tagging (Knop *et al*, 1999) using AMp1147
SGO1-2H3-2HA::HphMX6	PCR-based tagging (Longtine *et al*, 1998) using AMp1200
REC8-HKMT::His3MX6	PCR-based tagging (Longtine *et al*, 1998) using AMp1199
Promoter replacements	
spo13::KanMX6::pCUP1-SPO13-3FLAG::xhsv	PCR-based promoter replacement (Longtine *et al*, 1998) using AMp408
spo13::KanMX6::pCUP1-spo13-m2-3FLAG::xhsv	PCR-based promoter replacement (Longtine *et al*, 1998) using AMp408
Point mutants	
spo13::spo13-m2::LEU2	PCR-based amplification of *spo13-m2::LEU2* from AMp1062, followed by transformation into SK1
spo13::spo13-m2::HphMX6	*LEU2* marker in *spo13::spo13-m2::LEU2* strain was replaced with *HphMX6* marker using AMp969
Multi-step constructs	
cdc5::KanMX6::pCUP1-CDC5-3V5	1. PCR-based promoter replacement (Longtine *et al*, 1998) using AMp408 2. PCR-based tagging (Moqtaderi & Struhl, 2008) using AMp729
sgo1::sgo1(Δdb)::KanMX6	1. *sgo1::sgo1(Δdb)::LEU2* was created by PCR using AMp899; the forward PCR primer carries the destruction box deletion 2. *LEU2* marker in *sgo1::sgo1(Δdb)::LEU2* strain was replaced with *KanMX6* marker using AMp195
sgo1::sgo1(Δdb)-yEGFP::KanMX6	1. *sgo1::sgo1(Δdb)::LEU2* was created by PCR using AMp899; the forward PCR primer carries the destruction box deletion 2. PCR-based tagging (Knop *et al*, 1999) using AMp476

Allele	**Source**
ndd1::HphMX6::pSCC1-NDD1	1. PCR-based promoter replacement (Longtine *et al*, 1998) using AMp373 2. *KanMX6* marker in *ndd1::KanMX6::pSCC1-NDD1* strain was replaced with *HphMX6* marker using AMp969
sgo1::HphMX6::pCLB2-SGO1	1. PCR-based promoter replacement (Longtine *et al*, 1998) using AMp372 2. *KanMX6* marker in *sgo1::KanMX6::pCLB2-SGO1* strain was replaced with *HphMX6* marker using AMp969
bub1::HphMX6::pCLB2-BUB1	1. PCR-based promoter replacement (Longtine *et al*, 1998) using AMp372 2. *KanMX6* marker in *bub1::KanMX6::pCLB2-BUB1* strain was replaced with *HphMX6* marker using AMp969
cdc5::HphMX6::pSPO21-CDC5-nfGFP::xhsv	1. PCR-based tagging (Knop *et al*, 1999) with *nfGFP::KanMX6* using AMp1128 2. removal of *KanMX6* marker using AMp728 (Moqtaderi & Struhl, 2008) 3. PCR-based promoter replacement (Longtine *et al*, 1998) using AMp1139
nkp1::KanMX6::pIME2-NKP1-nfGFP::HphMX6	1. PCR-based tagging (Knop *et al*, 1999) using AMp1128 2. *KanMX6* marker in *NKP1-nfGFP::KanMX6* strain was replaced with *HphMX6* marker using AMp969 3. PCR-based promoter replacement (Longtine *et al*, 1998) using AMp375
Other constructs	
trp1::TetR-ymEos3.2::LEU2	*TetR-ymEos3.2::LEU2* was amplified from AMp1138 by PCR and inserted into the *TRP1* locus by transformation
ura3::pCLB2-CDC5::URA3	NcoI-digested AMp502 was transformed into SK1

Table 6.2: Origin of alleles for yeast genetic mutation

6.2.2.2. Yeast media

Media	Composition	Concentration
YEPD	Bacto-peptone	2% (w/v)
	Bacto-yeast extract	1% (w/v)
	Glucose	2% (w/v)
	Adenine	0.3mM
	Agar (solid media only)	2% (w/v)
YPG	Bacto-peptone	2% (w/v)
	Bacto-yeast extract	1% (w/v)
	glycerol	2.5% (v/v)
	Agar	2% (w/v)
4%YPDA	Bacto-peptone	2% (w/v)
	Bacto-yeast extract	1% (w/v)
	Glucose	4% (w/v)
	Adenine	0.3mM
	Agar	2% (w/v)
YPA	Bacto-peptone	2% (w/v)
	Bacto-yeast extract	1% (w/v)
	KAc	1% (w/v)
BYTA	Bacto-tryptone	2% (w/v)
	Bacto-yeast extract	1% (w/v)
	KAc	1% (w/v)
	K phthalate	50mM
SPO	KAc	0.3% (w/v)
	Agar (solid media only)	2% (w/v)
Dropout media	Yeast nitrogen base	1% (w/v)
	Formedium synthetic complete dropout	1x
	Glucose	2% (w/v)
	Adenine	0.3mM
	Agar	2% (w/v)

Table 6.3: Yeast growth media

6.2.2.3. Drugs

The following drugs were used in YPDA plates to select for the indicated resistance markers: 400µg/ml G418 (*KanMX*), 100µg/ml Clonat (*NatMX*) and 300µg/ml Hygromycin (*HphMX*).

Benomyl was used at 90µg/ml in SPO media to depolymerise microtubules. SPO media was boiled prior to addition of benomyl.

β-estradiol was added to SPO media at 1µM to release cells from pachytene block (Carlile & Amon, 2008).

Hrr25-as1 and Cdc7-as3 were inhibited by addition of 5µM 1NM-PP1 and 20µm PP1 to SPO media. While Cdc7-as3 responds to inhibition by both PP1 and 1NM-PP1 (Wan *et al*, 2006), the effect of PP1 on Hrr25-as1 has not been tested (Petronczki *et al*, 2006).

6.2.2.4. Lithium acetate transformation

A 50ml culture of yeast at OD_{600} = 0.1 was grown for 3.5 hours at 30˚C. Cells were pelleted by spinning at 3000rpm and subsequently washed in 10ml of water, 1ml of water and 1ml of LiTE. Cells were resuspended in 250µl LiTE. 50µl of this cell suspension was mixed with precipitated PCR product from 400µl of PCR and 10µl sonicated, single-stranded salmon sperm DNA. 300µl of LiTE in 40% PEG was added and cells were shaken at 30˚C and 250rpm in an Eppendorf tube. Cells were heat-shocked at 42˚C for 15 minutes before pelleting at 2500rpm for 3min. Yeast pellets were resuspended in 300µl YPDA and plated onto either YPDA plates (for drug selection markers) or dropout plates and incubated at 30˚C. For drug selection YPDA were replica plated onto appropriate drug-selection plates one day after transformation.

6.2.2.5. Yeast crosses

Yeast of opposite mating types were crossed on YPDA plates. If one strain contained a unique selective marker the other stain did not carry, a small amount of the former strain was used and mixed with a large amount of the latter strain. If both yeast carried the same markers, little of the MATα strain was used. Crossed yeast were incubated at 30˚C for at least 7 hours before streaking onto plates selecting for the unique selection marker or onto YPDA plates spread with 200µl 1mg/ml α-factor (WHWLQLKPGQPMY; synthesised by Peptide Protein research). Single colonies were patched onto YPDA, grown over night and patches transferred to SPO plates. Yeast were left to sporulate for at least 32 hours before dissection.

6.2.2.6. Tetrad dissection

Sporulated yeast were resuspended in 20µl 0.1mg/ml zymolyase (AMS Biotechnology), diluted in 1M sorbitol. Cells were left to digest for 15 minutes before addition of 1ml of sterile distilled water. 20µl of yeast solution were transferred to a YPDA plate and dissected using a Singer MSM 400 micromanipulator. Cells were incubated at 30˚C for 2-3 days and resulting colonies patched on YPDA. Patches were incubated over night and replica plated onto selective plates. Colony PCR was carried out to identify constructs, if required.

6.2.2.7. Storage of yeast strains

Yeast were patched on YPG plates to select for cells containing mitochondria. Cells were grown over night and subsequently resuspended in 20% glycerol for long-term storage at -80˚C. To retrieve strains from storage, a small amount of frozen yeast were patched onto YPG and grown over night at 30˚C.

6.2.2.8. Growth conditions

Yeast were grown in YPDA and shaken at 250rpm at 30˚C. Diploid yeast were transferred to fresh media or 4%YPDA plates at least every 24 hours to prevent sporulation.

6.2.2.9. Induction of sporulation

Diploid yeast were removed from long-term storage and plated onto YPG plates. Cells were left to grow over night and patched onto 4% YPDA plates the next morning. After 8 hour incubation, cells were resuspended in YPDA and left to shake at 250rpm and 30˚C for 24 hours. The culture was then diluted to OD_{600} = 0.2 in either YPA or BYTA and grown at 30˚C, shaking at 250rpm for 14-16 hours. Cells

were spun down and washed in sterile distilled water before resuspending in SPO media at an OD_{600} = 1.8.

6.2.2.10. Meiosis

To arrest cells in metaphase, cells carrying *pCLB2-CDC20* were left to shake for 6 hours at 250rpm at 30˚C after transfer to SPO. Benomyl-treated cells were arrested for 5.5 hours, spun down at 3000rpm and subsequently resuspended in fresh SPO containing 90µg/ml benomyl. Cells were shaken at 30˚C and 250rpm for a further 30 minutes. For *SPO13* overexpression experiments, $CuSO_4$ was added at 50µM to cultures 4.5 hours into the metaphase arrest.

Cells carrying either *ndt80Δ* or *pGAL1-NDT80* were arrested in prophase for 5 hours after transfer to SPO. To release cells from *pGAL-NDT80* block, β-estradiol was added to cultures at 1µM after 5 hours in SPO. To overexpress *SPO13*, $CuSO_4$ was added at 50µM 30 minutes before release from the prophase arrest. *CDC5* overexpression was induced at the same time as release from the prophase arrest.

To determine whether specific mutants might influence cell cycle arrests in ChIP experiments, tubulin immunofluorescence samples were taken and assessed for the percentage of metaphase I spindles. Data was collected for the experiments shown in Figs. 2.3, 3.5 and 4.1 only.

6.3. Nucleic acid methods

6.3.1. Plasmids

Plasmid	Description	Publication/Source
AMp190	pFA6a-His3MX6 Gene knockout plasmid with *His3MX6* marker.	(Longtine *et al*, 1998)
AMp195	pFA6a-KanMX6 Gene knockout plasmid with *KanMX6* marker.	(Longtine *et al*, 1998)
AMp372	pFA6a-KanMX6-pCLB2 Plasmid for promoter replacement with *pCLB2*.	Angelika Amon lab

Plasmid	Description	Publication/Source
AMp373	pFA6a-KanMX6-pSCC1 Plasmid for promoter replacement with *pSCC1*.	Angelika Amon lab
AMp375	pFA6a-KanMX6-pIME2 Plasmid for promoter replacement with *pIME2*.	Angelika Amon lab
AMp408	pFA6a-KanMX6-pCUP1 Plasmid for promoter replacement with *pCUP1*.	Angelika Amon lab
AMp476	*yEGFP* tagging plasmid with *KanMX6* marker.	pYM12 (Knop *et al*, 1999)
AMp502	YIplac211-pCLB2-CDC5 *URA3* integration plasmid carrying *pCLB2-CDC5*.	Angelika Amon lab
AMp680	pFA6a-3FLAG-NatMX6 *3FLAG* tagging plasmid with *NatMX6* marker.	Robin Allshire lab
AMp683	pFA6a-NatMX6 Gene knockout plasmid with *NatMX6* marker.	Hardwick lab
AMp728	Plasmid for markerless tagging with *3HSV*.	ZM473 (Moqtaderi & Struhl, 2008)
AMp729	Plasmid for markerless tagging with *3V5*.	ZM474 (Moqtaderi & Struhl, 2008)
AMp751	pFA6a-tdTomato-NatMX6 tdTomato tagging plasmid with *NatMX6* marker.	Taxis *et al* (2006)
AMp894	pFA6a-3FLAG-KanMX6 *3FLAG* tagging plasmid with *KanMX6* marker.	Robin Allshire lab
AMp899	YIplac128-SGO1 *LEU2* integration plasmid carrying *SGO1*.	Lab stock Creator: Adèle Marston
AMp968	pFA6a-6xGLY-HSV-KanMX6 *HSV* tagging plasmid with *KanMX6* marker.	Addgene (Funakoshi & Hochstrasser, 2009)
AMp969	pFA6a-6xGLY-V5-KanMX6 *V5* tagging plasmid with *KanMX6* marker.	Addgene (Funakoshi & Hochstrasser, 2009)
AMp1041	Plasmid for N-terminal or internal *6HA*-tagging of essential genes.	Euroscarf pOM13 (Gauss *et al*, 2005)
AMp1062	YIplac128-spo13-m2 *LEU2* integration plasmid carrying *spo13-m2*.	This study Site-directed mutagenesis was performed on AMp178 (YIplac128-SPO13) to introduce S132T and S134T mutations.

Plasmid	Description	Publication/Source
AMp1077	pFA6a-LEU2 Gene knockout plasmid with *LEU2* marker.	This study AMp195 was digested with BglII and PmeI to replace the *KanMX6* marker with *LEU2*.
AMp1128	*nfGFP* tagging plasmid with *KanMX6* marker.	This study Site-directed mutagenesis was performed on AMp476 to introduce S65T and G67A mutations into *GFP*.
AMp1138	YIplac128-TetR-ymEos3.2 *LEU2* integration plasmid carrying *TetR-ymEos3.2*.	This study Yeast codon-optimised mEos3.2 was amplified from a synthetic gene construct (GeneArt) and used to replace *GFP* in AMp326 (YIplac128-TetR-GFP) using Gibson assembly.
AMp1139	pFA6a-HphMX6-pSPO21 Plasmid for promoter replacement with *pSPO21*.	This study Gibson assembly was used to replace the *KanMX6* marker in AMp34 (pFA6a-KanMX6-pSPO21; from Angelika Amon lab) with *HphMX6*.
AMp1147	*GBP* tagging plasmid with *His3MX6* marker.	This study *GBP* was amplified by PCR from AMp961 (pFA6a-GBP-mRFP) and cloned to replace *3MYC* in AMp472 (pYM5 (Knop *et al*, 1999)) by Gibson assembly.
AMp1199	pFA6a-6xGLY-HKMT-His3MX6 *HKMT* tagging plasmid with *His3MX6* marker.	This study *HKMT* was amplified from AMp1184 (pYES2-myc-HKMT-GL (Zuzuarregui *et al*, 2012)) and cloned into AMp967 (pFA6a-6xGLY-HSV-HisMX6) to replace the *HSV* tag.
AMp1200	pFA6a-6xGLY-2H3-2HA-hphMX4 *2H3-2HA* tagging plasmid with *HphMX6* marker.	This study *2H3-2HA* was amplified from AMp1183 (pYX242-3H3-2HA-GL-Net1(1-600) (Zuzuarregui *et al*, 2012)) and cloned into AMp969 (pFA6a-6xGLY-HSV-HphMX6) to replace the *HSV* tag.

Table 6.4: Plasmids used in this study

6.3.2. Cloning

6.3.2.1. Restriction enzyme-based cloning

For vector digestion, 20µl of plasmid prepared with mini-prep were digested in the presence of 1x NEB buffer (appropriate to the restriction enzyme), 2µl restriction enzyme (per enzyme used) in a 50µl reaction. After 2 hours of incubation at 37˚C, 2µl calf intestinal phosphatase (CIP) (NEB) was added and reactions incubated at 37˚C for 1 hour. Vectors were purified either with a PCR purification kit (Qiagen) or after gel electrophoresis.

Inserts were prepared by PCR using Q5 polymerase (NEB) in a total of 200µl of reaction volume (4 x 50µl reactions). PCR product was purified using a kit (Qiagen). Digestions used 15µl of purified PCR product with 1x NEB buffer (appropriate to enzyme) and 1µl of restriction enzyme (per enzyme used). Inserts were purified either with a PCR purification kit (Qiagen) or after gel electrophoresis.

For ligation, 100µg of vector were mixed in a 1:5 ratio with the desired insert and ligated using Quick ligase (NEB) before transformation into *E. coli* by electroporation.

6.3.2.2. Gibson assembly cloning

For cloning by Gibson assembly (NEB), both insert and vector were amplified by PCR either from plasmid DNA (100µg) or genomic DNA (500µg) using Q5 polymerase (NEB). If plasmid DNA was used as template, 8µl of PCR product were incubated with 1µl CutSmart buffer (NEB) and 1µl DpnI (NEB) to digest template DNA. 100µg of vector were assembled with insert in 1:5 ratio and transformed into *E. coli* according to manufacturer's instructions.

6.3.3. Plasmid sequencing

Plasmids prepared by mini-prep or midi-prep were sequenced by mixing 2µl plasmid DNA, 2µl Big Dye terminator v3.1 (Applied Biosystems), 0.5µl 5µM

primer, 2µl Big Dye (Applied Biosystems) and 3.5µl water. Reactions were subjected to PCR using the following conditions:

Pre-incubation	95˚C	30 seconds
Amplification (25 cycles)	95˚C	30 seconds
	55˚C	15 seconds
	60˚C	4 minutes
Final extension	72˚C	5 minutes

Samples were sequenced on an ABI 3730 DNA analyser (Applied Biosystems) by the School of Biological Sciences sequencing service, University of Edinburgh.

6.3.4. Site-directed mutagenesis

Point mutants were created using the Quikchange XL II site-directed mutagenesis kit (Agilent) according to manufacturer's instructions.

6.3.5. *E. coli* mini-prep

2ml of LB + ampicillin were inoculated with a single colony of transformed *E. coli* and left to grow at 37˚C, shaking at 200rpm for 8 hours. Cells were spun at 13000rpm and the pellet resuspended in 100µl GTE. 150µl of alkaline SDS and 150µl of high salt buffer were added and the mixture left on ice for 15 minutes. The mixture was spun down at 13000rpm at 4˚C and the supernatant added to 1ml of cold ethanol. The mixture was spun again at 13000rpm and 4˚C and the pellet washed with 200µl 70% ethanol. The pellet was left to air-dry and then resuspended in 50µl TE.

6.3.6. *E. coli* midi-prep

50ml of LB + ampicillin were inoculated with a single colony of transformed *E. coli* and left to grow at 37˚C, shaking at 200rpm for 16 hours. Cells were spun at 3600rpm for 15 minutes and the pellet resuspended in 2.5ml GTE. 5ml of alkaline

SDS and 2.5ml of high salt buffer were added and the mixture spun at 3600rpm and 4˚C for 15 minutes. The solution was poured through a thin paper tissue to collect the supernatant. 10ml of isopropanol were added and the mixture spun at 3600rpm and 4˚C for 5 minutes. The resulting pellet was resuspended in 750µl TE and before addition of 1ml 5M LiCl. The mixture was left on ice for 20 minutes to precipitate RNA and subsequently spun at 3600rpm and 4˚C for 5 minutes. The supernatant was collected and 3.5ml of ethanol added. The mixture was left at -20˚C for 10 minutes before spinning at 3600rpm and 4˚C for 5 minutes. The pellet was resuspended in 200µl TE and precipitated once more after addition of 20µl 3M NaAc and 500µl ethanol by centrifuging at 13000rpm and 4˚C for 5 minutes. Pellets were air-dried and resuspended in 100µl-200µl TE, depending on pellet size.

6.3.7. Polymerase chain reaction (PCR)

In general, PCR reactions for gene knockouts and colony PCR contained 50-500ng template DNA, 200µM dNTPs (Roche), PCR buffer, 1µM of each oligonucleotide primer, 2% (v/v) lab-prepared Taq polymerase and sterile water to make up the desired reaction volume. To epitope-tag genes, I used Ex-Taq polymerase (TaKaRa) along with the supplied buffer and dNTPs. For cloning, I amplified constructs with Q5 polymerase and supplied buffer according to manufacturer's instructions with an annealing temperature 5-7˚C below the suggested temperature (http://tmcalculator.neb.com/). PCRs were performed using the following conditions:

Pre-incubation	95˚C	5 minutes
Amplification (25 cycles)	95˚C	30 seconds
	52-62˚C	30 seconds
	72˚C	1 minute/kb
Final extension	72˚C	10 minutes

For colony PCR, pre-incubation was extended to 10 minutes. Furthermore, a small amount of yeast or bacterial colony was used as template instead of plasmid or genomic DNA.

6.3.8. Agarose gel electrophoresis

DNA products were visualised on an agarose gel. Gels were prepared by adding agarose (Melford) to TAE at the desired percentage (w/v) and microwaving the mixture to dissolve the agarose. Ethidium bromide was added to the cooled mixture at 0.5µg/ml. Gels were poured in a pre-cast form. DNA samples were mixed with Orange G loading dye. DNA samples were run at 90-130V. 1kb ladder (NEB) was used as a size marker.

6.3.9. DNA extraction from agarose gels

For DNA extraction, agarose gels were prepared with low melting temperature agarose (Thermo Scientific) at 0.5% (w/v). Desired DNA bands were excised from the gel and purified using a commercial gel purification kit (Qiagen).

6.3.10. Smash and grab preparation of yeast genomic DNA

A small amount of yeast was resuspended in 200µl DNA breakage buffer. Approximately 100µl of silica beads (Biospec) and 200µl phenol:chloroform were added and the mixture vortexed for 4 minutes. Samples were centrifuged at 13000rpm for 5 minutes before adding the upper aqueous layer of the supernatant to 900µl cold ethanol. Samples were spun once more at 13000rpm and the pellet washed with 70% ethanol. Pellets were left to air-dry and subsequently resuspended in 50µl TE.

6.3.11. Sequencing of yeast strains

To confirm point mutations in yeast strains, the desired gene was amplified from genomic DNA by PCR using ExTaq polymerase (TaKaRa). 3µl of PCR products were treated with 0.5µl ExoI (NEB) and 0.5µl thermo-sensitive alkaline phosphatase (Promega). Reactions were incubated at 37˚C for 15 minutes and then at 80˚C for 15 minutes to deactivate enzymes. 4µl of Big Dye (Applied Biosystems) and 2µl 8µM

primer were added to reactions. PCR was then carried out with the following conditions:

Pre-incubation	96˚C	30 seconds
Amplification (25 cycles)	96˚C	30 seconds
	55˚C	15 seconds
	60˚C	4 minutes
Final extension	72˚C	5 minutes

Samples were sequenced on an ABI 3730 DNA analyser (Applied Biosystems) by the School of Biological Sciences sequencing service, University of Edinburgh.

6.3.12. Quantitative PCR (qPCR)

qPCR reaction mixtures are as follows: 5µl template DNA (Input or ChIP sample), 0.4µl 20µM primer (each forward and reverse), 1µl qPCR buffer, 5µl SYBR Green ER mix (Life Technologies) and 8.2µl DEPC-treated sterile water (VWR). Reactions were set up in triplicate and run on a LightCycler 480 system (Roche) in 96-well plates (Roche). Data was collected from LightCycler 480 system software and analysed in Microsoft Excel.

qPCR primer efficiency was determined using standard curves. Primers used in this study are outlined in Table 6.5 below.

Chro-mosome	**Location (as depicted in graphs)**	**Distance from centromere**	**Pri-mer pair**	**Sequence**	**Amp-licon size (bp)**	**Efficiency**
III	Centromere	250bp downstream	1279	TGTTGATGGGTTTACAATTT	91	1.958
			1280	CTTTCAATGATTGCTCTAAATC		
IV	Arm	95kb upstream	782	AGATGAAACTCAGGCTACCA	93	2.013
			783	TGCAACATCGTTAGTTCTTG		
IV	Peri-centromere	9.5kb upstream	1319	ATGATTCAATGGATTTAGCC	103	1.919
			1320	GTCAGTCTTATGCTGTTCCC		
IV	Left boundary	9.3kb upstream	4877	TACAGCAAATGTTGGTGATT	118	2.033
			4878	ACCTGCTTGTTCAACTCTCT		
IV	Centromere	150bp downstream	794	CCGAGGCTTTCATAGCTTA	80	2.061
			795	ACCGGAAGGAAGAATAAGAA		
IV	Right boundary	6.5kb downstream	4885	AGAAACCACCCATAATTGAG	92	2.05
			4886	ACGATAGTCAAATTTCCGTT		
V	Centromere	200bp downstream	945	TGAAGGTGAGCTTAAGACAG	115	1.891
			946	CAACCATGTTCGTAGCTAAA		

Table 6.5: qPCR primers

6.4. Protein methods

6.4.1. TCA whole cell extract preparation

4.5ml of meiotic culture were spun down at 3000rpm and the pellet resuspended in 5ml TCA. The mixture was left on ice for 10 minutes before spinning down at 3000rpm and 4˚C. The pellet was then transferred to a Fastprep tube (MP Biomedicals) and spun again at 13000rpm and 4˚C. Any remaining liquid was removed and cells snap-frozen in liquid nitrogen for storage at -80˚C.

Frozen cells were thawed and washed in 1ml acetone. Pellets were then air-dried for at least 3 hours and resuspended in 100µl protein breakage buffer. About 50µl of silica beads (Biospec) were added and cells lysed in a Fastprep Bio-Pulveriser FP120 three times for 45 seconds at 6.5 speed. 50µl of 3x SDS sample buffer were added and tubes boiled at 100˚C for 5 minutes. Tubes were spun at 13000rpm and supernatant transferred to a new Eppendorf. Samples were either loaded on a gel or stored at -20˚C.

6.4.2. SDS polyacrylamide gel electrophoresis (SDS-PAGE)

6.4.2.1. Biometra V15.17 system

Two glass plates were assembled with 1.5mm spacer in between and 30ml of polyacrylamide gel at the desired acrylamide concentration poured in between. The gel was topped with a layer of isopropanol and left to set. Once set, the isopropanol was poured off and the stacking gel solution poured on top of the separation gel. A comb was immediately inserted into the stacking gel. Once polymerised, the gel was moved to a Biometra V15.17 electrophoresis unit. 10µl of whole cell extract were loaded alongside 7.5µl pre-stained protein marker, broad range (NEB) or colour pre-stained protein standard, broad range (NEB). Gels were run at 55mA for 45 minutes followed by 12mA over night.

6.4.2.2. Bio-Rad mini transblot system

Glass plates provided by the manufacturer with 1mm spacing were assembled and gels poured similarly to the Biometra system, using 4.5ml of separation gel mix. Poured gels were transferred to a Mini Trans-Blot apparatus (Bio-Rad). 7.5µl of sample were loaded for 10-well gels, with 5µl of markers mentioned above.

6.4.3. Western blotting

For semi-dry transfer, gels were soaked in transfer buffer and sandwiched between 6 sheets of blotting paper (Whatman) and a protran BA 85 nitrocellulose membrane (Whatman), all previously soaked in transfer buffer. The stack was transferred to a semi-dry transfer apparatus (Amershan TE70). Proteins were transferred at $1mA/cm^2$ for 2.5 hours.

For wet transfer of mini-gels, soaked gels were sandwiched between 2 sheets of blotting paper and a nitrocellulose membrane. Gels were assembled in a Mini Trans-Blot apparatus (Bio-Rad) according to manufacturer's instructions. Gels were transferred at 100V for 1.5 hours.

Following transfer, gels were stained with Ponceau S. The membrane was blocked in 5% milk (in PBS-T) and then incubated with primary antibody in 2% milk (in PBS-T) over night. Membranes were rinsed with PBS three times and then washed in PBS-T three times for 15 minutes. Membranes were then incubated with secondary antibody in 2% milk for 1 hour. After incubation membranes were rinsed as before and washed three times in PBS-T for 5 minutes each. Proteins were visualised using the SuperSignal West Pico or Femto chemiluminescence kit (Thermo Scientific) according to manufacturer's instructions. Signal was detected using Kodak Bio-Max light film and films were developed using a Konica-Minolta SRX-101A developer. Antibodies used for western blotting are listed below in Table 6.6.

Antibody	Species	Dilution	Source
HA.11 (α-Ha)	Mouse	1:1000	Covance
9E10 (α-Myc)	Mouse	1:1000	Covance
M2 (α-Flag)	Mouse	1:1000	Sigma Aldrich
α-V5	Mouse	1:1000	Bio-Rad
α-H3K9me3	Mouse	1:2000	Bio-Techne
α-Pgk1	Mouse	1:5000	Life Technologies
α-Pgk1	Rabbit	1:10000	Lab stock (Colette Connor)
α-Mouse-HRP	Sheep	1:5000	GE Healthcare
α-Rabbit-HRP	Donkey	1:5000	GE Healthcare

Table 6.6: Western blot antibodies

6.4.4. Chromatin immunoprecipitation

Per IP, 50ml of yeast cultures was grown and arrested in either prophase or metaphase. After removing samples for TCA extracts and tubulin immunofluorescence, cells were added to 5ml 11% formaldehyde (in ChIP diluent) (Sigma) and fixed for 2 hours in a Falcon tube under constant low frequency shaking. Cells were spun down at 3000rpm and 4˚C and washed twice in TBS and once in FA lysis buffer with 0.1% SDS. Cells were then transferred to Fastprep tubes (MP biomedicals), spun down at 13000rpm and the pellet snap-frozen in liquid nitrogen for storage at -80˚C.

Cells were thawed on ice and 300µl FA lysis buffer with 0.5% SDS was added together with about 200µl of silica beads (Biospec). Cells were lysed in a Fastprep Bio-Pulveriser FP120 twice for 30 seconds at 6.5 speed. Cell lysates were spun at 13000rpm and 4˚C for 15 minutes. Pellets were washed with 1ml FA lysis buffer/0.1% SDS and then resuspended in 500µl FA lysis buffer/0.1% SDS. To shear DNA, cells were sonicated in a BioRuptor Twin sonicator (Diagenode) at 'high' setting for 30 cycles at 30 second on/off intervals. Sonicated samples were centrifuged at 13000rpm and 4˚C for 15 minutes and the supernatant was added to 500µl FA lysis buffer/0.1% SDS. Samples were spun once more at 13000rpm and 4˚C for 15 minutes and the supernatant added to 300µl FA lysis buffer/0.1% SDS. Samples were mixed by inversion and 10µl removed as input sample. 1ml of sample was added to Protein G Dynabeads (15µl per IP), which had previously been washed four times with FA lysis buffer/0.1% SDS. The appropriate antibody was then added to the beads and lysate: 7.5µl of 12CA5 α-Ha (Roche), 10µl of 9E10 α-Myc

(Covance), 5µl of M2 α-Flag (Sigma) or 10µl α-V5 (Bio-Rad). ChIP samples were incubated under rotation at 4˚C over night.

Beads were subsequently washed in 1ml of ChIP wash buffers 1-4, with 5 minute rotations in between. 200µl of 10% Chelex (Bio-Rad) slurry was added to both beads and the input samples. Samples were boiled at 100˚C for 10 minutes, spun down briefly at 2000rpm and treated with 2.5µl 10mg/ml proteinase K (Promega) at 55˚C for 30 minutes. To inactivate proteinase K, samples were boiled once more at 100˚C for 10 minutes. Samples were spun down at 2000rpm for 30 seconds and 130µl of supernatant removed for qPCR analysis.

6.5. Microscopy

6.5.1. Tubulin immunofluorescence

300µl of meiotic samples was spun down at 13000rpm and the pellet resuspended in 500µl 3.7% formaldehyde (Sigma), diluted in KP_i buffer. Samples were left to fix at 4˚C over night and then washed three times with 1ml KP_i buffer and 1ml 1.2M sorbitol-citrate. Samples were then frozen for storage at -20˚C.

Immunofluorescence slides were prepared by rinsing with water and treating wells with 5µl 0.1% poly-lysine for 5 minutes. Slides were rinsed again and left to air-dry. Stored samples were thawed and cells pelleted at 10000rpm for 3 minutes. Pellets were resuspended in digestion mix containing 200µl 1.2M sorbitol-citrate, 20µl glusulase (Perkin Elmer) and 6µl 1mg/ml zymolyase (AMS biotechnology). Cells were digested for 2-2.5 hours at 30˚C until they mostly appeared phase dark with jagged edges under the light microscope. Cells were spun at 3000rpm for 3 minutes and the supernatant removed apart from about 30µl. Pellets were resuspended and 5µl pipetted onto wells on the prepared immunofluorescence slides. Cells were left to attach for 10 minutes and liquid aspirated off. Cells were fixed onto slides by submerging slides in methanol for 3 minutes, followed by a 10 second wash in acetone. 5µl of rat α-tubulin (Bio-Rad), diluted 1:50 in PBS-BSA, were added to each well and left at room temperature for 1 hour in a moist, dark chamber. The liquid was removed by aspiration and wells washed five times with 5µl PBS-BSA.

5µl donkey α-rat FITC-conjugated antibody (Jackson ImmunoResearch), diluted 1:100 in PBS-BSA, was added to wells and left at room temperature for 1 hour in a moist, dark chamber. Liquid was aspirated once more and wells washed five times with 5µl PBS-BSA. 3µl DAPI-mount was added to each well, slides were covered with a glass coverslip (Marienfeld-Superior), sealed with nail varnish and stored at -20˚C.

Tubulin staining was assessed using a Zeiss Axioplan 2 fluorescence microscope with 100x Plan ApoChromat NA 1.4 oil lens.

6.5.2. Sample preparation for live cell imaging

For live cell imaging, meiotic cultures were shaken for 2.5 hours and then transferred to a microfluidics system. Prophase block-release strains were transferred onto a microfluidics plate or 8-well µ-slides (ibidi) 15 minutes after release from pachytene.

6.5.2.1. Microfluidics system

Microfluidics plates (Millipore) were prepared by sealing the plates to the manifold of an ONIX microfluidics system (CellASIC) and using the manufacturer's purging protocol to restore soft PDMS after vacuum storage of plates. Wells on the plate were then washed three times with 200µl SPO media and media appropriate for the experimental design was then added to wells. The plate was pre-heated at 30˚C for 30 minutes. Cells were then added to the appropriate wells and the plate sealed to the manifold. Cells were loaded using the manufacturer's recommended protocol. Cells were supplied with new media at a pressure of 2psi for the duration of the experiment.

6.5.2.2. 8-well µ-slide

8-well µ-slides (ibidi) were prepared by first washing wells with ethanol. 45µl of concanavalin A was added to each well and left at 30˚C for 15 minutes. Wells were

washed three times with 500µl sterile distilled water. Cells equivalent to 1.8ml culture, resuspended in 300µl SPO were loaded into each well and left at 30˚C for 20 minutes. Cells were aspirated and wells washed with conditioned SPO media (SPO media used in a previous experiment, filtered with 0.45µm bottle top filter (Nalgene)). 500µl of conditioned SPO media was added to each well, containing drugs as required.

6.5.3. Microscopy

Live cell imaging was carried out on a DeltaVision Elite system (Applied Precision) connected to an inverted Olympus IX-71 microscope with a 100x UPlanSApo NA 1.4 oil lens. Images were taken using a Photometrics Cascade II EMCCD camera. Camera, shutters and stage were controlled through the SoftWorx software (Applied precision) on a Linux operating system.

Cells were imaged at 15 minute intervals for a total of 12 hours (for prophase block-release experiments) or 15 hours (for asynchronous meiotic cultures). 6-8 points were imaged per strain, with 7 z-stacks typically being acquired at each point with 0.85µm spacing. For imaging of TetR-ymEos3.2 only 6 z-stacks were acquired because ymEos3.2 was found to bleach very quickly. Imaging conditions for different proteins are outlined in table 6.7. Images were analysed and processed using Image Pro Premier (Media Cybernetics) and ImageJ software (National Institutes of Health).

Protein	**Camera gain**	**Exposure time**	**% transmitted light**
Rec8-GFP	290	0.3 seconds	10%
Sgo1-GFP	290	0.3 seconds	10%
TetR-GFP	290	0.2 seconds	5%
MTW1-tdTomato/ PDS1-tdTomato	290	0.2 seconds	5%
SPC42-tdTomato/ PDS1-tdTomato	290	0.2 seconds	5%
TetR-tdTomato	290	0.1 seconds	5%
TetR-ymEos3.2	380	0.035 seconds	32%

Table 6.7: Typical imaging conditions

REFERENCES

Agarwal R & Cohen-Fix O (2002) Phosphorylation of the mitotic regulator Pds1/securin by Cdc28 is required for efficient nuclear localization of Esp1/separase. *Genes Dev.* **16:** 1371–1382

Agarwal S & Roeder GS (2000) Zip3 provides a link between recombination enzymes and synaptonemal complex proteins. *Cell* **102:** 245–255

Alexandru G, Uhlmann F, Mechtler K, Poupart M-A & Nasmyth K (2001a) Phosphorylation of the Cohesin Subunit Scc1 by Polo/Cdc5 Kinase Regulates Sister Chromatid Separation in Yeast. *Cell* **105:** 459–472

Alexandru G, Uhlmann F, Mechtler K, Poupart MA & Nasmyth K (2001b) Phosphorylation of the cohesin subunit Scc1 by Polo/Cdc5 kinase regulates sister chromatid separation in yeast. *Cell* **105:** 459–472

Asakawa H, Hayashi A, Haraguchi T & Hiraoka Y (2005) Dissociation of the Nuf2-Ndc80 complex releases centromeres from the spindle-pole body during meiotic prophase in fission yeast. *Mol. Biol. Cell* **16:** 2325–2338

Attner MA & Amon A (2012) Control of the mitotic exit network during meiosis. *Mol. Biol. Cell* **23:** 3122–3132

Attner MA, Miller MP, Ee L-S, Elkin SK & Amon A (2013) Polo kinase Cdc5 is a central regulator of meiosis I. *Proc. Natl. Acad. Sci. U.S.A.* **110:** 14278–14283

Azzam R, Chen SL, Shou W, Mah AS, Alexandru G, Nasmyth K, Annan RS, Carr SA & Deshaies RJ (2004) Phosphorylation by Cyclin B-Cdk Underlies Release of Mitotic Exit Activator Cdc14 from the Nucleolus. *Science* **305:** 516–519

Bannister LA, Reinholdt LG, Munroe RJ & Schimenti JC (2004) Positional cloning and characterization of mouse mei8, a disrupted allele of the meiotic cohesin Rec8. *genesis* **40:** 184–194

Basto R, Gomes R & Karess RE (2000) Rough deal and Zw10 are required for the metaphase checkpoint in Drosophila. *Nat. Cell Biol.* **2:** 939–943

Bausch C, Noone S, Henry JM, Gaudenz K, Sanderson B, Seidel C & Gerton JL (2007) Transcription alters chromosomal locations of cohesin in Saccharomyces cerevisiae. *Mol. Cell. Biol.* **27:** 8522–8532

Beckouët F, Srinivasan M, Roig MB, Chan K-L, Scheinost JC, Batty P, Hu B, Petela N, Gligoris T, Smith AC, Strmecki L, Rowland BD & Nasmyth K (2016) Releasing Activity Disengages Cohesin's Smc3/Scc1 Interface in a Process Blocked by Acetylation. *Mol. Cell* **61:** 563–574

Ben-Shahar TR, Heeger S, Lehane C, East P, Flynn H, Skehel M & Uhlmann F (2008) Eco1-Dependent Cohesin Acetylation During Establishment of Sister

Chromatid Cohesion. *Science* **321:** 563–566

Benjamin KR, Zhang C, Shokat KM & Herskowitz I (2003) Control of landmark events in meiosis by the CDK Cdc28 and the meiosis-specific kinase Ime2. *Genes Dev.* **17:** 1524–1539

Berchowitz LE, Gajadhar AS, van Werven FJ, De Rosa AA, Samoylova ML, Brar GA, Xu Y, Xiao C, Futcher B, Weissman JS, White FM & Amon A (2013) A developmentally regulated translational control pathway establishes the meiotic chromosome segregation pattern. *Genes Dev.* **27:** 2147–2163

Bernard P, Maure JF, Partridge JF, Genier S, Javerzat JP & Allshire RC (2001) Requirement of heterochromatin for cohesion at centromeres. *Science* **294:** 2539–2542

Biggins S (2013) The composition, functions, and regulation of the budding yeast kinetochore. *Genetics* **194:** 817–846

Bizzari F & Marston AL (2011) Cdc55 coordinates spindle assembly and chromosome disjunction during meiosis. *J. Cell Biol.* **193:** 1213–1228

Blanco MA, Pelloquin L & Moreno S (2001) Fission yeast mfr1 activates APC and coordinates meiotic nuclear division with sporulation. *J. Cell. Sci.* **114:** 2135–2143

Blat Y & Kleckner N (1999) Cohesins bind to preferential sites along yeast chromosome III, with differential regulation along arms versus the centric region. *Cell* **98:** 249–259

Blitzblau HG & Hochwagen A (2013) ATR/Mec1 prevents lethal meiotic recombination initiation on partially replicated chromosomes in budding yeast. *elife* **2:** e00844

Bowles J, Knight D, Smith C, Wilhelm D, Richman J, Mamiya S, Yashiro K, Chawengsaksophak K, Wilson MJ, Rossant J, Hamada H & Koopman P (2006) Retinoid signaling determines germ cell fate in mice. *Science* **312:** 596–600

Brar GA, Hochwagen A, Ee L-SS & Amon A (2009) The multiple roles of cohesin in meiotic chromosome morphogenesis and pairing. *Mol. Biol. Cell* **20:** 1030–1047

Brar GA, Kiburz BM, Zhang Y, Kim J-E, White F & Amon A (2006) Rec8 phosphorylation and recombination promote the step-wise loss of cohesins in meiosis. *Nature* **441:** 532–536

Buckingham LE, Wang HT, Elder RT, McCarroll RM, Slater MR & Esposito RE (1990) Nucleotide sequence and promoter analysis of SPO13, a meiosis-specific gene of Saccharomyces cerevisiae. *Proc. Natl. Acad. Sci. U.S.A.* **87:** 9406–9410

Buffin E, Lefebvre C, Huang J, Gagou ME & Karess RE (2005) Recruitment of

Mad2 to the Kinetochore Requires the Rod/Zw10 Complex. *Current Biology* **15:** 856–861

Buonomo SB, Clyne RK, Fuchs J, Loidl J, Uhlmann F & Nasmyth K (2000) Disjunction of homologous chromosomes in meiosis I depends on proteolytic cleavage of the meiotic cohesin Rec8 by separin. *Cell* **103:** 387–398

Buonomo SBC, Rabitsch KP, Fuchs J, Gruber S, Sullivan M, Uhlmann F, Petronczki M, Tóth A & Nasmyth K (2003) Division of the nucleolus and its release of CDC14 during anaphase of meiosis I depends on separase, SPO12, and SLK19. *Dev. Cell* **4:** 727–739

Burton JL & Solomon MJ (2007) Mad3p, a pseudosubstrate inhibitor of APCCdc20 in the spindle assembly checkpoint. *Genes Dev.* **21:** 655–667

Carlile TM & Amon A (2008) Meiosis I is established through division-specific translational control of a cyclin. *Cell* **133:** 280–291

Chambon J-P, Touati SA, Berneau S, Cladière D, Hebras C, Groeme R, McDougall A & Wassmann K (2013) The PP2A Inhibitor I2PP2A Is Essential for Sister Chromatid Segregation in Oocyte Meiosis II. *Curr. Biol.* **23:** 485–490

Chan GK, Jablonski SA, Starr DA, Goldberg ML & Yen TJ (2000) Human Zw10 and ROD are mitotic checkpoint proteins that bind to kinetochores. *Nat. Cell Biol.* **2:** 944–947

Chan K-L, Roig MB, Hu B, Beckouët F, Metson J & Nasmyth K (2012) Cohesin's DNA Exit Gate Is Distinct from Its Entrance Gate and Is Regulated by Acetylation. *Cell* **150:** 961–974

Chao WCH, Kulkarni K, Zhang Z, Kong EH & Barford D (2012) Structure of the mitotic checkpoint complex. *Nature* **484:** 208–213

Charles JF, Jaspersen SL, Tinker-Kulberg RL, Hwang L, Szidon A & Morgan DO (1998) The Polo-related kinase Cdc5 activates and is destroyed by the mitotic cyclin destruction machinery in S. cerevisiae. *Curr. Biol.* **8:** 497–507

Cheeseman IM, Anderson S, Jwa M, Green EM, Kang JS, Yates JR, Chan CSM, Drubin DG & Barnes G (2002) Phospho-regulation of kinetochore-microtubule attachments by the Aurora kinase Ipl1p. *Cell* **111:** 163–172

Chelysheva L, Diallo S, Vezon D, Gendrot G, Vrielynck N, Belcram K, Rocques N, Márquez-Lema A, Bhatt AM, Horlow C, Mercier R, Mézard C & Grelon M (2005) AtREC8 and AtSCC3 are essential to the monopolar orientation of the kinetochores during meiosis. *J. Cell. Sci.* **118:** 4621–4632

Cheng C-H, Lo Y-H, Liang S-S, Ti S-C, Lin F-M, Yeh C-H, Huang H-Y & Wang T-F (2006) SUMO modifications control assembly of synaptonemal complex and polycomplex in meiosis of Saccharomyces cerevisiae. *Genes Dev.* **20:** 2067–2081

Chikashige Y, Ding DQ, Funabiki H, Haraguchi T, Mashiko S, Yanagida M & Hiraoka Y (1994) Telomere-led premeiotic chromosome movement in fission yeast. *Science* **264:** 270–273

Chu S, DeRisi J, Eisen M, Mulholland J, Botstein D, Brown PO & Herskowitz I (1998) The transcriptional program of sporulation in budding yeast. *Science* **282:** 699–705 Available at: http://www.sciencemag.org/content/282/5389/699.full.html

Chu T, Henrion G, Haegeli V & Strickland S (2001) Cortex, a Drosophila gene required to complete oocyte meiosis, is a member of the Cdc20/fizzy protein family. *genesis* **29:** 141–152

Ciferri C, Pasqualato S, Screpanti E, Varetti G, Santaguida S, Reis Dos G, Maiolica A, Polka J, De Luca JG, De Wulf P, Salek M, Rappsilber J, Moores CA, Salmon ED & Musacchio A (2008) Implications for kinetochore-microtubule attachment from the structure of an engineered Ndc80 complex. *Cell* **133:** 427–439

Ciosk R, Shirayama M, Shevchenko A, Tanaka T, Tóth A, Shevchenko A & Nasmyth K (2000) Cohesin's Binding to Chromosomes Depends on a Separate Complex Consisting of Scc2 and Scc4 Proteins. *Mol. Cell* **5:** 243–254

Ciosk R, Zachariae W, Michaelis C, Shevchenko A, Mann M & Nasmyth K (1998) An ESP1/PDS1 complex regulates loss of sister chromatid cohesion at the metaphase to anaphase transition in yeast. *Cell* **93:** 1067–1076

Clarke AS, Tang TT-L, Ooi DL-Y & Orr-Weaver TL (2005) POLO kinase regulates the Drosophila centromere cohesion protein MEI-S332. *Dev. Cell* **8:** 53–64

Clift D, Bizzari F & Marston AL (2009) Shugoshin prevents cohesin cleavage by PP2A(Cdc55)-dependent inhibition of separase. *Genes Dev.* **23:** 766–780

Cloud V, Chan Y-L, Grubb J, Budke B & Bishop DK (2012) Rad51 is an accessory factor for Dmc1-mediated joint molecule formation during meiosis. *Science* **337:** 1222–1225

Clute P & Pines J (1999) Temporal and spatial control of cyclin B1 destruction in metaphase. *Nat. Cell Biol.* **1:** 82–87

Clyne RK, Katis VL, Jessop L, Benjamin KR, Herskowitz I, Lichten M & Nasmyth K (2003) Polo-like kinase Cdc5 promotes chiasmata formation and cosegregation of sister centromeres at meiosis I. *Nat. Cell Biol.* **5:** 480–485

Cohen-Fix O, Peters JM, Kirschner MW & Koshland D (1996) Anaphase initiation in Saccharomyces cerevisiae is controlled by the APC-dependent degradation of the anaphase inhibitor Pds1p. *Genes Dev.* **10:** 3081–3093

Corbett KD & Harrison SC (2012) Molecular architecture of the yeast monopolin complex. *Cell Rep* **1:** 583–589

Corbett KD, Yip CK, Ee L-S, Walz T, Amon A & Harrison SC (2010) The monopolin complex crosslinks kinetochore components to regulate chromosome-microtubule attachments. *Cell* **142:** 556–567

De Antoni A, Pearson CG, Cimini D, Canman JC, Sala V, Nezi L, Mapelli M, Sironi L, Faretta M, Salmon ED & Musacchio A (2005) The Mad1/Mad2 complex as a template for Mad2 activation in the spindle assembly checkpoint. *Curr. Biol.* **15:** 214–225

Ding D-Q, Yamamoto A, Haraguchi T & Hiraoka Y (2004) Dynamics of homologous chromosome pairing during meiotic prophase in fission yeast. *Dev. Cell* **6:** 329–341

Dirick L, Goetsch L, Ammerer G & Byers B (1998) Regulation of meiotic S phase by Ime2 and a Clb5,6-associated kinase in Saccharomyces cerevisiae. *Science* **281:** 1854–1857

Dreier MR, Bekier ME & Taylor WR (2011) Regulation of sororin by Cdk1-mediated phosphorylation. *J. Cell. Sci.* **124:** 2976–2987

Eichinger CS & Jentsch S (2010) Synaptonemal complex formation and meiotic checkpoint signaling are linked to the lateral element protein Red1. *Proc. Natl. Acad. Sci. U.S.A.* **107:** 11370–11375

Eijpe M, Heyting C, Gross B & Jessberger R (2000) Association of mammalian SMC1 and SMC3 proteins with meiotic chromosomes and synaptonemal complexes. *J. Cell. Sci.* **113 (Pt 4):** 673–682

Eijpe M, Offenberg H, Jessberger R, Revenkova E & Heyting C (2003) Meiotic cohesin REC8 marks the axial elements of rat synaptonemal complexes before cohesins SMC1β and SMC3. *J. Cell Biol.* **160:** 657–670

Elbatsh AMO, Haarhuis JHI, Petela N, Chapard C, Fish A, Celie PH, Stadnik M, Ristic D, Wyman C, Medema RH, Nasmyth K & Rowland BD (2016) Cohesin Releases DNA through Asymmetric ATPase-Driven Ring Opening. *Mol. Cell* **61:** 575–588

Elserafy M, Sarić M, Neuner A, Lin T-C, Zhang W, Seybold C, Sivashanmugam L & Schiebel E (2014) Molecular Mechanisms that Restrict Yeast Centrosome Duplication to One Event per Cell Cycle. *Curr. Biol.* **24:** 1456–1466 Available at: http://www.sciencedirect.com/science/article/pii/S0960982214005971

Eshleman HD & Morgan DO (2014) Sgo1 recruits PP2A to chromosomes to ensure sister chromatid bi-orientation in mitosis. *J. Cell. Sci.*

Espeut J, Cheerambathur DK, Krenning L, Oegema K & Desai A (2012) Microtubule binding by KNL-1 contributes to spindle checkpoint silencing at the kinetochore. *J. Cell Biol.* **196:** 469–482

Eytan E, Wang K, Miniowitz-Shemtov S, Sitry-Shevah D, Kaisari S, Yen TJ, Liu ST

& Hershko A (2014) Disassembly of mitotic checkpoint complexes by the joint action of the AAA-ATPase TRIP13 and p31(comet). *Proc. Natl. Acad. Sci. U.S.A.* **111:** 12019–12024

Fernius J & Hardwick KG (2007) Bub1 kinase targets Sgo1 to ensure efficient chromosome biorientation in budding yeast mitosis. *PLoS Genet.* **3:** e213

Fernius J & Marston AL (2009) Establishment of cohesion at the pericentromere by the Ctf19 kinetochore subcomplex and the replication fork-associated factor, Csm3. *PLoS Genet.* **5:** e1000629

Fernius J, Nerusheva OO, Galander S, Alves F de L, Rappsilber J & Marston AL (2013) Cohesin-Dependent Association of Scc2/4 with the Centromere Initiates Pericentromeric Cohesion Establishment. *Curr. Biol.*

Fraschini R, Beretta A, Sironi L, Musacchio A, Lucchini G & Piatti S (2001) Bub3 interaction with Mad2, Mad3 and Cdc20 is mediated by WD40 repeats and does not require intact kinetochores. *EMBO J.* **20:** 6648–6659

Funabiki H, Yamano H, Kumada K, Nagao K, Hunt T & Yanagida M (1996) Cut2 proteolysis required for sister-chromatid seperation in fission yeast. *Nature* **381:** 438–441

Funakoshi M & Hochstrasser M (2009) Small epitope-linker modules for PCR-based C-terminal tagging in Saccharomyces cerevisiae. *Yeast* **26:** 185–192

Furuya K, Takahashi K & Yanagida M (1998) Faithful anaphase is ensured by Mis4, a sister chromatid cohesion molecule required in S phase and not destroyed in G1 phase. *Genes Dev.* **12:** 3408–3418

Gandhi R, Gillespie PJ & Hirano T (2006) Human Wapl is a cohesin-binding protein that promotes sister-chromatid resolution in mitotic prophase. *Curr. Biol.* **16:** 2406–2417

Gassmann R, Holland AJ, Varma D, Wan X, Çivril F, Cleveland DW, Oegema K, Salmon ED & Desai A (2010) Removal of Spindly from microtubule-attached kinetochores controls spindle checkpoint silencing in human cells. *Genes Dev.* **24:** 957–971

Gauss R, Trautwein M, Sommer T & Spang A (2005) New modules for the repeated internal and N-terminal epitope tagging of genes in Saccharomyces cerevisiae. *Yeast* **22:** 1–12

Gerlich D, Koch B, Dupeux F, Peters J-M & Ellenberg J (2006) Live-cell imaging reveals a stable cohesin-chromatin interaction after but not before DNA replication. *Curr. Biol.* **16:** 1571–1578

Gladstone MN, Obeso D, Chuong H & Dawson DS (2009) The synaptonemal complex protein Zip1 promotes bi-orientation of centromeres at meiosis I. *PLoS Genet.* **5:** e1000771

Glynn EF, Megee PC, Yu H-G, Mistrot C, Unal E, Koshland DE, DeRisi JL & Gerton JL (2004) Genome-wide mapping of the cohesin complex in the yeast Saccharomyces cerevisiae. *PLoS Biol.* **2:** E259

Goldstein LS (1981) Kinetochore structure and its role in chromosome orientation during the first meiotic division in male D. melanogaster. *Cell* **25:** 591–602

Gómez R, Valdeolmillos A, Parra MT, Viera A, Carreiro C, Roncal F, Rufas JS, Barbero JL & Suja JA (2007) Mammalian SGO2 appears at the inner centromere domain and redistributes depending on tension across centromeres during meiosis II and mitosis. *EMBO Rep.* **8:** 173–180

Grandin N & Reed SI (1993) Differential function and expression of Saccharomyces cerevisiae B-type cyclins in mitosis and meiosis. *Mol. Cell. Biol.* **13:** 2113–2125

Griffis ER, Stuurman N & Vale RD (2007) Spindly, a novel protein essential for silencing the spindle assembly checkpoint, recruits dynein to the kinetochore. *J. Cell Biol.* **177:** 1005–1015

Gruber S, Haering CH & Nasmyth K (2003) Chromosomal cohesin forms a ring. *Cell* **112:** 765–777

Gyuricza MR, Manheimer KB, Apte V, Krishnan B, Joyce EF, McKee BD & McKim KS (2016) Dynamic and Stable Cohesins Regulate Synaptonemal Complex Assembly and Chromosome Segregation. *Curr. Biol.* **26:** 1688–1698

Haase J, Stephens A, Verdaasdonk J, Yeh E & Bloom K (2012) Bub1 kinase and Sgo1 modulate pericentric chromatin in response to altered microtubule dynamics. *Curr. Biol.* **22:** 471–481

Habu T, Kim SH, Weinstein J & Matsumoto T (2002) Identification of a MAD2-binding protein, CMT2, and its role in mitosis. *EMBO J.* **21:** 6419–6428

Haering CH, Farcas A-M, Arumugam P, Metson J & Nasmyth K (2008) The cohesin ring concatenates sister DNA molecules. *Nature* **454:** 297–301

Haering CH, Löwe J, Hochwagen A & Nasmyth K (2002) Molecular architecture of SMC proteins and the yeast cohesin complex. *Mol. Cell* **9:** 773–788

Hara K, Zheng G, Qu Q, Liu H, Ouyang Z, Chen Z, Tomchick DR & Yu H (2014) Structure of cohesin subcomplex pinpoints direct shugoshin-Wapl antagonism in centromeric cohesion. *Nat. Struct. Mol. Biol.* **21:** 864–870

Hardwick KG, Johnston RC, Smith DL & Murray AW (2000) MAD3 encodes a novel component of the spindle checkpoint which interacts with Bub3p, Cdc20p, and Mad2p. *J. Cell Biol.* **148:** 871–882

Harigaya Y, Tanaka H, Yamanaka S, Tanaka K, Watanabe Y, Tsutsumi C, Chikashige Y, Hiraoka Y, Yamashita A & Yamamoto M (2006) Selective elimination of messenger RNA prevents an incidence of untimely meiosis.

Nature **442:** 45–50

Hartwell LH & Kastan MB (1994) Cell cycle control and cancer. *Science* **266:** 1821–1828

Hassold T & Hunt P (2001) To err (meiotically) is human: the genesis of human aneuploidy. *Nat. Rev. Genet.* **2:** 280–291

Hauf S, Roitinger E, Koch B, Dittrich CM, Mechtler K & Peters J-M (2005) Dissociation of cohesin from chromosome arms and loss of arm cohesion during early mitosis depends on phosphorylation of SA2. *PLoS Biol.* **3:** e69

Henderson KA, Kee K, Maleki S, Santini PA & Keeney S (2006) Cyclin-dependent kinase directly regulates initiation of meiotic recombination. *Cell* **125:** 1321–1332

Hepworth SR, Friesen H & Segall J (1998) NDT80 and the meiotic recombination checkpoint regulate expression of middle sporulation-specific genes in Saccharomyces cerevisiae. *Mol. Cell. Biol.* **18:** 5750–5761

Hirano M & Hirano T (2002) Hinge- mediated dimerization of SMC protein is essential for its dynamic interaction with DNA. *EMBO J.* **21:** 5733–5744

Hochwagen A, Wrobel G, Cartron M, Demougin P, Niederhauser-Wiederkehr C, Boselli MG, Primig M & Amon A (2005) Novel response to microtubule perturbation in meiosis. *Mol. Cell. Biol.* **25:** 4767–4781

Holt LJ, Hutti JE, Cantley LC & Morgan DO (2007) Evolution of Ime2 phosphorylation sites on Cdk1 substrates provides a mechanism to limit the effects of the phosphatase Cdc14 in meiosis. *Mol. Cell* **25:** 689–702

Honigberg SM & Esposito RE (1994) Reversal of cell determination in yeast meiosis: postcommitment arrest allows return to mitotic growth. *Proc. Natl. Acad. Sci. U.S.A.* **91:** 6559–6563

Hornig NCD & Uhlmann F (2004) Preferential cleavage of chromatin-bound cohesin after targeted phosphorylation by Polo-like kinase. *EMBO J.* **23:** 3144–3153

Hornig NCD, Knowles PP, McDonald NQ & Uhlmann F (2002) The dual mechanism of separase regulation by securin. *Curr. Biol.* **12:** 973–982

Hotz M & Barral Y (2014) The Mitotic Exit Network: new turns on old pathways. *Trends in Cell Biology* **24:** 145–152

Howell BJ, McEwen BF, Canman JC, Hoffman DB, Farrar EM, Rieder CL & Salmon ED (2001) Cytoplasmic dynein/dynactin drives kinetochore protein transport to the spindle poles and has a role in mitotic spindle checkpoint inactivation. *J. Cell Biol.* **155:** 1159–1172

Hoyt MA, Totis L & Roberts BT (1991) S. cerevisiae genes required for cell cycle

arrest in response to loss of microtubule function. *Cell* **66:** 507–517

Huang H, Feng J, Famulski J, Rattner JB, Liu ST, Kao GD, Muschel R, Chan GKT & Yen TJ (2007) Tripin/hSgo2 recruits MCAK to the inner centromere to correct defective kinetochore attachments. *J. Cell Biol.* **177:** 413–424

Indjeian VB & Murray AW (2007) Budding yeast mitotic chromosomes have an intrinsic bias to biorient on the spindle. *Curr. Biol.* **17:** 1837–1846

Indjeian VB, Stern BM & Murray AW (2005) The centromeric protein Sgo1 is required to sense lack of tension on mitotic chromosomes. *Science* **307:** 130–133

Ishiguro K-I, Kim J, Nakamura SF, Kato S & Watanabe Y (2011) A new meiosis-specific cohesin complex implicated in the cohesin code for homologous pairing. *EMBO Rep.* **12:** 267–275

Ivanov D, Schleiffer A, Eisenhaber F, Mechtler K, Haering CH & Nasmyth K (2002) Eco1 is a novel acetyltransferase that can acetylate proteins involved in cohesion. *Curr. Biol.* **12:** 323–328

Iwabuchi M, Ohsumi K, Yamamoto TM, Sawada W & Kishimoto T (2000) Residual Cdc2 activity remaining at meiosis I exit is essential for meiotic M–M transition in Xenopus oocyte extracts. *EMBO J.* **19:** 4513–4523

Izawa D, Goto M, Yamashita A, Yamano H & Yamamoto M (2005) Fission yeast Mes1p ensures the onset of meiosis II by blocking degradation of cyclin Cdc13p. *Nature* **434:** 529–533

Jelluma N, Brenkman AB, van den Broek NJF, Cruijsen CWA, van Osch MHJ, Lens SMA, Medema RH & Kops GJPL (2008) Mps1 Phosphorylates Borealin to Control Aurora B Activity and Chromosome Alignment. *Cell* **132:** 233–246

Kagami A, Sakuno T, Yamagishi Y, Ishiguro T, Tsukahara T, Shirahige K, Tanaka K & Watanabe Y (2011) Acetylation regulates monopolar attachment at multiple levels during meiosis I in fission yeast. *EMBO Rep.* **12:** 1189–1195

Kalantzaki M, Kitamura E, Zhang T, Mino A, Novak B & Tanaka TU (2015) Kinetochore-microtubule error correction is driven by differentially regulated interaction modes. *Nat. Cell Biol.* **17:** 421–433

Kamieniecki RJ, Liu L & Dawson DS (2005) FEAR but not MEN genes are required for exit from meiosis I. *Cell Cycle* **4:** 1093–1098 Available at: http://www.tandfonline.com/doi/abs/10.4161/cc.4.8.1857#.Vxag_5MrJE4

Kassir Y, Granot D & Simchen G (1988) IME1, a positive regulator gene of meiosis in S. cerevisiae. *Cell* **52:** 853–862

Katis VL, Gálová M, Rabitsch KP, Gregan J & Nasmyth K (2004a) Maintenance of cohesin at centromeres after meiosis I in budding yeast requires a kinetochore-associated protein related to MEI-S332. *Curr. Biol.* **14:** 560–572

Katis VL, Lipp JJ, Imre R, Bogdanova A, Okaz E, Habermann B, Mechtler K, Nasmyth K & Zachariae W (2010) Rec8 phosphorylation by casein kinase 1 and Cdc7-Dbf4 kinase regulates cohesin cleavage by separase during meiosis. Supplement. *Dev. Cell* **18:** 397–409

Katis VL, Matos J, Mori S, Shirahige K, Zachariae W & Nasmyth K (2004b) Spo13 facilitates monopolin recruitment to kinetochores and regulates maintenance of centromeric cohesion during yeast meiosis. *Curr. Biol.* **14:** 2183–2196

Kawashima SA, Yamagishi Y, Honda T, Ishiguro K-I & Watanabe Y (2010) Phosphorylation of H2A by Bub1 prevents chromosomal instability through localizing shugoshin. *Science* **327:** 172–177

Keeney S, Giroux CN & Kleckner N (1997) Meiosis-specific DNA double-strand breaks are catalyzed by Spo11, a member of a widely conserved protein family. *Cell* **88:** 375–384

Kelly AE, Ghenoiu C, Xue JZ, Zierhut C, Kimura H & Funabiki H (2010) Survivin Reads Phosphorylated Histone H3 Threonine 3 to Activate the Mitotic Kinase Aurora B. *Science* **330:** 235–239

Kerrebrock AW, Miyazaki WY, Birnby D & Orr-Weaver TL (1992) The Drosophila mei-S332 gene promotes sister-chromatid cohesion in meiosis following kinetochore differentiation. *Genetics* **130:** 827–841

Kiburz BM, Amon A & Marston AL (2008) Shugoshin promotes sister kinetochore biorientation in Saccharomyces cerevisiae. *Mol. Biol. Cell* **19:** 1199–1209

Kiburz BM, Reynolds DB, Megee PC, Marston AL, Lee BH, Lee TI, Levine SS, Young RA & Amon A (2005) The core centromere and Sgo1 establish a 50-kb cohesin-protected domain around centromeres during meiosis I. *Genes Dev.* **19:** 3017–3030

Kim J, Ishiguro K-I, Nambu A, Akiyoshi B, Yokobayashi S, Kagami A, Ishiguro T, Pendás AM, Takeda N, Sakakibara Y, Kitajima TS, Tanno Y, Sakuno T & Watanabe Y (2014) Meikin is a conserved regulator of meiosis-I-specific kinetochore function. *Nature* **517:** 466–471

Kitajima TS, Hauf S, Ohsugi M, Yamamoto T & Watanabe Y (2005) Human Bub1 defines the persistent cohesion site along the mitotic chromosome by affecting Shugoshin localization. *Curr. Biol.* **15:** 353–359

Kitajima TS, Kawashima SA & Watanabe Y (2004) The conserved kinetochore protein shugoshin protects centromeric cohesion during meiosis. *Nature* **427:** 510–517

Kitajima TS, Miyazaki Y, Yamamoto M & Watanabe Y (2003a) Rec8 cleavage by separase is required for meiotic nuclear divisions in fission yeast. *EMBO J.* **22:** 5643–5653

Kitajima TS, Sakuno T, Ishiguro K-I, Iemura S-I, Natsume T, Kawashima SA & Watanabe Y (2006) Shugoshin collaborates with protein phosphatase 2A to protect cohesin. *Nature* **441:** 46–52

Kitajima TS, Yokobayashi S, Yamamoto M & Watanabe Y (2003b) Distinct cohesin complexes organize meiotic chromosome domains. *Science* **300:** 1152–1155

Kitamura K, Katayama S, Dhut S, Sato M, Watanabe Y, Yamamoto M & Toda T (2001) Phosphorylation of Mei2 and Ste11 by Pat1 Kinase Inhibits Sexual Differentiation via Ubiquitin Proteolysis and 14-3-3 Protein in Fission Yeast. *Dev. Cell* **1:** 389–399

Klapholz S & Esposito RE (1980a) Isolation of SPO12-1 and SPO13-1 from a natural variant of yeast that undergoes a single meiotic division. *Genetics* **96:** 567–588

Klapholz S & Esposito RE (1980b) Recombination and chromosome segregation during the single division meiosis in SPO12-1 and SPO13-1 diploids. *Genetics* **96:** 589–611

Klapholz S, Waddell CS & Esposito RE (1985) The role of the SPO11 gene in meiotic recombination in yeast. *Genetics* **110:** 187–216

Klein F, Mahr P, Gálová M, Buonomo SB, Michaelis C, Nairz K & Nasmyth K (1999) A central role for cohesins in sister chromatid cohesion, formation of axial elements, and recombination during yeast meiosis. *Cell* **98:** 91–103

Knop M, Siegers K, Pereira G, Zachariae W, Winsor B, Nasmyth K & Schiebel E (1999) Epitope tagging of yeast genes using a PCR-based strategy: more tags and improved practical routines. *Yeast* **15:** 963–972

Kops GJPL, Kim Y, Weaver BAA, Mao Y, McLeod I, Yates JR, Tagaya M & Cleveland DW (2005) ZW10 links mitotic checkpoint signaling to the structural kinetochore. *J. Cell Biol.* **169:** 49–60

Koubova J, Menke DB, Zhou Q, Capel B, Griswold MD & Page DC (2006) Retinoic acid regulates sex-specific timing of meiotic initiation in mice. *Proc. Natl. Acad. Sci. U.S.A.* **103:** 2474–2479

Krantz ID, McCallum J, DeScipio C, Kaur M, Gillis LA, Yaeger D, Jukofsky L, Wasserman N, Bottani A, Morris CA, Nowaczyk MJM, Toriello H, Bamshad MJ, Carey JC, Rappaport E, Kawauchi S, Lander AD, Calof AL, Li H-H, Devoto M, et al (2004) Cornelia de Lange syndrome is caused by mutations in NIPBL, the human homolog of Drosophila melanogaster Nipped-B. *Nat. Genet.* **36:** 631–635

Krenn V, Overlack K, Primorac I, van Gerwen S & Musacchio A (2014) KI motifs of human Knl1 enhance assembly of comprehensive spindle checkpoint complexes around MELT repeats. *Curr. Biol.* **24:** 29–39

Kueng S, Hegemann B, Peters BH, Lipp JJ, Schleiffer A, Mechtler K & Peters J-M (2006) Wapl controls the dynamic association of cohesin with chromatin. *Cell* **127:** 955–967

Kutrowska BW, Narczyk M, Buszko A, Bzowska A & Clark PL (2007) Folding and unfolding of a non-fluorescent mutant of green fluorescent protein. *J Phys Condens Matter* **19:** 285223

Lafont AL, Song J & Rankin S (2010) Sororin cooperates with the acetyltransferase Eco2 to ensure DNA replication-dependent sister chromatid cohesion. *Proc. Natl. Acad. Sci. U.S.A.* **107:** 20364–20369

Lampert F, Hornung P & Westermann S (2010) The Dam1 complex confers microtubule plus end-tracking activity to the Ndc80 kinetochore complex. *J. Cell Biol.* **189:** 641–649

Lee BH & Amon A (2003) Role of Polo-like kinase CDC5 in programming meiosis I chromosome segregation. *Science* **300:** 482–486

Lee BH, Amon A & Prinz S (2002) Spo13 regulates cohesin cleavage. *Genes Dev.* **16:** 1672–1681

Lee BH, Kiburz BM & Amon A (2004) Spo13 maintains centromeric cohesion and kinetochore coorientation during meiosis I. *Curr. Biol.* **14:** 2168–2182

Lee J, Kitajima TS, Tanno Y, Yoshida K, Morita T, Miyano T, Miyake M & Watanabe Y (2008) Unified mode of centromeric protection by shugoshin in mammalian oocytes and somatic cells. *Nat. Cell Biol.* **10:** 42–52

Lengronne A, Katou Y, Mori S, Yokobayashi S, Kelly GP, Itoh T, Watanabe Y, Shirahige K & Uhlmann F (2004) Cohesin relocation from sites of chromosomal loading to places of convergent transcription. *Nature* **430:** 573–578

Lengronne A, McIntyre J, Katou Y, Kanoh Y, Hopfner K-P, Shirahige K & Uhlmann F (2006) Establishment of Sister Chromatid Cohesion at the S. cerevisiae Replication Fork. *Mol. Cell* **23:** 787–799

Leu J-Y & Roeder GS (1999) The Pachytene Checkpoint in S. cerevisiae Depends on Swe1-Mediated Phosphorylation of the Cyclin-Dependent Kinase Cdc28. *Mol. Cell* **4:** 805–814

Li P & McLeod M (1996) Molecular Mimicry in Development: Identification of ste11+ As a Substrate and mei3+ As a Pseudosubstrate Inhibitor of ran1+ Kinase. *Cell* **87:** 869–880

Li R & Murray AW (1991) Feedback control of mitosis in budding yeast. *Cell* **66:** 519–531

Li X & Dawe RK (2009) Fused sister kinetochores initiate the reductional division in meiosis I. *Nat. Cell Biol.* **11:** 1103–1108

Lin F-M, Lai Y-J, Shen H-J, Cheng Y-H & Wang T-F (2010) Yeast axial-element protein, Red1, binds SUMO chains to promote meiotic interhomologue recombination and chromosome synapsis. *EMBO J.* **29:** 586–596

Lin Z, Luo X & Yu H (2016) Structural basis of cohesin cleavage by separase. *Nature*

Lindgren A, Bungard D, Pierce M, Xie J, Vershon A & Winter E (2000) The pachytene checkpoint in Saccharomyces cerevisiae requires the Sum1 transcriptional repressor. *EMBO J.* **19:** 6489–6497

Liu D, Vader G, Vromans MJM, Lampson MA & Lens SMA (2009) Sensing Chromosome Bi-Orientation by Spatial Separation of Aurora B Kinase from Kinetochore Substrates. *Science* **323:** 1350–1353

Liu D, Vleugel M, Backer CB, Hori T, Fukagawa T, Cheeseman IM & Lampson MA (2010) Regulated targeting of protein phosphatase 1 to the outer kinetochore by KNL1 opposes Aurora B kinase. *J. Cell Biol.* **188:** 809–820

Liu H, Jia L & Yu H (2013a) Phospho-H2A and Cohesin Specify Distinct Tension-Regulated Sgo1 Pools at Kinetochores and Inner Centromeres. *Curr. Biol.*

Liu H, Rankin S & Yu H (2013b) Phosphorylation-enabled binding of SGO1-PP2A to cohesin protects sororin and centromeric cohesion during mitosis. *Nat. Cell Biol.* **15:** 40–49

Lo H-C, Kunz RC, Chen X, Marullo A, Gygi SP & Hollingsworth NM (2012) Cdc7-Dbf4 Is a Gene-Specific Regulator of Meiotic Transcription in Yeast. *Mol. Cell. Biol.* **32:** 541–557

Lo H-C, Wan L, Rosebrock A, Futcher B & Hollingsworth NM (2008) Cdc7-Dbf4 regulates NDT80 transcription as well as reductional segregation during budding yeast meiosis. *Mol. Biol. Cell* **19:** 4956–4967

London N & Biggins S (2014) Mad1 kinetochore recruitment by Mps1-mediated phosphorylation of Bub1 signals the spindle checkpoint. *Genes Dev.* **28:** 140–152

London N, Ceto S, Ranish JA & Biggins S (2012) Phosphoregulation of Spc105 by Mps1 and PP1 regulates Bub1 localization to kinetochores. *Curr. Biol.* **22:** 900–906

Longtine MS, McKenzie A, Demarini DJ, Shah NG, Wach A, Brachat A, Philippsen P & Pringle JR (1998) Additional modules for versatile and economical PCR-based gene deletion and modification in Saccharomyces cerevisiae. *Yeast* **14:** 953–961

Lopez-Serra L, Lengronne A, Borges V, Kelly G & Uhlmann F (2013) Budding Yeast Wapl Controls Sister Chromatid Cohesion Maintenance and Chromosome Condensation. *Current Biology* **23:** 64–69

Losada A, Hirano M & Hirano T (1998) Identification of Xenopus SMC protein complexes required for sister chromatid cohesion. *Genes Dev.* **12:** 1986–1997

Luo X, Tang Z, Rizo J & Yu H (2002) The Mad2 spindle checkpoint protein undergoes similar major conformational changes upon binding to either Mad1 or Cdc20. *Mol. Cell* **9:** 59–71

Luo X, Tang Z, Xia G, Wassmann K, Matsumoto T, Rizo J & Yu H (2004) The Mad2 spindle checkpoint protein has two distinct natively folded states. *Nat. Struct. Mol. Biol.* **11:** 338–345

Madgwick S, Hansen DV, Levasseur M, Jackson PK & Jones KT (2006) Mouse Emi2 is required to enter meiosis II by reestablishing cyclin B1 during interkinesis. *J. Cell Biol.* **174:** 791–801

Mapelli M, Filipp FV, Rancati G, Massimiliano L, Nezi L, Stier G, Hagan RS, Confalonieri S, Piatti S, Sattler M & Musacchio A (2006) Determinants of conformational dimerization of Mad2 and its inhibition by p31comet. *EMBO J.* **25:** 1273–1284

Marston AL, Lee BH & Amon A (2003) The Cdc14 phosphatase and the FEAR network control meiotic spindle disassembly and chromosome segregation. *Dev. Cell* **4:** 711–726

Marston AL, Tham W-H, Shah H & Amon A (2004) A genome-wide screen identifies genes required for centromeric cohesion. *Science* **303:** 1367–1370

Martini E, Diaz RL, Hunter N & Keeney S (2006) Crossover homeostasis in yeast meiosis. *Cell* **126:** 285–295

Matos J, Lipp JJ, Bogdanova A, Guillot S, Okaz E, Junqueira M, Shevchenko A & Zachariae W (2008) Dbf4-dependent CDC7 kinase links DNA replication to the segregation of homologous chromosomes in meiosis I. *Cell* **135:** 662–678

McGuinness BE, Hirota T, Kudo NR, Peters J-M & Nasmyth K (2005) Shugoshin prevents dissociation of cohesin from centromeres during mitosis in vertebrate cells. *PLoS Biol.* **3:** e86

Megee PC & Koshland D (1999) A Functional Assay for Centromere-Associated Sister Chromatid Cohesion. *Science* **285:** 254–257

Meyer RE, Chuong HH, Hild M, Hansen CL, Kinter M & Dawson DS (2015) Ipl1/Aurora-B is necessary for kinetochore restructuring in meiosis I in Saccharomyces cerevisiae. *Mol. Biol. Cell* **26:** 2986–3000

Meyer RE, Kim S, Obeso D, Straight PD, Winey M & Dawson DS (2013) Mps1 and Ipl1/Aurora B act sequentially to correctly orient chromosomes on the meiotic spindle of budding yeast. *Science* **339:** 1071–1074

Michaelis C, Ciosk R & Nasmyth K (1997) Cohesins: chromosomal proteins that

prevent premature separation of sister chromatids. *Cell* **91:** 35–45

Miki F, Okazaki K, Shimanuki M, Yamamoto A, Hiraoka Y & Niwa O (2002) The 14-kDa dynein light chain-family protein Dlc1 is required for regular oscillatory nuclear movement and efficient recombination during meiotic prophase in fission yeast. *Mol. Biol. Cell* **13:** 930–946

Miller MP, Unal E, Brar GA & Amon A (2012) Meiosis I chromosome segregation is established through regulation of microtubule-kinetochore interactions. *elife* **1:** e00117 Available at: http://elife.elifesciences.org/content/1/e00117

Mimitou EP & Symington LS (2008) Sae2, Exo1 and Sgs1 collaborate in DNA double-strand break processing. *Nature* **455:** 770–774

Moldovan G-L, Pfander B & Jentsch S (2006) PCNA controls establishment of sister chromatid cohesion during S phase. *Mol. Cell* **23:** 723–732

Monje-Casas F, Prabhu VR, Lee BH, Boselli M & Amon A (2007) Kinetochore orientation during meiosis is controlled by Aurora B and the monopolin complex. *Cell* **128:** 477–490

Moqtaderi Z & Struhl K (2008) Expanding the repertoire of plasmids for PCR-mediated epitope tagging in yeast. *Yeast* **25:** 287–292

Morimoto A, Shibuya H, Zhu X, Kim J, Ishiguro K-I, Han M & Watanabe Y (2012) A conserved KASH domain protein associates with telomeres, SUN1, and dynactin during mammalian meiosis. *J. Cell Biol.* **198:** 165–172

Moyle MW, Kim T, Hattersley N, Espeut J, Cheerambathur DK, Oegema K & Desai A (2014) A Bub1-Mad1 interaction targets the Mad1-Mad2 complex to unattached kinetochores to initiate the spindle checkpoint. *J. Cell Biol.* **204:** 647–657

Nasmyth K (2002) Segregating sister genomes: the molecular biology of chromosome separation. *Science* **297:** 559–565

Nasmyth K & Haering CH (2009) Cohesin: its roles and mechanisms. *Annu. Rev. Genet.* **43:** 525–558

Natsume T, Müller CA, Katou Y, Retkute R, Gierliński M, Araki H, Blow JJ, Shirahige K, Nieduszynski CA & Tanaka TU (2013) Kinetochores Coordinate Pericentromeric Cohesion and Early DNA Replication by Cdc7-Dbf4 Kinase Recruitment. *Mol. Cell* **50:** 661–674

Neale MJ, Pan J & Keeney S (2005) Endonucleolytic processing of covalent protein-linked DNA double-strand breaks. *Nature* **436:** 1053–1057

Nerusheva OO, Galander S, Fernius J, Kelly D & Marston AL (2014) Tension-dependent removal of pericentromeric shugoshin is an indicator of sister chromosome biorientation. *Genes Dev.* **28:** 1291–1309 Available at:

http://genesdev.cshlp.org/content/28/12/1291.full

Newnham L, Jordan P, Rockmill B, Roeder GS & Hoffmann E (2010) The synaptonemal complex protein, Zip1, promotes the segregation of nonexchange chromosomes at meiosis I. *Proc. Natl. Acad. Sci. U.S.A.* **107:** 781–785

Ng TM, Waples WG, Lavoie BD & Biggins S (2009) Pericentromeric sister chromatid cohesion promotes kinetochore biorientation. *Mol. Biol. Cell* **20:** 3818–3827

Nijenhuis W, Castelmur von E, Littler D, De Marco V, Tromer E, Vleugel M, van Osch MHJ, Snel B, Perrakis A & Kops GJPL (2013) A TPR domain–containing N-terminal module of MPS1 is required for its kinetochore localization by Aurora B. *J. Cell Biol.* **201:** 217–231

Nijenhuis W, Vallardi G, Teixeira A, Kops GJPL & Saurin AT (2014) Negative feedback at kinetochores underlies a responsive spindle checkpoint signal. *Nat. Cell Biol.* **16:** 1257–1264

Nishiyama T, Ladurner R, Schmitz J, Kreidl E, Schleiffer A, Bhaskara V, Bando M, Shirahige K, Hyman AA, Mechtler K & Peters J-M (2010) Sororin mediates sister chromatid cohesion by antagonizing Wapl. *Cell* **143:** 737–749

Nishiyama T, Sykora MM, Huis in 't Veld PJ, Mechtler K & Peters J-M (2013) Aurora B and Cdk1 mediate Wapl activation and release of acetylated cohesin from chromosomes by phosphorylating Sororin. *Proc. Natl. Acad. Sci. U.S.A.* **110:** 13404–13409

Niwa O, Shimanuki M & Miki F (2000) Telomere-led bouquet formation facilitates homologous chromosome pairing and restricts ectopic interaction in fission yeast meiosis. *EMBO J.* **19:** 3831–3840

Nonaka N, Kitajima T, Yokobayashi S, Xiao G, Yamamoto M, Grewal SIS & Watanabe Y (2002) Recruitment of cohesin to heterochromatic regions by Swi6/HP1 in fission yeast. *Nat. Cell Biol.* **4:** 89–93

Novak I, Wang H, Revenkova E, Jessberger R, Scherthan H & Höög C (2008) Cohesin Smc1β determines meiotic chromatin axis loop organization. *J. Cell Biol.* **180:** 83–90

Ocampo-Hafalla MT, Katou Y, Shirahige K & Uhlmann F (2007) Displacement and re-accumulation of centromeric cohesin during transient pre-anaphase centromere splitting. *Chromosoma* **116:** 531–544

Oelschlaegel T, Schwickart M, Matos J, Bogdanova A, Camasses A, Havlis J, Shevchenko A & Zachariae W (2005) The yeast APC/C subunit Mnd2 prevents premature sister chromatid separation triggered by the meiosis-specific APC/C-Ama1. *Cell* **120:** 773–788

Ohe M, Inoue D, Kanemori Y & Sagata N (2007) Erp1/Emi2 is essential for the

meiosis I to meiosis II transition in Xenopus oocytes. *Developmental Biology* **303:** 157–164

Okaz E, Argüello-Miranda O, Bogdanova A, Vinod PK, Lipp JJ, Markova Z, Zagoriy I, Novak B & Zachariae W (2012) Meiotic prophase requires proteolysis of M phase regulators mediated by the meiosis-specific APC/CAma1. *Cell* **151:** 603–618

Overlack K, Primorac I, Vleugel M, Krenn V, Maffini S, Hoffmann I, Kops GJPL & Musacchio A (2015) A molecular basis for the differential roles of Bub1 and BubR1 in the spindle assembly checkpoint. *elife* **4:** 1691

Page SL & Hawley RS (2004) The genetics and molecular biology of the synaptonemal complex. *Annu. Rev. Cell Dev. Biol.* **20:** 525–558

Pak J & Segall J (2002) Role of Ndt80, Sum1, and Swe1 as targets of the meiotic recombination checkpoint that control exit from pachytene and spore formation in Saccharomyces cerevisiae. *Mol. Cell. Biol.* **22:** 6430–6440

Paliulis LV & Nicklas RB (2000) The reduction of chromosome number in meiosis is determined by properties built into the chromosomes. *J. Cell Biol.* **150:** 1223–1232

Panizza S, Mendoza MA, Berlinger M, Huang L, Nicolas A, Shirahige K & Klein F (2011) Spo11-accessory proteins link double-strand break sites to the chromosome axis in early meiotic recombination. *Cell* **146:** 372–383

Pasierbek P, Jantsch M, Melcher M, Schleiffer A, Schweizer D & Loidl J (2001) A Caenorhabditis elegans cohesion protein with functions in meiotic chromosome pairing and disjunction. *Genes Dev.* **15:** 1349–1360

Pelttari J, Hoja M-R, Yuan L, Liu J-G, Brundell E, Moens P, Santucci-Darmanin S, Jessberger R, Barbero JL, Heyting C & Höög C (2001) A Meiotic Chromosomal Core Consisting of Cohesin Complex Proteins Recruits DNA Recombination Proteins and Promotes Synapsis in the Absence of an Axial Element in Mammalian Meiotic Cells. *Mol. Cell. Biol.* **21:** 5667–5677

Petronczki M, Matos J, Mori S, Gregan J, Bogdanova A, Schwickart M, Mechtler K, Shirahige K, Zachariae W & Nasmyth K (2006) Monopolar attachment of sister kinetochores at meiosis I requires casein kinase 1. *Cell* **126:** 1049–1064

Pierce M, Benjamin KR, Montano SP, Georgiadis MM, Winter E & Vershon AK (2003) Sum1 and Ndt80 proteins compete for binding to middle sporulation element sequences that control meiotic gene expression. *Mol. Cell. Biol.* **23:** 4814–4825

Pinsky BA, Nelson CR & Biggins S (2009) Protein phosphatase 1 regulates exit from the spindle checkpoint in budding yeast. *Curr. Biol.* **19:** 1182–1187

Pittman DL, Cobb J, Schimenti KJ, Wilson LA, Cooper DM, Brignull E, Handel MA

& Schimenti JC (1998) Meiotic prophase arrest with failure of chromosome synapsis in mice deficient for Dmc1, a germline-specific RecA homolog. *Mol. Cell* **1:** 697–705

Primorac I, Weir JR, Chiroli E, Gross F, Hoffmann I, van Gerwen S, Ciliberto A & Musacchio A (2013) Bub3 reads phosphorylated MELT repeats to promote spindle assembly checkpoint signaling. *elife* **2:** 213

Queralt E & Uhlmann F (2008) Separase cooperates with Zds1 and Zds2 to activate Cdc14 phosphatase in early anaphase. *J. Cell Biol.* **182:** 873–883

Queralt E, Lehane C, Novak B & Uhlmann F (2006) Downregulation of PP2ACdc55 Phosphatase by Separase Initiates Mitotic Exit in Budding Yeast. *Cell* **125:** 719–732

Rabitsch KP, Petronczki M, Javerzat JP, Genier S, Chwalla B, Schleiffer A, Tanaka TU & Nasmyth K (2003) Kinetochore recruitment of two nucleolar proteins is required for homolog segregation in meiosis I. *Dev. Cell* **4:** 535–548

Rankin S, Ayad NG & Kirschner MW (2005) Sororin, a substrate of the anaphase-promoting complex, is required for sister chromatid cohesion in vertebrates. *Mol. Cell* **18:** 185–200

Revenkova E & Jessberger R (2006) Shaping meiotic prophase chromosomes: cohesins and synaptonemal complex proteins. *Chromosoma* **115:** 235–240

Revenkova E, Eijpe M, Heyting C, Hodges CA, Hunt PA, Liebe B, Scherthan H & Jessberger R (2004) Cohesin SMC1 beta is required for meiotic chromosome dynamics, sister chromatid cohesion and DNA recombination. *Nat. Cell Biol.* **6:** 555–562

Riedel CG, Katis VL, Katou Y, Mori S, Itoh T, Helmhart W, Gálová M, Petronczki M, Gregan J, Cetin B, Mudrak I, Ogris E, Mechtler K, Pelletier L, Buchholz F, Shirahige K & Nasmyth K (2006) Protein phosphatase 2A protects centromeric sister chromatid cohesion during meiosis I. *Nature* **441:** 53–61

Rollins RA, Korom M, Aulner N, Martens A & Dorsett D (2004) Drosophila nipped-B protein supports sister chromatid cohesion and opposes the stromalin/Scc3 cohesion factor to facilitate long-range activation of the cut gene. *Mol. Cell. Biol.* **24:** 3100–3111

Romanos MA, Scorer CA & Clare JJ (1992) Foreign gene expression in yeast: a review. *Yeast* **8:** 423–488

Rosenberg JS, Cross FR & Funabiki H (2011) KNL1/Spc105 Recruits PP1 to Silence the Spindle Assembly Checkpoint. *Current Biology* **21:** 942–947

Rothbauer U, Zolghadr K, Tillib S, Nowak D, Schermelleh L, Gahl A, Backmann N, Conrath K, Muyldermans S, Cardoso MC & Leonhardt H (2006) Targeting and tracing antigens in live cells with fluorescent nanobodies. *Nat. Methods* **3:** 887–

889 Available at: http://www.cardoso-lab.org/publications/Rothbauer_2006.pdf

Rowland BD, Roig MB, Nishino T, Kurze A, Uluocak P, Mishra A, Beckouët F, Underwood P, Metson J, Imre R, Mechtler K, Katis VL & Nasmyth K (2009) Building sister chromatid cohesion: smc3 acetylation counteracts an antiestablishment activity. *Mol. Cell* **33:** 763–774

Rudner AD & Murray AW (2000) Phosphorylation by Cdc28 activates the Cdc20-dependent activity of the anaphase-promoting complex. *J. Cell Biol.* **149:** 1377–1390

Rundlett SE, Carmen AA, Suka N, Turner BM & Grunstein M (1998) Transcriptional repression by UME6 involves deacetylation of lysine 5 of histone H4 by RPD3. *Nature* **392:** 831–835

Sakuno T, Tada K & Watanabe Y (2009) Kinetochore geometry defined by cohesion within the centromere. *Nature* **458:** 852–858

Salic A, Waters JC & Mitchison TJ (2004) Vertebrate shugoshin links sister centromere cohesion and kinetochore microtubule stability in mitosis. *Cell* **118:** 567–578

Sarangapani KK, Duro E, Deng Y, Alves F de L, Ye Q, Opoku KN, Ceto S, Rappsilber J, Corbett KD, Biggins S, Marston AL & Asbury CL (2014) Sister kinetochores are mechanically fused during meiosis I in yeast. *Science*

Sarkar S, Shenoy RT, Dalgaard JZ, Newnham L, Hoffmann E, Millar JBA & Arumugam P (2013) Monopolin subunit Csm1 associates with MIND complex to establish monopolar attachment of sister kinetochores at meiosis I. *PLoS Genet.* **9:** e1003610

Sasanuma H, Hirota K, Fukuda T, Kakusho N, Kugou K, Kawasaki Y, Shibata T, Masai H & Ohta K (2008) Cdc7-dependent phosphorylation of Mer2 facilitates initiation of yeast meiotic recombination. *Genes Dev.* **22:** 398–410

Saurin AT, van der Waal MS, Medema RH, Lens SMA & Kops GJPL (2011) Aurora B potentiates Mps1 activation to ensure rapid checkpoint establishment at the onset of mitosis. *Nature Communications* **2:** 316

Scherthan H, Weich S, Schwegler H, Heyting C, Härle M & Cremer T (1996) Centromere and telomere movements during early meiotic prophase of mouse and man are associated with the onset of chromosome pairing. *J. Cell Biol.* **134:** 1109–1125

Schwacha A & Kleckner N (1997) Interhomolog bias during meiotic recombination: meiotic functions promote a highly differentiated interhomolog-only pathway. *Cell* **90:** 1123–1135

Severson AF, Ling L, van Zuylen V & Meyer BJ (2009) The axial element protein HTP-3 promotes cohesin loading and meiotic axis assembly in C. elegans to

implement the meiotic program of chromosome segregation. *Genes Dev.* **23:** 1763–1778

Shepperd LA, Meadows JC, Sochaj AM, Lancaster TC, Zou J, Buttrick GJ, Rappsilber J, Hardwick KG & Millar JBA (2012) Phosphodependent recruitment of Bub1 and Bub3 to Spc7/KNL1 by Mph1 kinase maintains the spindle checkpoint. *Curr. Biol.* **22:** 891–899

Shin ME, Skokotas A & Winter E (2010) The Cdk1 and Ime2 Protein Kinases Trigger Exit from Meiotic Prophase in Saccharomyces cerevisiae by Inhibiting the Sum1 Transcriptional Repressor. *Mol. Cell. Biol.* **30:** 2996–3003

Shirayama M, Tóth A, Gálová M & Nasmyth K (1999) APC(Cdc20) promotes exit from mitosis by destroying the anaphase inhibitor Pds1 and cyclin Clb5. *Nature* **402:** 203–207

Shonn MA, McCarroll R & Murray AW (2000) Requirement of the spindle checkpoint for proper chromosome segregation in budding yeast meiosis. *Science* **289:** 300–303

Shonn MA, McCarroll R & Murray AW (2002) Spo13 protects meiotic cohesin at centromeres in meiosis I. *Genes Dev.* **16:** 1659–1671

Shou W, Seol JH, Shevchenko A, Baskerville C, Moazed D, Chen ZW, Jang J, Charbonneau H & Deshaies RJ (1999) Exit from mitosis is triggered by Tem1-dependent release of the protein phosphatase Cdc14 from nucleolar RENT complex. *Cell* **97:** 233–244

Shubassi G, Luca N, Pak J & Segall J (2003) Activity of phosphoforms and truncated versions of Ndt80, a checkpoint-regulated sporulation-specific transcription factor of Saccharomyces cerevisiae. *Mol. Genet. Genomics* **270:** 324–336

Sironi L, Mapelli M, Knapp S, De Antoni A, Jeang KT & Musacchio A (2002) Crystal structure of the tetrameric Mad1–Mad2 core complex: implications of a ‘safety belt’ binding mechanism for the spindle checkpoint. *EMBO J.* **21:** 2496–2506

Skibbens RV, Corson LB, Koshland D & Hieter P (1999) Ctf7p is essential for sister chromatid cohesion and links mitotic chromosome structure to the DNA replication machinery. *Genes Dev.* **13:** 307–319

Smith HE & Mitchell AP (1989) A transcriptional cascade governs entry into meiosis in Saccharomyces cerevisiae. *Mol. Cell. Biol.* **9:** 2142–2152

Sopko R, Raithatha S & Stuart D (2002) Phosphorylation and maximal activity of Saccharomyces cerevisiae meiosis-specific transcription factor Ndt80 is dependent on Ime2. *Mol. Cell. Biol.* **22:** 7024–7040

Sourirajan A & Lichten M (2008) Polo-like kinase Cdc5 drives exit from pachytene during budding yeast meiosis. *Genes Dev.* **22:** 2627–2632

Steber CM & Esposito RE (1995) UME6 is a central component of a developmental regulatory switch controlling meiosis-specific gene expression. *Proc. Natl. Acad. Sci. U.S.A.* **92:** 12490–12494

Stegmeier F, Visintin R & Amon A (2002) Separase, polo kinase, the kinetochore protein Slk19, and Spo12 function in a network that controls Cdc14 localization during early anaphase. *Cell* **108:** 207–220

Stuart D & Wittenberg C (1998) CLB5 and CLB6 are required for premeiotic DNA replication and activation of the meiotic S/M checkpoint. *Genes Dev.* **12:** 2698–2710

Sudakin V, Chan GK & Yen TJ (2001) Checkpoint inhibition of the APC/C in HeLa cells is mediated by a complex of BUBR1, BUB3, CDC20, and MAD2. *J. Cell Biol.* **154:** 925–936

Sugimoto A, Iino Y, Maeda T, Watanabe Y & Yamamoto M (1991) Schizosaccharomyces pombe ste11+ encodes a transcription factor with an HMG motif that is a critical regulator of sexual development. *Genes Dev.* **5:** 1990–1999

Sullivan M & Morgan DO (2007) A novel destruction sequence targets the meiotic regulator Spo13 for anaphase-promoting complex-dependent degradation in anaphase I. *J. Biol. Chem.* **282:** 19710–19715

Sutani T, Kawaguchi T, Kanno R, Itoh T & Shirahige K (2009) Budding yeast Wpl1(Rad61)-Pds5 complex counteracts sister chromatid cohesion-establishing reaction. *Curr. Biol.* **19:** 492–497

Talbert PB & Henikoff S (2010) Centromeres Convert but Don't Cross. *PLoS Biol.* **8:** e1000326

Tanaka K, Chang HL, Kagami A & Watanabe Y (2009) CENP-C functions as a scaffold for effectors with essential kinetochore functions in mitosis and meiosis. *Dev. Cell* **17:** 334–343

Tanaka K, Kitamura E, Kitamura Y & Tanaka TU (2007) Molecular mechanisms of microtubule-dependent kinetochore transport toward spindle poles. *J. Cell Biol.* **178:** 269–281

Tanaka K, Mukae N, Dewar H, van Breugel M, James EK, Prescott AR, Antony C & Tanaka TU (2005) Molecular mechanisms of kinetochore capture by spindle microtubules. *Nature* **434:** 987–994

Tanaka T, Cosma MP, Wirth K & Nasmyth K (1999) Identification of cohesin association sites at centromeres and along chromosome arms. *Cell* **98:** 847–858

Tanaka T, Fuchs J, Loidl J & Nasmyth K (2000) Cohesin ensures bipolar attachment of microtubules to sister centromeres and resists their precocious separation. *Nat. Cell Biol.* **2:** 492–499

Tang Z, Shu H, Qi W, Mahmood NA, Mumby MC & Yu H (2006) PP2A is required for centromeric localization of Sgo1 and proper chromosome segregation. *Dev. Cell* **10:** 575–585

Tang Z, Sun Y, Harley SE, Zou H & Yu H (2004) Human Bub1 protects centromeric sister-chromatid cohesion through Shugoshin during mitosis. *Proc. Natl. Acad. Sci. U.S.A.* **101:** 18012–18017

Taxis C, Maeder C, Reber S, Rathfelder N, Miura K, Greger K, Stelzer EHK & Knop M (2006) Dynamic organization of the actin cytoskeleton during meiosis and spore formation in budding yeast. *Traffic* **7:** 1628–1642

Tedesco M, La Sala G, Barbagallo F, De Felici M & Farini D (2009) STRA8 Shuttles between Nucleus and Cytoplasm and Displays Transcriptional Activity. *J. Biol. Chem.* **284:** 35781–35793

Tibbles KL, Sarkar S, Novak B & Arumugam P (2013) CDK-dependent nuclear localization of B-cyclin Clb1 promotes FEAR activation during meiosis I in budding yeast. *PLoS ONE* **8:** e79001

Tien JF, Umbreit NT, Gestaut DR, Franck AD, Cooper J, Wordeman L, Gonen T, Asbury CL & Davis TN (2010) Cooperation of the Dam1 and Ndc80 kinetochore complexes enhances microtubule coupling and is regulated by aurora B. *J. Cell Biol.* **189:** 713–723

Tomonaga T, Nagao K, Kawasaki Y, Furuya K, Murakami A, Morishita J, Yuasa T, Sutani T, Kearsey SE, Uhlmann F, Nasmyth K & Yanagida M (2000) Characterization of fission yeast cohesin: essential anaphase proteolysis of Rad21 phosphorylated in the S phase. *Genes Dev.* **14:** 2757–2770

Tonkin ET, Wang T-J, Lisgo S, Bamshad MJ & Strachan T (2004) NIPBL, encoding a homolog of fungal Scc2-type sister chromatid cohesion proteins and fly Nipped-B, is mutated in Cornelia de Lange syndrome. *Nat. Genet.* **36:** 636–641

Tóth A, Ciosk R, Uhlmann F, Gálová M, Schleiffer A & Nasmyth K (1999) Yeast Cohesin complex requires a conserved protein, Eco1p(Ctf7), to establish cohesion between sister chromatids during DNA replication. *Genes Dev.* **13:** 320–333

Tóth A, Rabitsch KP, Gálová M, Schleiffer A, Buonomo SB & Nasmyth K (2000) Functional genomics identifies monopolin: a kinetochore protein required for segregation of homologs during meiosis I. *Cell* **103:** 1155–1168

Trelles-Sticken E, Dresser ME & Scherthan H (2000) Meiotic telomere protein Ndj1p is required for meiosis-specific telomere distribution, bouquet formation and efficient homologue pairing. *J. Cell Biol.* **151:** 95–106

Tsubouchi T & Roeder GS (2005) A synaptonemal complex protein promotes homology-independent centromere coupling. *Science* **308:** 870–873

Tsubouchi T, MacQueen AJ & Roeder GS (2008) Initiation of meiotic chromosome synapsis at centromeres in budding yeast. *Genes Dev.* **22:** 3217–3226

Tsuchiya D, Yang Y & Lacefield S (2014) Positive feedback of NDT80 expression ensures irreversible meiotic commitment in budding yeast. *PLoS Genet.* **10:** e1004398

Tung KS, Hong EJ & Roeder GS (2000) The pachytene checkpoint prevents accumulation and phosphorylation of the meiosis-specific transcription factor Ndt80. *Proc. Natl. Acad. Sci. U.S.A.* **97:** 12187–12192

Uhlmann F, Lottspeich F & Nasmyth K (1999) Sister-chromatid separation at anaphase onset is promoted by cleavage of the cohesin subunit Scc1. *Nature* **400:** 37–42

Uhlmann F, Wernic D, Poupart M-A, Koonin EV & Nasmyth K (2000) Cleavage of Cohesin by the CD Clan Protease Separin Triggers Anaphase in Yeast. *Cell* **103:** 375–386

Unal E, Heidinger-Pauli JM, Kim W, Guacci V, Onn I, Gygi SP & Koshland DE (2008) A molecular determinant for the establishment of sister chromatid cohesion. *Science* **321:** 566–569

van Veen JE & Hawley RS (2003) Meiosis: when even two is a crowd. *Curr. Biol.* **13:** R831–3

van Werven FJ & Amon A (2011) Regulation of entry into gametogenesis. *Philos. Trans. R. Soc. Lond., B, Biol. Sci.* **366:** 3521–3531

Vanoosthuyse V & Hardwick KG (2009) A novel protein phosphatase 1-dependent spindle checkpoint silencing mechanism. *Curr. Biol.* **19:** 1176–1181

Vermeulen K, Van Bockstaele DR & Berneman ZN (2003) The cell cycle: a review of regulation, deregulation and therapeutic targets in cancer. *Cell Prolif.* **36:** 131–149

Verzijlbergen KF, Nerusheva OO, Kelly D, Kerr A, Clift D, de Lima Alves F, Rappsilber J & Marston AL (2014) Shugoshin biases chromosomes for biorientation through condensin recruitment to the pericentromere. *elife* **3:** e01374

Vincenten N, Kuhl L-M, Lam I, Oke A, Kerr AR, Hochwagen A, Fung J, Keeney S, Vader G & Marston AL (2015) The kinetochore prevents centromere-proximal crossover recombination during meiosis. *elife* **4:** 923

Vink M, Simonetta M, Transidico P, Ferrari K, Mapelli M, De Antoni A, Massimiliano L, Ciliberto A, Faretta M, Salmon ED & Musacchio A (2006) In vitro FRAP identifies the minimal requirements for Mad2 kinetochore dynamics. *Curr. Biol.* **16:** 755–766

Visintin R, Craig K, Hwang ES, Prinz S, Tyers M & Amon A (1998) The Phosphatase Cdc14 Triggers Mitotic Exit by Reversal of Cdk-Dependent Phosphorylation. *Mol. Cell* **2:** 709–718

Visintin R, Hwang ES & Amon A (1999) Cfi1 prevents premature exit from mitosis by anchoring Cdc14 phosphatase in the nucleolus. *Nature* **398:** 818–823

Vleugel M, Tromer E, Omerzu M, Groenewold V, Nijenhuis W, Snel B & Kops GJPL (2013) Arrayed BUB recruitment modules in the kinetochore scaffold KNL1 promote accurate chromosome segregation. *J. Cell Biol.* **203:** 943–955

Wan L, Niu H, Futcher B, Zhang C, Shokat KM, Boulton SJ & Hollingsworth NM (2008) Cdc28-Clb5 (CDK-S) and Cdc7-Dbf4 (DDK) collaborate to initiate meiotic recombination in yeast. *Genes Dev.* **22:** 386–397

Wan L, Zhang C, Shokat KM & Hollingsworth NM (2006) Chemical inactivation of cdc7 kinase in budding yeast results in a reversible arrest that allows efficient cell synchronization prior to meiotic recombination. *Genetics* **174:** 1767–1774

Wang E, Ballister ER & Lampson MA (2011a) Aurora B dynamics at centromeres create a diffusion-based phosphorylation gradient. *J. Cell Biol.* **194:** 539–549

Wang F, Dai J, Daum JR, Niedzialkowska E, Banerjee B, Stukenberg PT, Gorbsky GJ & Higgins JMG (2010) Histone H3 Thr-3 Phosphorylation by Haspin Positions Aurora B at Centromeres in Mitosis. *Science* **330:** 231–235

Wang HT, Frackman S, Kowalisyn J, Esposito RE & Elder R (1987) Developmental regulation of SPO13, a gene required for separation of homologous chromosomes at meiosis I. *Mol. Cell. Biol.* **7:** 1425–1435

Wang Y, Chang C-Y, Wu J-F & Tung K-S (2011b) Nuclear localization of the meiosis-specific transcription factor Ndt80 is regulated by the pachytene checkpoint. *Mol. Biol. Cell* **22:** 1878–1886

Washburn BK & Esposito RE (2001) Identification of the Sin3-binding site in Ume6 defines a two-step process for conversion of Ume6 from a transcriptional repressor to an activator in yeast. *Mol. Cell. Biol.* **21:** 2057–2069

Watanabe Y & Nurse P (1999) Cohesin Rec8 is required for reductional chromosome segregation at meiosis. *Nature* **400:** 461–464

Watanabe Y, Yokobayashi S, Yamamoto M & Nurse P (2001) Pre-meiotic S phase is linked to reductional chromosome segregation and recombination. *Nature* **409:** 359–363

Wei RR, Al-Bassam J & Harrison SC (2007) The Ndc80/HEC1 complex is a contact point for kinetochore-microtubule attachment. *Nat. Struct. Mol. Biol.* **14:** 54–59

Welburn JPI, Vleugel M, Liu D, Yates JR, Lampson MA, Fukagawa T & Cheeseman IM (2010) Aurora B phosphorylates spatially distinct targets to differentially

regulate the kinetochore-microtubule interface. *Mol. Cell* **38:** 383–392

Westhorpe FG, Tighe A, Lara-Gonzalez P & Taylor SS (2011) p31comet-mediated extraction of Mad2 from the MCC promotes efficient mitotic exit. *J. Cell. Sci.* **124:** 3905–3916

White JA, Ramshaw H, Taimi M, Stangle W, Zhang A, Everingham S, Creighton S, Tam S-P, Jones G & Petkovich M (2000) Identification of the human cytochrome P450, P450RAI-2, which is predominantly expressed in the adult cerebellum and is responsible for all-trans-retinoic acid metabolism. *Proc. Natl. Acad. Sci. U.S.A.* **97:** 6403–6408

Whitfield ZJ, Chisholm J, Hawley RS & Orr-Weaver TL (2013) A Meiosis-Specific Form of the APC/C Promotes the Oocyte-to-Embryo Transition by Decreasing Levels of the Polo Kinase Inhibitor Matrimony. *PLoS Biol.* **11:** e1001648

Wiedenmann J, Ivanchenko S, Oswald F, Schmitt F, Röcker C, Salih A, Spindler K-D & Nienhaus GU (2004) EosFP, a fluorescent marker protein with UV-inducible green-to-red fluorescence conversion. *Proc. Natl. Acad. Sci. U.S.A.* **101:** 15905–15910

Wurzenberger C & Gerlich DW (2011) Phosphatases: providing safe passage through mitotic exit. *Nat. Rev. Mol. Cell Biol.* **12:** 469–482

Xia G, Luo X, Habu T, Rizo J, Matsumoto T & Yu H (2004) Conformation-specific binding of p31(comet) antagonizes the function of Mad2 in the spindle checkpoint. *EMBO J.* **23:** 3133–3143

Xiang Y, Takeo S, Florens L, Hughes SE, Huo L-J, Gilliland WD, Swanson SK, Teeter K, Schwartz JW, Washburn MP, Jaspersen SL & Hawley RS (2007) The Inhibition of Polo Kinase by Matrimony Maintains G2 Arrest in the Meiotic Cell Cycle. *PLoS Biol.* **5:** e323

Xu H, Beasley MD, Warren WD, van der Horst GTJ & McKay MJ (2005) Absence of Mouse REC8 Cohesin Promotes Synapsis of Sister Chromatids in Meiosis. *Dev. Cell* **8:** 949–961

Xu L, Ajimura M, Padmore R, Klein C & Kleckner N (1995) NDT80, a meiosis-specific gene required for exit from pachytene in Saccharomyces cerevisiae. *Mol. Cell. Biol.* **15:** 6572–6581

Xu Z, Cetin B, Anger M, Cho US, Helmhart W, Nasmyth K & Xu W (2009) Structure and function of the PP2A-shugoshin interaction. *Mol. Cell* **35:** 426–441

Yaakov G, Thorn K & Morgan DO (2012) Separase Biosensor Reveals that Cohesin Cleavage Timing Depends on Phosphatase PP2A(Cdc55) Regulation. *Dev. Cell* **23:** 124–136

Yamagishi Y, Honda T, Tanno Y & Watanabe Y (2010) Two Histone Marks

Establish the Inner Centromere and Chromosome Bi-Orientation. *Science* **330:** 239–243

Yamagishi Y, Yang C-H, Tanno Y & Watanabe Y (2012) MPS1/Mph1 phosphorylates the kinetochore protein KNL1/Spc7 to recruit SAC components. *Nat. Cell Biol.*

Yamamoto A, West RR, McIntosh JR & Hiraoka Y (1999) A cytoplasmic dynein heavy chain is required for oscillatory nuclear movement of meiotic prophase and efficient meiotic recombination in fission yeast. *J. Cell Biol.* **145:** 1233–1249

Yeong FM, Lim HH, Padmashree CG & Surana U (2000) Exit from Mitosis in Budding Yeast. *Mol. Cell* **5:** 501–511

Yokobayashi S & Watanabe Y (2005) The kinetochore protein Moa1 enables cohesion-mediated monopolar attachment at meiosis I. *Cell* **123:** 803–817

Yokobayashi S, Yamamoto M & Watanabe Y (2003) Cohesins determine the attachment manner of kinetochores to spindle microtubules at meiosis I in fission yeast. *Mol. Cell. Biol.* **23:** 3965–3973

Yoshida K, Kondoh G, Matsuda Y, Habu T, Nishimune Y & Morita T (1998) The mouse RecA-like gene Dmc1 is required for homologous chromosome synapsis during meiosis. *Mol. Cell* **1:** 707–718

Yu H-G & Koshland D (2007) The Aurora kinase Ipl1 maintains the centromeric localization of PP2A to protect cohesin during meiosis. *J. Cell Biol.* **176:** 911–918

Zachariae W, Schwab M, Nasmyth K & Seufert W (1998) Control of Cyclin Ubiquitination by CDK-Regulated Binding of Hct1 to the Anaphase Promoting Complex. *Science* **282:** 1721–1724

Zaytsev AV, Mick JE, Maslennikov E, Nikashin B, DeLuca JG & Grishchuk EL (2015) Multisite phosphorylation of the NDC80 complex gradually tunes its microtubule-binding affinity. *Mol. Biol. Cell* **26:** 1829–1844

Zhang J, Shi X, Li Y, Kim B-J, Jia J, Huang Z, Yang T, Fu X, Jung SY, Wang Y, Zhang P, Kim S-T, Pan X & Qin J (2008) Acetylation of Smc3 by Eco1 Is Required for S Phase Sister Chromatid Cohesion in Both Human and Yeast. *Mol. Cell* **31:** 143–151

Zhang M, Chang H, Zhang Y, Yu J, Wu L, Ji W, Chen J, Liu B, Lu J, Liu Y, Zhang J, Xu P & Xu T (2012) Rational design of true monomeric and bright photoactivatable fluorescent proteins. *Nat. Methods* **9:** 727–729

Zhang N, Panigrahi AK, Mao Q & Pati D (2011) Interaction of Sororin protein with polo-like kinase 1 mediates resolution of chromosomal arm cohesion. *J. Biol. Chem.* **286:** 41826–41837

Zhou Q, Nie R, Li Y, Friel P, Mitchell D, Hess RA, Small C & Griswold MD (2008) Expression of stimulated by retinoic acid gene 8 (Stra8) in spermatogenic cells induced by retinoic acid: an in vivo study in vitamin A-sufficient postnatal murine testes. *Biol. Reprod.* **79:** 35–42

Zhu Z, Chung W-H, Shim EY, Lee SE & Ira G (2008) Sgs1 helicase and two nucleases Dna2 and Exo1 resect DNA double-strand break ends. *Cell* **134:** 981–994

Zuzuarregui A, Kupka T, Bhatt B, Dohnal I, Mudrak I, Friedmann C, Schüchner S, Frohner IE, Ammerer G & Ogris E (2012) M-Track: detecting short-lived protein-protein interactions in vivo. *Nat. Methods* **9:** 594–596

7. APPENDIX

7.1. Yeast strains

All yeast strains are diploid SK1-derivatives. Unless otherwise stated, the strain background is as follows: MATa/MAT, ho::LYS2/ho::LYS2, ura3/ura3, trp1::hisG/trp1::hisG, leu2::hisG/leu2::hisG, his3::hisG/his3::hisG. Strains marked with an asterisk (*) originate from lab stocks. All other strains were made in this study.

AMy strain	**Relevant genotype**
2261*	*cdc20::pCLB2-CDC20::KanMX6/cdc20::pCLB2-CDC20::KanMX6* *SGO1-6HA:TRP1/SGO1-6HA:TRP1*
4015*	*ndt80Δ::LEU2/ndt80Δ::LEU2* *REC8-3HA::URA3/ REC8-3HA::URA3*
5310*	*leu2::pURA3-TetR-GFP::LEU2/leu2::hisG* *CEN5::tetOx224::HIS3/CEN5* *cdc20::pCLB2-3HA-CDC20::KanMX6/cdc20::pCLB2-3HA-CDC20::KanMX6* *PDS1-18MYC::LEU2/PDS1-18MYC::LEU2*
5892*	*leu2::pURA3-TetR-GFP::LEU2/leu2::hisG* *CEN5::tetOx224::HIS3/CEN5* *cdc20::pCLB2-3HA-CDC20::KanMX6/cdc20::pCLB2-3HA-CDC20::KanMX6* *mam1Δ::TRP1/mam1Δ::TRP1* *PDS1-18MYC::LEU2/PDS1-18MYC::LEU2*
8067*	*cdc20::pCLB2-CDC20::KanMX6/cdc20::pCLB2-CDC20::KanMX6*
8068*	*cdc20::pCLB2-CDC20::KanMX6/cdc20::pCLB2-CDC20::KanMX6* *SGO1-6HA::TRP1/ SGO1-6HA::TRP1* *mam1Δ::KanMX6/ mam1Δ::KanMX6*
9102*	*cdc20::pCLB2-CDC20::KanMX6/cdc20::pCLB2-CDC20::KanMX6* *SGO1-9MYC::TRP1/SGO1-9MYC::TRP1*
9210*	*cdc20::pCLB2-CDC20::KanMX6/cdc20::pCLB2-CDC20::KanMX6* *SGO1-9MYC::TRP1/ SGO1-9MYC::TRP1* *mam1Δ::KanMX6/ mam1Δ::KanMX6*
9456*	*cdc20::pCLB2-CDC20::KanMX6/cdc20::pCLB2-CDC20::KanMX6* *SGO1-6HA::TRP1/ SGO1-6HA::TRP1* *mam1Δ::KanMX6/ mam1Δ::KanMX6* *spo13Δ::KanMX6/spo13Δ::KanMX6*
9464*	*cdc20::pCLB2-CDC20::KanMX6/cdc20::pCLB2-CDC20::KanMX6* *SGO1-6HA::TRP1/ SGO1-6HA::TRP1* *spo13Δ::KanMX6/spo13Δ::KanMX6*
10157	*cdc20::pCLB2-CDC20::KanMX6/cdc20::pCLB2-CDC20::KanMX6* *SGO1-6HA::TRP1/SGO1-6HA::TRP1* *cdc5::pCLB2-CDC5::KanMX6/cdc5::pCLB2-CDC5::KanMX6*

AMy strain	Relevant genotype
10617	*cdc20::pCLB2-CDC20::KanMX6/cdc20::pCLB2-CDC20::KanMX6* *spo11Δ::NatMX6/spo11Δ::NatMX6*
10618	*cdc20::pCLB2-CDC20::KanMX6/cdc20::pCLB2-CDC20::KanMX6* *spo11Δ::NatMX6/spo11Δ::NatMX6* *SGO1-9MYC::TRP1/SGO1-9MYC::TRP1*
11226	*cdc20::pCLB2-CDC20::KanMX6/cdc20::pCLB2-CDC20::KanMX6* *SGO1-9MYC::TRP1/ SGO1-9MYC::TRP1* *mam1Δ::KanMX6/mam1Δ::KanMX6* *spo11Δ□□NatMX6/spo11Δ□□NatMX6*
11633*	*ndt80Δ::LEU2/ndt80Δ::LEU2*
11699	*cdc20::pCLB2-CDC20::KanMX6/cdc20::pCLB2-CDC20::KanMX6* *SPO13-3FLAG::KanMX6/SPO13-3FLAG::KanMX6*
12700	*cdc20::pCLB2-CDC20::KanMX6/cdc20::pCLB2-CDC20::KanMX6* *SGO1-6HA::TRP1/SGO1-6HA::TRP1* *spo13Δ::hisG/spo13Δ::hisG*
12701	*cdc20::pCLB2-CDC20::KanMX6/cdc20::pCLB2-CDC20::KanMX6* *SGO1-6HA::TRP1/SGO1-6HA::TRP1* *spo13Δ::hisG/spo13Δ::hisG* *cdc5::pCLB2-CDC5::KanMX6/cdc5::pCLB2-CDC5::KanMX6*
13362	*leu2::pURA3-TetR-GFP::LEU2/leu2::hisG* *CEN5::tetOx224::HIS3/CEN5* *cdc20::pCLB2-3HA-CDC20::KanMX6/cdc20::pCLB2-3HA-CDC20::KanMX6* *PDS1-18MYC::LEU2/ PDS1-18MYC::LEU2* *spo11Δ::URA3/spo11Δ::URA3*
13363	*leu2::pURA3-TetR-GFP::LEU2/leu2::hisG* *CEN5::tetOx224::HIS3/CEN5* *cdc20::pCLB2-3HA-CDC20::KanMX6/cdc20::pCLB2-3HA-CDC20::KanMX6* *PDS1-18MYC::LEU2/ PDS1-18MYC::LEU2* *spo11Δ::URA3/spo11Δ::URA3* *mam1Δ::TRP1/mam1Δ::TRP1*
13431	*PDS1-tdTomato::KITRP1/PDS1-tdTomato::KITRP1* *CNM67-3mCherry::NatMX4/CNM67-3mCherry::NatMX4* *leu2::pURA3-TetR-GFP::LEU2/leu2::hisG* *CEN5::tetOx224::HIS3/CEN5*
13716	*REC8-GFP::URA3/ REC8-GFP::URA3* *PDS1-tdTomato::KITRP1/PDS1-tdTomato::KITRP1* *MTW1-tdTomato::NatMX6/MTW1-tdTomato::NatMX6*
13717	*REC8-GFP::URA3/ REC8-GFP::URA3* *PDS1-tdTomato::KITRP1/PDS1-tdTomato::KITRP1* *MTW1-tdTomato::NatMX6/MTW1-tdTomato::NatMX6* *mam1Δ::KanMX6/mam1Δ::KanMX6*
13718	*REC8-GFP::URA3/ REC8-GFP::URA3* *PDS1-tdTomato::KITRP1/PDS1-tdTomato::KITRP1* *MTW1-tdTomato::NatMX6/MTW1-tdTomato::NatMX6* *spo11Δ::NatMX6/spo11Δ::NatMX6*
13719	*REC8-GFP::URA3/ REC8-GFP::URA3* *PDS1-tdTomato::KITRP1/PDS1-tdTomato::KITRP1* *MTW1-tdTomato::NatMX6/MTW1-tdTomato::NatMX6* *spo11Δ::NatMX6/spo11Δ::NatMX6* *mam1Δ::KanMX6/mam1Δ::KanMX6*

AMy strain	Relevant genotype
13978	*PDS1-tdTomato::KITRP1/PDS1-tdTomato::KITRP1* *CNM67-3mCherry::NatMX4/CNM67-3mCherry::NatMX4* *leu2::pURA3-TetR-GFP::LEU2/leu2::hisG* *CEN5::tetOx224::HIS3/CEN5* *mam1Δ::KanMX6/mam1Δ::KanMX6*
13979	*PDS1-tdTomato::KITRP1/PDS1-tdTomato::KITRP1* *CNM67-3mCherry::NatMX4/CNM67-3mCherry::NatMX4* *leu2::pURA3-TetR-GFP::LEU2/leu2::hisG* *CEN5::tetOx224::HIS3/CEN5* *spo11Δ::NatMX6/spo11Δ::NatMX6*
13980	*PDS1-tdTomato::KITRP1/PDS1-tdTomato::KITRP1* *CNM67-3mCherry::NatMX4/CNM67-3mCherry::NatMX4* *leu2::pURA3-TetR-GFP::LEU2/leu2::hisG* *CEN5::tetOx224::HIS3/CEN5* *mam1Δ::KanMX6/mam1Δ::KanMX6* *spo11Δ::NatMX6/spo11Δ::NatMX6*
14051	*cdc20::pCLB2-CDC20::KanMX6/cdc20::pCLB2-CDC20::KanMX6* *CDC5-3V5/CDC5-3V5*
14052	*cdc20::pCLB2-CDC20::KanMX6/cdc20::pCLB2-CDC20::KanMX6* *CDC5-3V5/CDC5-3V5* *spo13Δ::KanMX6/spo13Δ::KanMX6*
14542	*cdc20::pCLB2-CDC20::KanMX6/cdc20::pCLB2-CDC20::KanMX6* *SGO1-6HA::TRP1/SGO1-6HA::TRP1* *RTS1-3PK::TRP1/RTS1-3PK::TRP1*
14544	*cdc20::pCLB2-CDC20::KanMX6/cdc20::pCLB2-CDC20::KanMX6* *SGO1-6HA::TRP1/SGO1-6HA::TRP1* *RTS1-3PK::TRP1/RTS1-3PK::TRP1* *cdc5::pCLB2-CDC5::KanMX6/cdc5::pCLB2-CDC5::KanMX6*
15118	*SPC42-tdTomato::NatMX6/SPC42-tdTomato::NatMX6* *PDS1-tdTomato::KITRP1/PDS1-tdTomato::KITRP1* *leu2::pURA3-TetR-GFP::LEU2/leu2::hisG* *CEN5::tetOx224::HIS3/CEN5* *spo13Δ::KanMX6/spo13Δ::KanMX6*
15119	*SPC42-tdTomato::NatMX6/SPC42-tdTomato::NatMX6* *PDS1-tdTomato::KITRP1/PDS1-tdTomato::KITRP1* *leu2::pURA3-TetR-GFP::LEU2/leu2::hisG* *CEN5::tetOx224::HIS3/CEN5* *mam1Δ::TRP1/mam1Δ::TRP1*
15120	*SPC42-tdTomato::NatMX6/SPC42-tdTomato::NatMX6* *PDS1-tdTomato::KITRP1/PDS1-tdTomato::KITRP1* *leu2::pURA3-TetR-GFP::LEU2/leu2::hisG* *CEN5::tetOx224::HIS3/CEN5* *spo13Δ::KanMX6/spo13Δ::KanMX6* *mam1Δ::TRP1/mam1Δ::TRP1*
15123	*cdc20::pCLB2-CDC20::KanMX6/cdc20::pCLB2-CDC20::KanMX6* *SGO1-6HA::TRP1/SGO1-6HA::TRP1* *RTS1-3PK::TRP1/RTS1-3PK::TRP1* *spo13Δ::KanMX6/spo13Δ::KanMX6*

AMy strain	Relevant genotype
15124	*cdc20::pCLB2-CDC20::KanMX6/cdc20::pCLB2-CDC20::KanMX6* *SGO1-6HA::TRP1/SGO1-6HA::TRP1* *RTS1-3PK::TRP1/RTS1-3PK::TRP1* *spo13::spo13-m2::LEU2/spo13::spo13-m2::LEU2*
15128	*cdc20::pCLB2-CDC20::KanMX6/cdc20::pCLB2-CDC20::KanMX6* *CDC5-3V5/CDC5-3V5* *spo13::spo13-m2::LEU2/spo13::spo13-m2::LEU2*
15132	*cdc20::pCLB2-CDC20::KanMX6/cdc20::pCLB2-CDC20::KanMX6* *SGO1-6HA::TRP1/SGO1-6HA::TRP1* *spo13::spo13-m2::LEU2/spo13::spo13-m2::LEU2* *cdc5::pCLB2-CDC5::KanMX6/cdc5::pCLB2-CDC5::KanMX6*
15133	*REC8-GFP::URA3/ REC8-GFP::URA3* *PDS1-tdTomato::KITRP1/PDS1-tdTomato::KITRP1* *MTW1-tdTomato::NatMX6/MTW1-tdTomato::NatMX6* *spo13Δ::KanMX6/spo13Δ::KanMX6*
15134	*REC8-GFP::URA3/ REC8-GFP::URA3* *PDS1-tdTomato::KITRP1/PDS1-tdTomato::KITRP1* *MTW1-tdTomato::NatMX6/MTW1-tdTomato::NatMX6* *mam1Δ::TRP1/mam1Δ::TRP1*
15135	*REC8-GFP::URA3/ REC8-GFP::URA3* *PDS1-tdTomato::KITRP1/PDS1-tdTomato::KITRP1* *MTW1-tdTomato::NatMX6/MTW1-tdTomato::NatMX6* *spo13Δ::KanMX6/spo13Δ::KanMX6* *mam1Δ::TRP1/mam1Δ::TRP1*
15137	*URA3/URA3* *cdc20::pCLB2-CDC20::KanMX6/cdc20::pCLB2-CDC20::KanMX6* *SGO1-yEGFP::KanMX6/SGO1-yEGFP::KanMX6* *MTW1-tdTomato::NatMX6/MTW1-tdTomato::NatMX6*
15138	*URA3/URA3* *cdc20::pCLB2-CDC20::KanMX6/cdc20::pCLB2-CDC20::KanMX6* *SGO1-yEGFP::KanMX6/SGO1-yEGFP::KanMX6* *MTW1-tdTomato::NatMX6/MTW1-tdTomato::NatMX6* *mam1Δ::KanMX6/mam1Δ::KanMX6*
15139	*URA3/URA3* *cdc20::pCLB2-CDC20::KanMX6/cdc20::pCLB2-CDC20::KanMX6* *SGO1-yEGFP::KanMX6/SGO1-yEGFP::KanMX6* *MTW1-tdTomato::NatMX6/MTW1-tdTomato::NatMX6* *spo11Δ::NatMX6/spo11Δ::NatMX6*
15140	*URA3/URA3* *cdc20::pCLB2-CDC20::KanMX6/cdc20::pCLB2-CDC20::KanMX6* *SGO1-yEGFP::KanMX6/SGO1-yEGFP::KanMX6* *MTW1-tdTomato::NatMX6/MTW1-tdTomato::NatMX6* *mam1Δ::KanMX6/mam1Δ::KanMX6* *spo11Δ::NatMX6/spo11Δ::NatMX6*
15190	*SPC42-tdTomato::NatMX6/SPC42-tdTomato::NatMX6* *PDS1-tdTomato::KITRP1/PDS1-tdTomato::KITRP1* *leu2::pURA3-TetR-GFP::LEU2/leu2::hisG* *CEN5::tetOx224::HIS3/CEN5*

AMy strain	Relevant genotype
15342	*ndt80Δ::LEU2/ndt80Δ::LEU2* *REC8-3HA::URA3/REC8-3HA::URA3* *mam1Δ::TRP1/mam1Δ::TRP1*
15343	*ndt80Δ::LEU2/ndt80Δ::LEU2* *REC8-3HA::URA3/REC8-3HA::URA3* *spo13Δ::KanMX6/spo13Δ::KanMX6*
15344	*ndt80Δ::LEU2/ndt80Δ::LEU2* *REC8-3HA::URA3/REC8-3HA::URA3* *spo13Δ::KanMX6/spo13Δ::KanMX6* *mam1Δ::TRP1/mam1Δ::TRP1*
15717	*cdc20::pCLB2-CDC20::KanMX6/cdc20::pCLB2-CDC20::KanMX6* *SPO13-3FLAG::KanMX6/SPO13-3FLAG::KanMX6* *CDC5-3V5/CDC5-3V5*
15718	*cdc20::pCLB2-CDC20::KanMX6/cdc20::pCLB2-CDC20::KanMX6* *spo13::spo13-m2-3FLAG::KanMX6/spo13::spo13-m2-3FLAG::KanMX6* *CDC5-3V5/CDC5-3V5*
15719	*cdc20::pCLB2-CDC20::KanMX6/cdc20::pCLB2-CDC20::KanMX6* *SGO1-6HA::TRP1/SGO1-6HA::TRP1* *RTS1-3PK::TRP1/RTS1-3PK::TRP1* *SPO13-3FLAG::KanMX6/ SPO13-3FLAG::KanMX6*
15790	*cdc20::pCLB2-CDC20::KanMX6/cdc20::pCLB2-CDC20::KanMX6* *SGO1-6HA::TRP1/SGO1-6HA::TRP1* *RTS1-3PK::TRP1/RTS1-3PK::TRP1* *spo13::spo13-m2-3FLAG::KanMX6/spo13::spo13-m2-3FLAG::KanMX6*
15797	*cdc20::pCLB2-CDC20::KanMX6/cdc20::pCLB2-CDC20::KanMX6* *CDC5-3V5/CDC5-3V5* *spo13::KanMX6::pCUP1-SPO13-3FLAG::xhsv/* *spo13::KanMX6::pCUP1-SPO13-3FLAG::xhsv*
15798	*cdc20::pCLB2-CDC20::KanMX6/cdc20::pCLB2-CDC20::KanMX6* *CDC5-3V5/CDC5-3V5* *spo13::KanMX6::pCUP1-spo13-m2-3FLAG::xhsv/* *spo13::KanMX6::pCUP1-spo13-m2-3FLAG::xhsv*
15996	*cdc20::pCLB2-CDC20::KanMX6/cdc20::pCLB2-CDC20::KanMX6* *SGO1-6HA::TRP1/SGO1-6HA::TRP1* *RTS1-3PK::TRP1/RTS1-3PK::TRP1* *spo13::KanMX6::pCUP1-SPO13-3FLAG::xhsv/* *spo13::KanMX6::pCUP1-SPO13-3FLAG::xhsv*
15997	*cdc20::pCLB2-CDC20::KanMX6/cdc20::pCLB2-CDC20::KanMX6* *SGO1-6HA::TRP1/SGO1-6HA::TRP1* *RTS1-3PK::TRP1/RTS1-3PK::TRP1* *spo13::KanMX6::pCUP1-spo13-m2-3FLAG::xhsv/* *spo13::KanMX6::pCUP1-spo13-m2-3FLAG::xhsv*
16001	*URA3/URA3, LEU2/LEU2* *cdc20::pCLB2-CDC20::KanMX6/cdc20::pCLB2-CDC20::KanMX6* *SGO1-yEGFP::KanMX6/SGO1-yEGFP::KanMX6* *MTW1-tdTomato::NatMX6/MTW1-tdTomato::NatMX6*

AMy strain	Relevant genotype
16059	*URA3/URA3, LEU2/LEU2* *cdc20::pCLB2-CDC20::KanMX6/cdc20::pCLB2-CDC20::KanMX6* *SGO1-yEGFP::KanMX6/SGO1-yEGFP::KanMX6* *MTW1-tdTomato::NatMX6/MTW1-tdTomato::NatMX6* *spo13Δ::KanMX6/spo13Δ::KanMX6*
16378	*pGAL1-NDT80::TRP1/pGAL1-NDT80::TRP1* *ura3::pGPD1-GAL4(848).ER::URA3/ura3::pGPD1-GAL4(848).ER::URA3* *REC8-GFP::URA3/ REC8-GFP::URA3* *PDS1-tdTomato::KITRP1/PDS1-tdTomato::KITRP1* *MTW1-tdTomato::NatMX6/MTW1-tdTomato::NatMX6* *SPO13-3FLAG::KanMX6/SPO13-3FLAG::KanMX6*
16379	*pGAL1-NDT80::TRP1/pGAL1-NDT80::TRP1* *ura3::pGPD1-GAL4(848).ER::URA3/ura3::pGPD1-GAL4(848).ER::URA3* *REC8-GFP::URA3/ REC8-GFP::URA3* *PDS1-tdTomato::KITRP1/PDS1-tdTomato::KITRP1* *MTW1-tdTomato::NatMX6/MTW1-tdTomato::NatMX6* *spo13::spo13-m2-3FLAG::KanMX6/spo13::spo13-m2-3FLAG::KanMX6*
16520	*pGAL1-NDT80::TRP1/pGAL1-NDT80::TRP1* *ura3::pGPD1-GAL4(848).ER::URA3/ura3::pGPD1-GAL4(848).ER::URA3* *REC8-GFP::URA3/ REC8-GFP::URA3* *PDS1-tdTomato::KITRP1/PDS1-tdTomato::KITRP1* *MTW1-tdTomato::NatMX6/MTW1-tdTomato::NatMX6* *spo13::KanMX6::pCUP1-SPO13-3FLAG::xhsv/* *spo13::KanMX6::pCUP1-SPO13-3FLAG::xhsv*
16521	*pGAL1-NDT80::TRP1/pGAL1-NDT80::TRP1* *ura3::pGPD1-GAL4(848).ER::URA3/ura3::pGPD1-GAL4(848).ER::URA3* *REC8-GFP::URA3/ REC8-GFP::URA3* *PDS1-tdTomato::KITRP1/PDS1-tdTomato::KITRP1* *MTW1-tdTomato::NatMX6/MTW1-tdTomato::NatMX6* *spo13::KanMX6::pCUP1-spo13-m2-3FLAG::xhsv/* *spo13::KanMX6::pCUP1-spo13-m2-3FLAG::xhsv*
16811	*ndd1::HphMX6::pSCC1-NDD1/ndd1::HphMX6::pSCC1-NDD1* *clb4Δ::His3MX6/clb4Δ::His3MX6* *cdc20::pCLB2-CDC20::KanMX6/cdc20::pCLB2-CDC20::KanMX6* *SGO1-6HA::TRP1/SGO1-6HA::TRP1*
16812	*ndd1::HphMX6::pSCC1-NDD1/ndd1::HphMX6::pSCC1-NDD1* *clb4Δ::His3MX6/clb4Δ::His3MX6* *cdc20::pCLB2-CDC20::KanMX6/cdc20::pCLB2-CDC20::KanMX6* *SGO1-6HA::TRP1/SGO1-6HA::TRP1* *cdc5::pCLB2-CDC5::KanMX6/cdc5::pCLB2-CDC5::KanMX6*
16813	*ndd1::HphMX6::pSCC1-NDD1/ndd1::HphMX6::pSCC1-NDD1* *clb4Δ::His3MX6/clb4Δ::His3MX6* *cdc20::pCLB2-CDC20::KanMX6/cdc20::pCLB2-CDC20::KanMX6* *SGO1-6HA::TRP1/SGO1-6HA::TRP1* *ama1Δ::NatMX6/ama1Δ::NatMX6*

AMy strain	Relevant genotype
16814	*ndd1::HphMX6::pSCC1-NDD1/ndd1::HphMX6::pSCC1-NDD1* *clb4Δ::His3MX6/clb4Δ::His3MX6* *cdc20::pCLB2-CDC20::KanMX6/cdc20::pCLB2-CDC20::KanMX6* *SGO1-6HA::TRP1/SGO1-6HA::TRP1* *cdc5::pCLB2-CDC5::KanMX6/cdc5::pCLB2-CDC5::KanMX6* *ama1Δ::NatMX6/ama1Δ::NatMX6*
16886	*ndd1::HphMX6::pSCC1-NDD1/ndd1::HphMX6::pSCC1-NDD1* *clb4Δ::His3MX6/clb4Δ::His3MX6* *cdc20::pCLB2-CDC20::KanMX6/cdc20::pCLB2-CDC20::KanMX6*
16887	*cdc20::pCLB2-CDC20::KanMX6/cdc20::pCLB2-CDC20::KanMX6* *loxp-6HA-Dbf4/loxp-6HA-Dbf4* *HRR25-3FLAG::NatMX6/HRR25-3FLAG::NatMX6*
16888	*cdc20::pCLB2-CDC20::KanMX6/cdc20::pCLB2-CDC20::KanMX6* *loxp-6HA-Dbf4/loxp-6HA-Dbf4* *HRR25-3FLAG::NatMX6/HRR25-3FLAG::NatMX6* *mam1Δ::TRP1/mam1Δ::TRP1*
16889	*cdc20::pCLB2-CDC20::KanMX6/cdc20::pCLB2-CDC20::KanMX6* *loxp-6HA-Dbf4/loxp-6HA-Dbf4* *HRR25-3FLAG::NatMX6/HRR25-3FLAG::NatMX6* *cdc5::pCLB2-CDC5::KanMX6/cdc5::pCLB2-CDC5::KanMX6*
16890	*cdc20::pCLB2-CDC20::KanMX6/cdc20::pCLB2-CDC20::KanMX6* *loxp-6HA-Dbf4/loxp-6HA-Dbf4* *HRR25-3FLAG::NatMX6/HRR25-3FLAG::NatMX6* *spo13Δ::LEU2/spo13Δ::LEU2*
16891	*cdc20::pCLB2-CDC20::KanMX6/cdc20::pCLB2-CDC20::KanMX6* *loxp-6HA-Dbf4/loxp-6HA-Dbf4* *HRR25-3FLAG::NatMX6/HRR25-3FLAG::NatMX6* *spo13::spo13-m2::LEU2/spo13::spo13-m2::LEU2*
17481	*pGAL1-NDT80::TRP1/pGAL1-NDT80::TRP1* *ura3::pGPD1-GAL4(848).ER::URA3/ura3::pGPD1-GAL4(848).ER::URA3* *REC8-GFP::URA3/ REC8-GFP::URA3* *PDS1-tdTomato::KITRP1/PDS1-tdTomato::KITRP1* *MTW1-tdTomato::NatMX6/MTW1-tdTomato::NatMX6* *SPO13-3FLAG::KanMX6/SPO13-3FLAG::KanMX6* *sgo1::HphMX6::pCLB2-SGO1/sgo1::HphMX6::pCLB2-SGO1*
17482	*pGAL1-NDT80::TRP1/pGAL1-NDT80::TRP1* *ura3::pGPD1-GAL4(848).ER::URA3/ura3::pGPD1-GAL4(848).ER::URA3* *REC8-GFP::URA3/ REC8-GFP::URA3* *PDS1-tdTomato::KITRP1/PDS1-tdTomato::KITRP1* *MTW1-tdTomato::NatMX6/MTW1-tdTomato::NatMX6* *spo13::KanMX6::pCUP1-SPO13-3FLAG::xhsv/spo13::KanMX6::pCUP1-SPO13-3FLAG::xhsv* *sgo1::HphMX6::pCLB2-SGO1/sgo1::HphMX6::pCLB2-SGO1*
17483	*ndd1::HphMX6::pSCC1-NDD1/ndd1::HphMX6::pSCC1-NDD1* *clb4Δ::His3MX6/clb4Δ::His3MX6* *SGO1-yEGFP::KanMX6/SGO1-yEGFP::KanMX6* *MTW1-tdTomato::NatMX6/MTW1-tdTomato::NatMX6* *PDS1-tdTomato::KITRP1/PDS1-tdTomato::KITRP1*

AMy strain	Relevant genotype
17484	*ndd1::HphMX6::pSCC1-NDD1/ndd1::HphMX6::pSCC1-NDD1* *clb4Δ::His3MX6/clb4Δ::His3MX6* *SGO1-yEGFP::KanMX6/SGO1-yEGFP::KanMX6* *MTW1-tdTomato::NatMX6/MTW1-tdTomato::NatMX6* *PDS1-tdTomato::KITRP1/PDS1-tdTomato::KITRP1* *ama1Δ::NatMX6/ama1Δ::NatMX6*
17485	*ndd1::HphMX6::pSCC1-NDD1/ndd1::HphMX6::pSCC1-NDD1* *clb4Δ::His3MX6/clb4Δ::His3MX6* *SGO1-yEGFP::KanMX6/SGO1-yEGFP::KanMX6* *MTW1-tdTomato::NatMX6/MTW1-tdTomato::NatMX6* *PDS1-tdTomato::KITRP1/PDS1-tdTomato::KITRP1* *spo13Δ::LEU2/spo13Δ::LEU2*
17486	*ndd1::HphMX6::pSCC1-NDD1/ndd1::HphMX6::pSCC1-NDD1* *clb4Δ::His3MX6/clb4Δ::His3MX6* *SGO1-yEGFP::KanMX6/SGO1-yEGFP::KanMX6* *MTW1-tdTomato::NatMX6/MTW1-tdTomato::NatMX6* *PDS1-tdTomato::KITRP1/PDS1-tdTomato::KITRP1* *spo13Δ::LEU2/spo13Δ::LEU2* *ama1Δ::NatMX6/ama1Δ::NatMX6*
17487	*ndd1::HphMX6::pSCC1-NDD1/ndd1::HphMX6::pSCC1-NDD1* *clb4Δ::His3MX6/clb4Δ::His3MX6* *sgo1::sgo1(Δdb)-yEGFP::KanMX6/sgo1::sgo1(Δdb)-yEGFP::KanMX6* *MTW1-tdTomato::NatMX6/MTW1-tdTomato::NatMX6* *PDS1-tdTomato::KITRP1/PDS1-tdTomato::KITRP1*
17488	*ndd1::HphMX6::pSCC1-NDD1/ndd1::HphMX6::pSCC1-NDD1* *clb4Δ::His3MX6/clb4Δ::His3MX6* *sgo1::sgo1(Δdb)-yEGFP::KanMX6/sgo1::sgo1(Δdb)-yEGFP::KanMX6* *MTW1-tdTomato::NatMX6/MTW1-tdTomato::NatMX6* *PDS1-tdTomato::KITRP1/PDS1-tdTomato::KITRP1* *ama1Δ::NatMX6/ama1Δ::NatMX6*
17492	*cdc20::pCLB2-CDC20::KanMX6/cdc20::pCLB2-CDC20::KanMX6* *SPO13-3FLAG::KanMX6/SPO13-3FLAG::KanMX6* *CDC5-3V5/CDC5-3V5* *mam1Δ::TRP1/mam1Δ::TRP1*
17493	*cdc20::pCLB2-CDC20::KanMX6/cdc20::pCLB2-CDC20::KanMX6* *spo13::spo13-m2-3FLAG::KanMX6/spo13::spo13-m2-3FLAG::KanMX6* *CDC5-3V5/CDC5-3V5* *mam1Δ::TRP1/mam1Δ::TRP1*
17494	*SPC42-tdTomato::NatMX6/SPC42-tdTomato::NatMX6* *PDS1-tdTomato::KITRP1/PDS1-tdTomato::KITRP1* *leu2::pURA3-TetR-GFP::LEU2/leu2::hisG* *CEN5::tetOx224::HIS3/CEN5* *spo13::spo13-m2::LEU2/spo13::spo13-m2::LEU2*
17544	*SPC42-tdTomato::NatMX6/SPC42-tdTomato::NatMX6* *PDS1-tdTomato::KITRP1/PDS1-tdTomato::KITRP1* *leu2::pURA3-TetR-GFP::LEU2/leu2::hisG* *CEN5::tetOx224::HIS3/CEN5* *spo13::spo13-m2::LEU2/spo13::spo13-m2::LEU2* *mam1Δ::TRP1/mam1Δ::TRP1*

AMy strain	Relevant genotype
17734	*ndd1::HphMX6::pSCC1-NDD1/ndd1::HphMX6::pSCC1-NDD1* *clb4Δ::His3MX6/clb4Δ::His3MX6* *sgo1::sgo1(Δdb)-yEGFP::KanMX6/sgo1::sgo1(Δdb)-yEGFP::KanMX6* *MTW1-tdTomato::NatMX6/MTW1-tdTomato::NatMX6* *PDS1-tdTomato::KITRP1/PDS1-tdTomato::KITRP1* *spo13Δ::LEU2/spo13Δ::LEU2*
17735	*ndd1::HphMX6::pSCC1-NDD1/ndd1::HphMX6::pSCC1-NDD1* *clb4Δ::His3MX6/clb4Δ::His3MX6* *sgo1::sgo1(Δdb)-yEGFP::KanMX6/sgo1::sgo1(Δdb)-yEGFP::KanMX6* *MTW1-tdTomato::NatMX6/MTW1-tdTomato::NatMX6* *PDS1-tdTomato::KITRP1/PDS1-tdTomato::KITRP1* *spo13Δ::LEU2/spo13Δ::LEU2* *ama1Δ::NatMX6/ama1Δ::NatMX6*
17888	*REC8-GFP::URA3/ REC8-GFP::URA3* *PDS1-tdTomato::KITRP1/PDS1-tdTomato::KITRP1* *MTW1-tdTomato::NatMX6/MTW1-tdTomato::NatMX6* *SGO1-GBP::His3MX6/SGO1-GBP::His3MX6*
17889	*REC8-GFP::URA3/ REC8-GFP::URA3* *PDS1-tdTomato::KITRP1/PDS1-tdTomato::KITRP1* *MTW1-tdTomato::NatMX6/MTW1-tdTomato::NatMX6* *SGO1-GBP::His3MX6/SGO1-GBP::His3MX6* *spo13Δ::KanMX6/spo13Δ::KanMX6*
18077	*cdc20::pCLB2-CDC20::KanMX6/ cdc20::pCLB2-CDC20::KanMX6* *SGO1-6HA::TRP1/SGO1-6HA::TRP1* *spo13::spo13-m2::LEU2/spo13::spo13-m2::LEU2*
18331	*cdc20::pCLB2-CDC20::KanMX6/ cdc20::pCLB2-CDC20::KanMX6* *SGO1-6HA::TRP1/SGO1-6HA::TRP1* *bub1::HphMX6::pCLB2-BUB1/bub1::HphMX6::pCLB2-BUB1*
18332	*cdc20::pCLB2-CDC20::KanMX6/ cdc20::pCLB2-CDC20::KanMX6* *SGO1-6HA::TRP1/SGO1-6HA::TRP1* *bub1::HphMX6::pCLB2-BUB1/bub1::HphMX6::pCLB2-BUB1* *cdc5::pCLB2-CDC5::KanMX6/cdc5::pCLB2-CDC5::KanMX6*
18507	*pGAL1-NDT80::TRP1/pGAL1-NDT80::TRP1* *ura3::pGPD1-GAL4(848).ER::URA3/ura3::pGPD1-GAL4(848).ER::URA3* *REC8-GFP::URA3/ REC8-GFP::URA3* *PDS1-tdTomato::KITRP1/PDS1-tdTomato::KITRP1* *MTW1-tdTomato::NatMX6/MTW1-tdTomato::NatMX6*
19273	*REC8-GFP::URA3/REC8-GFP::URA3* *leu2::pURA3-TetR-tdTomato::LEU2/leu2::hisG* *CEN5::tetOx224::HIS3/CEN5*
19274	*REC8-GFP::URA3/REC8-GFP::URA3* *leu2::pURA3-TetR-tdTomato::LEU2/leu2::hisG* *CEN5::tetOx224::HIS3/CEN5* *spo13Δ::HphMX6/spo13Δ::HphMX6*
19275	*REC8-GFP::URA3/REC8-GFP::URA3* *leu2::pURA3-TetR-tdTomato::LEU2/leu2::hisG* *CEN5::tetOx224::HIS3/CEN5* *SGO1-GBP::His3MX6/SGO1-GBP::His3MX6*

AMy strain	Relevant genotype
19276	*REC8-GFP::URA3/REC8-GFP::URA3* *leu2::pURA3-TetR-tdTomato::LEU2/leu2::hisG* *CEN5::tetOx224::HIS3/CEN5* *mam1Δ::KanMX6/ mam1Δ::KanMX6*
19282	*REC8-GFP::URA3/REC8-GFP::URA3* *leu2::pURA3-TetR-tdTomato::LEU2/leu2::hisG* *CEN5::tetOx224::HIS3/CEN5* *SGO1-GBP::His3MX6/SGO1-GBP::His3MX6* *spo13Δ::HphMX6/spo13Δ::HphMX6*
19283	*REC8-GFP::URA3/REC8-GFP::URA3* *leu2::pURA3-TetR-tdTomato::LEU2/leu2::hisG* *CEN5::tetOx224::HIS3/CEN5* *SGO1-GBP::His3MX6/SGO1-GBP::His3MX6* *mam1Δ::KanMX6/ mam1Δ::KanMX6*
19284	*REC8-GFP::URA3/REC8-GFP::URA3* *leu2::pURA3-TetR-tdTomato::LEU2/leu2::hisG* *CEN5::tetOx224::HIS3/CEN5* *spo13Δ::HphMX6/spo13Δ::HphMX6* *mam1Δ::KanMX6/ mam1Δ::KanMX6*
19285	*REC8-GFP::URA3/REC8-GFP::URA3* *leu2::pURA3-TetR-tdTomato::LEU2/leu2::hisG* *CEN5::tetOx224::HIS3/CEN5* *SGO1-GBP::His3MX6/SGO1-GBP::His3MX6* *mam1Δ::KanMX6/ mam1Δ::KanMX6* *spo13Δ::HphMX6/spo13Δ::HphMX6*
19286	*ura3::pCLB2-CDC5::URA3/ura3::pCLB2-CDC5::URA3,* *SPC42-tdTomato::NatMX6/SPC42-tdTomato::NatMX6* *PDS1-tdTomato::KITRP1/PDS1-tdTomato::KITRP1* *trp1::TetR-ymEos3.2::LEU2/trp1::TetR-ymEos3.2::LEU2* *CEN5::tetOx224::HIS3/CEN5* *MTW1-GBP::His3MX6/MTW1-GBP::His3MX6*
19287	*ura3::pCLB2-CDC5::URA3/ura3::pCLB2-CDC5::URA3,* *SPC42-tdTomato::NatMX6/SPC42-tdTomato::NatMX6* *PDS1-tdTomato::KITRP1/PDS1-tdTomato::KITRP1* *trp1::TetR-ymEos3.2::LEU2/trp1::TetR-ymEos3.2::LEU2* *CEN5::tetOx224::HIS3/CEN5* *MTW1-GBP::His3MX6/MTW1-GBP::His3MX6* *cdc5::HphMX6::pSPO21-CDC5-nfGFP::xhsv/CDC5*
19288	*ura3::pCLB2-CDC5::URA3/ura3::pCLB2-CDC5::URA3,* *SPC42-tdTomato::NatMX6/SPC42-tdTomato::NatMX6* *PDS1-tdTomato::KITRP1/PDS1-tdTomato::KITRP1* *trp1::TetR-ymEos3.2::LEU2/trp1::TetR-ymEos3.2::LEU2* *CEN5::tetOx224::HIS3/CEN5* *MTW1-GBP::His3MX6/MTW1-GBP::His3MX6* *spo13Δ::KanMX6/spo13Δ::KanMX6*

AMy strain	Relevant genotype
19289	*ura3::pCLB2-CDC5::URA3/ura3::pCLB2-CDC5::URA3,* *SPC42-tdTomato::NatMX6/SPC42-tdTomato::NatMX6* *PDS1-tdTomato::KITRP1/PDS1-tdTomato::KITRP1* *trp1::TetR-ymEos3.2::LEU2/trp1::TetR-ymEos3.2::LEU2* *CEN5::tetOx224::HIS3/CEN5* *MTW1-GBP::His3MX6/MTW1-GBP::His3MX6* *cdc5::HphMX6::pSPO21-CDC5-nfGFP::xhsv/CDC5* *spo13Δ::KanMX6/spo13Δ::KanMX6*
19290	*pGAL1-NDT80::TRP1/pGAL1-NDT80::TRP1* *ura3::pGPD1-GAL4(848).ER::URA3/ura3::pGPD1-GAL4(848).ER::URA3* *REC8-GFP::URA3/ REC8-GFP::URA3* *PDS1-tdTomato::KITRP1/PDS1-tdTomato::KITRP1* *MTW1-tdTomato::NatMX6/MTW1-tdTomato::NatMX6* *cdc5::KanMX6::pCUP1-CDC5-3V5/cdc5::KanMX6::pCUP1-CDC5-3V5*
19291	*pGAL1-NDT80::TRP1/pGAL1-NDT80::TRP1* *ura3::pGPD1-GAL4(848).ER::URA3/ura3::pGPD1-GAL4(848).ER::URA3* *REC8-GFP::URA3/ REC8-GFP::URA3* *PDS1-tdTomato::KITRP1/PDS1-tdTomato::KITRP1* *MTW1-tdTomato::NatMX6/MTW1-tdTomato::NatMX6* *spo13::spo13-(L26A)::HphMX6/spo13::spo13-(L26A)::HphMX6*
19292	*pGAL1-NDT80::TRP1/pGAL1-NDT80::TRP1* *ura3::pGPD1-GAL4(848).ER::URA3/ura3::pGPD1-GAL4(848).ER::URA3* *REC8-GFP::URA3/ REC8-GFP::URA3* *PDS1-tdTomato::KITRP1/PDS1-tdTomato::KITRP1* *MTW1-tdTomato::NatMX6/MTW1-tdTomato::NatMX6* *cdc5::KanMX6::pCUP1-CDC5-3V5/cdc5::KanMX6::pCUP1-CDC5-3V5* *spo13::spo13-(L26A)::HphMX6/spo13::spo13-(L26A)::HphMX6*
19560	*SPC42-tdTomato::NatMX6/SPC42-tdTomato::NatMX6* *PDS1-tdTomato::KITRP1/PDS1-tdTomato::KITRP1* *trp1::TetR-ymEos3.2::LEU2/leu2::hisG* *CEN5::tetOx224::HIS3/CEN5* *nkp1::KanMX6::pIME2-NKP1-nfGFP::HphMX6/* *nkp1::KanMX6::pIME2-NKP1-nfGFP::HphMX6*
19561	*SPC42-tdTomato::NatMX6/SPC42-tdTomato::NatMX6* *PDS1-tdTomato::KITRP1/PDS1-tdTomato::KITRP1* *trp1::TetR-ymEos3.2::LEU2/leu2::hisG* *CEN5::tetOx224::HIS3/CEN5* *nkp1::KanMX6::pIME2-NKP1-nfGFP::HphMX6/* *nkp1::KanMX6::pIME2-NKP1-nfGFP::HphMX6* *spo13Δ::KanMX6/spo13Δ::KanMX6*
19562	*SPC42-tdTomato::NatMX6/SPC42-tdTomato::NatMX6* *PDS1-tdTomato::KITRP1/PDS1-tdTomato::KITRP1* *trp1::TetR-ymEos3.2::LEU2/leu2::hisG* *CEN5::tetOx224::HIS3/CEN5* *nkp1::KanMX6::pIME2-NKP1-nfGFP::HphMX6/* *nkp1::KanMX6::pIME2-NKP1-nfGFP::HphMX6* *SGO1-GBP::His3MX6/SGO1-GBP::His3MX6*

AMy strain	Relevant genotype
19563	*SPC42-tdTomato::NatMX6/SPC42-tdTomato::NatMX6* *PDS1-tdTomato::KITRP1/PDS1-tdTomato::KITRP1* *trp1::TetR-ymEos3.2::LEU2/leu2::hisG* *CEN5::tetOx224::HIS3/CEN5* *nkp1::KanMX6::pIME2-NKP1-nfGFP::HphMX6/* *nkp1::KanMX6::pIME2-NKP1-nfGFP::HphMX6* *spo13Δ::KanMX6/spo13Δ::KanMX6* *SGO1-GBP::His3MX6/SGO1-GBP::His3MX6*
19944	*pGAL1-NDT80::TRP1/pGAL1-NDT80::TRP1* *ura3::pGPD1-GAL4(848).ER::URA3/ura3::pGPD1-GAL4(848).ER::URA3* *SPC42-tdTomato::NatMX6/SPC42-tdTomato::NatMX6* *PDS1-tdTomato::KITRP1/PDS1-tdTomato::KITRP1* *leu2::pURA3-TetR-GFP::LEU2/leu2::hisG* *CEN5::tetOx224::HIS3/CEN5*
19945	*pGAL1-NDT80::TRP1/pGAL1-NDT80::TRP1* *ura3::pGPD1-GAL4(848).ER::URA3/ura3::pGPD1-GAL4(848).ER::URA3* *SPC42-tdTomato::NatMX6/SPC42-tdTomato::NatMX6* *PDS1-tdTomato::KITRP1/PDS1-tdTomato::KITRP1* *leu2::pURA3-TetR-GFP::LEU2/leu2::hisG* *CEN5::tetOx224::HIS3/CEN5* *spo13Δ::HphMX6/spo13Δ::HphMX6*
19946	*pGAL1-NDT80::TRP1/pGAL1-NDT80::TRP1* *ura3::pGPD1-GAL4(848).ER::URA3/ura3::pGPD1-GAL4(848).ER::URA3* *SPC42-tdTomato::NatMX6/SPC42-tdTomato::NatMX6* *PDS1-tdTomato::KITRP1/PDS1-tdTomato::KITRP1* *leu2::pURA3-TetR-GFP::LEU2/leu2::hisG* *CEN5::tetOx224::HIS3/CEN5* *spo13Δ::HphMX6/spo13Δ::HphMX6* *cdc7::cdc7-as3::KanMX6/cdc7::cdc7-as3::KanMX6*
19947	*pGAL1-NDT80::TRP1/pGAL1-NDT80::TRP1* *ura3::pGPD1-GAL4(848).ER::URA3/ura3::pGPD1-GAL4(848).ER::URA3* *SPC42-tdTomato::NatMX6/SPC42-tdTomato::NatMX6* *PDS1-tdTomato::KITRP1/PDS1-tdTomato::KITRP1* *leu2::pURA3-TetR-GFP::LEU2/leu2::hisG* *CEN5::tetOx224::HIS3/CEN5* *spo13Δ::HphMX6/spo13Δ::HphMX6* *hrr25-as1::HIS3::hrr25Δ::KanMX4/hrr25-as1::HIS3::hrr25Δ::KanMX4*
19948	*pGAL1-NDT80::TRP1/pGAL1-NDT80::TRP1* *ura3::pGPD1-GAL4(848).ER::URA3/ura3::pGPD1-GAL4(848).ER::URA3* *SPC42-tdTomato::NatMX6/SPC42-tdTomato::NatMX6* *PDS1-tdTomato::KITRP1/PDS1-tdTomato::KITRP1* *leu2::pURA3-TetR-GFP::LEU2/leu2::hisG* *CEN5::tetOx224::HIS3/CEN5* *spo13Δ::HphMX6/spo13Δ::HphMX6* *hrr25-as1::HIS3::hrr25Δ::KanMX4/hrr25-as1::HIS3::hrr25Δ::KanMX4* *cdc7::cdc7-as3::KanMX6/cdc7::cdc7-as3::KanMX6*
19994	*REC8-GFP::URA3/ REC8-GFP::URA3* *PDS1-tdTomato::KITRP1/PDS1-tdTomato::KITRP1* *MTW1-tdTomato::NatMX6/MTW1-tdTomato::NatMX6* *sgo1::sgo1(Δdb)::KanMX6/sgo1::sgo1(Δdb)::KanMX6*

AMy strain	Relevant genotype
19995	*REC8-GFP::URA3/ REC8-GFP::URA3* *PDS1-tdTomato::KITRP1/PDS1-tdTomato::KITRP1* *MTW1-tdTomato::NatMX6/MTW1-tdTomato::NatMX6* *sgo1::sgo1(Δdb)::KanMX6/sgo1::sgo1(Δdb)::KanMX6* *spo13Δ::HphMX6/ spo13Δ::HphMX6*
19999	*pGAL1-NDT80::TRP1/pGAL1-NDT80::TRP1* *ura3::pGPD1-GAL4(848).ER::URA3/ura3::pGPD1-GAL4(848).ER::URA3* *SGO1-2H3-2HA::HphMX6/SGO1-2H3-2HA::HphMX6*
20000	*pGAL1-NDT80::TRP1/pGAL1-NDT80::TRP1* *ura3::pGPD1-GAL4(848).ER::URA3/ura3::pGPD1-GAL4(848).ER::URA3* *SGO1-2H3-2HA::HphMX6/SGO1-2H3-2HA::HphMX6* *REC8-HKMT::His3MX6/REC8-HKMT::His3MX6*
20001	*pGAL1-NDT80::TRP1/pGAL1-NDT80::TRP1* *ura3::pGPD1-GAL4(848).ER::URA3/ura3::pGPD1-GAL4(848).ER::URA3* *SGO1-2H3-2HA::HphMX6/SGO1-2H3-2HA::HphMX6* *REC8-HKMT::His3MX6/REC8-HKMT::His3MX6* *spo13Δ::HphMX6/spo13Δ::HphMX6*
20002	*pGAL1-NDT80::TRP1/pGAL1-NDT80::TRP1* *ura3::pGPD1-GAL4(848).ER::URA3/ura3::pGPD1-GAL4(848).ER::URA3* *SGO1-2H3-2HA::HphMX6/SGO1-2H3-2HA::HphMX6* *REC8-HKMT::His3MX6/REC8-HKMT::His3MX6* *spo13::spo13-m2::HphMX6/spo13::spo13-m2::HphMX6*
20003	*pGAL1-NDT80::TRP1/pGAL1-NDT80::TRP1* *ura3::pGPD1-GAL4(848).ER::URA3/ura3::pGPD1-GAL4(848).ER::URA3* *SGO1-2H3-2HA::HphMX6/SGO1-2H3-2HA::HphMX6* *REC8-HKMT::His3MX6/REC8-HKMT::His3MX6* *cdc5::pCLB2-CDC5::KanMX6/cdc5::pCLB2-CDC5::KanMX6*
20033	*REC8-GFP::URA3/ REC8-GFP::URA3* *PDS1-tdTomato::KITRP1/PDS1-tdTomato::KITRP1* *MTW1-tdTomato::NatMX6/MTW1-tdTomato::NatMX6* *spo13Δ::HphMX6/ spo13Δ::HphMX6*
20146	*SPC42-tdTomato::NatMX6/SPC42-tdTomato::NatMX6* *PDS1-tdTomato::KITRP1/PDS1-tdTomato::KITRP1* *leu2::pURA3-TetR-GFP::LEU2/leu2::hisG* *CEN5::tetOx224::HIS3/CEN5* *spo13Δ::HphMX6/spo13Δ::HphMX6*
20147	*SPC42-tdTomato::NatMX6/SPC42-tdTomato::NatMX6* *PDS1-tdTomato::KITRP1/PDS1-tdTomato::KITRP1* *leu2::pURA3-TetR-GFP::LEU2/leu2::hisG* *CEN5::tetOx224::HIS3/CEN5* *sgo1::sgo1(Δdb)::KanMX6/sgo1::sgo1(Δdb)::KanMX6*
20148	*SPC42-tdTomato::NatMX6/SPC42-tdTomato::NatMX6* *PDS1-tdTomato::KITRP1/PDS1-tdTomato::KITRP1* *leu2::pURA3-TetR-GFP::LEU2/leu2::hisG* *CEN5::tetOx224::HIS3/CEN5* *spo13Δ::HphMX6/spo13Δ::HphMX6* *sgo1::sgo1(Δdb)::KanMX6/sgo1::sgo1(Δdb)::KanMX6*

AMy strain	Relevant genotype
20218	*LEU2/LEU2* *RTS1-EGFP::KanMX4/RTS1-EGFP::KanMX4* *PDS1-tdTomato::KITRP1/PDS1-tdTomato::KITRP1* *MTW1-tdTomato::NatMX6/MTW1-tdTomato::NatMX6*
20219	*RTS1-EGFP::KanMX4/RTS1-EGFP::KanMX4* *PDS1-tdTomato::KITRP1/PDS1-tdTomato::KITRP1* *MTW1-tdTomato::NatMX6/MTW1-tdTomato::NatMX6* *spo13Δ::LEU2/spo13Δ::LEU2*
20317	*pGAL1-NDT80::TRP1/pGAL1-NDT80::TRP1* *ura3::pGPD1-GAL4(848).ER::URA3/ura3::pGPD1-GAL4(848).ER::URA3* *SPC42-tdTomato::NatMX6/SPC42-tdTomato::NatMX6* *PDS1-tdTomato::KITRP1/PDS1-tdTomato::KITRP1* *leu2::pURA3-TetR-GFP::LEU2/leu2::hisG* *CEN5::tetOx224::HIS3/CEN5* *cdc7::cdc7-as3::KanMX6/cdc7::cdc7-as3::KanMX6*
20318	*pGAL1-NDT80::TRP1/pGAL1-NDT80::TRP1* *ura3::pGPD1-GAL4(848).ER::URA3/ura3::pGPD1-GAL4(848).ER::URA3* *SPC42-tdTomato::NatMX6/SPC42-tdTomato::NatMX6* *PDS1-tdTomato::KITRP1/PDS1-tdTomato::KITRP1* *leu2::pURA3-TetR-GFP::LEU2/leu2::hisG* *CEN5::tetOx224::HIS3/CEN5* *hrr25-as1::HIS3::hrr25Δ::KanMX4/hrr25-as1::HIS3::hrr25Δ::KanMX4*
20319	*pGAL1-NDT80::TRP1/pGAL1-NDT80::TRP1* *ura3::pGPD1-GAL4(848).ER::URA3/ura3::pGPD1-GAL4(848).ER::URA3* *SPC42-tdTomato::NatMX6/SPC42-tdTomato::NatMX6* *PDS1-tdTomato::KITRP1/PDS1-tdTomato::KITRP1* *leu2::pURA3-TetR-GFP::LEU2/leu2::hisG* *CEN5::tetOx224::HIS3/CEN5* *hrr25-as1::HIS3::hrr25Δ::KanMX4/hrr25-as1::HIS3::hrr25Δ::KanMX4* *cdc7::cdc7-as3::KanMX6/cdc7::cdc7-as3::KanMX6*

Table 7.1: Yeast strains used in this study

7.2. Buffers and solutions

Solution	Composition	Protocol
Alkaline SDS	200mM NaOH 1% SDS	Mini-prep Midi-prep
ChIP diluent	0.143M NaCl 1.43mM EDTA 71.43mM Hepes-KOH, pH 7.5	ChIP
ChIP washing buffer 1	FA lysis buffer 0.1% SDS 275mM NaCl	ChIP
ChIP washing buffer 2	FA lysis buffer 0.1% SDS 500mM NaCl	ChIP

Solution	Composition	Protocol
ChIP washing buffer 3	10mM Tris-HCl 250mM LiCl 1mM EDTA 0.5% NP-40 0.5% Sodium deoxycholate	ChIP
DAPI mount	1mg/ml p-phenylenediamine 0.04M K_2HPO_4 0.01M KH_2PO_4 0.15M NaCl 0.1% NaN_3 0.05ug/ml DAPI 90% glycerol	Immunofluorescence
DNA breakage buffer	2% Triton X-100 1% SDS 100mM NaCl 10mM Tris-Cl (pH8.0) 1mM EDTA	Smash and grab genomic DNA isolation
2x FA lysis buffer	100mM Hepes-KOH, pH 7.5 300mM NaCl 2mM EDTA 2% Triton X-100 0.2% sodium deoxycholate	ChIP
GTE	50 mM glucose 25 mM Tris 10 mM EDTA	Mini-prep Midi-prep
High salt buffer	75g KAc 90ml glacial acetic acid H_2O up to 300ml	Mini-prep Midi-prep
KP_i buffer	0.1M K_2HPO_4 0.1M KH_2PO_4	Immunofluorescence
LiTE	0.1M LiAc (pH 7.5) 10µM Tris-HCl 1µM EDTA, pH 7.5	Transformation
Orange G loading dye	40% sucrose 0.1g Orange G H_2O up to 50ml	Gel electrophoresis
PBS-BSA	1% BSA 0.04M K_2HPO_4 0.01M KH_2PO_4 0.15M NaCl 0.1% NaN_3	Immunofluorescence
PBS for PBS-Tween	137mM NaCl 2.7mM KCl 10mM Na_2HPO_4 1.8mM KH_2PO_4 0.05% (v/v) Tween 20	Western blot

Solution	Composition	Protocol
PCR buffer (10x)	100mM Tris, pH 8.3 500mM KCl 20mM $MgCl_2$ 0.1% Gelatin	PCR
Ponceau S	2.1g Ponceau S (dry) 13.5g TCA 4.5ml glacial acetic acid H_2O up to 450ml	Western blot
qPCR buffer (10x)	200mM Tris pH 8.3 500 mM KCl 20 mM $MgCl_2$ 50 mM $(NH_4)_2SO_4$	qPCR
SDS-PAGE separation gel (10%)	10ml 30% acrylamide 7.5ml 4x separation buffer (pH 8.8) 12.5ml H_2O 450µl 10% APS 30µl TEMED	SDS-PAGE
SDS-PAGE stacking gel (4%)	2ml 30% acrylamide 7.5ml 2x stacking buffer (pH 6.8) 5.3ml H_2O 150µl 10% APS 15µl TEMED	SDS-PAGE
SDS running buffer (10x)	121.2g Tris base 576g glycine 40g SDS H_2O up to 4l	SDS-PAGE
SDS sample buffer (3x)	187mM Tris (pH 6.8) 6% β-mercaptoethanol 30% glycerol 9% SDS 0.05% bromophenol blue	SDS-PAGE
Separation buffer (pH8.8) (4x)	363.3 g Trizma base 8 g SDS H_2O up to 2l	SDS-PAGE
Stacking buffer (pH 6.8) (2x)	60.55 g Trizma base 4 g SDS H_2O up to 2l	SDS-PAGE
1.2M sorbitol citrate	17.4g anhydrous K_2HPO_4 7g citric acid 218.64g sorbitol H_2O up to 1l	Immunofluorescence
TAE (10x)	400mM Tris 1.14% (v/v) glacial acetic acid 10mM EDTA	Gel electrophoresis

Solution	Composition	Protocol
TBS	20 mM Tris-HCl, pH7.5 150 mM NaCl	ChIP
10x TE	0.1 M Tris-HCl 0.01 M EDTA, pH 7.5	Various
Transfer buffer (10x)	60.6g Trizma base 288.2g glycine 20ml SDS H_2O up to 2l	Western blot

Table 7.2: Buffers and solutions used in this study.

7.3. Abbreviations

APC/C	Anaphase promoting complex/cyclosome
CDK	cyclin-dependent kinase
CEN	centromere
ChIP	Chromatin immuno-precipitation
CPC	chromosomal passenger complex
DDK	Dbf4-dependent kinase
DNA	Deoxyribonucleic acid
DSR	Determinant of selective removal
FEAR	Cdc14 early release
GBP	GFP binding protein
GFP	Green fluorescent protein
HKMT	Histone lysine methyl transferase
KMN	KNL1-Mis12-Ndc80
MCC	Mitotic checkpoint complex
MEN	Mitotic exit network
MRX	Mre11-Rad50-Xrs2
MSE	Middle sporulation element
PCR	Polymerase chain reaction
PGC	Primordial germ cell
PP1	Protein phosphatase 1
PP2A	Protein phosphatase 2A
qPCR	Quantitative PCR

RC	Recombination checkpoint
SC	Synaptonemal complex
SPB	Spindle pole body
SPO	Sporulation media
TCA	Trichloric acid
tetO	Tet operators
TetR	Tet repressor
ymEos3.2	yeast codon-optimised mEos3.2